Development of Aptamers as Diagnostic and Therapeutic Agents

Thesis

DEVELOPMENT OF APTAMERS AS DIAGNOSTIC AND THERAPEUTIC AGENTS

A thesis submitted for the degree of Doctor of Philosophy in Chemistry and Analytical Sciences

Suzanne Clare Simmons

BSc.

February 2010

Department of Chemistry and Analytical Sciences

The Open University

Walton Hall

Milton Keynes

Buckinghamshire

MK7 6AA

United Kingdom

STATEMENT

The work presented in this thesis was carried out during the period 1st March 2006 to 26th February 2010 under supervision of Dr Sotiris Missailidis, Dr Maria Velasco-Garcia and Dr Jim Iley of The Open University, UK, with external supervision of Professor Paul Brenchley and Dr Edward McKenzie of The University of Manchester, UK.

ACKNOWLEDGEMENTS

Firstly I must thank my rather large team of supervisors and colleagues, Drs Sotiris Missailidis, Maria Velasco-Garcia, Eddie McKenzie, Jim Iley, Chiara DaPieve, Professor Paul Brenchley, plus Vaidehi Makwana and Steve Arnold for all of their help and support throughout what has been an emotional experience. I definitely couldn't have done it without all of your input and consider myself lucky to have worked with all of you.

An enormous thank you is deserved by Pam and Clive Simmons, my Mum and Dad, for continuously being there to help emotionally, financially and in any other way possible. Maybe now that I am finally leaving 'school' after 21 solid years I'll be able to support myself!

A big thank you goes to Martin Nurton, my husband, for doing his best to understand what it has been like and for making me laugh by trying to help me find the answers in my work...I'm fairly sure "this is the answer because it is" wouldn't really cut the mustard here though! Thanks also to Troy for reminding me that no matter how busy I am with lab work, writing, keeping house and answering Martin's phones, a Cockatoo still needs his cuddles and in doing so, will help with the toughest of days.

Thanks to my fellow Technical Milkers; Claire Kotecki, Sarah Mason and more recently, Lizzie Angus, who are probably the only ones who really know what it's like and are there on a daily basis to discuss, over boh!, when things go horribly wrong with supervisors, relationships, lab work or piercings.

During my PhD, I had the pleasure of being able to visit and work with a wonderful group of people at the Institute of Dentistry, University of Oulu in Finland. As well as gaining a lot of experimental results from the three weeks I spent with them, I gained an insight into how quiet, efficient and completely lovely and helpful Finnish people are (or these Finnish people anyway!). So many thanks to Sirpa, Pia, Sini and Tuula for everything. Similarly, many thanks go to Dr Lynda Harris, whom I worked with whilst in Manchester, for helping me with experiments and making me feel so welcome. Thanks also to Drs Dilson Silva and Celia Cortez for their expert help with the serum albumin assays.

Also, a big thank you to all my family and friends, past and present, who have helped to keep me sane by making me laugh on many occasions; I am lucky there are so many of you that you wont all fit on one page, and now that I can have my life back I have some catching up and repaying of laughter and support to pay back to all of you.

This thesis is dedicated to everyone above.

The Open University

EX12 Revised 27 January 2010

RESEARCH SCHOOL

Library Authorisation Form

Please return this form to the Research School with the two bound copies of your thesis to be deposited with the University Library. All candidates should complete parts one and two of the form. Part three only applies to PhD candidates.

Part One: Candidates Details

Name: SUZANNE CLARE SIMMONS PI: W8190101

Degree: PhD

Thesis title: DEVELOPMENT OF APTAMERS AS DIAGNOSTIC AND THERAPEUTIC AGENTS

Part Two: Open University Library Authorisation

I confirm that I am willing for my thesis to be made available to readers by The Open University Library, and that it may be photocopied, subject to the discretion of the Librarian.

Signed: S Simmons Date: 02/09/2010

Part Three: British Library Authorisation [PhD candidates only]

If you want like a copy of your PhD thesis to be available on loan to the British Library Thesis Service as and when it is requested, please tick Section A of this form.

The University has agreed that your participation in the British Library Thesis Service should be voluntary. Please tick either (a) or (b) to indicate your intentions.

(a) ☑ I am willing for The Open University to loan the British Library a copy of my thesis.

(b) ☐ I do not wish The Open University to loan the British Library a copy of my thesis.

Signed: S Simmons Date: 02/09/2010

a truncated aptamer '1.5M short', suggesting a possible application for this aptamer would be as an anticancer or anti-angiogenesis therapy or in a diagnostic assay for the detection of heparanase. Also, this aptamer and its full length counterpart have been applied to a quartz crystal to test the sensitivity of detection of heparanase using microbalance apparatus, with promising results.

LIST OF ABBREVIATIONS

Ab	Antibody
AMD	Age-related Macular Degeneration
APS	Ammonium PerSulphate
BAFB	(2-{4-[(E)-3-(4-bromophenyl) acryloylamino]-3-fluorophenyl} benzooxazol-5-yl) acetic acid
Bcl-2	B cell Lymphoma 2
bFGF	basic Fibroblast Growth Factor
BLAST	Basic Local Alignment Search Tool
BSA	Bovine Serum Albumin
CK-7	CytoKeratin 7
COX-2	CycloOXygenase 2
DAB	3,3'-DiAminoBenzidine tetrahydrochloride
DAG	DiAcylGlycerol
DMA	N,N-DiMethylAcetamide
DMSO	DiMethylSulfOxide
DNA	DeoxyriboNucleic Acid
dNTP	deoxyNucleotideTriPhosphates
DSP	3,3'-DithiodiPropionic acid
(N)ECEEM	(Non) Equilibrium Capillary Electrophoresis of Equilibrium Mixtures
ECM	ExtraCellular Matrix
EDTA	EthyleneDiamineTetraAcetic acid
EGF-R	Epidermal Growth Factor Receptor
EIA	Enzyme ImmunoAssay
ELISA	Enzyme-Linked ImmunoSorbent Assay
EMSA	Electrophoretic Mobility Shift Assay
ERK	Extracellular signal Regulated Kinase
FET	Field-Effect Transistors
FIS	Faradic Impedance Spectroscopy
FITC	Fluorescein IsoThioCyanate
FSH	Follicle Stimulating Hormone
GH-A	Clan A Glycosyl Hydrolase
GlcA	D-glucoronate

GlcN	Glucosamine
GlcNAc	Glucosamine (acetylated)
$GlcNSO_3$	Glcosamine (sulphated)
GnRH	Gonadotropin Releasing Hormone
GPI	Glycosylphosphatidyl inositol-linked
GST	Glutathione Transferase
hCG	human Chorionic Gonadotropin
HGF	Hepatocyte Growth Factor
Hpa	Heparanase
HRP	HorseRadish Peroxidase
HS	Heparan Sulphate
HSA	Human Serum Albumin
HSPG	Heparan Sulphate ProteoGlycan
IdoA	L-iduronate
IGF-1	Insulin-like Growth Factor 1
IHC	ImmunoHistoChemistry
IF	ImmunoFluorescence
IFE	Inner Filter Effect (primary; p, or secondary; s)
IFNγ	InterFeron γ
IgG	Immunoglobulin G
IL-8	InterLeukin 8
K_A	Association (or Affinity) constant
K_D	Dissociation constant
KGF	Keratinocyte Growth Factor
LH	Luteinising Hormone
MAP	Mitogen Activated Protein
MUC1	MUCin 1
NHS	N-Hydroxy-Succinimide
nt	nucleotide
PAGE	PolyAcrylamide Gel Electrophoresis
PBS	Phosphate Buffered Saline
PCR	Polymerase Chain Reaction
PDGF(R)	Platelet-Derived Growth Factor (Receptor)
PEG	PolyEthylene Glycol

PF4	Platelet Factor 4
PG	ProteoGlycan
PI	Propidium Iodide
pI	Isoelectric point
PI3-K	PhosphatidylInositol 3-Kinase
PI-88	Phosphomannopentaose sulphate
PKA	Protein Kinase A
PKC	Protein Kinase C
POC	Point Of Care
PTEN	Phosphatase and TENsin homolog
QCM	Quartz Crystal Microbalance
Rb	Retinoblasoma protein
RBD	Ras Binding Domain
RIA	RadioImmunoAssay
RK-682	(R)-3-hexadecanoyl-5-hydroxymethyltetronic acid
RNA	RiboNucleic Acid (sometimes messenger RNA or mRNA)
RTK	Receptor Tyrosine Kinase
SELEX	Systematic Evolution of Ligands by EXponential enrichment
SOC	Super Optimal broth with Catabolite repression
SNP	Single Nucleotide Polymorphism
SPRi	Surface Plasmon Resonance imaging
TBE	Tris Borate EDTA
TBS	Tris Buffered Saline
TEMED	TEtraMethylEthyleneDiamine
TGF	Transforming (or Tumour) Growth Factor
TIM	TriosephosphateIsoMerase
TMB	TetraMethyl Benzidine
TN-C	TeNascin C
VEGF(R)	Vascular Endothelial Growth Factor (Receptor)
vWF	von Willebrand Factor
XAM	Xylene Alternative Mountant

AMINO ACIDS; THEIR THREE AND ONE LETTER CODES, SIDE CHAIN POLARITY AND CHARGE AT pH 7.4

Alanine	Ala	A	nonpolar	neutral
Arginine	Arg	R	polar	positive
Asparagine	Asn	N	polar	neutral
Aspartic Acid	Asp	D	polar	negative
Cysteine	Cys	C	nonpolar	neutral
Glutamic Acid	Glu	E	polar	negative
Glutamine	Gln	Q	polar	neutral
Glycine	Gly	G	nonpolar	neutral
Histidine	His	H	polar	positive (10%) neutral (90%)
Isoleucine	Ile	I	nonpolar	neutral
Leucine	Leu	L	nonpolar	neutral
Lysine	Lys	K	polar	positive
Methionine	Met	M	nonpolar	neutral
Phenylalanine	Phe	F	nonpolar	neutral
Proline	Pro	P	nonpolar	neutral
Serine	Ser	S	polar	neutral
Threonine	Thr	T	polar	neutral
Tryptophan	Trp	W	nonpolar	neutral
Tyrosine	Tyr	Y	polar	neutral
Valine	Val	V	nonpolar	neutral

LIST OF INSERTIONS

LIST OF CONTENTS

CHAPTER ONE

INTRODUCTION

1.1 What is cancer?

Cancer is one of the principal causes of death in developed countries. It is a class of diseases which are characterised by uncontrolled proliferation of cells and invasion of the surrounding tissue around the body to different organs. This is initially caused by damage, or mutations, to DNA that encode for proteins controlling cell division, differentiation and survival, by carcinogens such as radiation, chemicals, physical agents or viruses [1]. However, cancer has been suggested not to be a one-step process but rather a multistep progressive one, with intermediate changes occurring in the genome, which when combined, help drive the change from normal healthy cells into malignant and metastatic cells. As observed clinically, a mutation causes a genetic lesion within a healthy cell, leading to a benign hyperplasia or polyp, which with further genetic mutation causes dysplasia (disorderliness of the cells caused by further mutation), and finally, cancer. The cancer itself then progresses and more mutations occur; leading to acquired ability to metastasise and invade other tissues where space and nutrients are not in limited supply. This is reflected in cell culture of both rodent and human cells, where more than two induced genetic alterations are required to generate tumorigenic variants [2] and is expected due to the many complex anti-cancer mechanisms shared by all cells in the body.

1.1.1 Why and what makes molecules in cancer a good target?

Due to the many steps required for formation of an invasive tumour there are a number of targets and approaches available to investigate possible therapeutics [1], which fall into the following main areas [2, 3]:

- Mutations can arise in the genes responsible for coordinating checking and repair of DNA, thus leaving it unchecked or unrepaired before cell division [1]. An example of this is p53; a gene involved in key areas of cell regulation which is mutated in approximately 50% of all human tumours, hence losing its function. In a healthy cell, p53 activates cell cycle arrest at checkpoint G1/S, upon detection of DNA damage, allowing the cell to repair the damage or induce apoptosis if the damage is too severe. Loss of function of p53 leads to damaged DNA remaining unrepaired and apoptosis from being triggered. Various cyclin-dependent kinase inhibitors are in development to halt the cell cycle, including Flavopiridol, Ispinesib and SNS-032 [3].
- Mutations can arise in proto-oncogenes, which are responsible for regulating cell growth and differentiation, creating oncogenes, which allow the cells to act self-sufficiently with respect to growth signals [1]. Healthy cells require activation from mitogenic growth signals to progress from non-proliferative to proliferative cells. These signals can come from growth factors, extracellular matrix (ECM) components or cell-cell adhesion/interaction molecules. A key difference between healthy and tumour cells is that tumour cells are able to synthesise their own growth signals and can 'switch on' and proliferate independently from other cells. Examples of this include the synthesis and response to growth factors platelet-derived growth factor and tumour growth factor alpha (PDGF and TGFα) by glioblastomas and sarcomas [2]. Numbers of Tyrosine Kinase receptors themselves are also increased in many cancers, for example, epidermal growth factor receptors (EGF-R) are increased in stomach tumours, leading to an increased response in the presence of typical levels of growth factors [2]. Gefitinib is an EGFR targeted inhibitor, which competes with ATP for binding of the

intracellular tyrosine kinase domain; inhibiting autophosphorylation and therefore, signal transduction and proliferation of the cell [3].

- Mutations occur in tumour suppressor genes, preventing the proteins they code for from being synthesised or being active, strongly increasing the probability of a tumour forming [1]. These are known as loss-of-function mutations as they form due to a loss of tumour suppression and are recessive, as both copies of the particular tumour suppressor gene need to be mutated before an effect is seen. Retinoblastoma protein (Rb) is responsible for blocking entry into S phase by the inactivation of growth factors such as E2F. Transforming growth factor beta (TGFβ) disrupts the phosphorylation of Rb protein in a normal healthy cell, which maintains its activity. However, many human tumours have shown downregulation of, or dysfunctional TGFβ receptors, hence allowing Rb to be phosphorylated and inactivated, leading to activation of growth factors and progression through S phase.
- Mutations occur in pathways responsible for cell death, therefore allowing the cell to escape apoptosis [1]. Intrinsic examples of this are Bcl-2 and IGF-1 overexpression; both of which are cell survival signals. PTEN, which acts by blocking the cell survival action of IGF-1 and is therefore a tumour suppressor, shows an inactivation of both alleles on an almost equal frequency to p53 mutations. Extrinsically, decoy receptors for the Fas ligand are upregulated in lung and colorectal tumours, which bind Fas but do not transmit its signal for apoptosis of the cell. Obatoclax is currently the only small molecule inhibitor target for apoptosis regulation and acts via inhibition of the Bcl-2 family of cell-survival proteins [3].

- Mutations occur that allow cells to evade terminal differentiation and replicative senescence, and hence they do not lose the ability to divide [1]. Normally, cells will only divide a finite number of times due to the shortening of telomeres with each round of replication, and then they will be subject to cell cycle arrest via the p53 pathway. However, if a tumour cell had the mutation and subsequent loss of p53; it could proceed with replication but would gain increasing genetic instability due to loss of genetic material from each round that would not be repaired. Thus, tumour cells have acquired the ability to reactivate telomerase; an enzyme which is normally expressed at low levels or even absent from somatic cells and is responsible for lengthening telomeres. This scenario has been proven in approximately 85% of human tumours, leading to telomerase forming another potential target for cancer therapeutics in the form of antisense oligonucleotides, reverse transcriptase inhibitors and G-quadruplex DNA-binding drugs.
- Tumours acquire a blood and lymph supply through mutated cells' ability to carry out angiogenesis (production of new blood vessels from pre-existing blood vessels) [1]. This is essential because in order for tumour cells to proliferate, they must be able to metabolise or they will suffer necrosis. Therefore, growth factors promoting growth and differentiation into new capillaries and their components, such as vascular endothelial growth factor (VEGF), fibroblast growth factor (FGF) and platelet-derived growth factor (PDGF), plus many others have all been shown to be expressed and sometimes overexpressed by tumour cells. Inhibitors such as anti-VEGF antibodies, decoy VEGF receptors, inhibitors of the tyrosine kinase pathway and inhibitors directed against endothelial cell proliferation and migration have all been developed as anti-cancer therapeutics [3].

- Cancerous cells can mutate further to allow travel and metastasis throughout the body [1]. To achieve this, tumour cells must have the ability to break the cell-cell and cell-ECM interactions that are normally present. In some cancers, notably breast and stomach, expression of E-cadherin, a cell-cell adhesion molecule present in epithelial cells, is lost. Tumour cells may also achieve access to the target organ through upregulation and release of extracellular proteases such as serine and threonine proteases and matrix metalloproteinases (MMPs). Specifically, MMPs 2 and 9 have shown type IV collagen degradation of the basement membrane and have shown to be expressed by tumour cells. Furthermore, tumour metastasis has shown to be markedly reduced in mice deficient in both MMPs 2 and 9, suggesting their importance in tumour metastasis [4]. Another such protease, heparanase, forms the topic of these studies.

1.2 Heparanase as a target

Metastasis accounts for 90% of cancer-related deaths in humans [1]. Metastatic tumour cells are able to degrade cell surface and extracellular matrix glycoproteins such as fibronectin and heparan sulphate proteoglycans, therefore breaching the endothelial cell layer and basement membrane to invade the target organ (ectopic site) [5-7]. They are able to do this by secreting enzymes, one of which has been identified and named heparanase (Hpa1) [8, 9].

1.2.1 Heparan sulphate

Heparan sulphate (HS) is a highly evolutionarily conserved molecule that is widely distributed on cell surfaces, extracellular matrices (ECM) and in basement membranes in mammals. It is a linear polysaccharide, expressed as a component of proteoglycan (PG) molecules [10].

A PG molecule comprises a core protein, to which two or three HS chains are covalently attached. There are two major proteoglycans found at the cell surface (figure 1.1): transmembrane syndecans with HS near the extracellular tips, and glycosylphosphatidyl inositol-linked (GPI) glypicans, with HS located near the plasma membrane. Agrin and Perlecan are two types of PG bound and comprising much of the ECM [10].

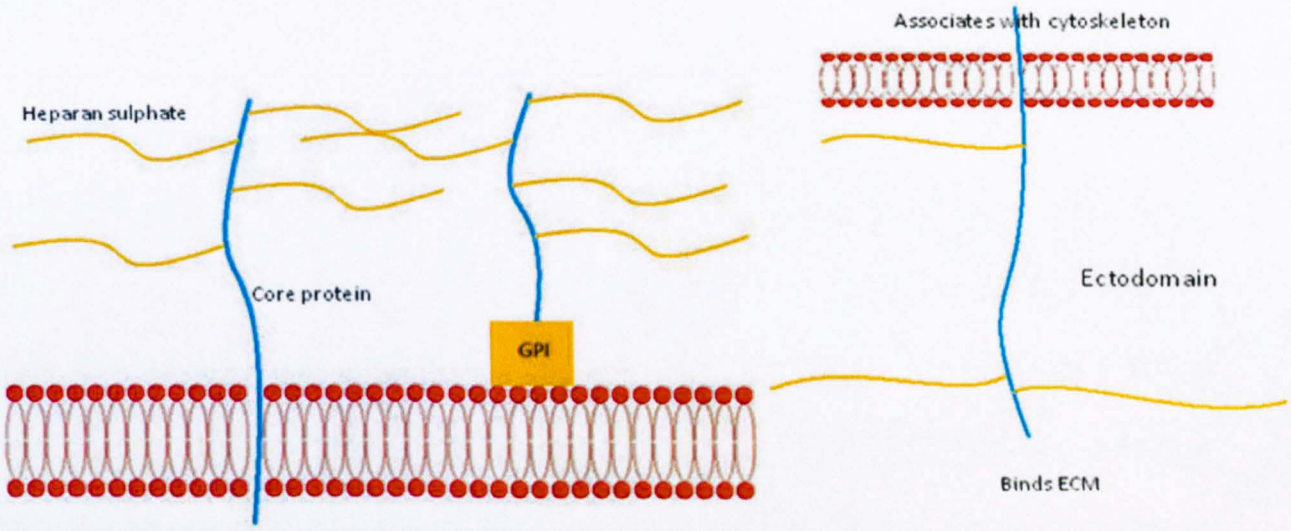

Figure 1.1 – Cell surface syndecans and GPI-linked glypicans (left) and ECM bound HSPGs (right). Core proteins are shown in blue, plasma membranes in red and HS chains in yellow.

HSPGs are synthesised in the Golgi system firstly by formation of a linkage region comprised of four sugars attached to a serine residue on the core protein [10]. The HS chains are elongated and modified, unit by unit, with alternating hexuronic acid and glucosamine residues [11]. Hexuronate can be either D-glucoronate (GlcA) or L-iduronate (IdoA), and the amine of the glucosamine is usually acetylated (GlcNAc), sulphated ($GlcNSO_3$), or unsubstituted [11], as shown in figure 1.2.

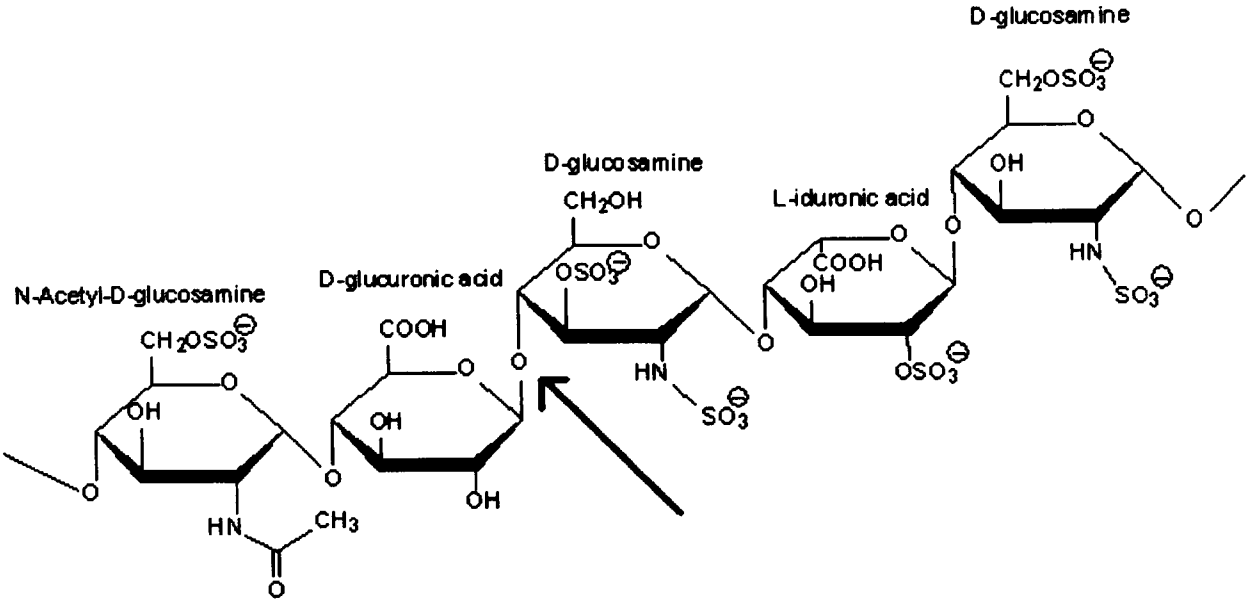

Figure 1.2 – A snapshot of a heparan sulphate chain showing different residues. The blue arrow indicates the site of cleavage of heparanase; between GlcA and GlcN. (Modified from [12])

In addition to their roles of anchoring cells and maintaining the structure of the tissue, HSPGs have major roles in development, homeostasis and protein regulation [13-15]. They are also able to protect the cell from cationic molecules and macromolecules, to bind and assemble ECM proteins such as laminin, fibronectin and collagen, to mediate interactions between numbers of different proteins by acting as co-stimulatory receptors, and to protect type IV collagen from proteolytic attack [16]. Cell-surface HSPG of endothelial cells are able to aid diapedesis and chemotaxis of leukocytes to sites of injury by interacting with selectins, together with activation and presentation of chemokines and interleukins to slow and attract the moving leukocyte so it 'rolls' along the cells' surface [10]. HS then activates and presents integrins to adhere and stop the rolling leukocyte, enabling it to migrate from the blood vessel into the injured tissue [10]. HSPGs also have an important storage role as they are able to bind many cytokines and growth factors [17] such as basic fibroblast growth factor (bFGF), vascular endothelial growth factor (VEGF), hepatocyte growth factor (HGF), keratinocyte growth factor (KGF),

transforming growth factor beta (TGF-β), interleukin-8 (IL-8) [18], interferon-γ (IFNγ) [19] and platelet factor 4 (PF4) [20].

1.2.2 Formation of Heparanase

Heparanase is a β-1,4-endoglycosidase enzyme which cleaves glycosidic bonds of heparan sulphate chains by hydrolysis to 10-20 sugar units long [21], between glucoronic acid (GlcA) and glucosamine (GlcN) [10], as seen in figure 1.2. Chromosome location of the human heparanase gene is at 4q21.3 [22]; represented as 14 exons separated by 13 introns, and encodes 543 amino acids, some of which are cleaved to form the active enzyme. Full length pre-proheparanase is shown in figure 1.3. It contains a 35 amino acid signal peptide sequence (Met^{1}-Ala^{35}), which is firstly removed upon entering the endoplasmic reticulum. It is then heavily N-glycosylated at six asparagine sites before being secreted, which is thought to have a role in kinetics of transport from the endoplasmic reticulum to the Golgi apparatus, and in secretion and solubility of the enzyme [23, 24]. Glycosylation is not thought to contribute to the enzyme's activity.

After being secreted as a 65KDa protein, proheparanase is transferred to late endosomes/lysosomes, sometimes via the cell surface, where it undergoes proteolytic processing at site 1: Glu^{109}-Ser^{110} and site 2: Gln^{157}-Lys^{158}, giving an 8KDa polypeptide at the N-terminus, a 50KDa polypeptide at the C-terminus, and a 6KDa linker polypeptide. The two larger polypeptides then associate non-covalently to form the active enzyme: a heterodimer [23, 25]. The fate of the linker peptide after its excision is unknown, although the hydrophobic Tyr^{156} is required for correct processing of the enzyme at site 2 [26].

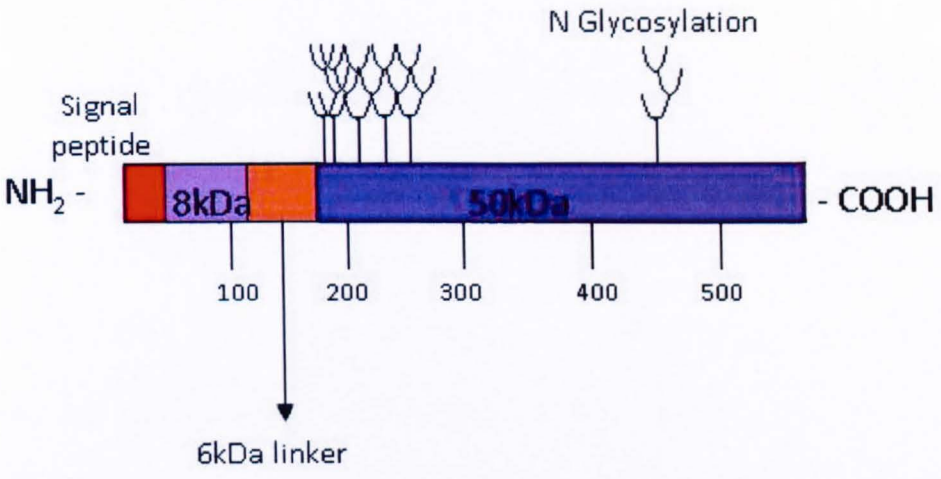

Figure 1.3 – A schematic diagram of pre-proheparanase showing N-Glycosylation sites (not to scale).

Investigations have revealed that cathepsin L is the most probable culprit of processing of proheparanase as in a cell line to which cell-permeable inhibitors of cathepsin L were added, heparanase remained inactive and in a cell free system, recombinant proheparanase was processed and activated by addition of cathepsin L [26].

Expression of Hpa protein correlates with expression of Hpa mRNA, suggesting that overexpression of the protein is regulated at the transcriptional level [27]. Cells with low heparanase mRNA expression were treated with an inhibitor of DNA methylation and expression of Hpa mRNA increased, although in the presence of cycloheximide (an inhibitor of protein synthesis) it had no effect, suggesting that de-methylation of transcription factors can regulate heparanase mRNA expression [28, 29]. Early growth response transcription factor [30], p53 [31], inflammatory cytokines [32] and hypoxia [33] are all responsible for regulation of heparanase gene expression. Notably, tumour variants of p53 are unable to bind to the promoter region of heparanase, hence were unable to suppress transcription [31]. Secretion of active enzyme was stimulated extracellularly, by activation of the protein kinase A (PKA) and C (PKC) pathways [34]. Formation and secretion of the heparanase protein in its latent form allows for tight regulation of its activity post-translation as well as at the transcriptional level.

Heparanase activity has been established when full length Hpa cDNA in a vector was transfected into mammalian cells and when the 65KDa proenzyme was added to mammalian cell cultures, which compared with no activity when just the 50KDa enzyme and cDNA were expressed, suggesting that just the 50KDa cDNA and enzyme are not sufficient for activity without the 8KDa subunit [25, 35]. However, when full length cDNA was expressed in insect cells, it resulted in low activity and expression, suggesting that proteolytic processing only occurs in mammalian cells [24].

Experiments have also shown evidence for heterodimer formation by means of a pull down assay, to demonstrate the physical association of both subunits and it has been found that the region Glu^{288}-Lys^{417} on the 50KDa subunit is the region which interacts with the 8KDa subunit [23]. It is not known what function the 8KDa peptide has as the active site and heparan binding domains are all found in the 50KDa subunit [24]. Attempts are being made to establish the minimum sequence from the 8KDa subunit needed for the enzyme to be fully functional by using site-directed mutagenesis; however, it is thought that complete removal of the linker peptide must be carried out for the enzyme to be fully active [24] as leaving only a 1kDa portion of it behind is sufficient to inhibit the activity of heparanase [36].

1.2.3 Heparanase Structure

Although a structure has not been determined for heparanase, the enzyme has been modelled on the structure of endo-1,4-β-xylanase as there is evidence that heparanase may be related to it in the family of clan A glycosyl hydrolases (GH-A), and the predicted structure is shown in figure 1.4 [37].

This group uses an acid catalysis mechanism for hydrolysing glycosidic bonds, using a proton donor and a nucleophile, and BLAST searches show similar sequences between heparanase and the xylanase family of enzymes [37]. The proton donor site in human heparanase is predicted to be Glu^{225} and the nucleophile, Glu^{343}. Site directed mutagenesis was carried out on these residues and this rendered the enzyme inactive, suggesting that the predictions were correct [37]. There are also 2 heparin binding domains present on the 50kDa subunit, located at Lys^{158}-Asp^{162} and Pro^{271}-Met^{278} [38]. These are predicted to reside closely to the proton donor and nucleophile sites to comprise the active site of the enzyme [37]. A peptide containing the Lys^{158}-Asp^{162} sequence showed binding of HS and subsequent inhibition of heparanase uptake and activity [38], suggesting that cell surface HS is another important regulatory factor responsible for uptake of secreted heparanase.

The structure prediction suggests that heparanase adopts a TIM barrel fold [37] shown in figure 1.4; comprised of six alternating α-helices and β-sheets from the 50kDa subunit and a further two α-helices and β-sheets from the 8kDa subunit [39]. Heparanase is currently being subjected to x-ray crystallographic analysis at Imperial College, London, to determine its structure.

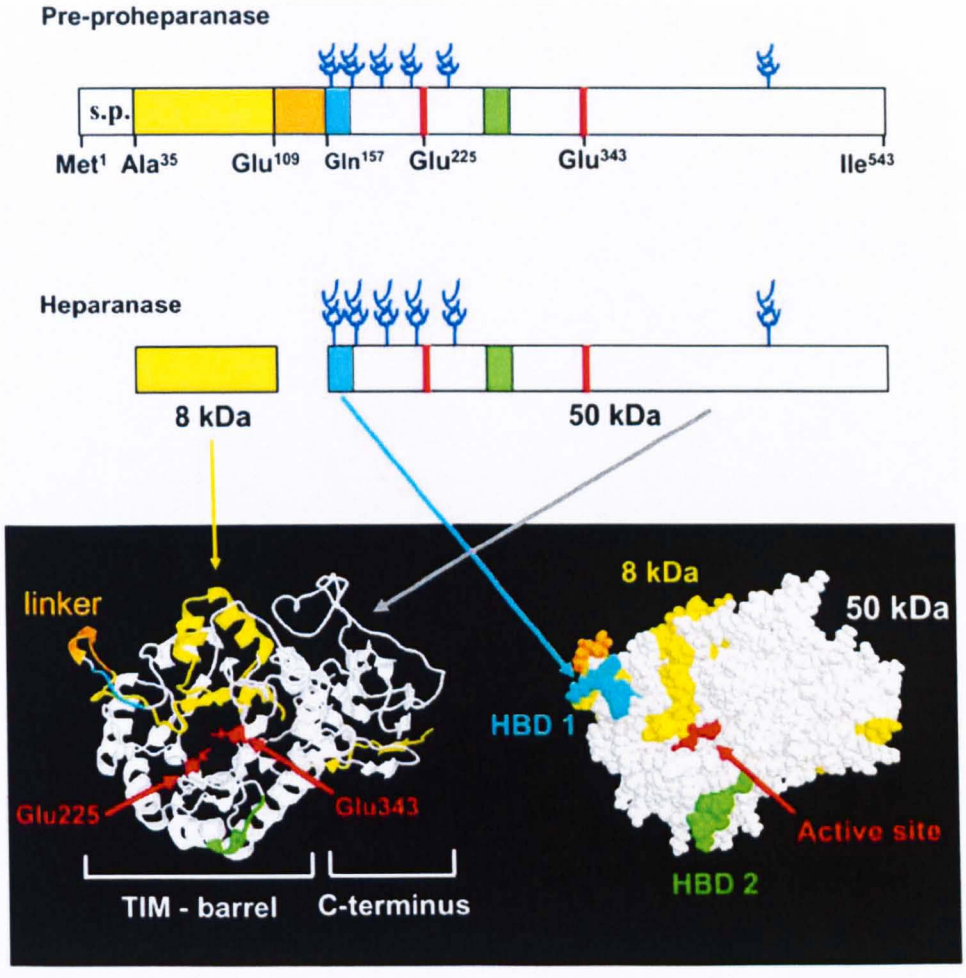

Figure 1.4 – A structural diagram of human heparanase (Hpa1) from [36]. Balls and sticks represent the predicted proton donor, Glu225 and nucleophile, Glu343.

1.2.4 Heparanase Activity

Heparanase activity has been seen in activated leukocytes, mast cells and macrophages and is secreted by activated $CD4^+$ T cells [40-42], platelets [43], neutrophils and metastatic tumour cells [44].

Heparanase secreted by metastatic tumour cells targets heparan sulphate proteoglycans in the basement membrane of blood vessels for degradation, leading to an increase in permeability of the target cell and allowing the tumour cell to penetrate it (shown in figure 1.5). By degradation of the basement membrane, heparanase is also responsible for the release of the once-bound bioactive molecules in stimulating movement and

proliferation of endothelial cells to the site of angiogenic stimulus, hence promoting neovascularisation.

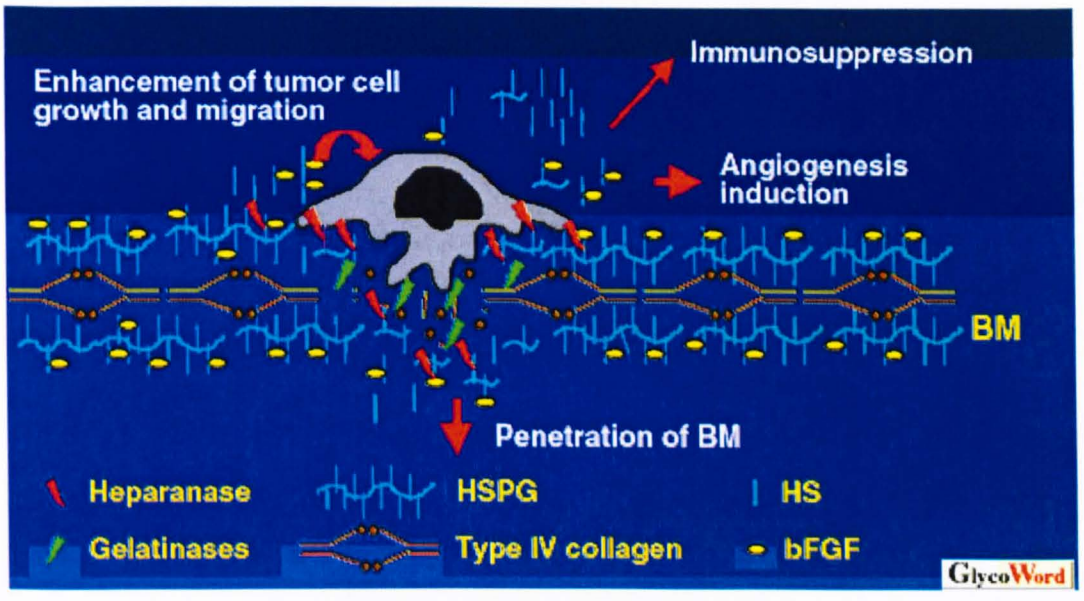

Figure 1.5 – Degradation of the basement membrane by an invading tumour cell (taken from [45]).

High levels of heparanase expression in tumour cells correlate with their metastatic potential, i.e. their ability to progress through the ECM and basement membrane [8]. Heparanase mRNA expression is also increased in tumour sites compared with surrounding healthy tissues [46]. Many groups have reported positive correlations between high heparanase expression and tumour size, stage, classification, vascularisation, postoperative and metastatic recurrence and poor prognosis. In some models, fragments of degraded heparan sulphate have been seen to down-regulate T cell functions [45].

Elevated levels of heparanase mRNA and protein have been found in cancer patients, who show significantly shorter postoperative survival times than patients without elevated Hpa mRNA levels [27, 47]. In experiments using non-metastatic lymphoma cells transfected with either chicken (secreted form), human (not so readily secreted form), or chimeric (human enzyme with chicken signal sequence) heparanase, it was found *in vitro*

that the chicken and chimeric heparanases showed a 3-10 fold increase in invasion of a reconstituted basement membrane compared to human and control heparanase transfected cells, suggesting that cell surface expression and secretion of heparanase facilitates lymphoma cell invasion through basement membranes [48]. Mice injected with chicken or chimeric heparanase showed accelerated mortality compared to mice injected with human heparanase, without the primary tumours exceeding 1% of their body weights, suggesting that they died because of the high level of metastasis found in the liver. Control mice, with no transfected heparanase showed no infiltration of tumour cells into the liver, emphasising the importance of cell surface expression and secretion of heparanase in tumour metastasis. High vascularity and vessel density and functionality of tumours in mice transfected with chicken and chimeric heparanase was also observed, when compared to human transfected and control mice, supporting the theory that heparanase also causes angiogenesis [48].

In addition to these well known effects, heparanase is also known to have other roles in tumour progression, including activation of signalling molecules that promote cell proliferation and survival, and increasing cell motility and blood vessel density [36]. Heparanase upregulation correlates with increased phosphorylation and activation of signalling molecules Akt [49], p38 [50], Pyk2, integrins and Src [50]. Vascular endothelial growth factor (VEGF), a vasculogenesis promoter, has shown to be activated by Src and latent or active heparanase [50]. Interestingly, Src inhibitors prevented VEGF activation by heparanase in addition to heparanase-enhanced cell migration, suggesting that Src and its inhibitors may be able to mediate heparanase functions too [50].

Heparanase enzymatic activity is dependent on the pH of the local environment [42]. *In vitro* experiments have shown that at pH 3.4 heparanase remains inactive, at pHs greater than 6.8 or less than 5.4 there is low activity, but for slightly more acidic than

physiological pHs 5.4, 6.4 and 6.8, there is a maximal release of degraded heparan sulphate, with an optimum pH of 6.0 [42, 51, 52]. This correlates well with the conditions *in vivo*, where cleavage of HS occurs in the slightly acidic pH areas of inflammation and in tumours [42, 53]. Heparanase was found to be inactive at pH 8.5 and above [10].

Single nucleotide polymorphisms (SNPs) of heparanase have been investigated [54]. Among them, a G to A polymorphism in exon 8, which provides an amino acid substitution of arginine for lysine at site 307, has been shown to have no significant effect on FIGO (Federation of Gynaecology and Obstetrics) classification of stage of disease [54]. However, a polymorphism in intron 2, which shows a substitution of T for C is significantly associated with stage of disease, even though it does not directly change the sequence of pre-proheparanase [54]. It is thought that through moderation of protein binding to this region, the SNP could affect splicing of areas concerned with signal peptide or activation cleavage, or that it could be in association with another SNP with a more functional role in heparanase protein sequence [54].

It has been suggested from the evidence that heparanase plays a crucial role in invasion of a target organ by metastatic tumour cells, also that it promotes angiogenesis from the release of sequestered growth factors, hence allowing the tumour cell to proliferate. Furthermore, heparanase expression has been implicated in a number of different cancers, for example, acute myeloid leukaemia [55], bladder [56], brain [57], breast [58], colon [59], gastric [60], oesophageal [61], oral [62], and pancreatic [27, 63, 64]. This, together with its practical advantages of solubility, being a secreted enzyme (hence facilitating its manipulation in the laboratory) and its availability as an active, recombinant enzyme expressed in insect cells, suggests that this enzyme may be a very exciting target for drug therapy.

1.2.5 Heparanase Inhibitors

Heparanase has been the target for a number of drug development efforts. Current inhibitors of heparanase include various mono- and polyclonal antibodies [65, 66], heparin [67], laminaran sulphate [48], phosphomannopentaose sulphate (PI-88) [68, 69] and suramin [70].

The inhibitor PI-88 is one of many sulphated oligosaccharides which have been shown to inhibit heparanase activity, and is a structural mimic of heparan sulphate [69]. In an *in vitro* angiogenesis assay system, testing a number of different oligosaccharides of which the results are represented in figure 1.6, PI-88 has been found to inhibit human angiogenesis by 50% at a concentration of 2μg/ml, showing a 25-fold increased inhibitory activity than suramin; which has entered clinical trials for its antiangiogenic properties [69]. Further investigation of PI-88 showed inhibition of tumour metastasis by >90% in high doses of 16-32mg/kg and by 50% in lower doses of 2mg/kg [69]. The drug has entered phase II clinical trials in combination therapies with other drugs, under Progen Pharmaceuticals Limited, for treatment of prostate cancer, metastatic myeloma, advanced lung cancer, primary liver cancer, advanced melanoma and multiple myeloma [71, 72].

The nature and length of the oligosaccharide backbone have shown to be important, as oligosaccharides composed of more than 4 monosaccharides have the highest inhibitory activity, but sulphonated cyclohexa, hepta and octaamyloses and sulphated chondroitin tetra, hexa and octasaccharides displayed little or no inhibitory activity respectively [69]. Experiments testing heparanase inhibition found a similar scenario where the length and nature of the oligosaccharide backbone affected the degree of inhibition and that PI-88 and maltohexaose sulphate were the most potent inhibitors. Results of an *in vitro* study

to test the antimetastatic activity of the oligosaccharides further confirmed this observation [69].

Heparin, which has been used in the clinic as a potent anticoagulant for more than half a century and is similar in structure to HS, showed no antiangiogenic properties in the same assay, although showed the most promising inhibition of heparanase; with an IC_{50} of 1μg/ml [69].

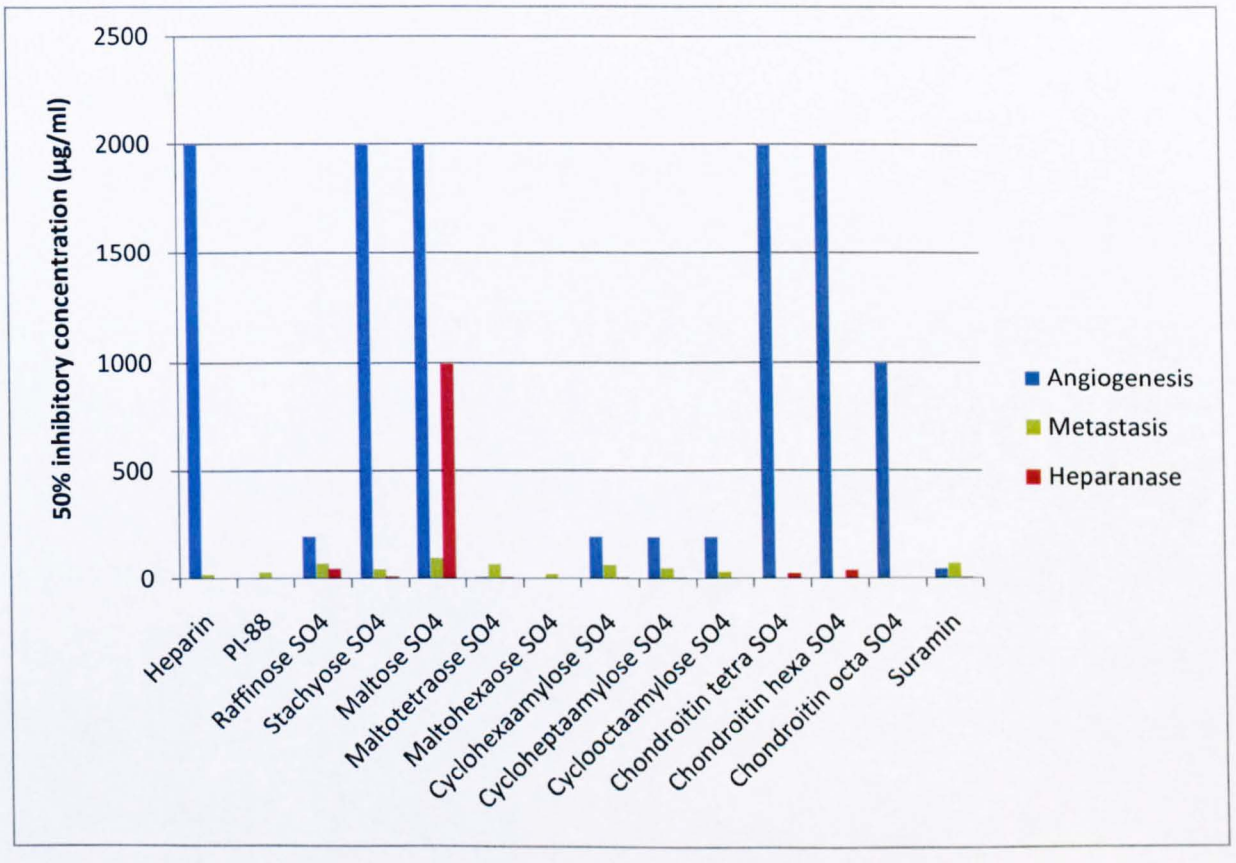

Figure 1.6 – 50% inhibitory concentrations (μg/ml) for angiogenesis, metastasis and heparanase inhibition of different sulphated oligosaccharides in comparison with heparin and suramin. Data from [69].

(R)-3-hexadecanoyl-5-hydroxymethyltetronic acid (RK-682) has been found to inhibit heparanase activity by directly binding to the enzyme, among other enzymes, and it has been found that by benzylation of the 4-position of RK-682 it is able to selectively inhibit heparanase only, with a 50% inhibitory concentration of 17μmol/L, which is comparable to other inhibitors found to date [73].

Another class of heparanase inhibitor are derivatives of furanyl-1,3-thiazol-2-yl and benzoxazol-5-yl acetic acids, which after optimisation, yielded (2-{4-[(E)-3-(4-bromophenyl) acryloylamino]-3-fluorophenyl} benzooxazol-5-yl) acetic acid, and showed an IC_{50} of heparanase inhibition of 0.4μM, an IC_{50} of angiogenesis of 1μM and after introduction into mice, displayed improved solubility, modest cell penetration and did not inhibit cytochrome P450 enzymes [74].

In an experiment linking heparanase with restenosis (re-occurrence of narrowing of blood vessel or organ) by release of bFGF from heparan sulphate chains in the ECM, an anti-heparanase IgG was found to inhibit bFGF release by 60% [66]. And in a cell invasion assay, another heparanase polyclonal IgG antibody reduced the invasiveness of an ovarian carcinoma cell line by up to 95% in a dose-dependent manner [65]. However, as with all antibodies, the prospect of using them as potential therapeutics is difficult as due to their large size, they are easily recognised as 'non-self' and destroyed by the immune system before being able to carry out their function. For this reason, aptamers have been chosen as the focus of this study, due to their superior binding properties in terms of specificity and selectivity, lower molecular weight and non immunogenic properties.

1.3 What are aptamers?

Aptamers are short oligonucleotides, which can be single or double stranded DNA or RNA. They have been developed for diagnostic and therapeutic uses and are characterised by high binding affinity and specificity to their target molecules [75-77]. Typically, aptamers can be from 22 to 100 bases (or base pairs) in length, and carry two distinct regions: a region of fixed sequence, used for amplification and identification purposes; and a

variable region, for which each base could potentially be an A, C, G or T/U. This creates a large number of different sequence combinations, typically in the region of 10^{15}, which is responsible for the different folding arrangements, specificities for different molecules, and binding affinities of the aptamers. Aptamers can be generated against small molecules, purified peptides and proteins, and even against cells and tissues, which allows for the target to remain in its native environment and conformation [78, 79], although it is more difficult to establish optimal conditions and there is more chance of experiencing non-specific binding or selecting aptamers against unwanted targets, due to the complexity of such environments. The affinity of aptamers has been compared to that of antibodies (i.e. in the nanomolar range), but as aptamers are mostly smaller (8-15kDa compared to 150kDa), they can penetrate tissues and be cleared from the system quicker than antibodies, which can be useful in diagnostic and imaging applications [78]. Being cleared from the plasma within minutes of intravenous administration is also a disadvantage, when using aptamers in the treatment of disease, as a suitable concentration cannot be maintained in the body without constant dosing; hence it is often important to modify the aptamers without affecting their activity before they can be used effectively in this way [80].

1.3.1 How are aptamers produced?

Aptamers are primarily produced based on the SELEX (Systematic Evolution of Ligands by EXponential enrichment) procedure [81] (figure 1.7) where the target is immobilised on a matrix, aptamer library solution is incubated with it, so that the different sequences effectively compete for binding with the target, unbound aptamers are removed by introducing wash steps, and finally, bound aptamers are removed by using a solution with

a high salt content or by heating them to a high enough temperature to denature the target, thus releasing the aptamers. The binding aptamers are then amplified by PCR. Typically, this procedure is repeated over many (usually ten) rounds, so that the amplified aptamers are incubated with the target molecules again, creating many copies of the aptamer sequences with the highest affinity, and removing the ones with lower affinities; hence the term: 'exponential enrichment'. Matrices used can be columns packed with sepharose containing a coupling reagent such as N-hydroxy-succinamide (NHS), which couples the N-terminus of proteins and peptides, nitrocellulose filters, or 'ELISA type' PCR tubes, which encourage protein binding. The SELEX procedure has been modified by many groups [78, 82-85], and some groups have even developed non-SELEX procedures to yield aptamers [86-88], however, the underlying principle remains the same.

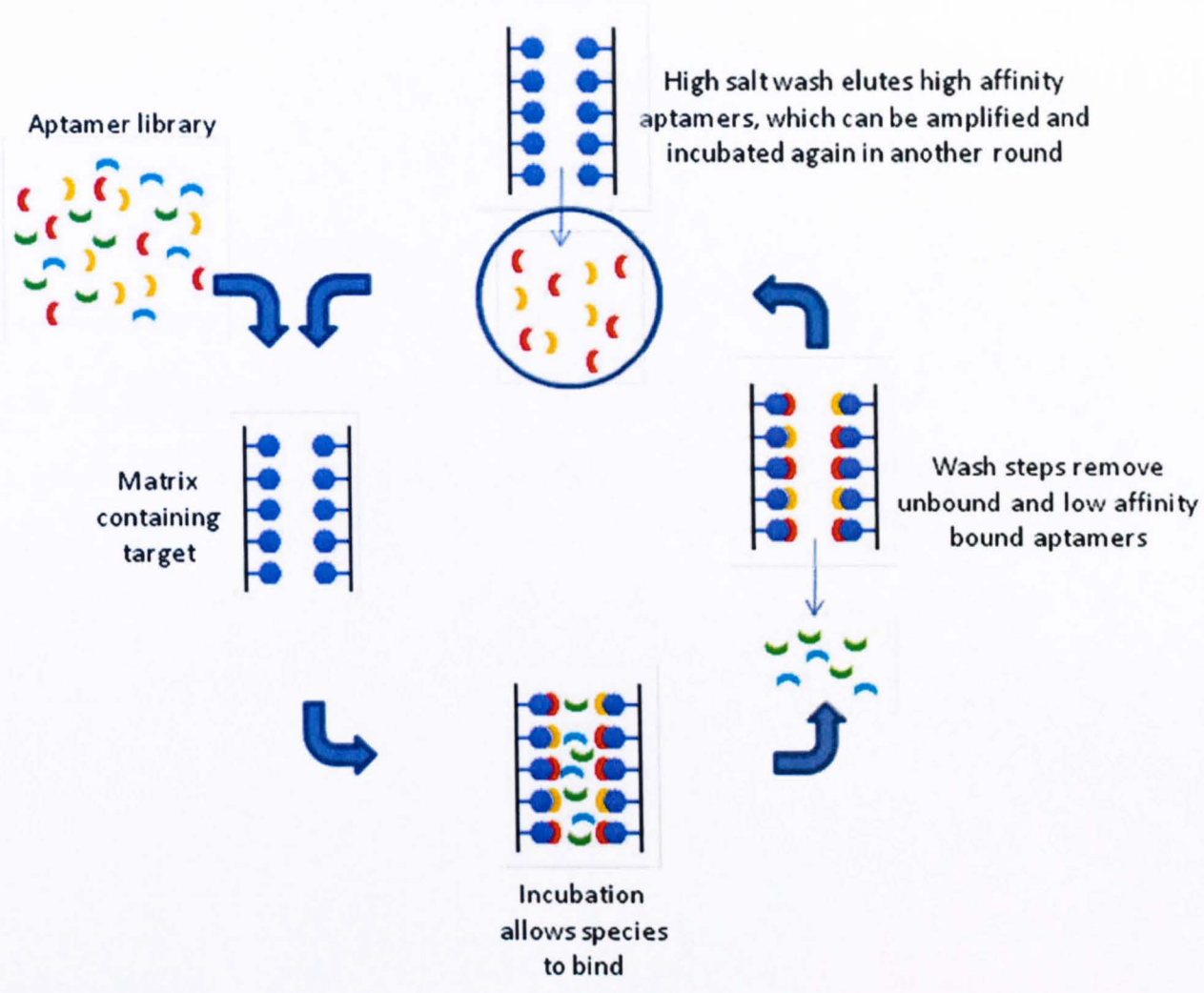

Figure 1.7 – A diagram of one round of SELEX-type selection. Eluted aptamers can be amplified and incubated again to enrich the pool with high affinity species. Rounds can be repeated for a number of times (usually 5-10) before adequate enrichment is achieved to result in only a few high-affinity and specificity binding species.

1.3.2 Structures of aptamers

Aptamers are often GC rich, so are able to form complex three-dimensional structures. Their folding allows them to maximise hydrogen bonding with complimentary bases, by utilising Watson and Crick binding sites, similar to double stranded DNA. In addition to utilising Watson and Crick binding sites, the formation of G-quadruplex structures (see figure 1.9) requires Hoogsteen hydrogen bonding sites, which are critical to the stability of tetrads.

These interactions result in the formation of hairpin loop (see figure 1.8 for an example) and G-quadruplex structures, which are both highly stable. Folding of the aptamers in this way is another characteristic which contributes to their high affinity and specificity. Groups have manipulated these characteristics by creating highly stable DNA aptamers to thrombin [89] using natural nucleotides to avoid potential toxic degradation products, only by circularisation of the exposed termini of the aptamers so they do not become susceptible to degradation by plasma exonucleases [89].

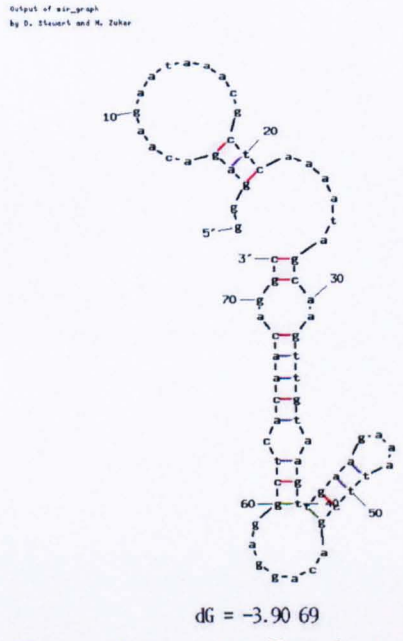

Figure 1.8 – Predicted structure of an aptamer sequence showing its folding to maximise hydrogen bonding with complimentary bases. In doing so, this has created many hairpin loops within the structure and is therefore highly stable [90].

Also, the aptamer AS-1411 to nucleolin is an unmodified 26nt DNA aptamer, which is not subject to nuclease resistance through the formation of the G-quadruplex structure [91, 92].

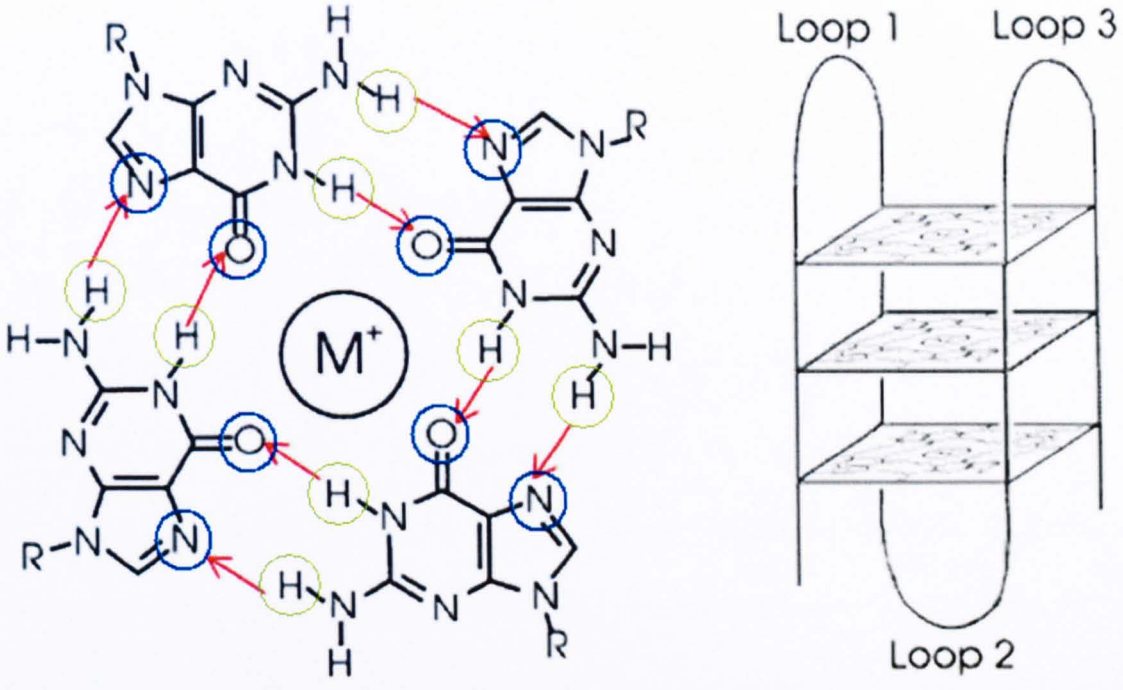

Figure 1.9 - Formation of G-quadruplex structure showing the basic unit or tetrad (left) containing the monovalent metal ion in the centre for further stability. Hydrogen bonding acceptors and donors are shown by the red arrows, Watson and Crick binding faces are shown in green and Hoogsteen in blue. Tetrads then stack on top of each other to form the G-quadruplex (right). Images were modified from [93].

1.3.3 Modifications to the aptamer

It is well known that the bloodstream contains many nucleases, and that an aptamer in its native state administered intravenously into the body, would be rapidly broken down in the bloodstream and the liver, and excreted within minutes through the kidneys. This is a useful property in cancer diagnostics or imaging studies, because any circulating aptamers are rapidly eliminated from the system, leaving only the aptamers that are bound to the disease site present, thus reducing any background interference. This property, however, is not useful in therapeutic applications, because a constant level of drug has to be maintained within the body for long periods of time. Most drugs require doses only once or twice a day, whereas unmodified aptamers would require doses on a smaller timescale

or continuous drip, with more than 90% of the molecules excreted without ever having the opportunity to exert their therapeutic effect, making them very inconvenient and expensive.

To overcome this adverse characteristic, aptamers would need to be appropriately modified. However, one very useful property of aptamers is that they can be readily coupled with other moieties and modified appropriately to suit any application.

Aptamers can be truncated by carrying out tests to determine the minimum sequence required to carry out their function, and removing the unnecessary bases. Groups on purine or pyrimidine bases can be replaced with amino, methyl or fluoro groups (2'-NH_2, 2'-OCH_3, 2'-F), or inverted bases to confer nuclease resistance [78, 94, 95]. Furthermore, aptamers can be coupled to large molecules, for example, polyethylene glycol (PEG) [96], a polymer with varying molecular weights (this can also be with or without a radionuclide) at their 5' or 3' end [97, 98]. This is designed to improve stability, solubility and reduce toxicity and plasma clearance. Another large molecule that has been used is a diacylglycerol (DAG) molecule, a dephosphorylated glycerol-3-phosphate molecule with 2 fatty acid chains attached, which can then also be incorporated into a liposome. This also reduces plasma clearance, as the liposome has a large molecular weight, and the liposome can also be filled with a cytotoxic drug, for example, Cisplatin [99].

Finally, aptamers are currently being developed in nuclear medicine applications for diagnosing abnormalities in tissues and organs, offering the possibility of early stage detection of cancer and other diseases. Using a chelator, radionuclides such as ^{99}Technetium and ^{188}Rhenium can be attached to aptamers designed to bind to a particular target of interest, thus making them suitable for gamma camera imaging [100].

1.3.4 Administration of aptamers

Of the three aptamers that have entered clinical trials, only one has been approved for therapeutic use. This anti-VEGF aptamer; Pegaptanib, was originally designed to treat cancer, but was found to be more promising in treating age-related macular degeneration (AMD) and involves administration directly into the eye by intra-vitreal injection [101]. The remaining two aptamers, an anti-nucleolin aptamer named AS1411, developed by Antisoma has entered phase I clinical trials for treatment of renal and non-small cell lung cancers, and acute myelogenous leukaemia [102] and an aptamer developed by Archemix; ARC1779, which inhibits platelet aggregation and thrombosis by inhibiting the action of von Willebrand Factor (vWF) [103]; are both administered intravenously.

1.3.5 Aptamers as therapeutics

Aptamers have been developed for use as cancer therapeutics against many targets involved in pathways leading to cell growth, proliferation and angiogenesis and are in various stages of development.

To date, there is only one aptamer developed for the treatment of cancer in clinical trials. This aptamer has been developed by Antisoma, and binds to nucleolin, a ubiquitous protein expressed in the nucleolus and on the cell surface of proliferating cells, and overexpressed in malignant cells in cancers such as prostate, cervical and breast [91, 92]. The aptamer is unmodified; however it is G-rich and adopts a dimeric G-quadruplex formation which confers nuclease resistance. Once bound to nucleolin, the complex is internalised and causes arrest of cell division in S phase, leading to apoptosis of the

tumour cells [91]. This is thought to occur by inhibition of helicase activity in the replication fork and subsequent inhibition of DNA replication [92].

Vascular endothelial growth factor (VEGF) is a protein involved in the production of *de novo* blood vessels (vasculogenesis), as well as angiogenesis and in increasing the permeability of microvessels [95]. VEGF has a number of different splice variants, $VEGF_{121}$, $VEGF_{145}$, $VEGF_{165}$, $VEGF_{189}$, and $VEGF_{206}$, correlating with the number of amino acids in the protein. VEGF is the substrate for tyrosine kinase receptors, which are thought to lead to angiogenesis, and, although the exact mechanism it has in the promotion of tumours is unclear, overexpression of VEGF in people with tumours is associated with poor prognosis [95]. A PEGylated anti-VEGF aptamer was the first aptamer to reach clinical trials and be used as an approved therapeutic, but although it was developed originally to treat cancer, it has not been approved for this use, but instead for the treatment of age-related macular degeneration (AMD) [104] in order to avoid issues related to systemic administration. The aptamer is injected intravitreally and binds to the $VEGF_{165}$ variant, preventing vascularisation of blood vessels and progression of AMD.

VEGF was also the target used by Ruckman *et al.*[95]. RNA aptamers were generated against the $VEGF_{165}$ form and modified to make them as small as possible. Their K_D's ranged from 49-130pM. They specifically bound to this form and did not bind to $VEGF_{121}$ or the closely related placental growth factor ($PlGF_{129}$), and showed promise in inhibiting the binding of $VEGF_{165}$ to its receptors VEGFR-1 and VEGFR-2. One aptamer in the study had the ability to reduce VEGF induced vascular permeability *in vivo* using the Miles assay [105].

Basic fibroblast growth factor (bFGF) is also a potent angiogenic factor [94, 106] and belongs to a family with at least eight other members [106-108]. Jellinek *et al.* [94]

produced a 2'aminopyrimidine modified RNA aptamer to bFGF with a K_D of 35nM. The modification ensured that the aptamer was 1000-fold more stable in 90% human serum than an unmodified version [94]. Binding studies carried out on the aptamer to denatured bFGF and other members of the FGF family; acidic FGF, FGF-4, FGF-5, FGF-6 and FGF-7 plus four other heparin binding proteins, showed considerably lower affinity, ranging from $4.1x10^{-2}$ to $>10^{-6}$M [94]. In a cell culture system, the aptamer inhibited bFGF binding to the FGF receptor 1.

Platelet derived growth factor (PDGF) is another protein responsible for regulating cell growth and division. There are five known ligands: PDGF-A, B, C, D and an AB heterodimer; and two receptors PDGFRA and PDGFRB, which are tyrosine kinase receptors (RTK's). This is part of the phosphatidylinositol 3-kinase (PI3-K) pathway [1, 109], and activates protein kinase B (PKB) which is involved in mediating cell survival signals, and protein kinase C (PKC) [1, 109]. PDGF-B has been implicated in many renal diseases and it is thought to induce glomerular mesangial cell proliferation and matrix accumulation [110]. A DNA aptamer was produced to target PDGF-B, and coupled with 40kDa PEG for stability *in vivo* [96]. Treatment *in vivo* of a rat with initiated mesangioproliferative glomerulonephritis on day three of the disease with the PEG coupled aptamer, reduced overexpression of PDGF-B in mesangial cells, and arrested mesangial cell proliferation [96].

Raf-1 is a serine threonine kinase – the first in the mitogen activated protein (MAP) kinase cascade, which is activated by a chain of events from the receptor tyrosine kinase (RTK), leading to cell growth and proliferation [1, 109]. Raf-1 is activated upon binding of Ras to the Ras binding domain (RBD); amino acids 51-131 of Raf-1. Ras binds to Raf-1 with an affinity of 18nM [111-113]. Using only the RBD of Raf-1 for selection, RNA aptamers were produced, which were all similar to one of two different sequences; RNA 9A and 9B. The

two sequences showed binding affinities of 152 and 361nM respectively [114] for the RBD of Raf-1 [114]. In a competition experiment, the addition of the two aptamers significantly reduced Ras binding to the RBD of Raf-1. RNA aptamer 9A also bound to a GST fusion form of Raf-1 RBD; B-Raf RBD, with an affinity of 285nM, but in the competition experiment it showed specificity for RBD of Raf-1 and did not inhibit the interaction between Ras and B-Raf RBD [114]. It was found that RNA 9A and B inhibited the Raf-1 activation reaction in an experiment using full length Raf-1, but that addition of the aptamers after the activation reaction had occurred provoked no inhibition by the aptamers [114], suggesting that the aptamers function as inhibitors of the activation reaction and not to Raf-1 itself. These experiments showed that the most potent aptamer, RNA 9A, could be a useful regulatory drug for mediating Ras and Raf-1 interactions in cells, therefore influencing cell growth and proliferation.

Angiogenin is another molecule involved in angiogenesis and cell proliferation [115]. It is a ribonuclease which is thought to become active when it translocates to the nucleolus of the cell [116, 117]. DNA aptamers were produced, which showed inhibition of angiogenin's ribonucleolytic activity by >50% when present in a threefold excess [118]. The aptamer was then truncated and tested for specificity by observing its effect on RNase A (another ribonuclease which is 33% homologous to angiogenin) for its substrate poly(C), to which there was no significant inhibition, showing that the aptamer was specific for angiogenin [118]. In an assay with human endothelial cells, it was found that the aptamer inhibited angiogenin induced cell proliferation by 65% at a concentration of 1μM and by 100% at 5μM, although not inhibiting, rather cotranslocating with angiogenin to the nucleus [118].

The production of aptamers has been of use in isolating a protein thought to be a marker for angiogenesis, by selecting against microvessels of rat glioma [119]. SELEX was carried

out on transformed endothelial cells to produce the single stranded DNA aptamers. One aptamer selectively bound to microvessels of rat brain glioblastoma, but not to normal vessels in the rat brain [119]. This aptamer was used to identify its specific target, which was found to be a rat homologue of mouse pigpen protein, and thought to contribute to angiogenesis, although little else is known about this protein. This aptamer served as a useful probe, and could be developed further as a therapeutic measure to treat glioblastoma *in vivo* [119].

1.3.6 Aptamers as diagnostics

A number of aptamers have also been developed for diagnostic applications, due to their inherent properties.

RNA aptamers have been produced that bind to protein kinase C with the intention of investigating their role in signal transduction pathways other than those involved with phospholipid hydrolysis [120]. Aptamers were used because of their substrate specificity in the hope that they would inhibit one enzyme but none of the others with high sequence homology. An RNA aptamer selected against protein kinase C βII showed a K_D of 7nM, and exhibited one order of magnitude lower potency for protein kinase C βI, which is 96% homologous to the βII isozyme [121], and showed no potency for the α isozyme [120].

Another way in which aptamers have been used as diagnostic agents is exemplified by the aptamer produced against neutrophil elastase to provide a useful imaging tool [122-124]. Neutrophil elastase is a serine protease which can degrade a variety of proteins, including connective tissue, and is found in the granules of neutrophils. When there is infection and inflammation in the body, neutrophils are recruited to the site [125-127], whereupon

they release their granules, and hence, neutrophil elastase [128]. This is thought to be a good marker of inflammation as neutrophil elastase is highly localised in the site of inflammation by a protease inhibitor α-1 [127, 129-131]. Aptamers were generated that showed a rate constant of 1-3 x $10^8 M^{-1} min^{-1}$ for neutrophil elastase [122, 123, 132] and were shown by flow cytometry to bind preferentially to activated neutrophils. The aptamers were tested for their imaging properties *in vivo* in a rat model and it was found that, compared with an anti-elastase IgG (which is the method clinically used), not only was the overall intensity higher, but the background signal was lower, all over a shorter time period [122, 123]. This is due to the rapid clearance that the aptamer has from the blood because of its smaller size, and minimal perfusion into the surrounding tissues. The results showed that aptamers could be a viable alternative in imaging compared to antibodies [122, 123].

An anti-MUC-1 aptamer is also in developent for diagnostic imaging in breast cancer [100] by conjugation to ^{99m}technetium via chelator MAG2, and has shown high resistance to nuclease degradation and high renal clearance and therefore, less toxic effect.

The field of biosensors coupled with aptamers has recently developed due to the huge potential of biosensor development in point of care (POC) applications and the ability of aptamers to fulfil some of the requirements for such applications [133]. The majority of the methods developed so far have been based on the 15 nucleotide aptamer to Thrombin [134], as this has been well characterised in terms of structure and binding and has used as a model system. This aptamer adopts a G-quadruplex structure comprised of two tetrads connected by T-T or T-G-T loops and has been used in a number of electrochemical sensors, for example, faradic impedance spectroscopy (FIS), measuring changes in the electron transfer resistance upon binding of target to aptamer [133, 135].

Other targets used for aptasensors include a biotinylated aptamer for Immunoglobulin E to detect atopic diseases such as asthma and dermatitis; used in an electrochemical device by an extravidin-alkaline phosphatase label [133], as well as in surface plasmon resonance imaging (SPRi), in combination with carbon nanotubes using field-effect transistors (FET) and in a piezoelectric quartz crystal microbalance device [135].

DNA aptamers selected for platelet-derived growth factor (PDGF) were selected for use in an electrochemical biosensor using non-faradic impedance spectroscopy, showing a detection limit of 40nM; as was an aptamer selected for interferon-γ, which was able to detect the target down to a level of 1pM [133].

Both Cocaine and 17-β estradiol aptamers have also been used in electrochemical detection systems and measured using a redox reaction; the detection limit of 17-β estradiol being 10pM [133].

1.3.7 Modifications to the selection procedure:

Extracellular signal-related kinase (ERK) is the third protein in the MAP kinase cascade. It is activated downstream of Raf-1 by MEK, and once activated, it can also lead to cell proliferation and differentiation [1, 109]. Bianchini *et al.* [82] wanted to shorten the length of time taken to run selection, whilst still yielding high affinity binding aptamers, and used a process with only two selection steps against the target, ERK2. The first selection step utilised a synthetic peptide target corresponding to a fragment of ERK2, which contained the two phosphorylation (and therefore, activation) sites, T^{183} and Y^{185} [136]. After PCR amplification of the bound product, the target was then 'switched' [83, 84] to an extract of proteins from a cell line, containing the full-length ERK2 protein. The amplified products were incubated with this, and separated on a nitrocellulose

membrane to yield ERK2 specific polyclonal aptamers, which were then amplified by PCR and cloned. After screening of clones, an aptamer was found to selectively inhibit ERK2 with a binding affinity of 63nM [82].

A problem that White *et al.* [85] attempted to overcome with selecting RNA aptamers for Thrombin was cross-reactivity between different species. When an aptamer is selected using a protein target derived from an animal model and tested in the same model, it may show high affinity and specificity. However, it may not exhibit the same properties when tested in humans, unless the protein is very highly evolutionarily conserved, risking failure in clinical trials [85]. Using a modified SELEX procedure, they hoped to overcome this by alternating porcine and human thrombin as the target in each SELEX round. Thrombin is a serine protease which acts as a coagulation protein by converting fibrinogen into fibrin and by activating other reactions in the coagulation cascade. It has been suggested that it also has a role in cellular proliferation after damage occurring to the vascular system [85]. This method of SELEX removed non-binding aptamers and aptamers that only bound to one of the two targets, leaving high affinity aptamers, which bound to both targets, and were then truncated to 25 nucleotides in length. One truncated RNA aptamer bound to human thrombin with a K_D of 0.54±0.1nM and porcine thrombin with a K_D of 1.4±0.3nM, showing that this method not only angled the selection process towards the more evolutionarily conserved region of the target, but that, in doing so, no compromise was made on the affinity for either target, as the aptamer bound to both with a very high affinity [85].

Tenascin-C (TN-C), an extracellular matrix glycoprotein which is overexpressed during tissue remodelling, including tumour growth, was a target for Hicke *et al.*[78]. Recent evidence has shown that the fibrinogen-like domain of TN-C may bind to a critical integrin involved in angiogenesis, $\alpha_v\beta_3$ [137], and that expression of TN-C in tumours correlates

with poor prognosis. Hicke *et al.* used a method of 'target switching' between purified protein and cell SELEX on TN-C expressing U251 glioblastoma cells, to generate aptamers to TN-C [78]. The reasons behind this were to exploit the advantages of easy and rapid selection on purified proteins, and expression of the protein in its native state in cell SELEX. This would ensure that the enriched aptamers recognise and bind to both the purified and native protein, and would make testing *in vitro* and hopefully *in vivo* more successful. A 13kDa aptamer was produced and then modified by substituting 15 of the 19 purines with 2'-OCH_3 groups to ensure it was more stable against nucleases. It then showed a binding affinity of $5x10^{-9}$M with the fibrinogen-like domain of TN-C, potentially interfering with the binding to $\alpha_V\beta_3$ and hence, angiogenesis.

Aptamers have also been produced using non-SELEX methods. Berezovski *et al.* [86-88] developed equilibrium and nonequilibrium capillary electrophoresis of equilibrium mixtures (ECEEM and NECEEM). NECEEM attempts to overcome the problems of the heterogeneous methods of selection described above, where the target is immobilised to a solid phase, as this is quite often expensive, time-consuming and unreliable as not only non-specific binding of ligand to the surface may be experienced, but by immobilising the target to a solid phase, it may change its conformation [86-88]. These techniques are carried out by incubating the aptamers and target to obtain an equilibrium mixture, which is then injected into a capillary and run under electrophoresis to remove unbound aptamers and secondly, to measure the fraction of aptamer·target complexes and dissociated aptamers from these complexes. These methods not only simplify the selection procedure by carrying it out in one round, but allow simultaneous calculation of K_d and K_{off}, and has the potential to be automated to become of even more use [86-88].

1.3.8 Future research and scope

It is evident that the properties of aptamers make them excellent candidates for diagnostic use, with only relatively minor modifications needed. However, it is important when considering any drug for therapeutic use, to ensure that it can be administered effectively, is not broken down and excreted before it carries out its function, and that it does not cause an immune response. Aptamers have a high potential to do this, but modifications are often needed as the aptamer has many hurdles to overcome before it even reaches its target in the body. In time, research will deliver better and more competent aptamers for use *in vivo* and the modifications to selection procedures found to be successful will only aid this progress. A molecule called a spiegelmer has been developed as a therapeutic reagent in cancer [138] and is designed to overcome the problem of *in vivo* stability that has been associated with aptamers. Spiegelmers are comprised of L-ribose or L-2'-deoxyribose, creating mirror image oligonucleotides with enhanced *in vivo* stability compared with aptamers. One such spiegelmer inhibits the cascade for release of Gonadotropin-releasing hormone (GnRH) [138], the hormone responsible for releasing gonadotropins, luteinising hormone (LH) and follicle stimulating hormone (FSH) in mammalian reproduction [139]. This is important as prostate and breast cancers are caused by these hormones [140, 141], as well as endometriosis. The spiegelmer showed a K_D of 20nM for GnRH, and high specificity, as when GnRH was substituted with an analogue of GnRH (Buserelin), showing a closely related structure, the spiegelmer showed no antagonistic activity towards it [138]. Animal studies were conducted, which demonstrated that the coupling of the spiegelmer with PEG, not only did it not have any adverse effect on the spiegelmer's specificity and biological activity, but it caused the molecule to be retained for a longer period of time, causing its activity

to be comparable with the drug Cetrorelix, which is a marketed GnRH antagonist [138]. The spiegelmer also exhibited no immune response, which is important in assessing the safety of the molecule for long-term use [138].

1.4 Aims of This Project

The main aim of this project was to develop aptamers that bind to and selectively recognise human recombinant polymorphic heparanase and parts of the protein, for potential use in both diagnostic and therapeutic applications. As targets of the project we have identified the active heparanase heterodimer, comprised by the 50 and 8kDa subunits of heparanase, as well as the linker peptide of the protein, which is proteolytically excised from the proenzyme to result in the active enzyme. The reason for selecting these two targets of the enzyme was to verify if we could detect the presence and inhibit the action of the active enzyme or, in the case of the linker peptide, to see if we could block the proteolytic cleavage of this peptide, thus locking the enzyme in the inactive proenzymatic form as well as identify the as yet unknown fate of the cleaved peptide.

Experiments were designed to test generated aptamers using a number of different assays, then to select the most promising aptamer(s) for further development. Firstly, aptamers' binding and affinity were to be characterised using biochemical and physicochemical assays such as electrophoretic mobility shift assays (EMSA), fluorescence titrations, competition and sandwich enzyme-linked immunosorbent assays (ELISAs), using a heparanase polyclonal antibody as a positive control for comparison purposes.

Upon distinguishing aptamers with the highest binding affinities for heparanase, these would be tested using human tissue in immunohistochemistry and immunofluorescence experiments and compared to the heparanase polyclonal antibody as a positive control, plus a negative control, to examine if the aptamers bind heparanase specifically and the extent of their binding.

Subject to the aptamers' performance in these assays, they were then to be tested for their therapeutic and diagnostic potential. It was determined that to evaluate their therapeutic potential, their enzyme inhibiting function would be evaluated in different types of invasion assays, as well as their non-specific interaction with serum proteins and their susceptibility to nuclease degradation, crucial for the *in vivo* administration of the aptamers. To investigate the diagnostic potential of the aptamers and their ability to detect the presence of low levels of heparanase in biological media as an indication of metastasis and disease progression, the stability of the aptamers in serum would be crucial, as well as the performance of the aptamers in diagnostic assays. This would be evaluated in ELISA and quartz crystal microbalance assays that would be relevant for clinical settings. In this thesis I am presenting my findings from such studies and discussing my results and the future potential my studies open for the development of such heparanase aptamers into diagnostic or therapeutic agents.

References:

1. Cowley, S., D. Male, I. Romero, and J. Saffrey, *The Interactive Cell.* S377 Molecular and Cell Biology, ed. I. Nuttall, et al. Vol. 1. 2004: The Open University. 134-135.
2. Hanahan, D. and R.A. Weinberg, *The hallmarks of cancer.* Cell, 2000. **100**(1): p. 57-70.
3. Missailidis, S., ed. *Anticancer Therapeutics*. 2008, John Wiley & Sons, Ltd. 404.
4. Itoh, T., M. Tanioka, H. Matsuda, H. Nishimoto, T. Yoshioka, R. Suzuki, and M. Uehira, *Experimental metastasis is suppressed in MMP-9-deficient mice.* Clin Exp Metastasis, 1999. **17**(2): p. 177-81.
5. Nicolson, G.L., *Cancer metastasis. Organ colonization and the cell-surface properties of malignant cells.* Biochim Biophys Acta, 1982. **695**(2): p. 113-76.
6. Nicolson, G.L. and G. Poste, *Tumor cell diversity and host responses in cancer metastasis--part I--properties of metastatic cells.* Curr Probl Cancer, 1982. **7**(6): p. 1-83.
7. Poste, G. and I.J. Fidler, *The pathogenesis of cancer metastasis.* Nature, 1980. **283**(5743): p. 139-46.
8. Nakajima, M., T. Irimura, D. Di Ferrante, N. Di Ferrante, and G.L. Nicolson, *Heparan sulfate degradation: relation to tumor invasive and metastatic properties of mouse B16 melanoma sublines.* Science, 1983. **220**(4597): p. 611-3.
9. Nakajima, M., T. Irimura, N. Di Ferrante, and G.L. Nicolson, *Metastatic melanoma cell heparanase. Characterization of heparan sulfate degradation fragments produced by B16 melanoma endoglucuronidase.* J Biol Chem, 1984. **259**(4): p. 2283-90.

10. Li, J.P. and I. Vlodavsky, *Heparin, heparan sulfate and heparanase in inflammatory reactions.* Thromb Haemost, 2009. **102**(5): p. 823-8.

11. Kjellen, L. and U. Lindahl, *Proteoglycans: structures and interactions.* Annu Rev Biochem, 1991. **60**: p. 443-75.

12. Aldrich, S. *Heparan Sulphate.* [Webpage] 2006 [cited 05/05/2006]; Available from: http://www.sigmaaldrich.com/img/assets/19500/heparinase_heparin.gif.

13. Bernfield, M., M. Gotte, P.W. Park, O. Reizes, M.L. Fitzgerald, J. Lincecum, and M. Zako, *Functions of cell surface heparan sulfate proteoglycans.* Annu Rev Biochem, 1999. **68**: p. 729-77.

14. Lin, X., *Functions of heparan sulfate proteoglycans in cell signaling during development.* Development, 2004. **131**(24): p. 6009-21.

15. Whitelock, J.M. and R.V. Iozzo, *Heparan sulfate: a complex polymer charged with biological activity.* Chem Rev, 2005. **105**(7): p. 2745-64.

16. Laurie, G.W., C.P. Leblond, and G.R. Martin, *Localization of type IV collagen, laminin, heparan sulfate proteoglycan, and fibronectin to the basal lamina of basement membranes.* J Cell Biol, 1982. **95**(1): p. 340-4.

17. Lindahl, U., M. Kusche-Gullberg, and L. Kjellen, *Regulated diversity of heparan sulfate.* J Biol Chem, 1998. **273**(39): p. 24979-82.

18. Spillmann, D., D. Witt, and U. Lindahl, *Defining the interleukin-8-binding domain of heparan sulfate.* J Biol Chem, 1998. **273**(25): p. 15487-93.

19. Lortat-Jacob, H., J.E. Turnbull, and J.A. Grimaud, *Molecular organization of the interferon gamma-binding domain in heparan sulphate.* Biochem J, 1995. **310 (Pt 2)**: p. 497-505.

20. Stringer, S.E. and J.T. Gallagher, *Specific binding of the chemokine platelet factor 4 to heparan sulfate.* J Biol Chem, 1997. **272**(33): p. 20508-14.

21. Pikas, D.S., J.P. Li, I. Vlodavsky, and U. Lindahl, *Substrate specificity of heparanases from human hepatoma and platelets.* J Biol Chem, 1998. **273**(30): p. 18770-7.

22. Dong, J., A.K. Kukula, M. Toyoshima, and M. Nakajima, *Genomic organization and chromosome localization of the newly identified human heparanase gene.* Gene, 2000. **253**(2): p. 171-8.

23. Levy-Adam, F., H.Q. Miao, R.L. Heinrikson, I. Vlodavsky, and N. Ilan, *Heterodimer formation is essential for heparanase enzymatic activity.* Biochem Biophys Res Commun, 2003. **308**(4): p. 885-91.

24. McKenzie, E., K. Young, M. Hircock, J. Bennett, M. Bhaman, R. Felix, P. Turner, A. Stamps, D. McMillan, G. Saville, S. Ng, S. Mason, D. Snell, D. Schofield, H. Gong, R. Townsend, J. Gallagher, M. Page, R. Parekh, and C. Stubberfield, *Biochemical characterization of the active heterodimer form of human heparanase (Hpa1) protein expressed in insect cells.* Biochem J, 2003. **373**(Pt 2): p. 423-35.

25. Fairbanks, M.B., A.M. Mildner, J.W. Leone, G.S. Cavey, W.R. Mathews, R.F. Drong, J.L. Slightom, M.J. Bienkowski, C.W. Smith, C.A. Bannow, and R.L. Heinrikson, *Processing of the human heparanase precursor and evidence that the active enzyme is a heterodimer.* J Biol Chem, 1999. **274**(42): p. 29587-90.

26. Abboud-Jarrous, G., Z. Rangini-Guetta, H. Aingorn, R. Atzmon, S. Elgavish, T. Peretz, and I. Vlodavsky, *Site-directed mutagenesis, proteolytic cleavage, and activation of human proheparanase.* J Biol Chem, 2005. **280**(14): p. 13568-75.

27. Koliopanos, A., H. Friess, J. Kleeff, X. Shi, Q. Liao, I. Pecker, I. Vlodavsky, A. Zimmermann, and M.W. Buchler, *Heparanase expression in primary and metastatic pancreatic cancer.* Cancer Res, 2001. **61**(12): p. 4655-9.

28. Shteper, P.J., E. Zcharia, Y. Ashhab, T. Peretz, I. Vlodavsky, and D. Ben-Yehuda, *Role of promoter methylation in regulation of the mammalian heparanase gene.* Oncogene, 2003. **22**(49): p. 7737-49.

29. Simizu, S., K. Ishida, M.K. Wierzba, T.A. Sato, and H. Osada, *Expression of heparanase in human tumor cell lines and human head and neck tumors.* Cancer Lett, 2003. **193**(1): p. 83-9.

30. de Mestre, A.M., S. Rao, J.R. Hornby, T. Soe-Htwe, L.M. Khachigian, and M.D. Hulett, *Early growth response gene 1 (EGR1) regulates heparanase gene transcription in tumor cells.* J Biol Chem, 2005. **280**(42): p. 35136-47.

31. Baraz, L., Y. Haupt, M. Elkin, T. Peretz, and I. Vlodavsky, *Tumor suppressor p53 regulates heparanase gene expression.* Oncogene, 2006. **25**(28): p. 3939-47.

32. Chen, G., D. Wang, R. Vikramadithyan, H. Yagyu, U. Saxena, S. Pillarisetti, and I.J. Goldberg, *Inflammatory cytokines and fatty acids regulate endothelial cell heparanase expression.* Biochemistry, 2004. **43**(17): p. 4971-7.

33. Sandwall, E., S. Bodevin, N.J. Nasser, E. Nevo, A. Avivi, I. Vlodavsky, and J.P. Li, *Molecular structure of heparan sulfate from Spalax. Implications of heparanase and hypoxia.* J Biol Chem, 2009. **284**(6): p. 3814-22.

34. Shafat, I., I. Vlodavsky, and N. Ilan, *Characterization of mechanisms involved in secretion of active heparanase.* J Biol Chem, 2006. **281**(33): p. 23804-11.

35. Nadav, L., A. Eldor, O. Yacoby-Zeevi, E. Zamir, I. Pecker, N. Ilan, B. Geiger, I. Vlodavsky, and B.Z. Katz, *Activation, processing and trafficking of extracellular heparanase by primary human fibroblasts.* J Cell Sci, 2002. **115**(Pt 10): p. 2179-87.

36. Vlodavsky, I., N. Ilan, A. Naggi, and B. Casu, *Heparanase: structure, biological functions, and inhibition by heparin-derived mimetics of heparan sulfate.* Curr Pharm Des, 2007. **13**(20): p. 2057-73.

37. Hulett, M.D., J.R. Hornby, S.J. Ohms, J. Zuegg, C. Freeman, J.E. Gready, and C.R. Parish, *Identification of active-site residues of the pro-metastatic endoglycosidase heparanase.* Biochemistry, 2000. **39**(51): p. 15659-67.

38. Levy-Adam, F., G. Abboud-Jarrous, M. Guerrini, D. Beccati, I. Vlodavsky, and N. Ilan, *Identification and characterization of heparin/heparan sulfate binding domains of the endoglycosidase heparanase.* J Biol Chem, 2005. **280**(21): p. 20457-66.

39. Nardella, C., A. Lahm, M. Pallaoro, M. Brunetti, A. Vannini, and C. Steinkuhler, *Mechanism of activation of human heparanase investigated by protein engineering.* Biochemistry, 2004. **43**(7): p. 1862-73.

40. Adams, D.H. and S. Shaw, *Leucocyte-endothelial interactions and regulation of leucocyte migration.* Lancet, 1994. **343**(8901): p. 831-6.

41. Blotnick, S., G.E. Peoples, M.R. Freeman, T.J. Eberlein, and M. Klagsbrun, *T lymphocytes synthesize and export heparin-binding epidermal growth factor-like growth factor and basic fibroblast growth factor, mitogens for vascular cells and fibroblasts: differential production and release by CD4+ and CD8+ T cells.* Proc Natl Acad Sci U S A, 1994. **91**(8): p. 2890-94.

42. Gilat, D., R. Hershkoviz, I. Goldkorn, L. Cahalon, G. Korner, I. Vlodavsky, and O. Lider, *Molecular behavior adapts to context: heparanase functions as an extracellular matrix-degrading enzyme or as a T cell adhesion molecule, depending on the local pH.* J Exp Med, 1995. **181**(5): p. 1929-34.

43. Hulett, M.D., C. Freeman, B.J. Hamdorf, R.T. Baker, M.J. Harris, and C.R. Parish, *Cloning of mammalian heparanase, an important enzyme in tumor invasion and metastasis.* Nat Med, 1999. **5**(7): p. 803-9.

44. Vlodavsky, I., A. Eldor, A. Haimovitz-Friedman, Y. Matzner, R. Ishai-Michaeli, O. Lider, Y. Naparstek, I.R. Cohen, and Z. Fuks, *Expression of heparanase by platelets and circulating cells of the immune system: possible involvement in diapedesis and extravasation.* Invasion Metastasis, 1992. **12**(2): p. 112-27.

45. Nakajima, M. *Tumor Heparanase.* Glycoword - Proteoglycan [Webpage] 2001 30/06/2001 [cited 2010 05/08/2010]; Available from: www.gak.co.jp/FCCA/glycoword/PGA10/PGA10E.html.

46. Chen, X.P., Y.B. Liu, J. Rui, S.Y. Peng, C.H. Peng, Z.Y. Zhou, L.H. Shi, H.W. Shen, and B. Xu, *Heparanase mRNA expression and point mutation in hepatocellular carcinoma.* World J Gastroenterol, 2004. **10**(19): p. 2795-9.

47. Gohji, K., H. Hirano, M. Okamoto, S. Kitazawa, M. Toyoshima, J. Dong, Y. Katsuoka, and M. Nakajima, *Expression of three extracellular matrix degradative enzymes in bladder cancer.* Int J Cancer, 2001. **95**(5): p. 295-301.

48. Goldshmidt, O., E. Zcharia, R. Abramovitch, S. Metzger, H. Aingorn, Y. Friedmann, V. Schirrmacher, E. Mitrani, and I. Vlodavsky, *Cell surface expression and secretion of heparanase markedly promote tumor angiogenesis and metastasis.* Proc Natl Acad Sci U S A, 2002. **99**(15): p. 10031-6.

49. Gingis-Velitski, S., A. Zetser, M.Y. Flugelman, I. Vlodavsky, and N. Ilan, *Heparanase induces endothelial cell migration via protein kinase B/Akt activation.* J Biol Chem, 2004. **279**(22): p. 23536-41.

50. Zetser, A., Y. Bashenko, E. Edovitsky, F. Levy-Adam, I. Vlodavsky, and N. Ilan, *Heparanase induces vascular endothelial growth factor expression: correlation with p38 phosphorylation levels and Src activation.* Cancer Res, 2006. **66**(3): p. 1455-63.

51. Hoogewerf, A.J., J.W. Leone, I.M. Reardon, W.J. Howe, D. Asa, R.L. Heinrikson, and S.R. Ledbetter, *CXC chemokines connective tissue activating peptide-III and neutrophil activating peptide-2 are heparin/heparan sulfate-degrading enzymes.* J Biol Chem, 1995. **270**(7): p. 3268-77.

52. Oosta, G.M., L.V. Favreau, D.L. Beeler, and R.D. Rosenberg, *Purification and properties of human platelet heparitinase.* J Biol Chem, 1982. **257**(19): p. 11249-55.

53. Tannock, I.F. and D. Rotin, *Acid pH in tumors and its potential for therapeutic exploitation.* Cancer Res, 1989. **49**(16): p. 4373-84.

54. Ralph, S., P.E. Brenchley, A. Summers, D.D. Rosa, R. Swindell, and G.C. Jayson, *Heparanase gene haplotype (CGC) is associated with stage of disease in patients with ovarian carcinoma.* Cancer Sci, 2007. **98**(6): p. 844-9.

55. Vlodavsky, I., O. Goldshmidt, E. Zcharia, R. Atzmon, Z. Rangini-Guatta, M. Elkin, T. Peretz, and Y. Friedmann, *Mammalian heparanase: involvement in cancer metastasis, angiogenesis and normal development.* Semin Cancer Biol, 2002. **12**(2): p. 121-9.

56. Gohji, K., M. Okamoto, S. Kitazawa, M. Toyoshima, J. Dong, Y. Katsuoka, and M. Nakajima, *Heparanase protein and gene expression in bladder cancer.* J Urol, 2001. **166**(4): p. 1286-90.

57. Marchetti, D. and G.L. Nicolson, *Human heparanase: a molecular determinant of brain metastasis.* Adv Enzyme Regul, 2001. **41**: p. 343-59.

58. Maxhimer, J.B., R.M. Quiros, R. Stewart, K. Dowlatshahi, P. Gattuso, M. Fan, R.A. Prinz, and X. Xu, *Heparanase-1 expression is associated with the metastatic potential of breast cancer.* Surgery, 2002. **132**(2): p. 326-33.

59. Friedmann, Y., I. Vlodavsky, H. Aingorn, A. Aviv, T. Peretz, I. Pecker, and O. Pappo, *Expression of heparanase in normal, dysplastic, and neoplastic human colonic mucosa and stroma. Evidence for its role in colonic tumorigenesis.* Am J Pathol, 2000. **157**(4): p. 1167-75.

60. Tang, W., Y. Nakamura, M. Tsujimoto, M. Sato, X. Wang, K. Kurozumi, M. Nakahara, K. Nakao, M. Nakamura, I. Mori, and K. Kakudo, *Heparanase: a key enzyme in invasion and metastasis of gastric carcinoma.* Mod Pathol, 2002. **15**(6): p. 593-8.

61. Mikami, S., K. Ohashi, Y. Usui, T. Nemoto, K. Katsube, M. Yanagishita, M. Nakajima, K. Nakamura, and M. Koike, *Loss of syndecan-1 and increased expression of heparanase in invasive esophageal carcinomas.* Jpn J Cancer Res, 2001. **92**(10): p. 1062-73.

62. Ikuta, M., K.A. Podyma, K. Maruyama, S. Enomoto, and M. Yanagishita, *Expression of heparanase in oral cancer cell lines and oral cancer tissues.* Oral Oncol, 2001. **37**(2): p. 177-84.

63. Kim, A.W., X. Xu, E.F. Hollinger, P. Gattuso, C.V. Godellas, and R.A. Prinz, *Human heparanase-1 gene expression in pancreatic adenocarcinoma.* J Gastrointest Surg, 2002. **6**(2): p. 167-72.

64. Rohloff, J., J. Zinke, K. Schoppmeyer, A. Tannapfel, H. Witzigmann, J. Mossner, C. Wittekind, and K. Caca, *Heparanase expression is a prognostic indicator for postoperative survival in pancreatic adenocarcinoma.* Br J Cancer, 2002. **86**(8): p. 1270-5.

65. He, X., P.E. Brenchley, G.C. Jayson, L. Hampson, J. Davies, and I.N. Hampson, *Hypoxia increases heparanase-dependent tumor cell invasion, which can be inhibited by antiheparanase antibodies.* Cancer Res, 2004. **64**(11): p. 3928-33.

66. Myler, H.A., E.A. Lipke, E.E. Rice, and J.L. West, *Novel heparanase-inhibiting antibody reduces neointima formation.* J Biochem (Tokyo), 2006. **139**(3): p. 339-45.

67. Bar-Ner, M., A. Eldor, L. Wasserman, Y. Matzner, I.R. Cohen, Z. Fuks, and I. Vlodavsky, *Inhibition of heparanase-mediated degradation of extracellular matrix heparan sulfate by non-anticoagulant heparin species.* Blood, 1987. **70**(2): p. 551-7.

68. Chuang, W.L., M.D. Christ, J. Peng, and D.L. Rabenstein, *An NMR and molecular modeling study of the site-specific binding of histamine by heparin, chemically modified heparin, and heparin-derived oligosaccharides.* Biochemistry, 2000. **39**(13): p. 3542-55.

69. Parish, C.R., C. Freeman, K.J. Brown, D.J. Francis, and W.B. Cowden, *Identification of sulfated oligosaccharide-based inhibitors of tumor growth and metastasis using novel in vitro assays for angiogenesis and heparanase activity.* Cancer Res, 1999. **59**(14): p. 3433-41.

70. Nader, H.B., M.A. Porcionatto, I.L. Tersariol, M.A. Pinhal, F.W. Oliveira, C.T. Moraes, and C.P. Dietrich, *Purification and substrate specificity of heparitinase I and heparitinase II from Flavobacterium heparinum. Analyses of the heparin and heparan sulfate degradation products by 13C NMR spectroscopy.* J Biol Chem, 1990. **265**(28): p. 16807-13.

71. Khasraw, M., N. Pavlakis, S. McCowatt, C. Underhill, S. Begbie, P. de Souza, A. Boyce, F. Parnis, V. Lim, R. Harvie, and G. Marx, *Multicentre phase I/II study of PI-88, a heparanase inhibitor in combination with docetaxel in patients with metastatic castrate-resistant prostate cancer.* Ann Oncol, 2009.

72. Lewis, K.D., W.A. Robinson, M.J. Millward, A. Powell, T.J. Price, D.B. Thomson, E.T. Walpole, A.M. Haydon, B.R. Creese, K.L. Roberts, J.R. Zalcberg, and R. Gonzalez, *A phase II study of the heparanase inhibitor PI-88 in patients with advanced melanoma.* Invest New Drugs, 2008. **26**(1): p. 89-94.

73. Ishida, K., G. Hirai, K. Murakami, T. Teruya, S. Simizu, M. Sodeoka, and H. Osada, *Structure-based design of a selective heparanase inhibitor as an antimetastatic agent.* Mol Cancer Ther, 2004. **3**(9): p. 1069-77.

74. Courtney, S.M., P.A. Hay, R.T. Buck, C.S. Colville, D.J. Phillips, D.I. Scopes, F.C. Pollard, M.J. Page, J.M. Bennett, M.L. Hircock, E.A. McKenzie, M. Bhaman, R. Felix, C.R. Stubberfield, and P.R. Turner, *Furanyl-1,3-thiazol-2-yl and benzoxazol-5-yl acetic acid derivatives: novel classes of heparanase inhibitor.* Bioorg Med Chem Lett, 2005. **15**(9): p. 2295-9.

75. Famulok, M. and G. Mayer, *Aptamers as tools in molecular biology and immunology.* Curr Top Microbiol Immunol, 1999. **243**: p. 123-36.

76. Gold, L., B. Polisky, O. Uhlenbeck, and M. Yarus, *Diversity of oligonucleotide functions.* Annu Rev Biochem, 1995. **64**: p. 763-97.

77. Osborne, S.E., I. Matsumura, and A.D. Ellington, *Aptamers as therapeutic and diagnostic reagents: problems and prospects.* Curr Opin Chem Biol, 1997. **1**(1): p. 5-9.

78. Hicke, B.J., C. Marion, Y.F. Chang, T. Gould, C.K. Lynott, D. Parma, P.G. Schmidt, and S. Warren, *Tenascin-C aptamers are generated using tumor cells and purified protein.* J Biol Chem, 2001. **276**(52): p. 48644-54.

79. Morris, K.N., K.B. Jensen, C.M. Julin, M. Weil, and L. Gold, *High affinity ligands from in vitro selection: complex targets.* Proc Natl Acad Sci U S A, 1998. **95**(6): p. 2902-7.

80. Brody, E.N. and L. Gold, *Aptamers as therapeutic and diagnostic agents.* J Biotechnol, 2000. **74**(1): p. 5-13.

81. Ellington, A.D. and J.W. Szostak, *In vitro selection of RNA molecules that bind specific ligands.* Nature, 1990. **346**(6287): p. 818-22.

82. Bianchini, M., M. Radrizzani, M.G. Brocardo, G.B. Reyes, C. Gonzalez Solveyra, and T.A. Santa-Coloma, *Specific oligobodies against ERK-2 that recognize both the native and the denatured state of the protein.* J Immunol Methods, 2001. **252**(1-2): p. 191-7.

83. Radrizzani, M., M.G. Brocardo, C. Gonzalez Solveyra, M. Bianchini, G.B. Reyes, E.G. Cafferata, G. Vila Ortiz, and T.A. Santa-Coloma, *Development of monoclonal oligobodies and chemically synthesized oligobodies.* Medicina (B Aires), 2000. **60 Suppl 2**: p. 55-60.

84. Radrizzani, M., M. Broccardo, C. Gonzalez Solveyra, M. Bianchini, G.B. Reyes, E.G. Cafferata, and T.A. Santa-Coloma, *Oligobodies: bench made synthetic antibodies.* Medicina (B Aires), 1999. **59**(6): p. 753-8.

85. White, R., C. Rusconi, E. Scardino, A. Wolberg, J. Lawson, M. Hoffman, and B. Sullenger, *Generation of species cross-reactive aptamers using "toggle" SELEX.* Mol Ther, 2001. **4**(6): p. 567-73.

86. Berezovski, M., A. Drabovich, S.M. Krylova, M. Musheev, V. Okhonin, A. Petrov, and S.N. Krylov, *Nonequilibrium capillary electrophoresis of equilibrium mixtures: a universal tool for development of aptamers.* Journal of the American Chemical Society, 2005. **127**(9): p. 3165-3171.

87. Berezovski, M., M. Musheev, A. Drabovich, and S.N. Krylov, *Non-SELEX selection of aptamers.* Journal of the American Chemical Society, 2006. **128**(5): p. 1410-1411.

88. Drabovich, A., M. Berezovski, and S.N. Krylov, *Selection of smart aptamers by equilibrium capillary electrophoresis of equilibrium mixtures (ECEEM).* Journal of the American Chemical Society, 2005. **127**(32): p. 11224-11225.

89. Di Giusto, D.A. and G.C. King, *Construction, stability, and activity of multivalent circular anticoagulant aptamers.* J Biol Chem, 2004. **279**(45): p. 46483-9.

90. Zuker, M., *Mfold web server for nucleic acid folding and hybridization prediction.* Nucleic Acids Res, 2003. **31**(13): p. 3406-15.

91. Bates, P.J., J.B. Kahlon, S.D. Thomas, J.O. Trent, and D.M. Miller, *Antiproliferative activity of G-rich oligonucleotides correlates with protein binding.* The Journal of biological chemistry, 1999. **274**(37): p. 26369-26377.

92. Xu, X., F. Hamhouyia, S.D. Thomas, T.J. Burke, A.C. Girvan, W.G. McGregor, J.O. Trent, D.M. Miller, and P.J. Bates, *Inhibition of DNA replication and induction of S phase cell cycle arrest by G-rich oligonucleotides.* The Journal of biological chemistry, 2001. **276**(46): p. 43221-43230.

93. Laughlin, A.J., D.K. Male, S. Missailidis, R. Mileusnic, and M.C. Hirst, *From Molecules To Cells*. S377 Molecular and Cell Biology, ed. G. Bearman, et al. Vol. 1. 2004, Milton Keynes. 311.

94. Jellinek, D., L.S. Green, C. Bell, C.K. Lynott, N. Gill, C. Vargeese, G. Kirschenheuter, D.P. McGee, P. Abesinghe, W.A. Pieken, and et al., *Potent 2'-amino-2'-deoxypyrimidine RNA inhibitors of basic fibroblast growth factor.* Biochemistry, 1995. **34**(36): p. 11363-72.

95. Ruckman, J., L.S. Green, J. Beeson, S. Waugh, W.L. Gillette, D.D. Henninger, L. Claesson-Welsh, and N. Janjic, *2'-Fluoropyrimidine RNA-based aptamers to the 165-amino acid form of vascular endothelial growth factor (VEGF165). Inhibition of*

receptor binding and VEGF-induced vascular permeability through interactions requiring the exon 7-encoded domain. J Biol Chem, 1998. **273**(32): p. 20556-67.

96. Floege, J., T. Ostendorf, U. Janssen, M. Burg, H.H. Radeke, C. Vargeese, S.C. Gill, L.S. Green, and N. Janjic, *Novel approach to specific growth factor inhibition in vivo: antagonism of platelet-derived growth factor in glomerulonephritis by aptamers.* Am J Pathol, 1999. **154**(1): p. 169-79.

97. Da Pieve, C., P. Williams, D.M. Haddleton, R.M. Palmer, and S. Missailidis, *Modification of thiol functionalized aptamers by conjugation of synthetic polymers.* Bioconjug Chem. **21**(1): p. 169-74.

98. Hicke, B.J., A.W. Stephens, T. Gould, Y.-F. Chang, C.K. Lynott, J. Heil, S. Borkowski, C.-S. Hilger, G. Cook, S. Warren, and P.G. Schmidt, *Tumor Targeting by an Aptamer.* J Nucl Med, 2006. **47**(4): p. 668-678.

99. Cao, Z., R. Tong, A. Mishra, W. Xu, G.C. Wong, J. Cheng, and Y. Lu, *Reversible cell-specific drug delivery with aptamer-functionalized liposomes.* Angew Chem Int Ed Engl, 2009. **48**(35): p. 6494-8.

100. Pieve, C.D., A.C. Perkins, and S. Missailidis, *Anti-MUC1 aptamers: radiolabelling with (99m)Tc and biodistribution in MCF-7 tumour-bearing mice.* Nucl Med Biol, 2009. **36**(6): p. 703-10.

101. Gragoudas, E.S., A.P. Adamis, E.T. Cunningham, Jr., M. Feinsod, D.R. Guyer, and V.I.S.i.O.N.C.T.G. the, *Pegaptanib for Neovascular Age-Related Macular Degeneration.* N Engl J Med, 2004. **351**(27): p. 2805-2816.

102. Soundararajan, S., W. Chen, E.K. Spicer, N. Courtenay-Luck, and D.J. Fernandes, *The Nucleolin Targeting Aptamer AS1411 Destabilizes Bcl-2 Messenger RNA in Human Breast Cancer Cells.* Cancer Res, 2008. **68**(7): p. 2358-2365.

103. Gilbert, J.C., T. DeFeo-Fraulini, R.M. Hutabarat, C.J. Horvath, P.G. Merlino, H.N. Marsh, J.M. Healy, S. BouFakhreddine, T.V. Holohan, and R.G. Schaub, *First-in-Human Evaluation of Anti von Willebrand Factor Therapeutic Aptamer ARC1779 in Healthy Volunteers.* Circulation, 2007. **116**(23): p. 2678-2686.

104. Group, E.S., *Preclinical and phase 1A clinical evaluation of an anti-VEGF pegylated aptamer (EYE001) for the treatment of exudative age-related macular degeneration.* Retina (Philadelphia, Pa.), 2002. **22**(2): p. 143-152.

105. Miles, A.A. and E.M. Miles, *Vascular reactions to histamine, histamine-liberator and leukotaxine in the skin of guinea-pigs.* J Physiol, 1952. **118**(2): p. 228-57.

106. Basilico, C. and D. Moscatelli, *The FGF family of growth factors and oncogenes.* Adv Cancer Res, 1992. **59**: p. 115-65.

107. Miyamoto, M., K. Naruo, C. Seko, S. Matsumoto, T. Kondo, and T. Kurokawa, *Molecular cloning of a novel cytokine cDNA encoding the ninth member of the fibroblast growth factor family, which has a unique secretion property.* Mol Cell Biol, 1993. **13**(7): p. 4251-9.

108. Tanaka, A., K. Miyamoto, N. Minamino, M. Takeda, B. Sato, H. Matsuo, and K. Matsumoto, *Cloning and characterization of an androgen-induced growth factor essential for the androgen-dependent growth of mouse mammary carcinoma cells.* Proc Natl Acad Sci U S A, 1992. **89**(19): p. 8928-32.

109. Cowley, S., D. Male, R. Mileusnic, I. Romero, J. Saffrey, and R. Saunders, *The Dynamic Cell.* S377 Molecular and Cell Biology, ed. G. Bearman, et al. Vol. 2. 2004. 117-119.

110. Slomowitz, L.A., *Progression of renal disease.* N Engl J Med, 1988. **319**(23): p. 1547-8.

111. Chuang, E., D. Barnard, L. Hettich, X.F. Zhang, J. Avruch, and M.S. Marshall, *Critical binding and regulatory interactions between Ras and Raf occur through a small, stable N-terminal domain of Raf and specific Ras effector residues.* Mol Cell Biol, 1994. **14**(8): p. 5318-25.

112. Herrmann, C., G.A. Martin, and A. Wittinghofer, *Quantitative analysis of the complex between p21ras and the Ras-binding domain of the human Raf-1 protein kinase.* J Biol Chem, 1995. **270**(7): p. 2901-5.

113. Vojtek, A.B., S.M. Hollenberg, and J.A. Cooper, *Mammalian Ras interacts directly with the serine/threonine kinase Raf.* Cell, 1993. **74**(1): p. 205-14.

114. Kimoto, M., M. Shirouzu, S. Mizutani, H. Koide, Y. Kaziro, I. Hirao, and S. Yokoyama, *Anti-(Raf-1) RNA aptamers that inhibit Ras-induced Raf-1 activation.* Eur J Biochem, 2002. **269**(2): p. 697-704.

115. Bussolino, F., A. Mantovani, and G. Persico, *Molecular mechanisms of blood vessel formation.* Trends Biochem Sci, 1997. **22**(7): p. 251-6.

116. Moroianu, J. and J.F. Riordan, *Identification of the nucleolar targeting signal of human angiogenin.* Biochem Biophys Res Commun, 1994. **203**(3): p. 1765-72.

117. Moroianu, J. and J.F. Riordan, *Nuclear translocation of angiogenin in proliferating endothelial cells is essential to its angiogenic activity.* Proc Natl Acad Sci U S A, 1994. **91**(5): p. 1677-81.

118. Nobile, V., N. Russo, G. Hu, and J.F. Riordan, *Inhibition of human angiogenin by DNA aptamers: nuclear colocalization of an angiogenin-inhibitor complex.* Biochemistry, 1998. **37**(19): p. 6857-63.

119. Blank, M., T. Weinschenk, M. Priemer, and H. Schluesener, *Systematic evolution of a DNA aptamer binding to rat brain tumor microvessels. selective targeting of endothelial regulatory protein pigpen.* J Biol Chem, 2001. **276**(19): p. 16464-8.

120. Conrad, R., L.M. Keranen, A.D. Ellington, and A.C. Newton, *Isozyme-specific inhibition of protein kinase C by RNA aptamers.* J Biol Chem, 1994. **269**(51): p. 32051-4.

121. Ono, Y., T. Kurokawa, T. Fujii, K. Kawahara, K. Igarashi, U. Kikkawa, K. Ogita, and Y. Nishizuka, *Two types of complementary DNAs of rat brain protein kinase C. Heterogeneity determined by alternative splicing.* FEBS Lett, 1986. **206**(2): p. 347-52.

122. Charlton, J., G.P. Kirschenheuter, and D. Smith, *Highly potent irreversible inhibitors of neutrophil elastase generated by selection from a randomized DNA-valine phosphonate library.* Biochemistry, 1997. **36**(10): p. 3018-26.

123. Charlton, J., J. Sennello, and D. Smith, *In vivo imaging of inflammation using an aptamer inhibitor of human neutrophil elastase.* Chem Biol, 1997. **4**(11): p. 809-16.

124. Smith, D., G.P. Kirschenheuter, J. Charlton, D.M. Guidot, and J.E. Repine, *In vitro selection of RNA-based irreversible inhibitors of human neutrophil elastase.* Chem Biol, 1995. **2**(11): p. 741-50.

125. Repine, J.E., *Scientific perspectives on adult respiratory distress syndrome.* Lancet, 1992. **339**(8791): p. 466-9.

126. Varani, J. and P.A. Ward, *Mechanisms of neutrophil-dependent and neutrophil-independent endothelial cell injury.* Biol Signals, 1994. **3**(1): p. 1-14.

127. Weiss, S.J. and S. Regiani, *Neutrophils degrade subendothelial matrices in the presence of alpha-1-proteinase inhibitor. Cooperative use of lysosomal proteinases and oxygen metabolites.* J Clin Invest, 1984. **73**(5): p. 1297-303.

128. Wright, D.G., *Human neutrophil degranulation.* Methods Enzymol, 1988. **162**: p. 538-51.

129. Liou, T.G. and E.J. Campbell, *Nonisotropic enzyme--inhibitor interactions: a novel nonoxidative mechanism for quantum proteolysis by human neutrophils.* Biochemistry, 1995. **34**(49): p. 16171-7.

130. Rice, W.G. and S.J. Weiss, *Regulation of proteolysis at the neutrophil-substrate interface by secretory leukoprotease inhibitor.* Science, 1990. **249**(4965): p. 178-81.

131. Travis, J. and G.S. Salvesen, *Human plasma proteinase inhibitors.* Annu Rev Biochem, 1983. **52**: p. 655-709.

132. Oleksyszyn, J. and J.C. Powers, *Irreversible inhibition of serine proteases by peptide derivatives of (alpha-aminoalkyl)phosphonate diphenyl esters.* Biochemistry, 1991. **30**(2): p. 485-93.

133. Velasco-Garcia, M.N. and S. Missailidis, *New trends in aptamer-based electrochemical biosensors.* Gene Therapy and Molecular Biology, 2009. **13**(1): p. 1-9.

134. Bock, L.C., L.C. Griffin, J.A. Latham, E.H. Vermaas, and J.J. Toole, *Selection of single-stranded DNA molecules that bind and inhibit human thrombin.* Nature, 1992. **355**(6360): p. 564-6.

135. de-los-Santos-Álvarez, N., M.a.J. Lobo-Castañón, A.J. Miranda-Ordieres, and P. Tuñón-Blanco, *Aptamers as recognition elements for label-free analytical devices.* TrAC Trends in Analytical Chemistry, 2008. **27**(5): p. 437-446.

136. Seger, R. and E.G. Krebs, *The MAPK signaling cascade.* Faseb J, 1995. **9**(9): p. 726-35.

137. Yokoyama, K., H.P. Erickson, Y. Ikeda, and Y. Takada, *Identification of amino acid sequences in fibrinogen gamma -chain and tenascin C C-terminal domains critical for binding to integrin alpha vbeta 3.* J Biol Chem, 2000. **275**(22): p. 16891-8.

138. Wlotzka, B., S. Leva, B. Eschgfaller, J. Burmeister, F. Kleinjung, C. Kaduk, P. Muhn, H. Hess-Stumpp, and S. Klussmann, *In vivo properties of an anti-GnRH Spiegelmer: an example of an oligonucleotide-based therapeutic substance class.* Proc Natl Acad Sci U S A, 2002. **99**(13): p. 8898-902.

139. Conn, P.M. and W.F. Crowley, Jr., *Gonadotropin-releasing hormone and its analogs.* Annu Rev Med, 1994. **45**: p. 391-405.

140. Kettel, L.M. and W.P. Hummel, *Modern medical management of endometriosis.* Obstet Gynecol Clin North Am, 1997. **24**(2): p. 361-73.

141. Schally, A.V., *Luteinizing hormone-releasing hormone analogs: their impact on the control of tumorigenesis.* Peptides, 1999. **20**(10): p. 1247-62.

CHAPTER TWO

MATERIALS AND METHODS

2.1 Materials

Acrylamide/Bis-acrylamide 30% was purchased from Sigma-Aldrich Ltd (Gillingham, UK, product code A3699 100ml).

Agarose was purchased from Sigma-Aldrich Ltd (Gillingham, UK, product code A9539).

Agar Select was purchased from Sigma-Aldrich Ltd (Gillingham, UK, product number A5054).

Ampicillin sodium salt was purchased from Sigma-Aldrich Ltd (Gillingham, UK, product code A9518 5g).

Antibodies:

Anti-Rabbit IgG (whole molecule)–Peroxidase antibody produced in goat was purchased from Sigma-Aldrich Ltd (Gillingham, UK, product code A6154 1ml).

Rabbit polyclonal anti-Heparanase IgG [1] was supplied by Professor Paul Brenchley, University of Manchester at a concentration of 10mg/ml in buffer containing sodium azide.

Secondary swine-anti-rabbit and goat-anti-mouse biotinylated antibodies were supplied by Dako (Ely, UK).

Mouse monoclonal anti-cytokeratin-7 and control mouse antibody were supplied by Dako (Ely, UK).

Aptamers:

Aptamer library was supplied at a concentration of 40µmoles in sterile deionised water from the University of Nottingham. Internal forward and reverse primers were also supplied from the University of Nottingham at concentrations of 1mmole and 40µmoles respectively.

All aptamer and biotinylated aptamer specific sequences were purchased as custom single stranded oligonucleotides from Eurofins MWG Operon (Ebersberg, Germany).

Biopsy punch (8mm) was purchased from Kai Industries (Gifu, Japan).

Boric Acid was purchased from Sigma-Aldrich Ltd (Gillingham, UK, product code B6768 1Kg).

Bovine Serum Albumin (BSA) was purchased from Sigma-Aldrich Ltd (Gillingham, UK, product code A7030 10g).

Citric acid was purchased from Sigma-Aldrich Ltd (Gillingham, UK, product code C2404 500g).

Dimethylsulfoxide (DMSO) was purchased from Sigma-Aldrich Ltd (Gillingham, UK, product code D8418).

25bp DNA step ladder was purchased from Promega UK Ltd (Southampton, UK, product number G4511).

Ethylenediaminetetraacetic acid disodium salt dihydrate (EDTA) was purchased from Sigma-Aldrich Ltd (Gillingham, UK, product code E5513 50g).

Ethidium Bromide was purchased from Sigma-Aldrich Ltd (Gillingham, UK, product code E7637 1g).

Human recombinant polymorphic heparanase enzyme was supplied at a concentration of 0.5mg/ml and Linker Peptide at 1mg/ml in 25mM Tris, 0.7M NaCl pH 7.5, from the University of Manchester.

Hydrocortisone was purchased from Sigma-Aldrich Ltd (Gillingham, UK).

KCl was purchased from VWR (Lutterworth, UK, product code 10198 500g).

Matrigel was purchased from BD Discovery Labware (Bedford, MA, USA).

Media and supplements for cell culture were purchased from Invitrogen Ltd (Paisley, UK).

$MgCl_2 \cdot 6H_2O$ was purchased from Sigma-Aldrich Ltd (Gillingham, UK, product code M2393 500g).

Microcons Filters and Ultrafree-15 Centrifugal Filter Devices were purchased from Millipore, supplied by Fisher Scientific UK Ltd (Loughborough, UK).

NaCl was purchased from Fisher Scientific UK Ltd (Loughborough, UK, product code S/3120/60 1Kg).

NaSCN was ordered from Sigma-Aldrich Ltd (Gillingham, UK, product code 251410 100g).

PBS (phosphate buffered saline) was supplied in tablet form from Sigma-Aldrich Ltd (Gillingham, UK, product number P4417).

PCR reagents:

Taq DNA Polymerase supplied with 10x PCR buffer Sigma-Aldrich Ltd (Gillingham, UK, product code D1806);

25mM Magnesium Chloride solution supplied by Sigma-Aldrich Ltd (Gillingham, UK, product code A3513);

Deoxynucleotide Triphosphates supplied as dATP, dCTP, dGTP and dTTP at 100mM each were purchased from Promega UK Ltd (Southampton, UK, product code U1240).

Quartz crystals (5MHz) coated with gold and polished for use at 25°C were purchased from Testbourne Ltd (Basingstoke, UK).

REAL antibody diluent was purchased from Dako (Ely, UK).

Sodium acetate was purchased from VWR (Lutterworth, UK, product code 30104 1Kg).

StreptABComplex/HRP was purchased from Dako (Ely, UK).

Streptavidin-Biotinylated Horseradish Peroxidase Complex was purchased from GE Healthcare Life Sciences (Little Chalfont, UK, product number RPN1051).

Streptavidin coated tubes were ordered from Roche Diagnostics Ltd (Burgess Hill, UK, product code 11741772001).

Tris Buffered Saline (TBS) was supplied in tablet form from Sigma-Aldrich Ltd (Gillingham, UK, product number T5030).

Tetra-methyl benzidine (TMB) was purchased from Sigma-Aldrich Ltd (Gillingham, UK, product code 860336).

Tissue culture inserts (8μm pore size, 10mm diameter) were purchased from NUNC, supplied by Fisher Scientific UK Ltd (Loughborough, UK, product code 137443).

TOPO TA Cloning® Kit (with pCR®2.1-TOPO® vector) with One Shot® TOP10 Chemically Competent E. coli was purchased from Invitrogen Ltd (Paisley, UK, product code K4500-40).

Top Yield PCR tubes were purchased from NUNC, supplied by Fisher Scientific UK Ltd (Loughborough, UK, product code 248909)

Trizma base was purchased from Sigma-Aldrich Ltd (Gillingham, UK, product code T1503 1Kg).

Tryptone was ordered from Sigma-Aldrich Ltd (Gillingham, UK, product code T9410 1Kg).

Tubing for peristaltic pump (0.8mm pore size, 1.6mm wall thickness) was purchased from Fisher Scientific UK Ltd (Loughborough, UK, product code FB56465).

Tween 20 was purchased from Sigma-Aldrich Ltd (Gillingham, UK, product code P9416).

Xylene Cyanole FF was purchased from Sigma-Aldrich Ltd (Gillingham, UK, product code X4126 10g).

Yeast extract was ordered from Sigma-Aldrich Ltd (Gillingham, UK, product code Y1625 1Kg).

2.2 Buffers and Solutions

Carbonate buffer was prepared by adding 0.53g Na_2CO_3 and 0.42g $NaHCO_3$ and making up to 100ml with ultra pure water, pH 9.6.

Chromogen was prepared by adding 1.21ml 0.5M sodium acetate solution, 37.5µl 0.5M citric acid solution and 62.5µl 10% TMB in DMSO to 5ml ultra pure H_2O, then activated by adding 7.5µl 30% H_2O_2.

Citrate buffer is composed of 2.94g sodium citrate and 500µl Tween 20 in 1 litre of dH_2O, pH 6.0.

EIA Diluent was prepared by adding 125mg BSA and 500µl 5% tween 20 to 25ml PBS.

Elution buffer is composed of 1.5M NaCl, 20mM KCl, 5mM $MgCl_2$ pH 7.2.

PBS was prepared to working concentration (0.01M phosphate buffer, 0.0027M KCl, 0.137M NaCl pH 7.4) by adding one PBS tablet to 200ml ultra pure H_2O and sterilising in an autoclave.

Piranha solution comprised of 1 volume 30% H_2O_2 added to 4 volumes of concentrated H_2SO_4 (prepared in fume hood as extremely caustic and exothermic).

Salt solution is composed of 100mM NaCl, 20mM KCl and 5mM $MgCl_2$ at pHs 6.5 and 7.2.

TBE buffer is composed of 0.045M Trizma base, 0.045M Boric Acid and 0.001M EDTA.

TBS buffer was prepared to working concentration (0.05M Tris and 0.15M NaCl, pH 7.6) by adding one TBS tablet to 15ml ultra pure water.

5% Tween 20 is made by adding 1ml tween 20 to 19ml ultra pure H_2O.

Wash buffer is composed of PBS containing 2 ml 5% tween 20.

2.3 Cell lines and culture conditions

First trimester (8-12 weeks gestation) and term placenta and decidua were obtained surgically at termination or completion of pregnancy and both informed consent and local ethical committee approval was in place for use of both tissues.

Uterine leiomyoma tissue was obtained from routine surgical operations after informed consent of the donors. The study was approved by the Ethics Committee of the Oulu University Hospital. Only non-degenerated myomas were selected for the study. To prepare myoma discs for the organotypic culture, the tissue was cut into 3mm slices with a disposable scalpel then into discs with an 8mm biopsy punch. Macroscopically heterogeneous areas of the myoma tissue were omitted. The myoma discs were stored at -70°C in 1:1 DMEM/F12 media containing 10% DMSO.

All cell lines were cultured to 80% confluency and media were supplemented with 10% FBS, L-glutamine (2mM), penicillin (100IU/ml) and streptomycin (100µg/ml). Endometrial adenocarcinoma, Ishikawa cell line was cultured in DMEM; placental stromal cells (first trimester) were cultured in 50% DMEM 50% Ham's F12 supplemented with 1% non-essential amino acids; first trimester immortalised PL4 trophoblasts [2] were cultured in Ham's F10 medium; trophoblast carcinoma, BeWo cell line was cultured in 50% DMEM 50% Ham's F12, and ovarian carcinoma cell line OC-MZ6 [1, 2] was cultured in DMEM containing 10mM HEPES, 116mg/L arginine and 36mg/L asparagine. Human tongue squamous carcinoma cells [3]; HSC-3 (JCRB 0623; Osaka National Institute of Health Sciences, Osaka, Japan) were cultured in 50% DMEM 50% Ham's F-12 and additionally supplemented with 50µg/ml ascorbic acid, 250ng/ml fungizone, 5µg/ml insulin (bovine pancreas) and 0.4ng/ml hydrocortisone. Cells were incubated in 95% air/5% CO_2 at 37°C.

2.4 Equipment and Instrumentation

Pipettes used were Gilson Pipetman P1000, P200, P100 and P10 (Gilson S.A.S, Villiers Le Bel) and associated tips.

PCR machine used was an Eppendorf Mastercycler Personal with a heated lid, capable of holding 16 500µl or 25 200µl tubes and adjustment of time and temperature increments.

Fluorimeter used was an Horiba Jobin Yvon Fluoromax-P equipped with a photon counter and Peltier system for temperature control and stirring facility, coupled to a PC utilising Datamax software for spectral analysis.

ELISA plate reader was a Bio-Tek EL808 Ultra Microplate Reader capable of reading one 96-well ELISA plate at a time with a fixed wavelength, coupled to a PC using Bio-Tek Gen5 microplate data collection and analysis software.

Gel Imager used was a Kodak Image Station 440CF containing 5 filters for visualising chemiluminescent, fluorescent and chromogenic gels and blots, connected to a camera using a 6x optical zoom lens and a PC with Kodak 1D Image Analysis Software for visualisation and analysis.

RQCM was produced by Maxtek Inc with three separate channels for simultaneous measurement of crystals' frequency and resistance, over a wide frequency range 3.8 to 6.06MHz or 5.1 to 10MHz using a high performance phase lock oscillator (PLO) circuit. This equipment was connected to a PC and used Windows-based RQCM datalogging software for data collection and analysis.

UV experiments were conducted on a Bio-Tek Uvikon XL with a Peltier Thermosystem for temperature control and stirring facility, connected to a PC utilising Lab Power Junior software for data collection and analysis.

2.5 Selection

Selection protocols were modified from [4] and our group's previous optimisations [5].

2.5.1 Salt selection method

1. Aptamer Library PCR amplification. Before commencing selection, aptamer library was amplified in a 500µl thin-walled PCR tube by single stranded PCR, prepared on ice, as follows:

Library (40µM)	50
F primer (1mM)	50
R primer (40µM)	50
10x PCR buffer	20
25mM dNTP's	20
25mM $MgCl_2$	5.4
Taq	2
dH_2O	2.6
	200.0µl total volume

The conditions in the PCR programme were as follows:

Step 1: Initial denaturation at 95°C for 10 minutes,

Step 2: Denaturation at 95°C for 1 minute 30 seconds,

Step 3: Annealing of primers at 56°C for 30 seconds,

Step 4: Extension at 72°C for 1 minute 30 seconds, then steps 2-4 repeated 99 times,

Step 5: Final extension at 72°C for 10 minutes.

The amplified library was stored in the refrigerator until it was needed for use.

This protocol was eventually modified to generate more copies of each aptamer species by firstly double stranding the aptamer library before single stranding it, prepared on ice in a 500µl thin-walled PCR tube as follows:

Library (40µM)	50
F primer (1mM)	2
R primer (40µM)	50
10x PCR buffer	20
25mM dNTP's	20
25mM $MgCl_2$	5.4
Taq	2
dH_2O	50.6
	200µl total volume

The conditions in the PCR programme were as follows:

Step 1: Initial denaturation at 95°C for 10 minutes,

Step 2: Denaturation at 95°C for 1 minute 30 seconds,

Step 3: Annealing of primers at 56°C for 30 seconds,

Step 4: Extension at 72°C for 1 minute 30 seconds, then steps 2-4 repeated 30 times,

Step 5: Final extension at 72°C for 10 minutes.

This created enough cDNA to amplify to single-stranded DNA in the next step, which was again prepared on ice:

Product	100
F primer (1mM)	100
10x PCR buffer	30
25mM dNTP's	40
25mM $MgCl_2$	10.8
Taq	2
dH_2O	17.2
	300µl total volume

The conditions in the PCR programme were as follows:

Step 1: Initial denaturation at 95°C for 10 minutes,

Step 2: Denaturation at 95°C for 1 minute 30 seconds,

Step 3: Annealing of primers at 56°C for 30 seconds,

Step 4: Extension at 72°C for 1 minute 30 seconds, then steps 2-4 repeated 99 times,

Step 5: Final extension at 72°C for 10 minutes.

2. Human recombinant polymorphic heparanase was diluted in 100µl salt solution (see above) to 150nM final concentration in a Top Yield PCR tube. This was left to incubate overnight in the fume hood at room temperature.
3. The next day, the tube was washed four times with 200µl salt solution and blotted dry on blue roll to remove any unbound enzyme.
4. 150µl amplified aptamer library was added to the tube and incubated for 1 hour at room temperature, shaking slowly. This was then removed and the tube washed once in salt solution to remove any unbound aptamers.

5. From a stock solution of elution buffer, dilutions were made as follows:

Concentration NaCl (M)	Volume stock solution added (µl)	Volume ultra pure H_2O added (µl)
0.2	6.65	43.35
0.3	10	40
0.4	13.3	36.7
0.5	16.65	33.35
0.6	20	30
0.7	23.3	26.7
0.8	26.65	23.35
0.9	30	20
1.0	33.3	16.7
1.1	36.65	13.35
1.2	40	10
1.3	43.3	6.7
1.4	46.65	3.35
1.5	50	0
3.0M NaSCN	50	0

6. Beginning with the 0.2M elution buffer, 50µl was added to the tube in the same order as above for 1 minute and then removed to a clean PCR tube. Adding elution buffer in this way removes bound aptamers depending on their binding affinities; for example, the 0.2M removes aptamers with the lowest binding affinity, whilst the 1.5M and 3.0M NaSCN removes aptamers with the highest binding affinities.

7. Fractions from the higher salt concentrations were then desalted using Microcons centrifugal filters and double strand amplified by PCR, before being visualised on an agarose gel. This procedure was either terminated here or repeated a further 9 times to yield a ten-round selection method.

2.5.2 Heat selection method - one round

1. Aptamer Library PCR amplification. Before commencing selection, aptamer library was amplified as indicated above (see salt selection protocol) and the amplified library was stored in the refrigerator until it was needed for use.
2. Human recombinant polymorphic heparanase was diluted in 100µl salt solution (see buffers and solutions section) to 150nM final concentration in a Top Yield PCR tube. This was left to incubate overnight in the fume hood at room temperature.
3. The next day, the tube was washed four times with 200µl salt solution and blotted dry on blue roll to remove any unbound protein.
4. 150µl amplified aptamer library were added to the tube and incubated for 1 hour at room temperature, shaking slowly. This was then removed and the tube washed once in salt solution to remove any unbound aptamers.
5. 50µl ultra pure H_2O was added to the tube, the tube was sealed and placed in the PCR machine. A spare tube containing 1ml ultra pure water was kept in the PCR machine to provide water at the correct temperature for all the gradients.
6. The PCR machine was used to generate 5°C intervals from 25°C to 90°C with a two-minute hold on each temperature. After the 90°C temperature gradient, the temperatures chosen were 92°C, 94°C, 96°C and 98°C.

7. After 1 minute of the two-minute hold at each temperature, 50µl water was removed from the tube, placed in a fresh PCR tube and retained for double stranded PCR.
8. The 50µl water was replaced with 50µl water from the spare tube after each extraction, as this was at the same temperature as the water removed.
9. Collected fractions were subjected to double stranded PCR to prepare the aptamers for cloning.

2.5.3 Heat selection method – ten rounds

1. Aptamer Library PCR amplification. Before commencing selection, aptamer library was amplified in a 500µl thin-walled PCR tube by single stranded PCR, prepared on ice, as indicated above.
2. Human recombinant polymorphic heparanase was diluted in 100µl salt solution to 150nM in a Top Yield PCR tube. This was left to incubate overnight in the fume hood at room temperature.
3. The next day, the tube was washed four times in 200µl salt solution and blotted dry on blue roll to remove any unbound protein.
4. 150µl amplified aptamer library was added to the tube and incubated for 1 hour at room temperature, shaking slowly. This was then removed and the tube washed once in salt solution to remove any unbound aptamers.
5. From here PCR reagents were added to the tube as follows:

10x PCR buffer	10.0
25mM dNTP's	10.0
25mM $MgCl_2$	2.7

Taq	1.0
10μM F primer	0.4
0.4μM R primer	10
dH_2O	25.9
	60.0μl

The conditions in the PCR programme were as follows:

Step 1: Initial denaturation at 95°C for 10 minutes,

Step 2: Denaturation at 95°C for 1 minute 30 seconds,

Step 3: Annealing of primers at 56°C for 30 seconds,

Step 4: Extension at 72°C for 1 minute 30 seconds, then steps 2-4 repeated 99 times*,

Step 5: Final extension at 72°C for 10 minutes.

* After 30 cycles of the program, the machine was paused, 1μl more Taq and 39.6μl more forward primer was added and the program was resumed for the further 69 cycles. This was to create some cDNA (as equal concentrations of primers were used in the first part of the PCR reaction) that would allow the generation of single stranded DNA copies after addition of only the forward primer for the second part of the amplification (unidirectional PCR).

6. Another Top Yield PCR tube was sensitised with the protein target ready for the competion of the PCR amplification. PCR products were incubated in the Top Yield tube with the target protein instead of amplified library, eliminating at each step molecules that did not bind or were competed out by stronger binders in the PCR mixture. The process above was repeated nine times to create a ten-round selection and amplification protocol. The aim of this was to amplify the binding aptamers through each cycle and

discard the ones that did not bind or were weaker binders and were thus displaced at each further amplification by the stronger binders, thus resulting in only a few high affinity aptamers.

2.6 Desalting using Microcons filters

These were purchased from Millipore with a 3kDa molecular weight cut off to retain the generated aptamers (which are approximately 23kDa). Each spin cycle recommended by the manufacturer was 60 minutes at 14,000rpm.

1. 500µl ultra pure H_2O was added to the filter; the filter was capped and centrifuged to remove any contaminant glycerin.
2. The flow through was removed and sample plus ultra pure water was added to make a total volume of 500µl, the filter capped and centrifuged again.
3. Flow through was again removed and 500µl ultra pure water was added as a wash step, then spun again and removed, leaving in the filter a small volume of water containing the desalted aptamers.
4. 20µl ultra pure water was added to the filters to ensure enough volume was present to elute the DNA. This was pipetted up and down, and then the filters were inverted and placed into a clean eppendorf tube and spun at 3000rpm for 1 minute to collect the desalted DNA, as per manufacturer's recommendations.

2.7 Buffer exchange using Ultrafree-15 centrifugal filter devices

These were purchased from Millipore with a 10kDa molecular weight cut-off, to retain the 58kDa recombinant heparanase.

1. 15ml ultra pure water was transferred to the centrifugal filter and the cap closed, then placed into a 50ml falcon tube (which acted as the filtrate collection tube) and put into the centrifuge along with a balance tube. This was spun at 2000g for 30 minutes to wash through the membrane and remove any contaminant glycerin.
2. The filtrate was discarded from the collection tube.
3. 2ml human recombinant polymorphic heparanase was added to the filter and made up to 15ml by adding salt solution, the cap was fastened and the tube spun again at 2000g for long enough to concentrate the sample but not so that it dried on the membrane (approximately 20 minutes).
4. After 20 minutes the filtrate was removed, the sample topped up to 15ml with salt solution and spun again at 2000g, this time for long enough to concentrate the sample down to 1ml using the graduations on the filter. The heparanase was then pipetted into a clean stock tube for further use.

2.8 Double Stranded PCR

Double stranded PCRs were conducted at the end of each selection to amplify retained aptamers in preparation for cloning, a sample of which was visualised on an agarose gel to confirm their presence. The double stranded aptamers were then cloned into vector in *E. coli* cells.

Double stranded PCR reaction was prepared on ice, as follows:

DNA	50
10x Buffer	7

dNTPs (25mM)	0.7
Taq	0.7
F primer (1/100)	1.75
R primer (conc)	0.44
$MgCl_2$ (25mM)	1.87
dH_2O	7.55
	70.0µl total volume

The conditions in the PCR programme were as follows:

Step 1: Initial denaturation at 95°C for 10 minutes,

Step 2: Denaturation at 95°C for 1 minute 30 seconds,

Step 3: Annealing of primers at 56°C for 30 seconds,

Step 4: Extension at 72°C for 1 minute 30 seconds, then steps 2-4 were repeated 30 times,

Step 5: Final extension at 72°C for 10 minutes to create poly A tails for cloning into vector.

2.9 Colony PCR

Testing of colonies for insertion of the aptamer into the plasmid was carried out using a PCR of a single colony from the agar plate and putting it directly into the PCR reagents (which were mixed on ice) below:

10x PCR buffer	2.0
25mM dNTP's	0.4

25mM $MgCl_2$	0.53
Taq	0.2
F primer (internal 10µM/M13 100µM)	0.5/0.25
R primer (internal 0.4µM/M13 100µM)	12.5/0.25
dH_2O	3.87/16.37
	20.0µl (per colony)

The conditions in the PCR programme were as follows:

Step 1: Initial denaturation at 95°C for 10 minutes,

Step 2: Denaturation at 95°C for 1 minute 30 seconds,

Step 3: Annealing of primers at 56°C for 30 seconds,

Step 4: Extension at 72°C for 1 minute 30 seconds, then steps 2-4 were repeated 30 times,

Step 5: Final extension at 72°C for 10 minutes.

Two different primers were used to test each colony, internal and M13. The primers referred to as internal are the same ones used in selection, named so because they are internal to the M13, which outflank them. The fragment size generated from these primers in the PCR should be either 75bp if the colonies' DNA contained aptamer or no band if it didn't. The M13 primers were supplied with the cloning kit and recognise loci within the vector spanning across the insert site, hence show a 200bp if there is no aptamer inserted in the vector, or 275bp if there is aptamer inserted in the vector (200bp plus the size of the aptamer). The PCR mix was prepared as above for each colony and then each colony was picked, swiped first on a clean agar patch plate containing 50mg/ml

ampicillin, labelled with colony numbers for identification purposes, and then put into the PCR tube.

2.10 Agarose gel

Extreme care was taken with the use of ethidium bromide due to its carcinogenic properties.

1. Using a balance, 2g agarose was measured into a conical flask with 100ml TBE buffer.
2. The conical flask was heated in the microwave to dissolve the agarose in buffer and make it molten. This then was cooled to approximately 50°C before adding 5µl 10mg/ml ethidium bromide.
3. Masking tape was fixed to the ends of the gel tray to seal them and the gel was poured into the tray. The well comb was added, and this was left to set for 30 minutes.
4. The well comb was removed and the gel tray was put into the gel tank and filled with TBE buffer to the level.
5. 6x gel loading buffer was added to each sample to be loaded. 10µl 25/100bp ladder (see figure 2.1) was also prepared with loading dye.
6. 10µl of each sample was loaded into each well of the gel, with 5µl of ladder loaded into the wells at either end of the gel.
7. The power supply was connected and the gel was run at 100 volts for one hour.
8. The equipment was turned off; the gel was removed and viewed in the imaging apparatus.

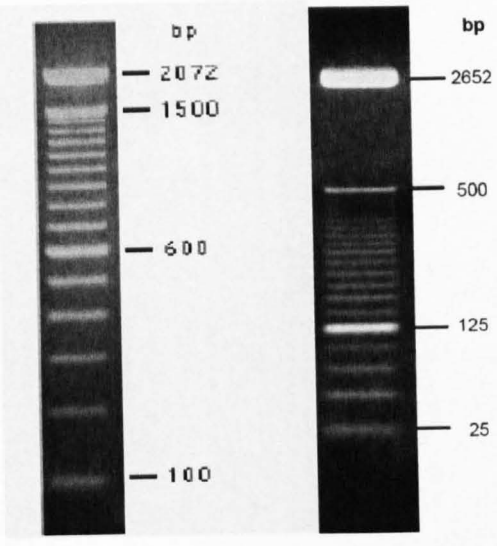

Figure 2.1 – 100bp (left) and 25bp (right) DNA ladders used in agarose gel electrophoresis.

2.11 Cloning

Cloning was carried out using the Topo TA cloning kit with chemically competent Top10 *E. coli* cells.

1. 0.5µl double stranded PCR product was added to 1µl salt solution (supplied with the kit), 1µl TOPO vector and 3.5µl sterile deionised water and incubated for 5 minutes at room temperature.
2. 2µl was taken from the mix above, added to a vial of chemically competent Top10 *E. coli* cells and incubated for 30 minutes on ice.
3. The cells were heat shocked for 30 seconds without shaking at 42°C, then immediately transferred back to ice.
4. 250µl SOC medium (supplied with the kit) was added to the cells, the caps were sealed tightly on the tubes and they were placed in a shaking incubator at 180rpm, 37°C for one hour to recuperate.

5. 10 and 50µl volumes of cells were spread on pre-warmed agar plates (containing 50mg/ml ampicillin) and left overnight in an incubator at 37°C to allow colonies to grow.

2.12 ELISA (enzyme linked immuno sorbent assay)

This was carried out in accordance with [6].

1. An ELISA plate or Top Yield 'ELISA type' PCR tubes were sensitised overnight at room temperature with 100-200µl human recombinant polymorphic heparanase at 150nM concentration.
2. The solution was removed and 10mg/ml BSA in PBS were added and incubated for 20 minutes at room temperature to block the tubes.
3. The solution was removed and the tubes were washed three times in wash buffer and blotted dry on blue roll.
4. 100-200µl primary antibody in EIA diluent was added to each of the samples. Depending on the nature of the ELISA it may have been appropriate to vary the concentration of the antibody, and a dilution series was often used. For a competition ELISA, where it was needed to measure the activity of the competing agent (i.e. aptamer) with the substrate, in comparison to the antibody, either a set concentration of antibody and a dilution series of aptamer was used, or a set concentration of aptamer and a dilution series of antibody. This was left to incubate at room temperature for one hour.
5. The solution was removed and the tubes were washed three times in wash buffer and blotted dry on blue roll.
6. 100µl biotinylated antibody at 2.5µg/ml concentration (in EIA diluent) was added to each of the tubes and incubated for one hour at room temperature.

7. The solution was removed and the tubes were washed three times in wash buffer and blotted dry on blue roll.
8. 100µl streptavidin peroxidase at a 1/500 dilution in EIA diluent was added to each of the tubes and incubated for one hour at room temperature.
9. The solution was removed and the tubes were washed three times in wash buffer and blotted dry on blue roll.
10. 50µl chromogen was added and incubated for 30 minutes at room temperature. There should have been a colour change from colourless to blue.
11. 25µl 10% H_2SO_4 was added to stop the reaction and the plate was put in the plate reader to analyse at 450nm.

2.13 ELISA (enzyme linked immuno sorbent assay) using Streptavidin coated PCR tubes/plates

Streptavidin-coated PCR tubes were purchased pre-coated; however, later ELISA plates were coated with streptavidin/neutravidin/extravidin/avidin to save on cost. This method was modified from [6].

1. For coating of ELISA plates, a 4:1 molar ratio of aptamer:avidin molecule were added in a tube and made to the correct concentration with EIA diluent. After 2 hours, 100µl was plated in the relevant wells of the plate and left to incubate overnight at 4°C. Strips of streptavidin-coated PCR tubes were sensitised overnight at room temperature with 100µl 5'biotinylated aptamer at varying concentrations, often using a dilution series.
2. The solution was removed the next day and the tubes were blocked by incubating them with 10mg/ml BSA in PBS for 20 minutes at room temperature.

3. The solution was removed and the tubes were washed three times in wash buffer and blotted dry on blue roll.
4. Concentrations of human recombinant polymorphic heparanase were added to the tubes and incubated for one hour at room temperature. The concentrations were either fixed if the aptamer concentration was varied, or varied using a dilution series, whilst keeping the aptamer concentration fixed.
5. 100µl rabbit polyclonal anti-heparanase IgG primary antibody in EIA diluent was added to each of the samples at a concentration of 165nM. This was left to incubate at room temperature for one hour.
6. The solution was removed and the tubes were washed three times in wash buffer and blotted dry on blue roll.
7. 100µl biotinylated antibody at a 2.5µg/ml concentration (in EIA diluent) was added to each of the tubes and incubated for one hour at room temperature.
8. The solution was removed and the tubes were washed three times in wash buffer and blotted dry on blue roll.
9. 100µl streptavidin peroxidase at a 1/500 dilution in EIA diluent was added to each of the tubes and incubated for one hour at room temperature.
10. The solution was removed and the tubes were washed three times in wash buffer and blotted dry on blue roll.
11. 50µl chromogen was added and incubated for 30 minutes at room temperature. There should have been a colour change from colourless to blue.
12. 25µl 10% H_2SO_4 was added to stop the reaction and the plate was put in the plate reader to analyse at 450nm.

2.14 EMSA (electrophoretic mobility shift assay)

For 2 gels (µl)	1%	8%	10%	15%	18%
Acrylamide	300	2400	3000	4500	5400
Water	6742.5	4642.5	4042.5	2542.5	1642.5
5x TBE	1800	1800	1800	1800	1800
100mg/ml APS	150	150	150	150	150
TEMED	7.5	7.5	7.5	7.5	7.5

Extreme care was taken whilst using unpolymerised acrylamide due to its carcinogenic properties.

1. Gel plates were carefully washed in water and dried with blue roll. They were then clipped into the casting apparatus and into the gel plate.
2. The gel was made as per the quantities above, leaving the APS and TEMED until last, as these caused the gel to polymerise. The gels were poured quickly using a pipette, the well combs were subsequently inserted and the gel was left to set for 2 hours.
3. Meanwhile the reactions were prepared: A 1:1 ratio of aptamer to protein at 4µM concentration was used. The volumes required were added to 5µl 5x TBE, and the volume was made up to 20µl with ultra pure water. These were then left to incubate for one hour at room temperature.
4. Before loading the samples, the gel was set to pre-run. The castor was unclipped from the gel plate and transferred to the tank. Fresh 1x TBE was added up to the level and the well combs were removed. The wells were cleaned out using a syringe and hypodermic needle to dislodge any excess gel. The voltage supply was connected and run for 1 hour at 120 volts.

5. 6x loading dye were added to the samples and ladder and they were loaded on to the gel using a pipette. The gel was either run overnight (preferable) at 15-20 volts or for about 3-4 hours at 70 volts, until the bottom of the loading dye reached the bottom of the gel.
6. After running the gel, the equipment was switched off, the gel was removed from the plates and the equipment was washed. The gel was transferred to a container with 100ml 1x TBE containing 0.5µg/ml ethidium bromide (the running buffer was re-used for this). A lid was put on the container and shook slowly for one hour.
7. After the hour, the gel was removed, rinsed in water and viewed under the gel imaging equipment.

2.15 Fluorescence Quenching Titrations

These were conducted based on the method described by Missailidis *et al.* [7].

1. The fluorimeter and computer were switched on and left to equilibrate for 30 minutes.
2. Settings were calibrated for the experiment: emission acquisitions were taken with an excitation wavelength of 280nm. Emission spectra were measured from 300nm to 420nm every 5nm, with 1 second at each measurement and the slits were ±5nm.
3. In a 100µl fluorescence cuvette, which was washed with water prior to using, human recombinant polymorphic heparanase or linker peptide were diluted to 100µl at the appropriate concentration in salt solution.
4. The cuvette was immediately placed into the fluorimeter and a scan taken.
5. Immediately after the scan, appropriate volume additions of 100µM unmodified aptamer to be tested were added to the cuvette so that the total ratios of heparanase:aptamer were 10:1, 5:1, 2.5:1, 1.25:1 and 0.625:1.

6. After each addition a scan was taken and then after all scans had been taken, the cuvette was washed in water, methanol and then nitric acid, ready for the next experiment.
7. Data were analysed using Microsoft Excel, then Microcal Origin to estimate K_A values by using the relevant quadratic equation [7] as explained in chapter four.

2.16 Immunoperoxidase staining of paraffin embedded tissue (sections cut at 5μm)

These experiments were conducted at The University of Manchester within the Maternal and Foetal Research Group under supervision of Drs John Aplin and Lynda Harris, as follows [2].

1. Slides were warmed for 10 minutes at 60 degrees to soften wax.
2. Sections were deparaffinised in three consecutive baths of xylene for 5 minutes each, then 100%, 100% and 70% alcohol for one minute each.
3. Slides were rinsed in running water from tap.
4. Slides were immersed in a plastic dish containing citrate buffer (see section 2.2 buffers and solutions) and microwaved at high temperature for 5 minutes with lid on loosely. Buffer level was topped up after 5 minutes and then they were microwaved for a further 5 minutes.
5. Slides were left to cool for 20 minutes (in the microwave).
6. To block endogenous peroxide activity, slides were placed in methanol containing 0.4% (v/v) HCl and 0.5% (v/v) H_2O_2 for 30 minutes.
7. Slides were rinsed in running water from tap.
8. Slides were washed for 5 minutes in three baths containing TBS.

9. Excess moisture was wiped from the slides with a soft tissue and the sections were drawn around with a Dako pen.
10. Sections were blocked for 30 minutes with 5% BSA in TBS and then dabbed off without a washing step.
11. Primary antibody/aptamers were diluted using TBS (1:100 dilutions for anti-heparanase and anti-cytokeratin 7, neat for control mouse antibody and 1:200 dilution for all aptamers; generating similar concentrations), added to the sections and left overnight at 4°C in a humidity chamber. Concentrations and incubation times were previously optimised in this assay using antibodies [2].
12. Slides were washed for 5 minutes in three baths containing TBS.
13. Secondary antibodies were added at 1:200 dilutions for 1 hour at room temperature to relevant sections, aptamer-labelled sections were incubated with TBS only.
14. Antibodies were washed off with TBS wash bottle and then slides were washed for 5 minutes in three baths containing TBS.
15. Excess moisture was wiped from the slides with a soft tissue, and then avidin peroxidase was added to all sections @ 5µg/ml in 0.125M TBS. These were incubated at room temperature for 1 hour and then washed off using a TBS wash bottle.
16. 3,3'-Diaminobenzidine tetrahydrochloride (DAB) was used to develop the avidin peroxidase. This was composed of 0.05% (w/v) DAB and 0.015% (v/v) H_2O_2 in TBS, and was firstly added to one section, observed under a microscope, then the reaction was stopped upon completion by rinsing in running water. The time for completion of the reaction was recorded and used when staining the rest of the sections.
17. Slides were rinsed in running water from tap.
18. Slides were counterstained with Mayers' haematoxylin for 5 minutes, and then rinsed under tap water.

19. Slides were put into acid alcohol solution to remove excess stain for five seconds and then rinsed in tap water for 5 minutes.
20. Slides were dehydrated in 70%, 100% and 100% alcohol, then two consecutive baths of xylene for 5 minutes each.
21. Slides were mounted with large coverslips using XAM.

2.17 FITC and PI-labelling cell culture coverslips

These experiments were conducted at The University of Manchester within the Maternal and Foetal Research Group under supervision of Drs John Aplin and Lynda Harris, as follows [2].

1. Cells were previously fixed in 4% paraformaldehyde for 15 minutes.
2. Cells were permeabilised by incubating them in 0.1% triton in PBS for 10 minutes.
3. Cells were washed in PBS three times.
4. Primary antibody/biotinylated aptamers were added and incubated for 1 hour at room temperature (1:100 dilutions for anti-heparanase and anti-cytokeratin 7, neat for control mouse antibody and 1:200 dilutions for all aptamers). Concentrations and incubation times were all previously optimised using this assay with antibodies and the aptamers used in this study were diluted to these same concentrations.
5. Cells were washed in PBS three times.
6. Secondary antibodies were added at 1:200 dilutions to heparanase and control mouse antibody-labelled coverslips only and incubated for 1 hour at room temperature (aptamer-labelled coverslips were left in PBS only).
7. Cells were washed in PBS three times.

8. Streptavidin-FITC conjugate was added to all coverslips at a 1:50 dilution of stock and incubated for 1 hour at room temperature underneath a cover to preserve the fluorescence.
9. Cells were washed in PBS three times.
10. Coverslips were blotted on a soft tissue and mounted onto slides using Vectashield mounting medium containing propidium iodide. To secure the coverslips to the slides, clear nail varnish was used around the edges.

2.18 Matrigel invasion assay method

These experiments were conducted at The University of Manchester within the Maternal and Foetal Research Group under the supervision of Drs John Aplin and Lynda Harris [2].

1. Transwell inserts were placed into each experimental well of a 24-well plate. One coverslip per experiment was sterilised in IMS to be used as an indicator of cell confluency throughout the experiment. 20µl Matrigel previously diluted to working concentration; (1:8 in serum-free medium) was added to each insert and spread around with a pipette tip then left to dry in the incubator for at least 30 minutes.
2. OC MZ-6 and PL4 cells for the experiment were passaged. Culture medium was removed from the flasks which were then washed twice with PBS, removed and replaced with 3ml trypsin EDTA. The flasks were incubated until the cells had detached and then the suspension was transferred to a centrifuge tube and spun for 5 minutes @ 1000rpm. The supernatant was removed and cells were resuspended in 2ml of their respective supplemented medium (specified in section 2.3; Cell lines and culture conditions) and

then counted with a haemocytometer. $6x10^4$ cells were required for each well so cell concentration was adjusted to $6x10^5$cells/ml.

3. 500µl medium was added around the edge of each insert and then 400µl medium plus 100µl cells into the insert. Cells were left in the incubator for one hour to adhere to the Matrigel.
4. The medium from both the insert and the well was removed then replaced with aptamer/antibody/control solution (all at 1:100 dilutions in fresh medium) 500µl each into the insert and the well and the plate incubated for 24 hours in the incubator.
5. After 24 hours the coverslip was viewed to make sure the cells had grown enough. If not, they were left for up to another 24 hours.
6. The cells were then fixed in 4% paraformaldehyde for 15 minutes and permeabilised in 0.1% triton for 10 minutes, then stored in PBS @4°C until they were ready to be stained.
7. The transwells were removed with forceps and the inside of the insides of each membrane wiped with a cotton bud to remove all cells. Freshly filtered haematoxylin was added both sides of the insert to stain the nuclei of the cells. Haematoxylin was replaced with PBS then the inserts were plunged into a beaker of hot water to activate the stain. The insides of the membranes were once again wiped with a cotton bud and then the membranes cut out, placed on the slides and mounted.
8. The slides were viewed under light microscope at x10 magnification, eight to ten representative areas were selected and the cells counted. Data were represented as the mean ± its standard deviation, and an unpaired two-tailed t-test was conducted to assess the significance of the results.

2.19 Myoma organotypic model method

These experiments were conducted at The University of Oulu, Finland, within the Institute of Dentistry and under supervision of Professor Tuula Salo, Drs Pia Nyberg and Sirpa Salo and Sini Nurmenniemi [3].

2.19.1 Day 1

1. Media was warmed prior to use on each day of experiment.
2. Previously frozen myomas from the same batch were transferred into a petri dish then into a 50ml tube containing fresh media for 1 hour as they were stored in media containing DMSO so need to be washed. Transwell plates were labelled.
3. Myomas in medium were transferred into a fresh Petri dish and using forceps, pushed down vertically into each transwell insert so there were no gaps where cells could fall.
4. HSC-3 tongue carcinoma cells were prepared by removing the medium, washing x2 in PBS then adding 3ml trypsin-EDTA and incubating until cells had detached.
5. The cell suspension was transferred to a 50ml falcon tube and spun down in a centrifuge so that the trypsin could be removed and replaced with fresh medium. The cells were then counted manually after pipetting 20µl suspension into the haemocytometer. 700,000 cells per myoma (50µl) were required so the cell suspension was diluted to 14,000,000 cells/ml with fresh medium.
6. Cells were prepared for the experiment in eppendorf tubes by adding 150 µl cells plus 1.5µl inhibitor. These volumes were correct for a 1/100 dilution of inhibitor, performed in triplicate samples.
7. Medium containing inhibitor was prepared for the whole experiment and stored in 15ml falcon tubes – 4 or 5 changes of 1ml per sample. This ensured that each change of media contained an equal concentration of inhibitor.

8. 1ml medium containing inhibitor was pipetted below the transwell and 50µl cell suspension plus inhibitor pipetted on top of the myoma. The plate was incubated for 24 hours at 37°C to allow cells to attach to the myoma surface.

2.19.2 Day 2

1. In fresh 12 well culture plates, a metal grid was transferred to each experimental well using sterile forceps. From the transwell plate, the medium (containing its respective inhibitor) below the transwell was pipetted to the corresponding well on the 12-well plate, then, using sterile forceps, one piece of sterile nylon membrane was added atop of each grid.
2. Using 2 pairs of forceps, the transwell membrane was perforated from the bottom and each myoma was carefully lifted out, maintaining its orientation, and placed on top of the corresponding grid.
3. The experiment was cultured for 2 weeks, changing (and retaining) the media on days 5, 8 and 11 with fresh inhibitor-containing medium.

2.19.3 Day 14

1. Media was removed and retained in eppendorf tubes, then frozen for later use.
2. Myoma tissues were transferred to cassettes and placed in 4% paraformaldehyde to dehydrate and fix the tissue.

2.19.4 Histology, IHC and visualisation

1. Myomas were fixed in formalin for 12 hours, then dehydrated, longitudinally bisected and embedded in paraffin.
2. 6μm sections were deparaffinised and endogenous peroxidase activity blocked by incubation in 0.3% H_2O_2 in methanol for 30 minutes.
3. Antigen retrieval was performed by microwaving the sections in Tris/EDTA (10mmol/L Tris, 1mmol/L EDTA, pH9) for 20 minutes, after which the sections were blocked with 2% BSA in PBS for 30 minutes and then incubated with mouse anti-cytokeratin antibody in REAL antibody diluent overnight at 4°C in a humidity chamber.
4. Sections were washed twice in PBS for ten minutes after each step.
5. Biotinylated anti-mouse secondary antibody was incubated for one hour, then StreptABComplex/HRP on 0.5M NaCl in PBS for 30 minutes.
6. 3,3'-diaminobenzidine was incubated on each section for 3 minutes to develop the stain on the antigen, then the sections were mounted using xylene.
7. Slides were viewed under light microscope at x100 magnification and nine representative images were taken from each of the three repeats of every treatment. Images were analysed using ImageJ software [8] to determine maximal invasion depth (distance from surface of tissue to deepest invaded cell), maximum invasion area and invasion index [1-(noninvading area/total area)]. Figures were analysed using Microsoft Office Excel and unpaired two-tailed t-tests were used to assess the statistical significance.

2.19.5 ELISA

All dilutions were carried out using EIA diluent (20mM Tris, 150mM NaCl, 0.1% BSA, 0.05% Tween 20, pH 7.5) unless otherwise stated. Experiments were performed in triplicate.

1. ELISA plates were sensitised with streptavidin and 10µg/ml biotinylated synthetic peptide SP102 (QYDSYDVKSGVAVGGGGGK-biotin), then washed three times in wash buffer (see section 2.2 buffers and solutions).
2. In a separate tube, media samples were diluted 1:200 and 135µl was added to 15µl of a 1:40 dilution of primary antibody raised in rabbit (against synthetic N terminal telopeptide QNYSPQYDSYDVKSGVAVGG from type III collagen). This was incubated for 30 minutes at room temperature, then 100µl was added to the corresponding well of the ELISA plate and incubated for one hour at room temperature.
3. Wells were then washed three times with wash buffer and blotted dry.
4. HRP-conjugated anti-rabbit secondary antibody at a 1:50,000 dilution in Quardian peroxidase conjugate stabiliser was added to each well and incubated for one hour at room temperature.
5. Wells were again washed three times with wash buffer.
6. 100µl chromogen containing substrate tetramethylbenzidine (TMB) was added to each well and after a 30 minute incubation the reaction was stopped by adding 100µl 2M H_2SO_4. The absorbance was taken at 450nm.

Controls included TMB substrate solution only and antibody only.

2.19.6 RIA

Each sample was processed in duplicate. Media from samples containing cells were diluted 1:10 or 1:2 for those without cells.

1. 200µl media sample was incubated with 200µl tracer (synthetic peptide GGVGAAAIAGIGGEKAGGFAPY – ^{125}I) and 200µl primary antibody (raised in rabbit immunised with synthetic peptide GGVGAAAIAGIGGEKAGGFAPY) for two hours at 37°C.
2. 500µl PEG containing anti-rabbit secondary antibody was added and incubated for 30 minutes at 4°C, the samples were spun in a centrifuge at 3000rpm for 30 minutes, supernatants were removed and the pellets were measured using a gamma reader.

Controls used:

Synthetic peptide (GGVGAAAIAGIGGEKAGGFAPY) diluted between 1:128,000 and 1:4,000 + tracer + primary antibody to form standards;

PBS-tween + tracer + unrelated rabbit antibody to generate no signal;

Synthetic peptide only to generate no signal;

PBS-tween + tracer + primary antibody, generating maximum signal;

Unrelated synthetic peptide + tracer + primary antibody, also generating maximum signal.

2.20 Serum Stability Assays

Extreme care was taken whilst using unpolymerised acrylamide due to its carcinogenic properties.

1. In one tube per time point, 1µl 100µM aptamer stock was incubated with 17µl human or mouse serum and left for the required time (30 minutes, 1, 2, 3, 4 and 5 hours) at room temperature. The reaction was stopped by adding 2µl 1M EDTA and the samples were kept at -20°C until ready to run on a native polyacrylamide gel.

2. A 12% native polyacrylamide gel was used: 3.6ml acrylamide, 3.4ml ultra pure water and 1.8ml 5x TBE were mixed in a 25ml universal bottle, then 150µl 100mg/ml APS and 7.5µl TEMED were added, quickly mixed, and the gel poured immediately. The well combs were subsequently inserted and the gel was left to set for 2 hours.
3. The gel was then pre-run and the samples loaded as the protocol for EMSA details.

2.21 Quartz Crystal Microbalance (QCM)

2.21.1 Immobilisation of 5'biotinylated aptamers to gold-coated quartz crystals.

Immobilisations were carried out according to Liss et al. [9].

1. Gold surfaces of each 5MHz crystal were cleaned with two injections of ice-cold piranha solution, with a 500µl wash of ice-cold water after each injection.
2. Crystals were immersed in ice-cold H_2O, and then transferred to an oven to dry at 100°C for at least an hour.
3. Activation of gold surfaces was achieved by adding 4mg/ml 3,3' dithiodipropionic acid (DSP) in water-free N,N-dimethylacetamide (DMA), sealing the crystal within a chamber and incubating for 15 minutes at room temperature.
4. The crystals were washed three times with sterile PBS.
5. 1mg/ml streptavidin diluted in sterile PBS was injected onto the crystal surface; the crystal sealed in a chamber and incubated overnight at 4°C.
6. The crystals were washed five times with PBS, and then the crystal was blocked by adding 0.025% BSA in PBS and incubating for one hour at room temperature.

7. 5' biotinylated aptamers, diluted to 2μM in PBS were added after being heated to 95°C and cooled on ice, and incubated for one hour at room temperature.
8. The crystals were washed well in PBS and used immediately.

2.21.2 Experiments:

Experiments were carried out, in accordance with Liss *et al.* [9], to measure the binding of heparanase to the aptamers immobilised on the crystal using solutions that were kept at room temperature, with care taken to avoid fluctuations in temperature, humidity, and pressure.

1. The crystal was placed in the flow cell, taking care to orientate it correctly, and the system was set up as shown in figure 2.2.
2. PBS was run through the system for one minute on fast flow, then the pump was halted, the program and monitoring switched on, the capacitance adjusted, and the crystal left to equilibrate in the PBS contained within the flow cell for one hour or until the reading was stabilised.
3. After pausing the program and taking care not to introduce any air into the system, human recombinant polymorphic heparanase diluted in PBS was added to the flow cell, using the pump to pull the liquid through very slowly, then the pump was halted and the program was resumed.
4. When the readings had stabilised, the program was paused and the crystal was washed using the pump to pull 10ml PBS through the system, the pump was ceased and the readings resumed.

5. After the readings had settled, the program was paused and the crystal was regenerated with 10ml 100mM EDTA, then 3.0M NaSCN before the experiment ended. The crystal was kept at 4°C in a chamber of PBS containing 0.02% sodium azide until the next experiment.

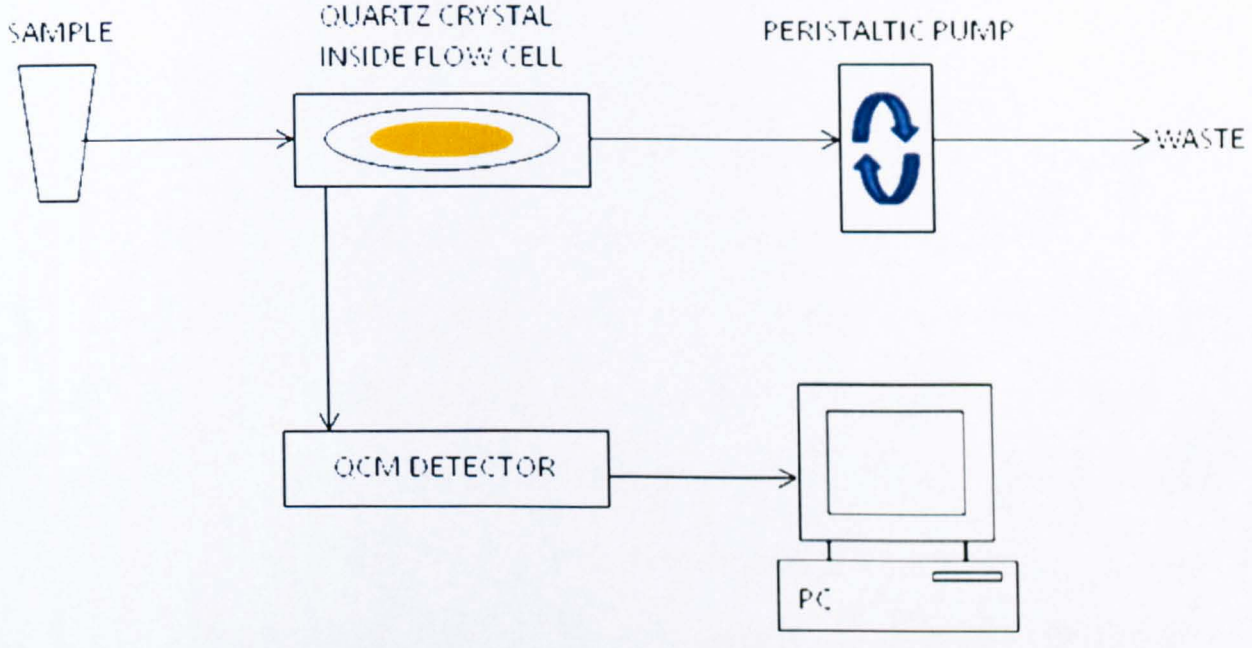

Figure 2.2 – Experimental set-up of QCM stop-flow equipment. The peristaltic pump pulls sample through the flow cell and all data are sent from the flow cell via the QCM detector to the PC for analysis.

2.22 Interaction of Aptamers with Serum Albumins

Experiments were conducted based on methods by Silva et al., [10-12]. Absorbance was measured using a UV spectrophotometer to generate a wavelength scan incorporating wavelengths of 280 and 290nm. Fluorescence emission was measured between 300 and 400nm using an excitation wavelength of 290nm, corresponding to the excitation wavelength of the tryptophan residues. Emission and excitation wavelength slits were set

to 3nm for all experiments. Both UV and fluorescence experiment were conducted at 37°C by use of the Peltier Thermosystems to automatically control the temperature.

2.22.1 UV titrations

1. In a 3ml cuvette, 1ml PBS was used to autozero the equipment, which was set up to measure samples as per the conditions outlined above.
2. 1ml HSA diluted to 6μM in PBS was transferred to a 3ml cuvette and the absorbance measured after allowing 5 minutes for the cuvette and solution to reach 37°C.
3. Additions of between 1 and 6.4μl of the selected aptamer were made after the previous reading had been completed. After making the addition, a pipette was used to mix the solution in the cuvette by gradually pipetting up and down. This was then left for one minute to mix and interact with the HSA before taking the absorbance measurement. Total concentration of aptamer in the cuvette began at 0.01μM and ended with 0.33μM.
4. All experiments were repeated at least three times to gain consistency, and data were plotted and analysed from Microsoft Office Excel and Microcal Origin.
5. At the end of the experiment, the cuvettes were washed in detergent and ultra-pure water.

2.22.2 Fluorescence titrations

1. The equipment was set up to measure samples as per the conditions outlined above.
2. 1ml HSA diluted to 60μM in PBS was transferred to a 3ml cuvette and the absorbance measured after allowing 5 minutes for the cuvette and solution to reach 37°C.

3. Additions of between 1 and 6.4µl of the selected aptamer were made after the previous reading had been completed and were set up to read every 90 seconds, leaving time to make the next addition, pipette up and down gently to mix, and interact before the following reading was taken. Total concentration of aptamers began at 0.12µM and ended with 7.1µM.
4. A total of three scans were taken per addition, which were then averaged and plotted in Microsoft Office Excel and Microcal Origin for analysis.
5. At the end of the experiment, the cuvettes were washed in detergent and ultra-pure water, and then soaked in nitric acid.

References:

1. He, X., P.E. Brenchley, G.C. Jayson, L. Hampson, J. Davies, and I.N. Hampson, *Hypoxia increases heparanase-dependent tumor cell invasion, which can be inhibited by antiheparanase antibodies.* Cancer Res, 2004. **64**(11): p. 3928-33.
2. Harris, L.K., P.N. Baker, P.E. Brenchley, and J.D. Aplin, *Trophoblast-derived Heparanase is Not Required for Invasion.* Placenta, 2008. **29**(4): p. 332-7.
3. Nurmenniemi, S., T. Sinikumpu, I. Alahuhta, S. Salo, M. Sutinen, M. Santala, J. Risteli, P. Nyberg, and T. Salo, *A novel organotypic model mimics the tumor microenvironment.* Am J Pathol, 2009. **175**(3): p. 1281-91.
4. Ellington, A.D. and J.W. Szostak, *In vitro selection of RNA molecules that bind specific ligands.* Nature, 1990. **346**(6287): p. 818-22.
5. Missailidis, S., D. Thomaidou, K.E. Borbas, and M.R. Price, *Selection of aptamers with high affinity and high specificity against C595, an anti-MUC1 IgG3 monoclonal antibody, for antibody targeting.* Journal of Immunological Methods, 2005. **296**(1-2): p. 45-62.
6. Ferreira, C.S., K. Papamichael, G. Guilbault, T. Schwarzacher, J. Gariepy, and S. Missailidis, *DNA aptamers against the MUC1 tumour marker: design of aptamer-antibody sandwich ELISA for the early diagnosis of epithelial tumours.* Anal Bioanal Chem, 2008. **390**(4): p. 1039-50.
7. Missailidis, S., *Targeting of antibodies using aptamers.* Methods Mol Biol, 2004. **248**: p. 547-55.
8. Abramoff, M.D., P.J. Magelhaes, and S.J. Ram, *Image Processing with ImageJ.* Biophotonics International, 2004. **11**(7): p. 36-42.

9. Liss, M., B. Petersen, H. Wolf, and E. Prohaska, *An aptamer-based quartz crystal protein biosensor.* Anal Chem, 2002. **74**(17): p. 4488-95.

10. Silva, D., C.M. Cortez, J. Cunha-Bastos, and S.R. Louro, *Methyl parathion interaction with human and bovine serum albumin.* Toxicol Lett, 2004. **147**(1): p. 53-61.

11. Silva, D., C.M. Cortez, and S.R. Louro, *Chlorpromazine interactions to sera albumins. A study by the quenching of fluorescence.* Spectrochim Acta A Mol Biomol Spectrosc, 2004. **60**(5): p. 1215-23.

12. Silva, D., M. Cortez-Moreira, V.L.F. Cunha Bastos, J. Cunha Bastos, and C. Martins Cortez, *The interaction of methyl-parathion with serum and albumin of the neo-tropical fish Piaractus mesopotamicus.* Ecotoxicology and Environmental Safety. **73**(1): p. 32-37.

CHAPTER THREE

SELECTION OF APTAMERS TO HEPARANASE AND LINKER PEPTIDE

3.1 Background

As described in the introduction, selection procedures were based on the SELEX methodology and protocol [1] with modifications based on the group's previous optimisations and according to the needs of the project. After incubation with target, aptamers were eluted using high salt concentrations or temperatures as both have the potential to denature or at least reversibly reconfigure the structure of heparanase, so that bound aptamers are released. It follows that at lower temperatures or salt concentrations, non-binders and weakly bound aptamers are released, whilst retaining the strongly bound. Therefore, using either tactic, the most promising aptamers should be found in the elutions of highest salt or temperature as will be described in this chapter.

3.1.1 Aptamer Library

The aptamer library used contained a 25 base-long variable sequence, of which each position could carry an A, C, G or T base, flanked at the 5' end by a 23-base fixed sequence (GGG AGA CAA GAA TAA ACG CTC AA) and at the 3' end by a 24-base sequence (TTC GAC AGG AGG CTC ACA ACA GGC). These fixed sequences are used for the purpose of recognition for primers (GGG AGA CAA GAA TAA ACG CTC AA and GCC TGT TGT GAG CCT CCT GTC GAA) whilst amplifying in PCR, and also add stability to the structure of the aptamer. The chosen length of variable sequence results in a total of 4^{25} (or 10^{15}) different sequence combinations, allowing all known structures to be formed, such as hairpins and superloops, and where the sequence is GC-rich, creates stability through the formation of quadruplex structures, formed between guanine bases.

The Avogadro constant states that one mole of substance contains 6.022×10^{23} entities or molecules, and therefore to ensure that an aptamer library theoretically contains at least one copy of each sequence of the 10^{15} different possibilities, there must be 1.7nmoles of aptamer library material. Each aptamer library was ordered to a scale of 40nmoles to contain approximately 24 copies of each sequence and then amplified forthwith to further enrich the availability of each species and ensure that high binders are not lost due to the vast excess of non-specific binders.

3.1.2 Heparanase and Heparanase Linker Peptide

Aptamers were generated against human polymorphic recombinant heparanase, expressed in insect cells [2], of which amino acids 1-36 (shown in red in diagram below) form the signal peptide sequence (not part of the active enzyme); amino acids 37-108 form the 8kDa subunit; 109-156 (in purple) form the 6kDa linker peptide, which is excised and hence not part of the active enzyme, and 157-543 show the 50kDa subunit. Amino acid 307 (in orange) shows the polymorphism; a point mutation from arginine to lysine.

MLLRSKPALP PPLMLLLLGP LGPLSPGALP RPAQAQDVVD LDFFTQEPLH LVSPSFLSVT
IDANLATDPR FLILLGSPKL RTLARGLSPA YLRFGGTKTD FLIFDPKKES TFEERSYWQS
QVNQDICKYG SIPPDVEEKL RLEWPYQEQL LLREHYQKKF KNSTYSRSSV DVLYTFANCS
GLDLIFGLNA LLRTADLQWN SSNAQLLLDY CSSKGYNISW ELGNEPNSFL KKADIFINGS
QLGEDFIQLH KLLRKSTFKN AKLYGPDVGQ PRRKTAKMLK SFLKAGGEVI DSVTWHHYYL
NGRTATKEDF LNPDVLDIFI SSVQKVFQVV ESTRPGKKVW LGETSSAYGG GAPLLSDTFA
AGFMWLDKLG LSARMGIEVV MRQVFFGAGN YHLVDENFDP LPDYWLSLLF KKLVGTKVLM

ASVQGSKRRK LRVYLHCTNT DNPRYKEGDL TLYAINLHNV TKYLRLPYPF SNKQVDKYLL RPLGPHGLLS KSVQLNGLTL KMVDDQTLPP LMEKPLRPGS SLGLPAFSYS FFVIRNAKVA ACI

Recombinant heparanase has been shown to exhibit maximum activity at pH 5, although still retains approximately 20% of this level of activity at pH 7 [2]. Furthermore, it has been shown to significantly degrade cell-surface heparan sulfate at pH 7.4, after 4 hours, with an indistinguishable profile of degradation of heparan sulfate from the native enzyme [2]. Analysis of the sequence of recombinant enzyme, based on Henderson-Hasselbalch parameters, suggests that the isoelectric point (pI) of the enzyme is approximately 9.5; therefore at pH 7.2 the enzyme will have a net charge of +17.8, and +34.39 at pH 5. This is considered generally advantageous and facilitating aptamer binding, as it offers an initial positive electrostatic interaction between the aptamer and the target enzyme, although it can also allow an increased non-specific interaction due to charge.

The linker peptide is a GST recombinant fusion peptide of 49 amino acids. It has a molecular weight of 6089.7 and a theoretical pI of 4.56. At pH 7.2 the peptide has an overall charge of approximately -3.04. The negative charge of the peptide may have implications on aptamer selection, as DNA sequences carry an overall negative charge, due to the DNA phosphate backbone. However, the presence of arginines in the peptide sequence can offer anchors that have been shown to facilitate aptamer binding [3]. Two different aptamer selection approaches have been adopted, based on different elution protocols, one based on heat denaturation and one on salt elution, as described below.

3.2 Heat One-Step Method

In an attempt to remove desalting steps and optimise the selection procedure from previously used protocols involving high salt or chaotropic agents, an alternative method of selection was performed. This method was based on using heat, instead of salt, to release the bound aptamers from the enzyme. A buffer exchange was carried out on recombinant heparanase using Millipore Ultrafree-15 centrifugal devices to replace the original 25mM Trizma base, 0.7M NaCl pH 7.5 with 0.1M salt solution, pH 6.5 in order to reduce the NaCl concentration of the solution and slightly decrease the pH of the solution, so as the enzyme to be positively charged. This solution was also used as adsorption buffer of the protein to ELISA plates and functionalised 'Top Yield' PCR tubes (see below), as carbonate buffer at pH 9.6 would confer a slightly positive charge on the enzyme due to it being above the theoretical pI of the protein, which could have an adverse effect on aptamer binding and selection.

Prior to selection, aptamer library was amplified using a single stranded PCR protocol, and human recombinant heparanase at a concentration of 10µg/ml, diluted in 0.1M salt solution pH 6.5, was adsorbed to 'Top Yield' PCR tubes overnight on ice in the fume hood. Aptamer library was incubated for one hour with heparanase and, after washing the tube with wash buffer, 50µl volumes of ultra pure H_2O were added to the tube, heated to increasing temperatures (50, 60, 70, 80, 90, 92, 94, 96, 98°C), and then removed and retained. A PCR was carried out on all of the temperature-eluted samples to double-strand the DNA for cloning, and a 2% agarose gel was run with 100bp ladder to check for presence of aptamers (figure 3.1). The gel showed that the only viable band at 75bp was present in the 92°C fraction, which was subsequently taken forward to the cloning stage.

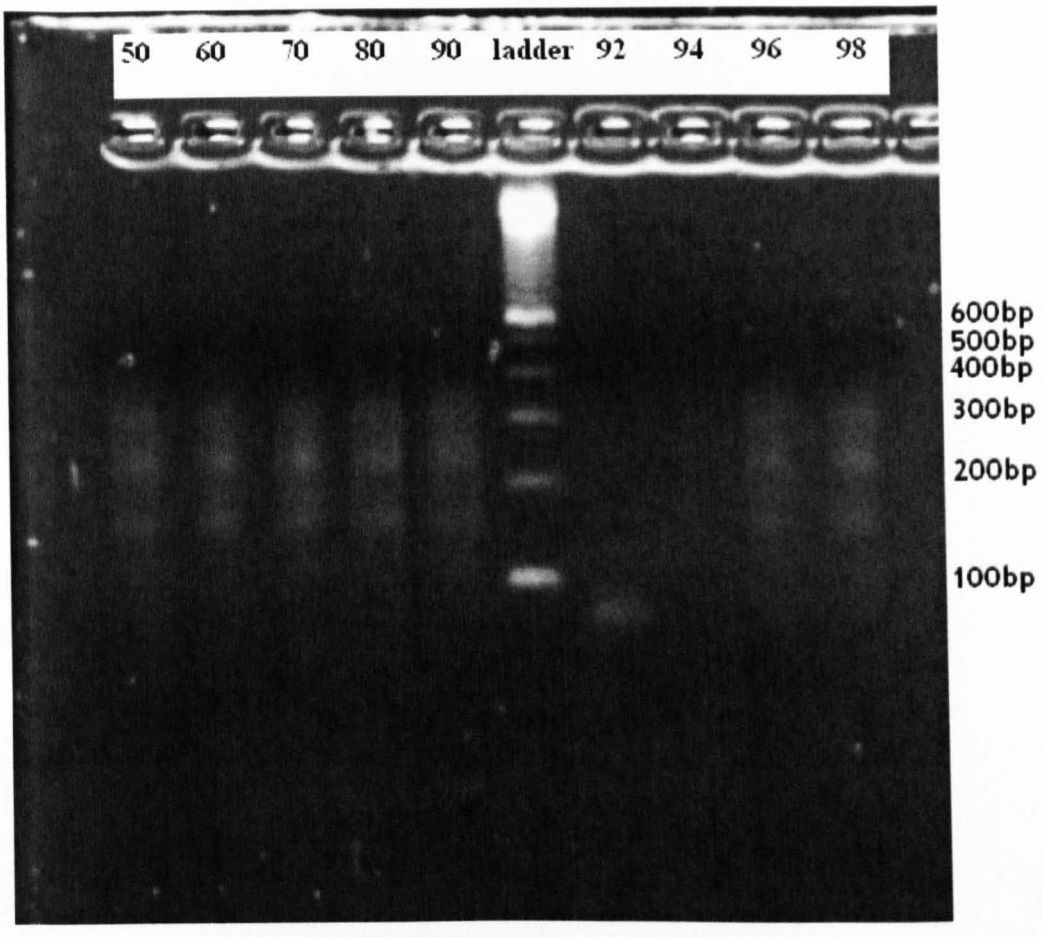

Figure 3.1 – A 2% agarose gel was used to check for presence of 75bp aptamers from the highest temperature elutions. Only one viable band was observed from the 92˚C elution, which was selected for cloning.

The product from the elution at 92˚C was cloned into TOPO vector and chemically competent *E. coli* cells according to the cloning protocol (see materials and methods). This generated single colonies on an agar plate containing ampicillin, which were then tested directly using two primer sets: internal forward and reverse primers, and M13 forward and reverse primers, according to the PCR method.

2% agarose gels were run to see if the correct size fragments were present following cloning (an example of which is shown in figure 3.2). Should cloning have been successful, the internal primers would show the full 75bp of the aptamer, whereas the M13 primer set would show a band at 200bp if the M13 gene were uninterrupted (i.e. no aptamer inserted) or a 275bp band with the aptamer present in the gene.

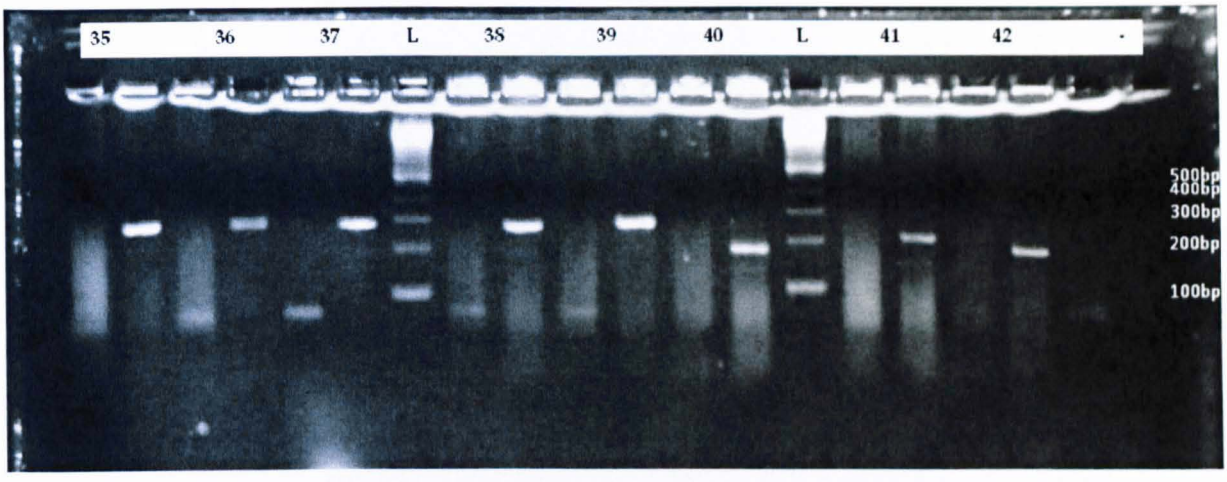

Figure 3.2 – A 2% agarose gel was used to test for positive colonies using internal and M13 primer sets. Clone numbers 35-39 were selected as positive and sent for sequencing analysis, whereas clones 40-42 were assumed negative as, even though a smear with the internal primer set is seen, the M13 primers suggest no insert is present. A smear on the internal negative control is also apparent, suggesting primer front.

The gels showed that the positive colonies (containing both 275 and 75bp fragments) were 35, 36, 37, 38, 39, 43, 44, 45, 46, 50, 51, 54 and 57. The agar patch plate containing these colonies was sent for sequencing (Macrogen Inc., Korea). The 5'-3' variable sequences that were generated were displayed using Clustal W [4], showing sequence homology using different colours as follows:

```
36                ----GATTCA-GTA-TACGATG--------- 16
38                --CTGATCAAAGTA-TAAGTAAAACATT--- 25
43                --AATAGCAAGTTG-TGAGTTGAAGAAA--- 25
35                ---GGAACCATATACTAAGTTTTTCTTT--- 25
44                --TTCAAGCTATTA-TAG-TCTCATACGG-- 25
46                --TTTAACGTATT--TAT-TCAAGCTCGTA- 25
50                --TATATATTCCTA-CACATCTAACTTA--- 25
39                --CCTAATAAGACTTAACCTTACTAAC---- 25
54                GATGTGGAATTATAGGACTTTAA-------- 23
45                ------GAGTTACG---------------- 8
37                AGGCAACAGGAACCTTAGTTG---------- 21
51                ------ATGGACTTTTGAATGTGGCAACAAA 25
```

The full-length sequences were 38, 39, 43, 44, 46, 50 and 51, which were ordered as oligonucleotides from MWG for testing, whereas the incomplete sequences were rejected. It was discovered, following further testing (see chapter four), that these

aptamers were false positives that did not bind heparanase, which led us to attempting further selections.

An additional attempt based on heat denaturation elution protocols was performed, where the heat selection protocol was repeated but modified slightly by running ten consecutive rounds of incubation followed by elution using high temperature (98°C). The aim was to re-amplify the bound aptamers through each cycle and discard the ones that did not bind, based on the protocol described by Missailidis [5]. As this method utilises ten cycles instead of one cycle, it should re-enforce the highest binding sequences and therefore produce a more reliable result. At the end of the ten cycles a double stranded PCR was carried out as above and the products were run on a 2% agarose gel. There were no bands observed on the gel and after repeating the double stranded PCR and agarose gel there were still no bands thus indicating that no aptamers were selected using this protocol. An ELISA (shown in chapter four) confirmed that the 'Top Yield' tubes were saturated with heparanase, so this was ruled out as a cause. The ELISA also showed a slight increase in signal at 450nm upon heating the enzyme, compared to not heating; suggesting that after applying heat to the enzyme, the antibody bound in a stable complex with the enzyme nevertheless. For this reason, it was decided to pursue the salt selection protocol, as it seemed possible that the aptamer-enzyme complex may also have been stable under the condition tested, thus resulting in insufficient elution and amplification of the bound aptamer during the heat denaturation processes.

3.3 Salt One-Step Method

3.3.1 Selection against the Heparanase active enzyme

Following the outcome of the heat selection, a more traditional approach, based on the elution of bound aptamers using high salt and chaotropic agent concentrations was followed. Aptamer library, theoretically containing at least one copy ($1.2x10^{15}$ entities) of each species, was amplified in a single stranded PCR to yield multiple copies of each sequence. This was essential as it would give each heparanase molecule a higher chance of encountering the tightest binding species and would ensure that higher binders would not be displaced by non specific binders due to their excess in the initial solution. Human recombinant heparanase was diluted to 10µg/ml in carbonate buffer solution, pH 9.6 in 'Top Yield' PCR tubes and allowed 24 hours on ice in a fume hood to adsorb to the walls of the well, after which, the well was washed three times with 0.1M salt solution to remove all unbound heparanase molecules. The amplified library was then incubated within the tube for one hour, library solution containing unbound species was removed and subsequently bound species were eluted by adding increasing concentrations in 0.1M increments (0.2-1.5M) of salt solution, pH 7.2, followed by an additional wash using 3M NaSCN to ensure that all binding aptamers were eluted. All the fractions were removed, retained, and desalted using microcon filters with a 3,000 molecular weight cut off (thus retaining any aptamers due to their molecular weight of approximately 22,281Da), to prevent inhibition of the subsequent PCR reaction by the salt present. The product of the desalting processes, eluted at approximately 60µl of pure water, was added to PCR reagents for double stranded PCR, using equal concentrations of both forward and reverse primers, to prepare the DNA for cloning into bacterial cells.

Prior to cloning, products were run on a 2% agarose gel containing ethidium bromide (figure 3.3) to check that aptamers had been generated and retained. Only the highest four salt concentrations were tested initially, as the aptamers with the highest affinities

should have been retained in lower concentrations and eluted only in higher salt concentrations. The samples were run against a 100bp DNA ladder.

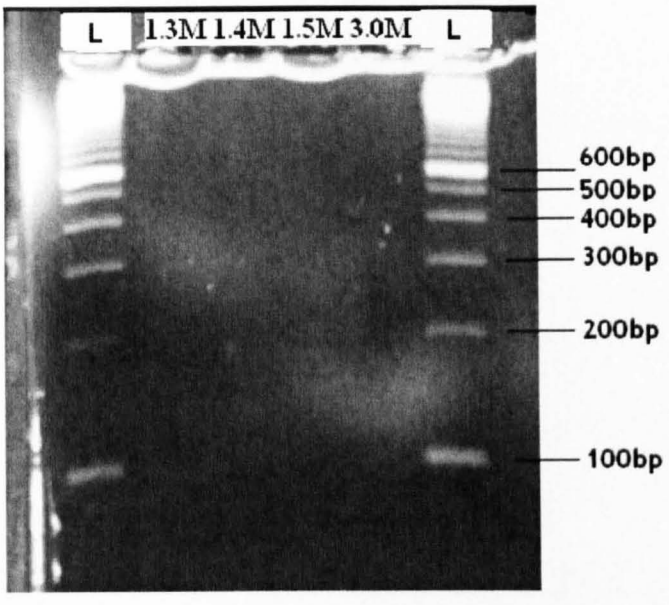

Figure 3.3 – A 2% agarose gel to check presence of 75bp aptamers from the highest salt elutions. No aptamers were visible on this gel.

There were no bands observed at 75bp on the gel, so the microcon filters were re-eluted to make sure DNA was not retained on the microcon membranes. The PCR was repeated and another agarose gel was run (figure 3.4) using the same conditions as above.

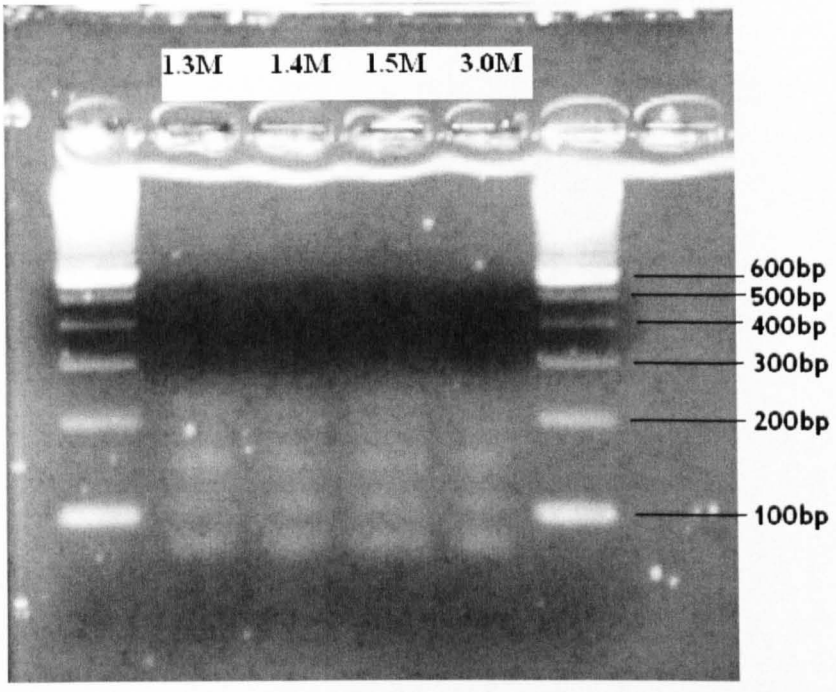

Figure 3.4 – A 2% agarose gel to check presence of 75bp aptamers from the highest salt elutions. Multiple bands were observed suggesting annealing of primers or some contamination of reagents in the PCR mix.

There were multiple bands observed on all samples in this gel, which suggested either the reagents were contaminated or that the primers or aptamers may have annealed to one another, so this selection could not progress any further, as single bands at 75bp are needed to ensure that the correct product is to be cloned. This highlighted the importance of using a negative control in PCR, as contamination or dimerisation of nucleic acids would be easily recognised.

It was considered that a possible reason why the salt selection method did not work was due to the potentially too low amount of individual aptamer species on the original library mixture. Therefore, it was decided to amplify the aptamer library in a slightly different way, with the aim of achieving more copies of each individual sequence. To do this, 50µl of aptamer library (theoretically containing two copies of each aptamer sequence) was included in a double-stranded PCR for 30 cycles and then 100µl of this product was included in a single stranded PCR for 99 cycles. This meant that the library

that was included in the single stranded PCR was more concentrated and included more copies of each sequence due to the exponential nature of the double stranded PCR. The salt selection protocol was then carried out on a tube sensitised with 0.15μM Hpa1 in 0.1M salt solution, pH 6.5. This was chosen so as to increase the positive charge of the protein and ensure increased aptamer binding (see heat protocol above). Furthermore, the method was modified slightly so that each salt elution was incubated in the tube for five minutes on the rotating mixer before being removed to a clean PCR tube. The purpose of this was to aid the removal of weakly bound aptamers into each elution from agitation together with salt content. The desalting was then carried out in microcon filters, using 60 minute spin times instead of 80 minutes, to lower the chance of the filters becoming dry. After elution, a PCR was carried out to produce double-stranded DNA, using new PCR reagents to exclude the possibility of contamination, and the products ran on a 2% agarose gel stained with ethidium bromide and containing a 25bp ladder (figure 3.5):

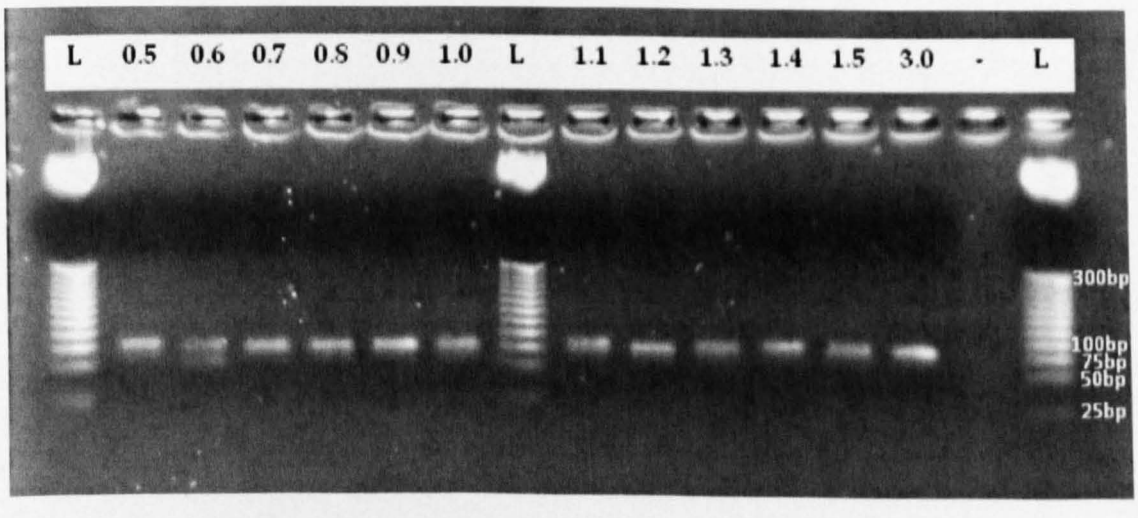

Figure 3.5 – A 2% agarose gel to determine the presence of aptamers in each salt elution from 0.5M NaCl to 3M NaSCN. 75bp bands were seen in all samples except the negative control, suggesting that different species of aptamer had bound with different affinities, which were removed with the different salt concentrations.

This gel shows single bands at 75bp in each sample, showing that aptamers were eluted from each salt concentration due to their differing affinities, as expected. The negative control shows no bands and suggests that multiple bands observed in previous occasions were a result of PCR reagent contamination. The 1.5M NaCl and 3.0M NaSCN elution products were cloned into TOPO and then into *E. coli*. PCRs were carried out on the appropriate sized colonies using internal and M13 primers, and 2% agarose gels were run (see figure 3.6 for an example), to see which colonies contained aptamers.

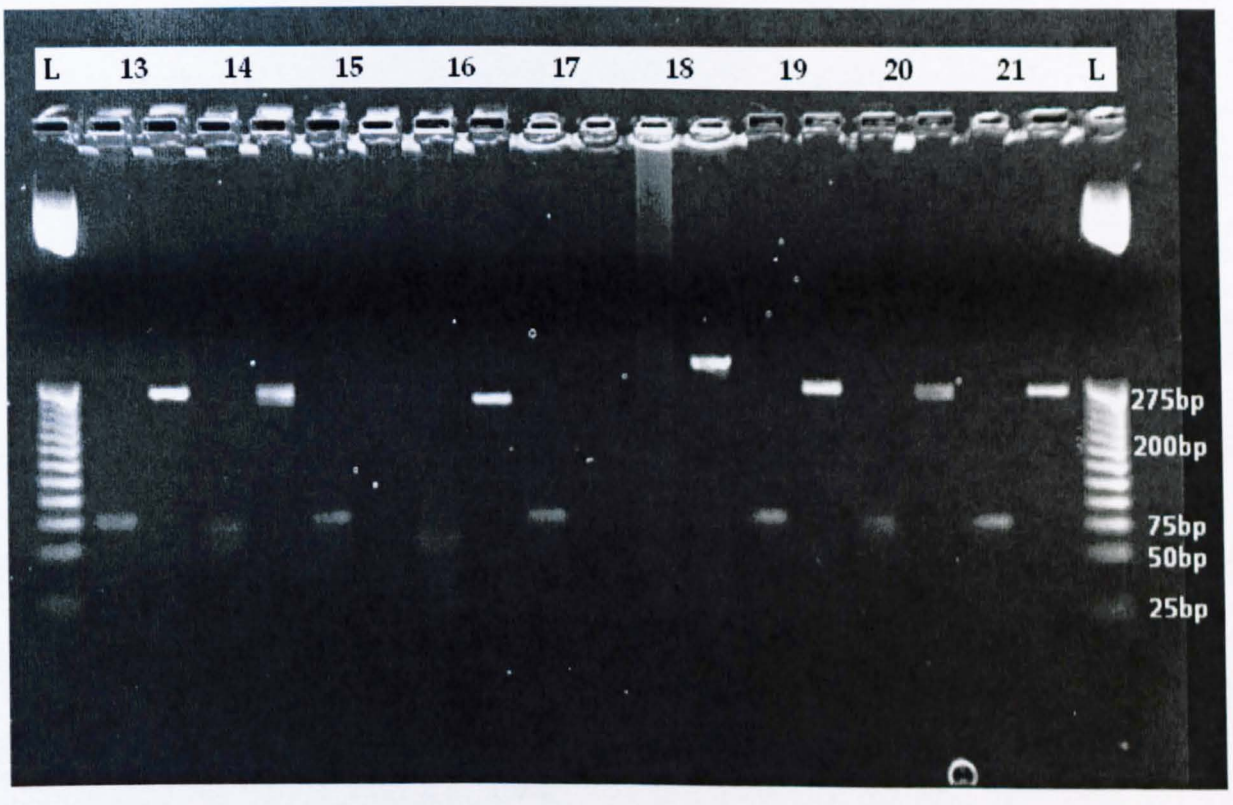

Figure 3.6 – A 2% agarose gel showing products of PCRs on colonies obtained following cloning of the 1.5M NaCl elution into *E. coli* cells. Primers used were M13 and internal, showing 275bp and 75bp fragments upon insertion of aptamers, respectively. From this gel, colony numbers 13, 14, 16, 19-21 were selected as positives as they display bands at both 275 and 75bp. Numbers 15, 17 and 18 were discarded.

The colonies from 1.5M NaCl selection products selected for sequencing were numbers 1-14, 16, 19-22, 24-36, 62, 65-67, 69-73, and the 5'-3' sequences of the aptamers, displayed using Clustal W [4] were as follows:

```
25          --------AAGAAGACTAGCGATGAAGAGCGCT--  25
72          CGGATTATTCGAACTCTTCCAATGA----------  25
34          ----TACTAACTACTCGTACGCAAACGGA------  25
```

```
69          -----AATAGCAAGTTGTAAGTTGAAGAAA----- 25
22          ---ACTTAATTTGCACTTACCATATGGC------- 25
62          --TAATTGCTTCACCCTTACAAACCAG-------- 25
2           -TCTCTTTCTTGACGCTCTATAAGCG--------- 25
7           GCGATCGGGATAATCTGCTATAAGA---------- 25
4           -------TATTCATACG--GAACAGAATTCTCCC- 25
71          ---------CCAATATAA-GAATATTATTGTCTCA 25
5           -----CATTGGAAAAATCCGAAAGTGATTA----- 25
20          -----CAGATTAACATACCAAATCTAATTA----- 25
1           ---------ATGGACTTTTGAATGTGGCAACAAA- 25
13          ---------ATGGACTTTTGAATGTGGCAACAAA- 25
19          ---------GTCGCCTTTTCACTTCACTAGGGTA- 25
11          GGACAGTCAGTCACCATGATTATTT---------- 25
32          -------CACTCAACAGCCTTATTTCCCAATG--- 25
24          -----GAAAGCAAACGTCCTAATTCCAGAA----- 25
29          -------AACTAAATCTCCAAACAACTTACTG--- 25
27          -CACCAGGTTCCATGTCCTAAACTTA--------- 25
21          -------TAATACCTCGCCAGCTACGTCACAG--- 25
```

The colony numbers selected for sequencing from the 3.0M NaSCN selection products were 1-7, 9-11, 13-26, 28, 31-32 and the sequences of the aptamers, again displayed using Clustal W [4] were as follows:

```
31          TTTAACGTATTTATTCAAGCTCGTA--- 25
32          TTTAACGTATTTATTCAAGCTCGTA--- 25
28          TTTAACGTATTTATTCAAGCTCGTA--- 25
26          TTTAACGTATTTATTCAAGCTCGTA--- 25
25          TTTAACGTATTTATTCAAGCTCGTA--- 25
23          TTTAACGTATTTATTCAAGCTCGTA--- 25
22          TTTAACGTATTTATTCAAGCTCGTA--- 25
21          TTTAACGTATTTATTCAAGCTCGTA--- 25
20          TTTAACGTATTTATTCAAGCTCGTA--- 25
19          TTTAACGTATTTATTCAAGCTCGTA--- 25
18          TTTAACGTATTTATTCAAGCTCGTA--- 25
17          TTTAACGTATTTATTCAAGCTCGTA--- 25
16          TTTAACGTATTTATTCAAGCTCGTA--- 25
15          TTTAACGTATTTATTCAAGCTCGTA--- 25
14          TTTAACGTATTTATTCAAGCTCGTA--- 25
13          TTTAACGTATTTATTCAAGCTCGTA--- 25
10          TTTAACGTATTTATTCAAGCTCGTA--- 25
9           TTTAACGTATTTATTCAAGCTCGTA--- 25
5           TTTAACGTATTTATTCAAGCTCGTA--- 25
4           TTTAACGTATTTATTCAAGCTCGTA--- 25
3           TTTAACGTATTTATTCAAGCTCGTA--- 25
6           TTTAACATATTTATTCAAGCTCGTA--- 25
1           ---TATATATTCCTACACATCTAACTTA 25
```

Sequences from the 1.5M NaCl products showed some similarities with 2 sequences being entirely homologous. Sequences from the 3.0M selection products showed that all except for two sequences were homologous. This is very exciting, as it suggests that this is the highest affinity aptamer for Hpa1 and that all the other sequences were eluted earlier during the selection process by salt elution, leaving this as the last aptamer. The fact that this aptamer remained bound even when exposed to 1.5M NaCl is significant in itself as it suggests that it has a very high affinity for Hpa1. These two sequences were chosen for structural analysis and functional analysis.

3.3.2 Selection against the Heparanase Linker Peptide

The same method, described above for the active enzyme, was used to select aptamers against the GST fusion linker peptide sequence. Library was amplified and selection carried out exactly as for heparanase, except that the concentration of linker peptide introduced to the 'Top Yield' PCR tubes for adsorption was 1.66μM. Desalting was carried out on elutions: 1.1, 1.2, 1.3, 1.4, 1.5M NaCl and 3.0M NaSCN, followed by a double stranded PCR and 2% agarose gel electrophoresis to analyse PCR products (figure 3.7).

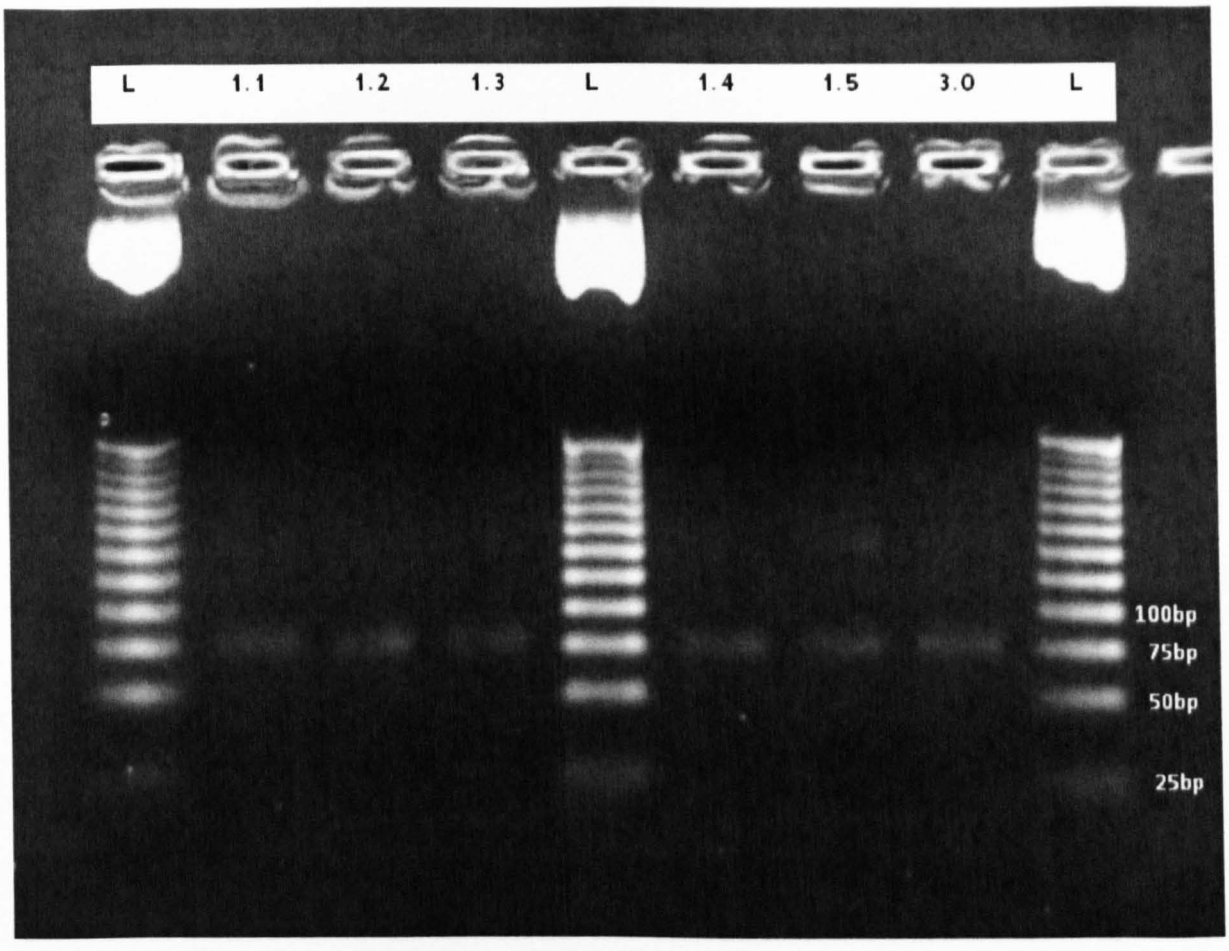

Figure 3.7 – A 2% agarose gel showing 25bp ladder, plus products of 1.1 to 1.5M NaCl and 3M NaSCN elutions. Bands at 75bp, confirming presence of aptamers, were seen in all elutions.

The gel shows bands at 75bp, hence aptamers, in all elutions; so the products from 3.0M NaSCN elution were cloned into TOPO vector, then into chemically competent *E. coli* cells. 45 colonies were analysed by double stranded PCR, using both M13 and internal primer sets, and 2% agarose gels were run to confirm insertion of aptamers into the vectors prior to sequencing. Figure 3.8 is an example of one such agarose gel.

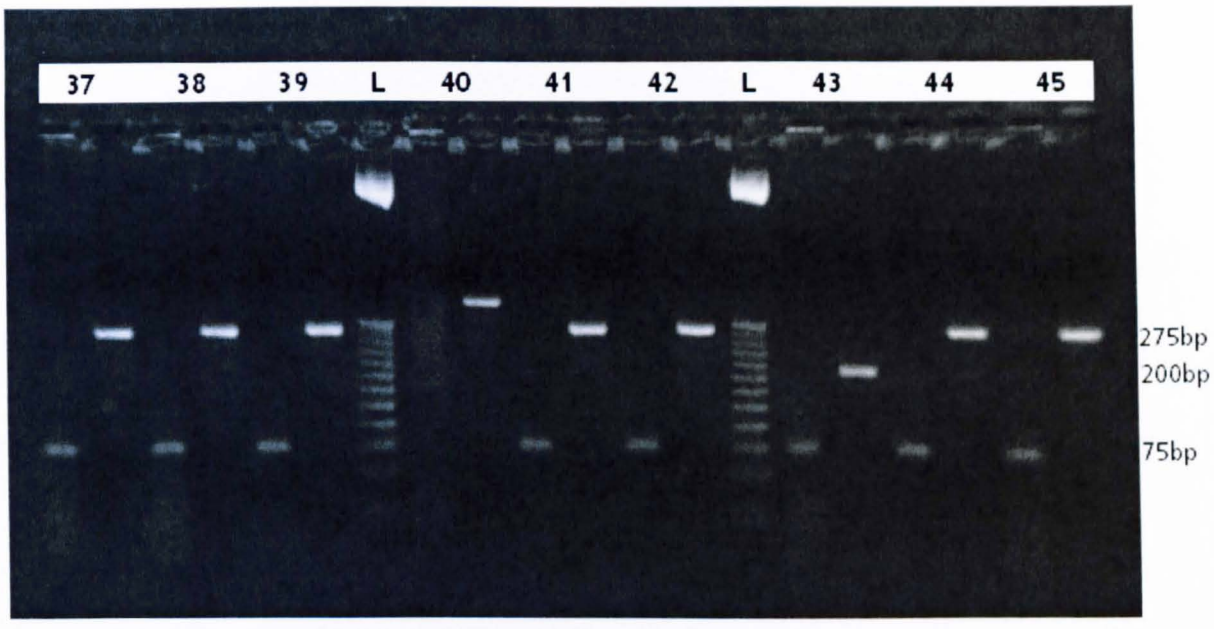

Figure 3.8 – A 2% agarose gel showing 25bp ladder and colony numbers 37-45 tested using internal and M13 primer sets. Numbers 40 and 43 were rejected as both the 75 and 275bp bands were not seen, whereas the rest were assumed positive and sequenced.

Of the 45 colonies, numbers 1, 2, 4-7, 9, 11-13, 15-18, 20-22, 24, 28, 30-32, 34-35, 37-39, 41-42 and 44-45 were analysed by sequencing, with the following results as displayed by Clustal W [4]:

```
1                -GTGCTGAACCAAGTCGGTTTGTCCA--------- 25
13               ----------AAACTCGGTATGCTCACCACCAATG 25
20               -AGTGATCAAAAAACGCACTGCCTGA--------- 25
34               --TCGAGCCACCATCTCACACCCATAA-------- 25
5                ------AAAACAATCTCACATATCGGGCTG----- 24
6                -------GGTACACTTAATAA-TGAACGATAAC-- 25
28               -----AAAGCACAACTTACAACTAGACTAT----- 25
9                AACTGACTACTATTTTCGTATTTGT---------- 25
42               ------TTTCTATTTAAATGTGTGTCTTCAT---- 25
30               -------ATGGACTTTTGAATGTGGCAACAAA--- 25
31               -----TTCTCGAGCTATTTGAATCCGGAC------ 24
41               -----TTCTCGAGCTATTTGAATCCGGAC------ 24
12               --CATCTATAGATCTTTTT---------------- 17
21               GGCTATGATAAGATCTGATTCTTTA---------- 25
22               ---AATCACAGATTTGTATTCATT----------- 21
39               ------TATATATTCCTACACATCTAACTTA---- 25
16               ---AATAGCAAGTTGTGAGTTGAAGAAA------- 25
37               ---AATAGCAAGTTGTGAGTTGAAGAAA------- 25
17               -----TCGCCCGTTCCAAGCAAAC-GCAGCC---- 25
32               -------TCGCGGTGCAACCAATTTATGAACA--- 25
2                --------TTGCTCCTTATAGAGCCGTCCGAGC-- 25
4                --------TTGCTCCTTATAGAGCCGTCCGAGC-- 25
35               --------TTGCTCCTTATAGAGCCGTCCGAGC-- 25
44               --------TTGCTCCTTATAGAGCCGTCCGAGC-- 25
```

```
38          GTAGAGACCCACCCCTAATCTAGAC---------- 25
7           CTAAAGTGCCTCACGCTGTTAACTC---------- 25
15          CTAAAGTGCCTCACGCTGTTAACTC---------- 25
18          CTAAAGTGCCTCACGCTGTTAACTC---------- 25
24          CTAAAGTGCCTCACGCTGTTAACTC---------- 25
45          CTAAAGTGCCTCACGCTGTTAACTC---------- 25
11          --------AGCCACTTGATCCAACCTGCCTTGG-- 25
```

Of the results obtained, the sequences highlighted in pink and yellow occurred with the highest frequency, suggesting that these were the ones with the highest binding affinity, as they were able to out-compete the other sequences. These were chosen for further structure-based and functional analysis.

3.4 Structure Predictions

To assess the potential structures of these aptamers, sequences were transcribed into Mfold [6]; a program used to predict the spontaneous three-dimensional structures of DNA/RNA molecules by calculating their minimum Gibbs free energy values [7] as well as the free energies of folding of any particular base pair at 37°C. The lower or more negative the value, the less energy is required for the predicted structure to be formed and, therefore, the more likely it is to be formed spontaneously. The variable and primer regions were both assessed as the primer regions help to confer stability upon the molecule and therefore are frequently implicated in the folded structure. Figure 3.9 shows predictions for the 1.5M elution product, whilst figure 3.10 shows predictions for the 3.0M NaSCN elution product, both from the heparanase active enzyme selection.

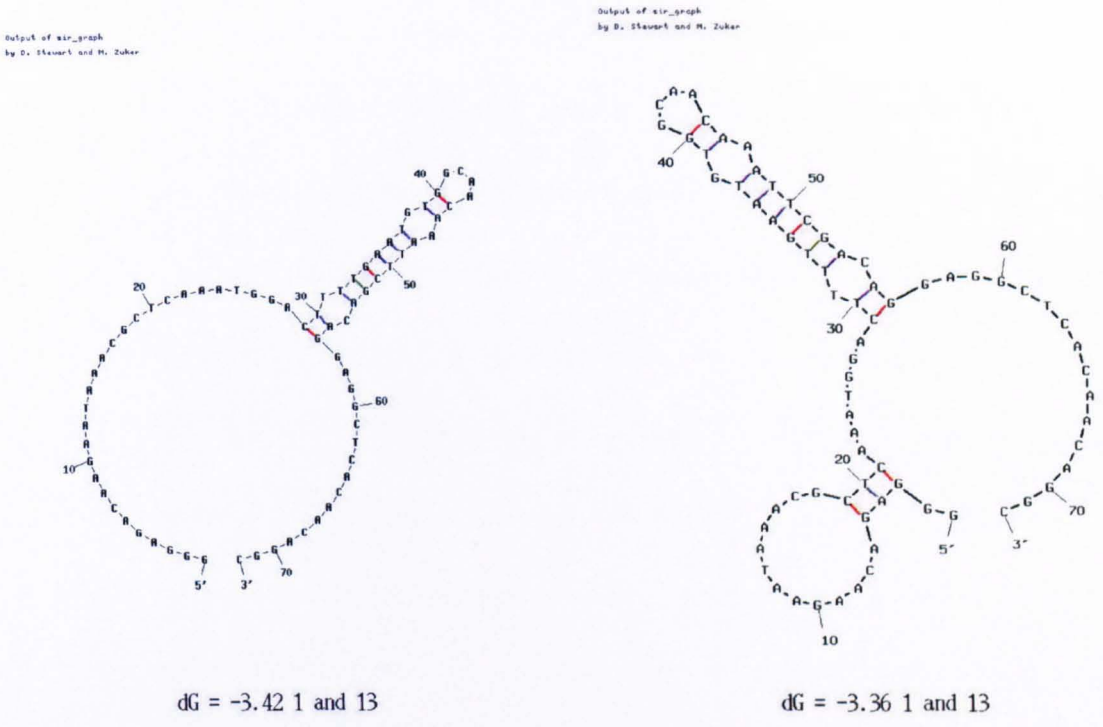

Figure 3.9 – Mfold energy dot plot predicted structures of clone numbers 1 and 13 from 1.5M NaCl elution of heparanase selection. ΔG at 37˚C for these structures is calculated at -3.42 and -3.36kcal/mol respectively [6].

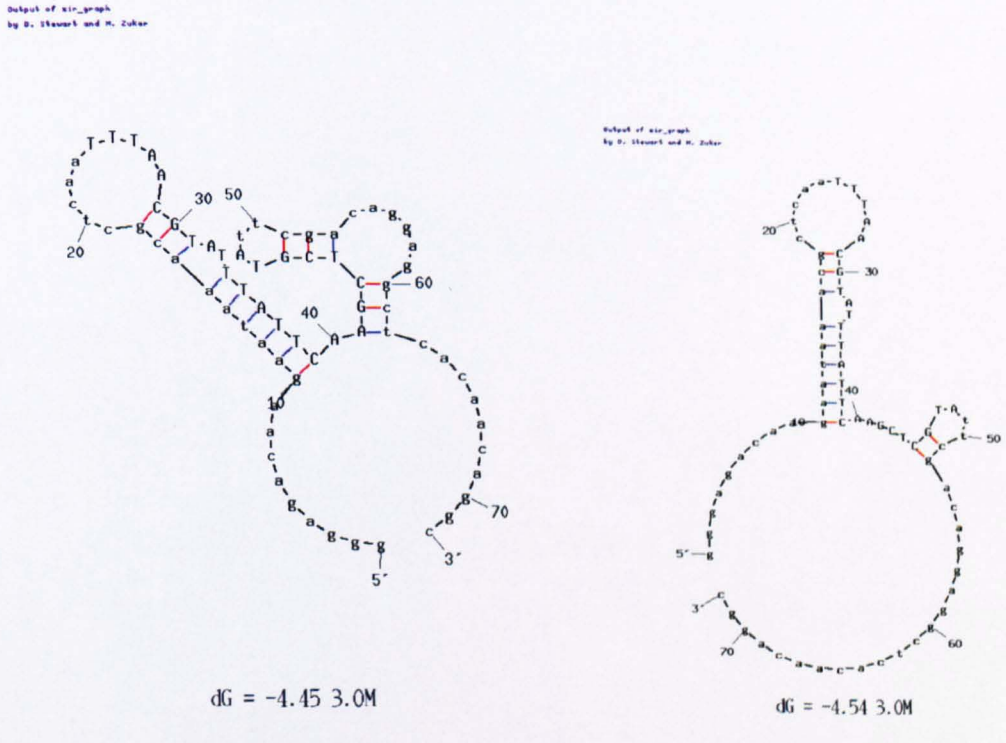

Figure 3.10 – Mfold energy dot plot predicted structures of homologous sequence generated from 3.0M NaSCN elution of heparanase selection. ΔG at 37˚C for this structure is -4.45 and -4.54 kcal/mol respectively [6].

Using the predicted structures generated by Mfold, it was decided to investigate the 3.0M NaSCN sequence as a slightly truncated sequence of 55 nucleotides, including some of

both primer regions as in both predicted structures the same sections of primer sequences were implicated. This sequence was further known as '3.0M'. For the 1.5M NaCl product, the two structure predictions varied significantly, with the one prediction implicating most of the primer regions in structure formation, and the other implicating neither primers in the structure (see figure 3.10). For this reason, it was decided to order this sequence as a full-length and also as a truncated version for further testing. These were further known as '1.5M short' and '1.5M long'.

The two sequences obtained from selection against the linker peptide were also transcribed into Mfold, where sequences were suggested having highly negative ΔG values (see figures 3.11 and 3.12).

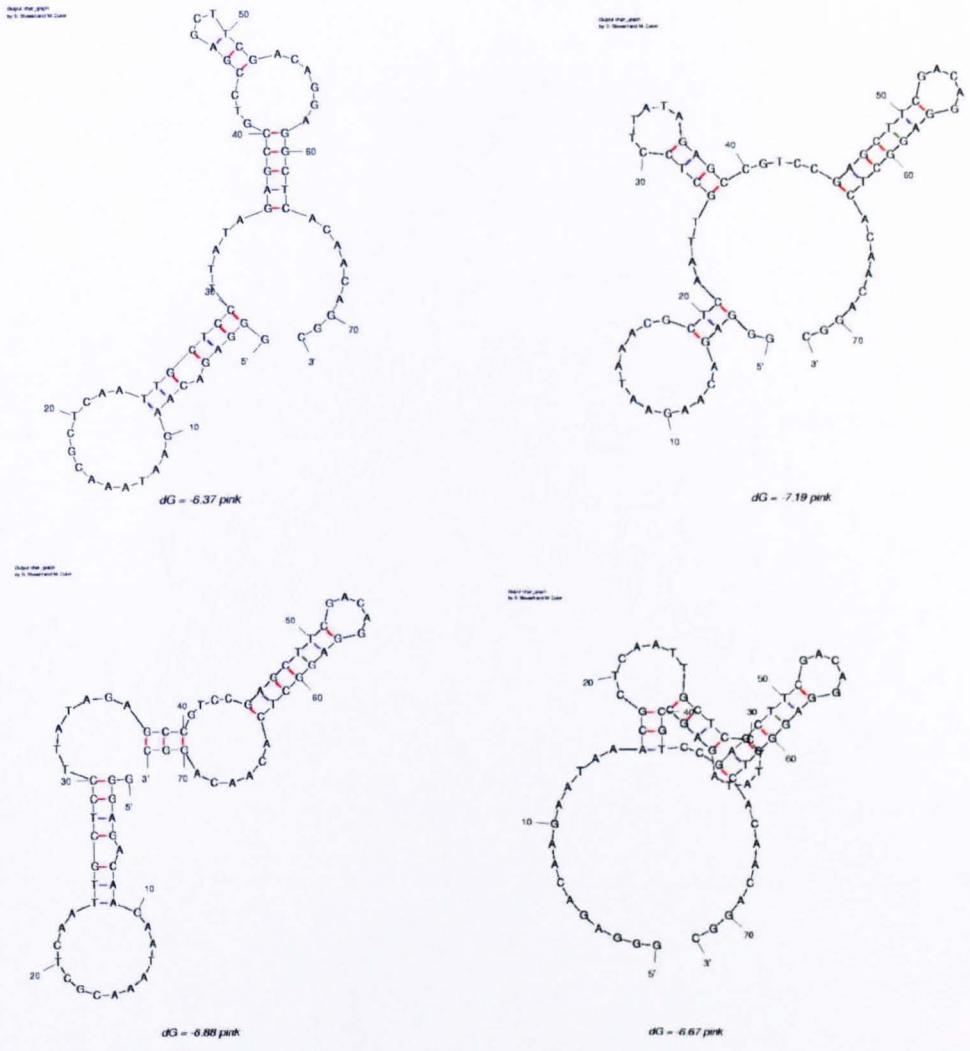

Figure 3.11 - Mfold energy dot plot predicted structures of homologous sequence generated from the pink sequence of 3.0M NaSCN elution of linker peptide selection. Four structures were predicted, with ΔG values at 37˚C of -6.37kcal/mol, -7.19kcal/mol, -6.88kcal/mol and -6.67kcal/mol respectively [6].

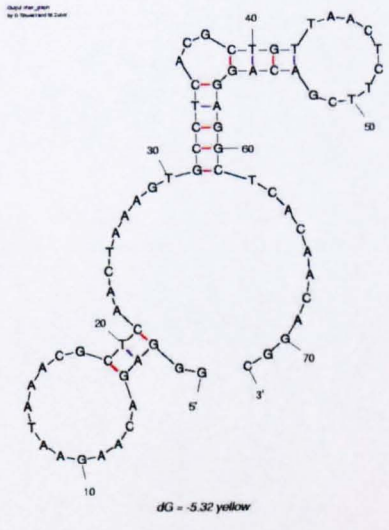

Figure 3.12 - Mfold energy dot plot predicted structure of homologous sequence generated from the yellow sequence of 3.0M NaSCN elution of linker peptide selection. ΔG at 37˚C for this structure is -5.32kcal/mol [6].

All predicted structures, both for the yellow and pink aptamer, seem to implicate the primer regions (see figures 3.11 and 3.12). Thus, these aptamers were also ordered as 72mer oligonucleotides to commence further testing and referred to as 'pink' and 'yellow'.

3.5 Discussion

Heparanase presented an interesting target for aptamer selection, and aptamers were selected for both the active enzyme and the linker peptide that is proteolytically cleaved from the pre pro enzyme to allow formation of the active enzyme. The results from the different selection processes indicate that selection of bound aptamers using a heat-based elution method was not suitable for this enzyme. Data obtained from an ELISA assay suggested that after heating of heparanase to 98°C, although this process may have reversibly or irreversibly damaged the enzyme, did not result in a reduced signal and the anti-heparanase polyclonal antibody was still able to recognise and bind to the enzyme, more so than in a system conducted at room temperature. This suggests that the structure of the enzyme was still mostly intact and that the antibody may even have been better able to bind to heparanase after heating. Furthermore, no aptamers were eluted from the heating of the heparanase-aptamer complex after heating to 98°C, in agreement with the above observation. For this reason, the selection based on a salt elution protocol was followed and subsequently optimised by incubation of the target in a solution closer to physiological pH to take advantage of the positive charge of the enzyme at these conditions, more rigorous amplification of aptamer library, and using agitation to aid the introduction/removal of aptamers to the target.

Although aptamer library was amplified in a single stranded PCR before incubation with the enzyme, these selection methodologies generated more promising results after amplifying the aptamer library exponentially in a double stranded PCR before a single stranded PCR. This suggests that initial library enrichment was advantageous due to the presence of more copies of each binding species, that better facilitated competitive binding to a limited pool of target and resulted in single or few aptamer sequences being selected.

Aptamers were successfully selected against human recombinant heparanase and the 6kDa linker peptide region using an optimised, modified SELEX protocol based on interruption of the interactions formed between protein and aptamer by high salt content. Aptamers generated from 1.5M NaCl and 3.0M NaSCN elutions each suggested one prominent species based on sequence homology, as the greater the number of times the species is encountered, the higher affinity for the target it is expected to have, due to its out-competing the other sequences. Two sequences from each target were analysed using structure predicting software known as Mfold, and ordered as full length and truncated single-stranded sequences for further testing both for their affinity for their target and for their ability to detect the target in media and/or inhibit its action, as described in the following chapters.

References:

1. Ellington, A.D. and J.W. Szostak, *In vitro selection of RNA molecules that bind specific ligands.* Nature, 1990. **346**(6287): p. 818-22.
2. McKenzie, E., K. Young, M. Hircock, J. Bennett, M. Bhaman, R. Felix, P. Turner, A. Stamps, D. McMillan, G. Saville, S. Ng, S. Mason, D. Snell, D. Schofield, H. Gong, R. Townsend, J. Gallagher, M. Page, R. Parekh, and C. Stubberfield, *Biochemical characterization of the active heterodimer form of human heparanase (Hpa1) protein expressed in insect cells.* Biochem J, 2003. **373**(Pt 2): p. 423-35.
3. Hermann, T. and D.J. Patel, *Adaptive recognition by nucleic acid aptamers.* Science, 2000. **287**(5454): p. 820-5.
4. Larkin, M.A., G. Blackshields, N.P. Brown, R. Chenna, P.A. McGettigan, H. McWilliam, F. Valentin, I.M. Wallace, A. Wilm, R. Lopez, J.D. Thompson, T.J. Gibson, and D.G. Higgins, *Clustal W and Clustal X version 2.0.* Bioinformatics, 2007. **23**(21): p. 2947-8.
5. Missailidis, S., *Targeting of antibodies using aptamers.* Methods Mol Biol, 2004. **248**: p. 547-55.
6. Zuker, M., *Mfold web server for nucleic acid folding and hybridization prediction.* Nucleic Acids Res, 2003. **31**(13): p. 3406-15.
7. SantaLucia, J., Jr., *A unified view of polymer, dumbbell, and oligonucleotide DNA nearest-neighbor thermodynamics.* Proc Natl Acad Sci U S A, 1998. **95**(4): p. 1460-5.

CHAPTER FOUR

FUNCTIONAL ASSAYS TO ASSESS BINDING OF APTAMERS TO HEPARANASE AND HEPARANASE FRAGMENTS

4.1 Background

Following the development and synthesis of aptamers directed against the human polymorphic recombinant heparanase and the GST fusion linker peptide, experiments were designed to test the affinity and specificity of the aptamers *in vitro*, in bench-top assays. The assays selected were ELISA (enzyme-linked immunosorbent assay), EMSA (electrophoretic mobility shift assay) and fluorescence quenching titrations. Unfortunately, due to the unavailability of an antibody for the GST fusion linker peptide, it was not possible to test the aptamers for this target using all the above techniques.

4.2 ELISA

4.2.1 Optimisation of ELISA

To optimise the conditions for an ELISA, it was necessary to examine the stoichiometry between enzyme and antibody by determining the concentration of antibody needed to saturate a plate sensitised with 150nM heparanase. An ELISA was carried out using a dilution series from 0 to 660nM polyclonal anti-heparanase antibody. The results, shown in figure 4.1, indicated that a 1:1 molar binding ratio was sufficient, as 160nM antibody formed the beginning of the plateau due to the free heparanase being mostly exhausted. There was a slight increase in signal upon increasing the antibody concentration over 160nM due to any remainder of heparanase becoming bound. However, this may also have been due to some antibody molecules binding to more than one site of heparanase as a polyclonal antibody was used. For this reason, 660nM was chosen as the optimum concentration and used in further assays.

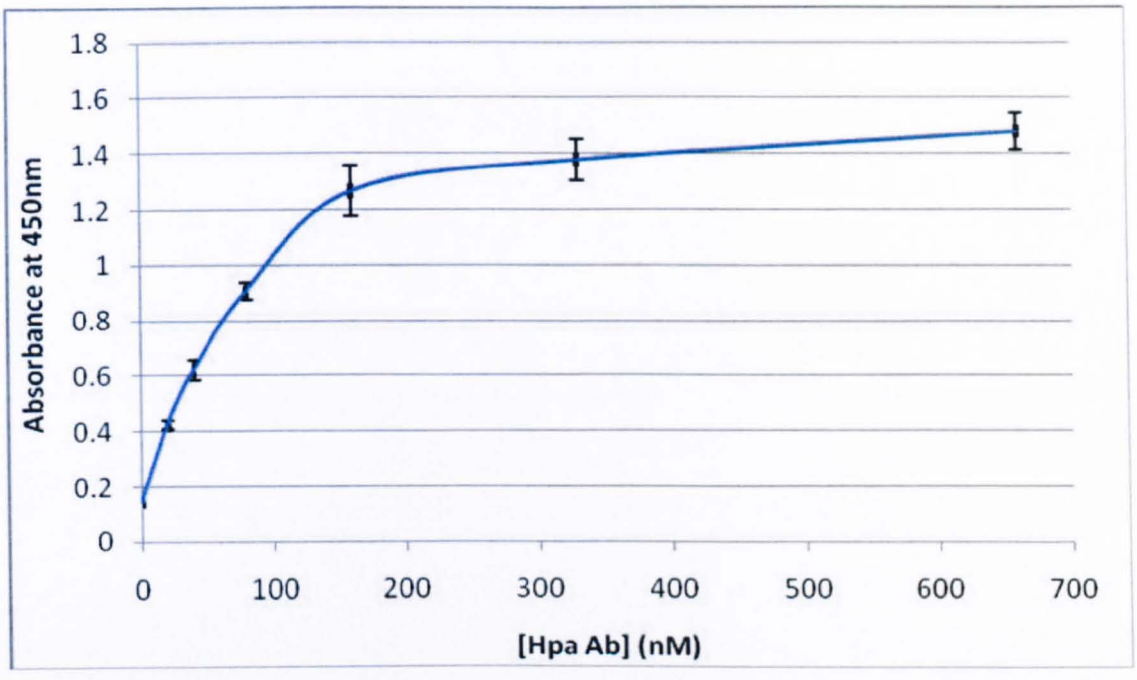

Figure 4.1 - An ELISA using a plate sensitised with 150nM human polymorphic recombinant heparanase with addition of increasing concentrations from 0-660nM polyclonal anti-heparanase IgG antibody to determine the optimum stoichiometry between heparanase and antibody. 660nM was determined to be the optimum concentration of antibody as although 160nM (a 1:1 molar binding ratio) gave a strong signal, it was important to exhaust all heparanase molecules with antibody.

In previous experiments carried out, it was determined that the optimum conditions for ELISA were to block the wells with 10mg/ml BSA in PBS to minimise any of the subsequent reagents from binding to the well surface and generating false-positive results.

The traditional competition ELISA was initially used between aptamer and antibody for these studies, aiming to demonstrate that the aptamer had the ability to compete out the heparanase-bound antibody, based on a protocol previously demonstrated by the MUC1 aptamer [1]. However, these studies would only show if the aptamer bound and competed with the antibody for the same site or bound in close enough proximity to disrupt one another's interactions. It is entirely possible, due to their small size compared to both antibody and enzyme, due to their negative charge, and due to the fact that a polyclonal antibody was used with no known epitope, that the aptamers may bind at a

completely different site from the antibody, which would explain the lack of positive results on this assay.

Hence, the ELISA was modified by immobilising 5' biotinylated aptamers via the use of avidin molecules to the surface of the wells, then after a blocking step, incubating heparanase, heparanase antibody and following the ELISA to completion. This was initially carried out in triplicate using pre-coated streptavidin PCR tubes and an example is shown of 1.5M short aptamer in figure 4.2.

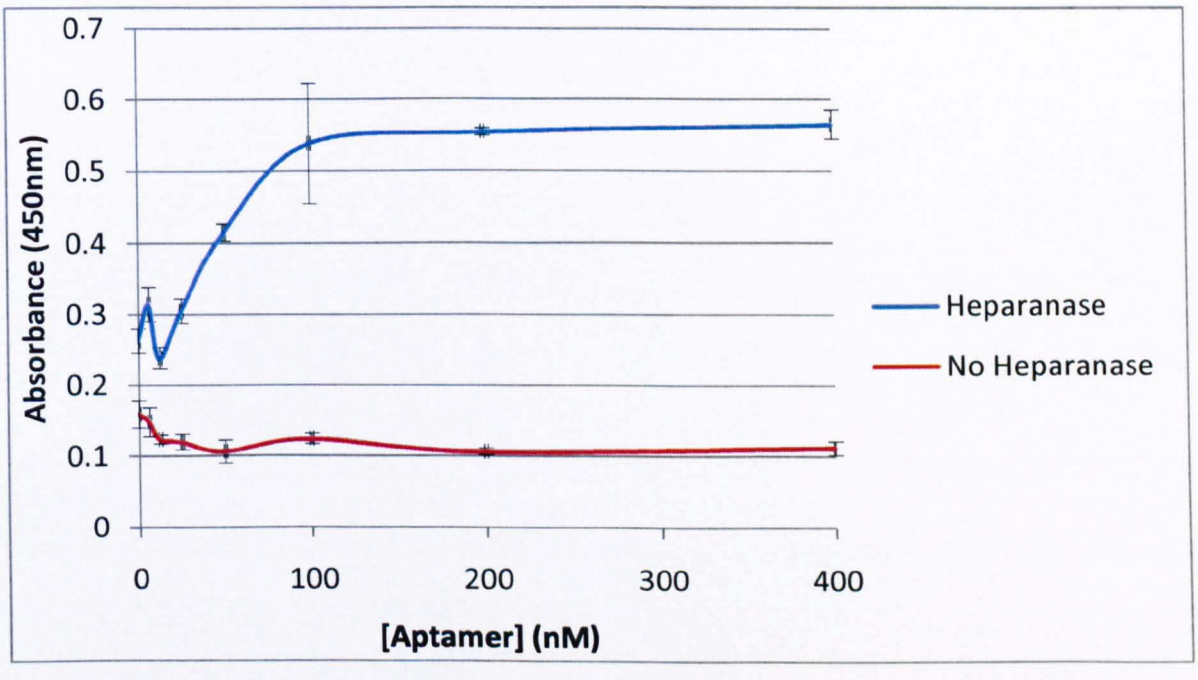

Figure 4.2 - An ELISA using streptavidin pre-coated PCR tubes with 5' biotinylated 1.5M short aptamer. After blocking, then addition of 160nM human recombinant polymorphic heparanase and its respective antibody, the ELISA was run to completion.

The experiments using all three aptamers without heparanase showed a marginal change in absorbance at a level between 0.1 and 0.3 absorbance units, compared to those with heparanase added. The latter increased in absorbance upon increasing the concentrations of aptamers, suggesting that the aptamers did indeed bind heparanase. However, this method needed further optimisation to increase consistency and reduce costs. Thus, it was decided to allow an interaction between streptavidin and each

aptamer for a period of two hours before aliquoting 100µl into the wells of an ELISA plate instead of using pre-coated streptavidin PCR tubes. Adding biotinylated aptamers in a 4x molar excess of streptavidin (due to the presence of 4 biotin binding sites per streptavidin molecule) would ensure that the streptavidin-biotin binding reaction had occurred before the exposed areas of streptavidin bound to the wells of the plate, leaving the aptamers exposed for recognition by heparanase. Using one preparation of streptavidin-aptamer, serially diluted to the appropriate concentrations in this way would make the absorbance readings more consistent, as some large error bars were observed in the original trials using PCR tubes. Carrying out the ELISA in the appropriate plate instead of PCR tubes would also make the absorbance readings more consistent as in using PCR tubes, the final solution had to be transferred to an ELISA plate to be analysed, which could have left behind some solution; leading to large error bars and non-reproducible results. The PCR tubes were also very expensive and modifying the ELISA in this way caused the experiment to be more cost-effective.

Unfortunately, due to an unavailability of antibody for the GST linker peptide, the ELISA was not a viable test of the linker peptide's interactions with its respective aptamers.

4.2.2 Troubleshooting selection

Due to no aptamers being detected at the end of the ten-round heat selection method, it was decided to conduct an ELISA in the 'Top Yield' PCR tubes used in selection, to make sure that there was heparanase adsorbed to the tubes as this may have been a reason why there were no aptamers found at the end of selection. Also, this ELISA was used to ascertain if the protein's interactions were being disrupted enough to release the aptamers to be amplified at 95°C. Experiments were conducted in triplicate as follows: 150nM heparanase was incubated in Top Yield PCR tubes overnight at room temperature.

Three tubes containing 0.1M salt solution were also incubated to act as the negative control. The next day, heparanase-containing tubes were incubated at 95°C for ten minutes, 95°C for one hour, 97°C for one hour or 98°C for one hour. The positive control was heparanase-adsorbed tubes that remained unheated. The rest of the ELISA was conducted with the removal of unbound heparanase by washing of the tubes, then the addition of primary antibody, streptavidin-conjugated secondary antibody and chromogen complex plus 10% H_2SO_4. The results are shown in figure 4.3.

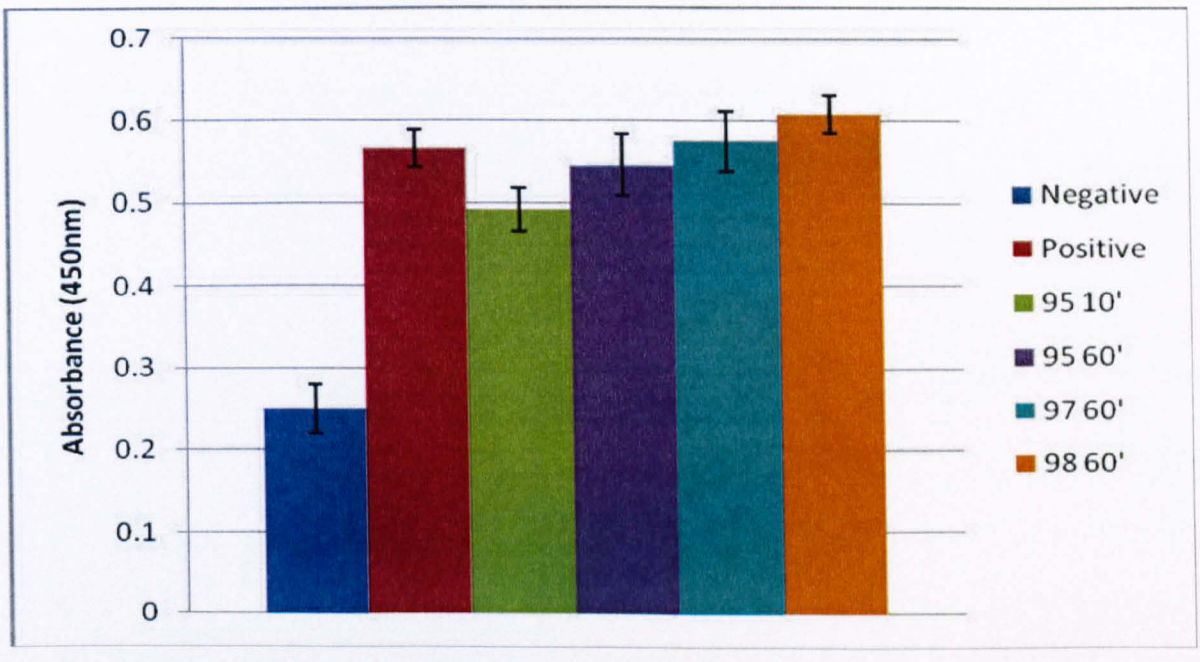

Figure 4.3 - An ELISA using 'Top Yield' ELISA-type PCR tubes sensitised with 150nM human polymorphic recombinant heparanase or 0.1M salt solution (negative control). After heating all but the negative and positive controls to either 95, 97 or 98°C for the times indicated and addition of 660nM anti-heparanase antibody, the ELISA was run to completion and it was determined that heparanase had saturated the tubes and remained bound during selection, also that the antibody bound to heparanase and not to the sides of the tubes, both seen by the difference in absorbance between the negative and positive controls. It was also observed that at high temperatures the heparanase remained bound to the tubes and furthermore, bound an equal or greater number of primary antibody molecules. Error bars represent standard deviation of the mean.

The results of this ELISA show that the 'Top Yield' tubes were saturated with heparanase due to the strong signal observed by the positive control, so this can be ruled out as the reason why there were no aptamers generated in this method. The difference in

absorbance seen between the negative and positive controls also shows that the antibody binds to heparanase and not to the sides of the tubes.

There was an increase in absorbance with a corresponding increase in temperature, which suggests that a greater amount of antibody binds to heparanase subjected to higher temperatures. This could be due to the heat causing a conformational change in the protein such that the antibody binding site is more accessible to the antibody, therefore allowing it to bind more tightly and more of it to bind. However, as this antibody was raised in rabbit against the recombinant enzyme [2] and not the heat denatured protein or an epitope or peptide component of the enzyme, one would expect the antibody to recognize the structured enzyme and not recognize it after heat denaturation.

Applying this to the selection method, this could mean that although the protein's conformation is changing, it may not be releasing any bound aptamers. Also, as the tubes are heated at the stage where aptamers are incubating with the protein during selection, the aptamers may also be adopting a different structure under heat and the heparanase and aptamer be stabilising each other and remaining bound. Due to the difficulty in establishing a solution for this technique, it was decided to pursue with and address the salt selection methods instead.

4.2.3 Heparanase-selected aptamers using one-round heat method

To test the binding of seven aptamers (38, 39, 43, 44, 46, 50 and 51) previously selected against heparanase using the one-step heat selection method, a competition ELISA was carried out by adsorbing 150nM heparanase in 0.1M binding solution to an ELISA plate, then incubating 660nM polyclonal heparanase antibody for one hour. Aptamer was added and incubated for one hour at concentrations from 0 to 700nM and the ELISA was

run to completion. The ELISA was measured to see if the addition of any of the aptamers had displaced the binding of the antibody to heparanase, and at what concentration. The results are shown in figure 4.4 below.

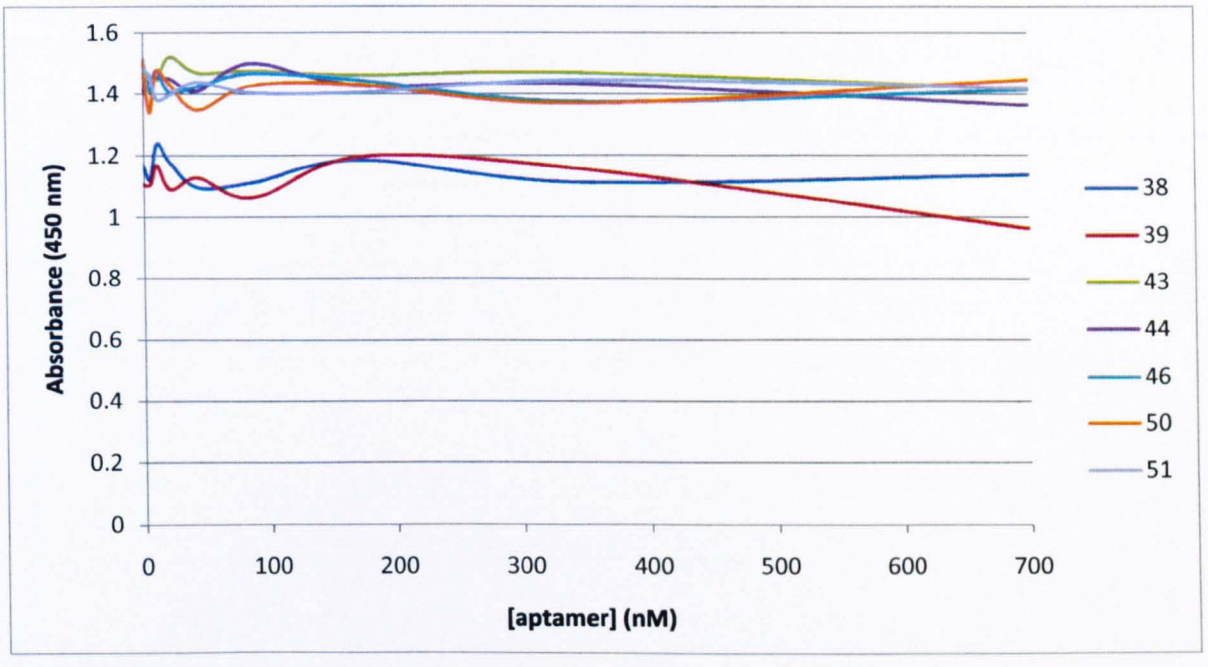

Figure 4.4 - An ELISA using a plate sensitised with 150nM heparanase, labelled with 660nM polyclonal anti-heparanase IgG antibody, and then incubated with 0-700nM of each heparanase-selected aptamer to observe if the antibody was displaced. Results showed that none of the aptamers displaced the antibody as the signal did not decrease significantly from the negative (no aptamer) controls and therefore the aptamers' affinities for heparanase were below that of the antibody.

Unfortunately, none of the aptamers displaced the binding of the antibody to heparanase as the absorbance at 450nm should have decreased upon displacement of antibody by aptamer but this was not demonstrated in any of the results for the aptamers tested. Therefore, a competition ELISA was carried out in reverse, similar to the one described above, but by adding the aptamers to the heparanase-sensitised wells first at a concentration of 600nM and then adding the antibody at concentrations from 5 to 330nM to allow the aptamers a chance to bind without the presence of antibody, to

investigate whether any would remain bound after addition of even lower concentrations of antibody. Figure 4.5 below shows the results.

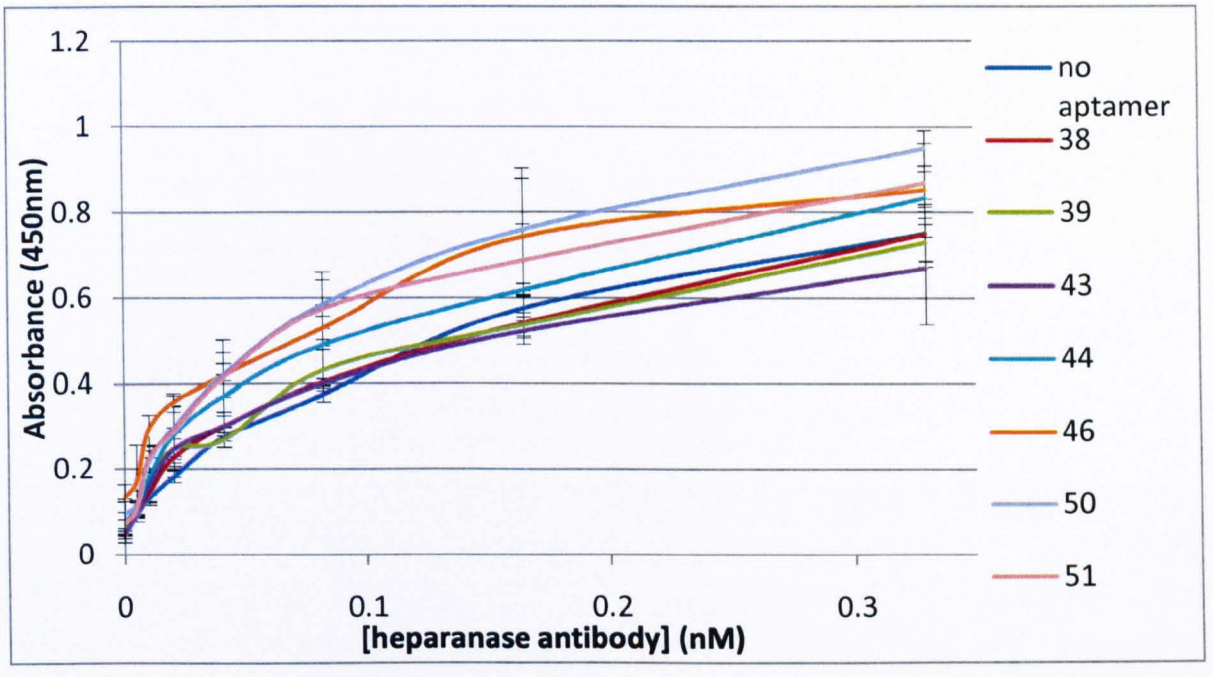

Figure 4.5 - An ELISA using a plate sensitised with 150nM heparanase, incubated with 600nM of each heparanase-selected aptamer, and then incubated with 0-330nM polyclonal heparanase antibody. A negative control containing no aptamer was used to demonstrate antibody binding with no aptamer interference. The results all clearly follow the pattern shown by the negative control suggesting that the aptamers either do not bind at the antibody binding site or do not stay bound to heparanase in the presence of heparanase antibody. Error bars represent standard deviation of the mean of triplicate samples.

The results showed that absorbance increased with concentration of antibody added, suggesting that if any aptamers were bound, the antibody displaced them. The results also did not deviate from the pattern of the negative control where no aptamer was added, suggesting that if any aptamers were bound then they were so with only a very low affinity. However, an EMSA was carried out to validate this as the ELISA only tests for binding to the same site as the antibody, and the aptamers may bind to a completely different site. None of these aptamers showed any shift in the EMSA (data not shown), thus confirming they did not bind to heparanase.

4.2.4 Heparanase aptamers selected using one-round salt method.

To test aptamers generated from one-round salt selection ('1.5M short', '1.5M long' and '3.0M') a competition ELISA was conducted by incubating 175nM heparanase polyclonal antibody in wells sensitised with 150nM heparanase. Aptamers were added in dilution series from 0-1.43µM and the ELISA was run to completion. The experiment was run in triplicate and results are shown in figure 4.6. Once again, to give aptamers a greater chance of competing with the antibody, an ELISA was conducted with aptamer and antibody added in opposite order, shown in figure 4.7, using 500nM each aptamer, followed by 0-175nM antibody. Error bars represent the standard deviation of the mean over the three experiments.

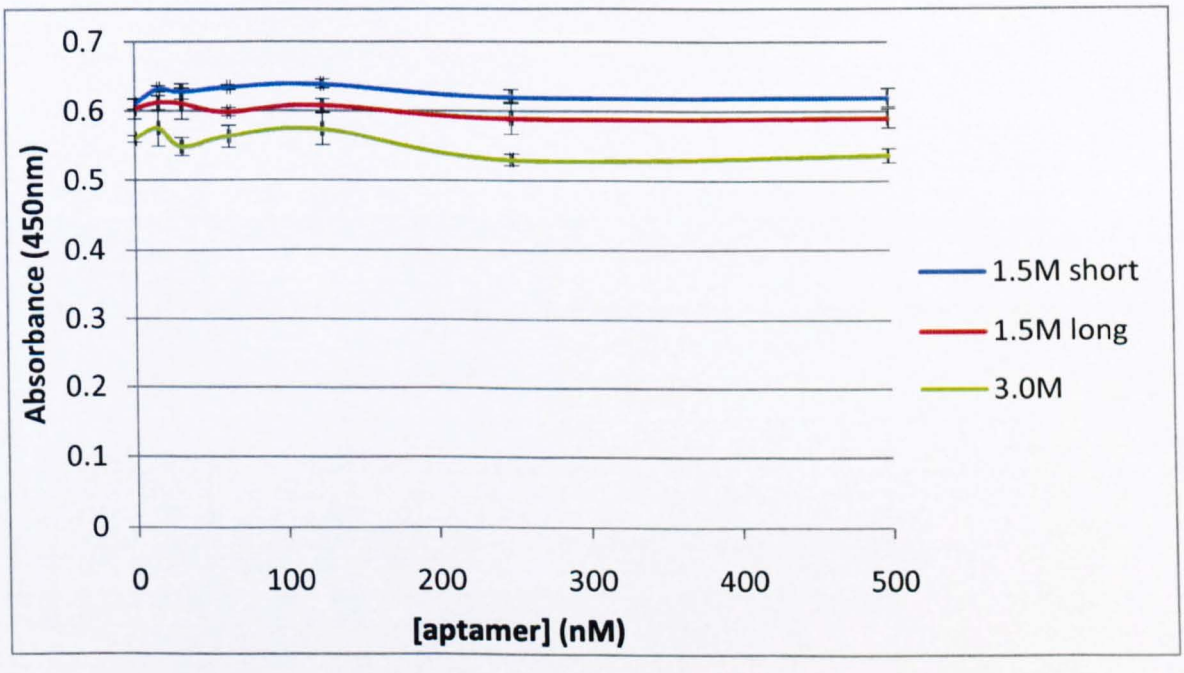

Figure 4.6 - A competition ELISA using a plate sensitised with 150nM human recombinant polymorphic heparanase, incubated with 175nM heparanase antibody, then a dilution series of 0-500nM each heparanase-selected aptamer. After completing the ELISA the results suggested that the aptamers did not displace the antibody as the absorbance did not decrease upon increasing aptamer concentration. Error bars represent standard deviation of the mean.

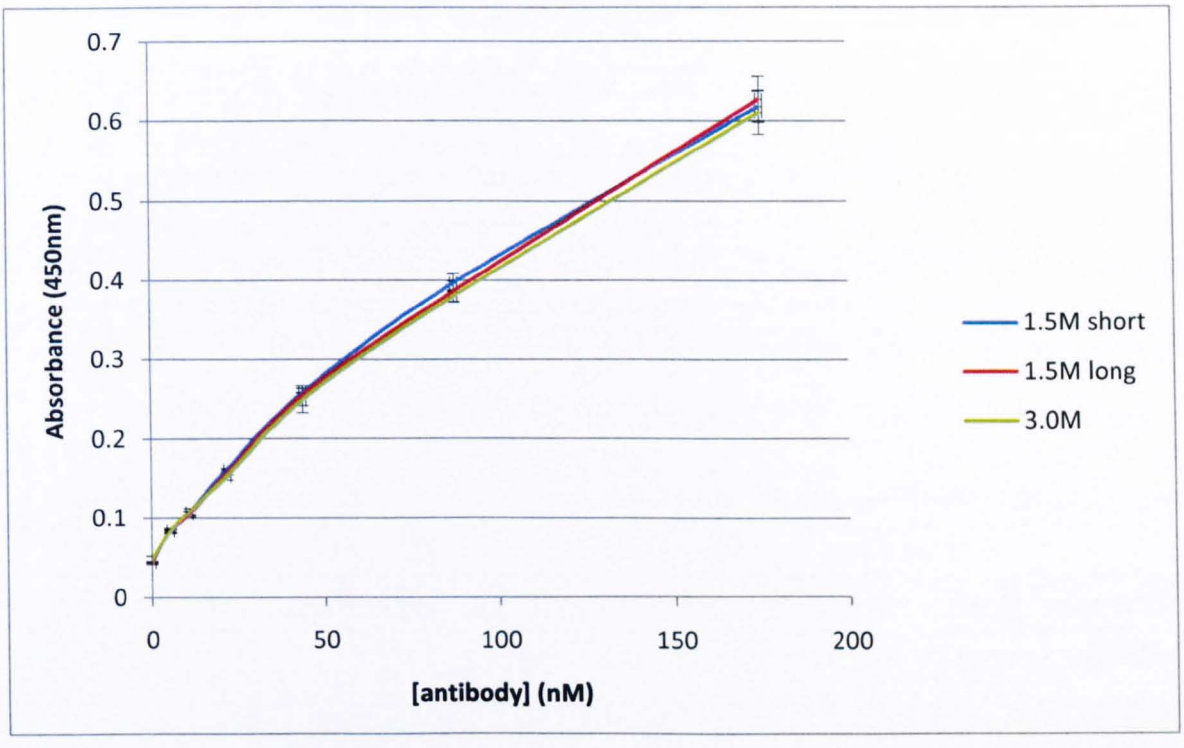

Figure 4.7 - A competition ELISA using a plate sensitised with 150nM human recombinant polymorphic heparanase incubated with 500nM each heparanase-selected aptamer then with 0-175nM heparanase polyclonal antibody. Error bars represent standard deviation of the mean.

Addition of either aptamer in these studies at any concentration did not affect the absorbance of these assays. In figure 4.6 the absorbance remained stable at 0.6 units from 0 to 500nM aptamer and in figure 4.7 the aptamer curves increased in absorbance in a fashion similar to the increase shown when no aptamer is present. This demonstrated that these aptamers do not interfere with the binding of heparanase to its antibody and therefore do not bind at the same site, if at all.

To determine whether the aptamers bound heparanase, but at a different site from the antibody, streptavidin ELISAs were performed with 187nM 5' biotinylated 1.5M short, long, 3.0M and an unrelated aptamer as detailed in the methods section; the results of which are shown in figure 4.8. The results for the heparanase-selected aptamers show that the absorbance increased as the heparanase concentration increased, which suggests the aptamers bind heparanase. The negative control (unrelated aptamer) has

also shown an increase in absorbance with heparanase concentration, although at a lower level than that observed by the heparanase-selected aptamers. This suggests that there is some binding due to electrostatic interactions from the positive charge of the enzyme and the strong negative charge of the aptamer. The graph of 1.5M long and 3.0M aptamers show a plateau at 100nM heparanase, with a plateau at 70nM for 1.5M short aptamer when binding sites become exhausted. Also, the absorbance reaches a higher maximum for the two longer aptamers which would suggest that more heparanase is retained by them, and may be explained by their size in that more 9kDa 1.5M short aptamers may be obscured and subject to steric hindrance by one 58kDa heparanase molecule than a 22kDa 1.5M long or 17kDa 3.0M aptamer. Therefore, more 1.5M long and 3.0M aptamers are available for binding heparanase.

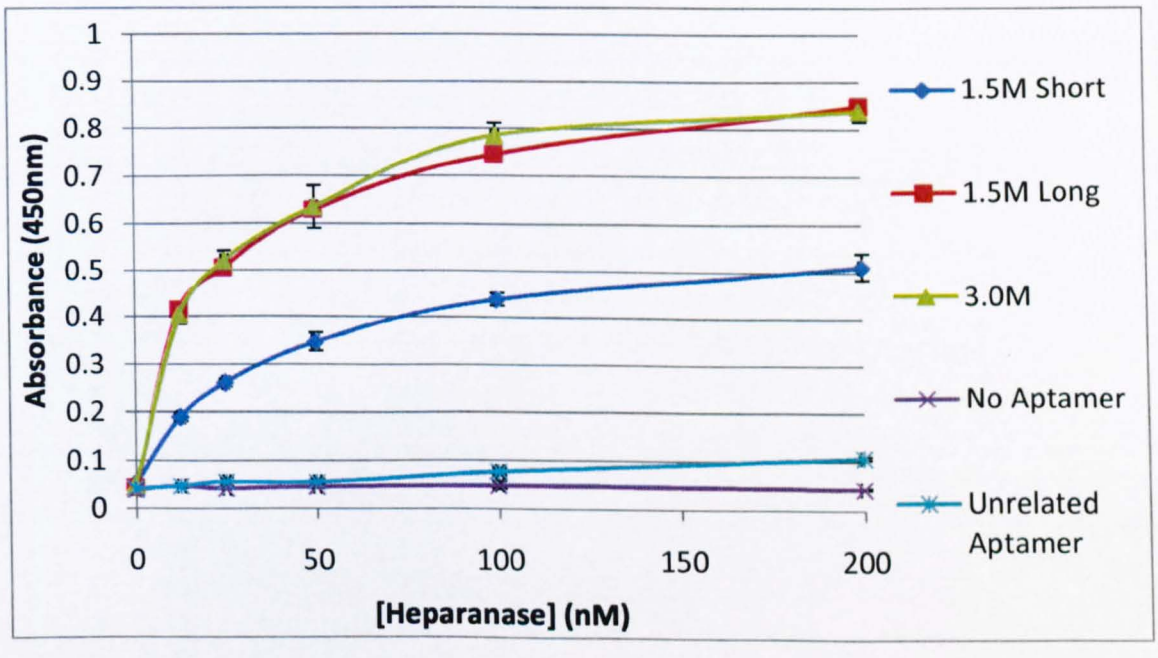

Figure 4.8 - A streptavidin ELISA carried out by immobilisation of 187nM of each 5' biotinylated aptamer (1.5M short, 1.5M long, 3.0M and an unrelated aptamer) with 41.5nM streptavidin and the wells of an ELISA plate. After blocking with 10mg/ml BSA in PBS, 0-200nM heparanase was incubated for one hour and then the ELISA was run to completion. All heparanase-selected aptamers showed an increase of absorbance upon increasing heparanase concentration above the negative controls, confirming binding. Error bars represent standard deviation of the mean from triplicate results.

The streptavidin ELISA method was applied to investigate binding and recognition of heparanase-selected aptamers to heat denatured and active heparanase. 200nM each 5' biotinylated aptamer were incubated in streptavidin-coated PCR tubes overnight, then blocked in 5mg/ml BSA in PBS. After the wash step, heparanase (some of which had been previously denatured by heating to 95°C for one hour), serially diluted from 0-400nM was incubated in its respective well for one hour and the ELISA was run to completion. Figures 4.9 to 4.11 show the results of each aptamer.

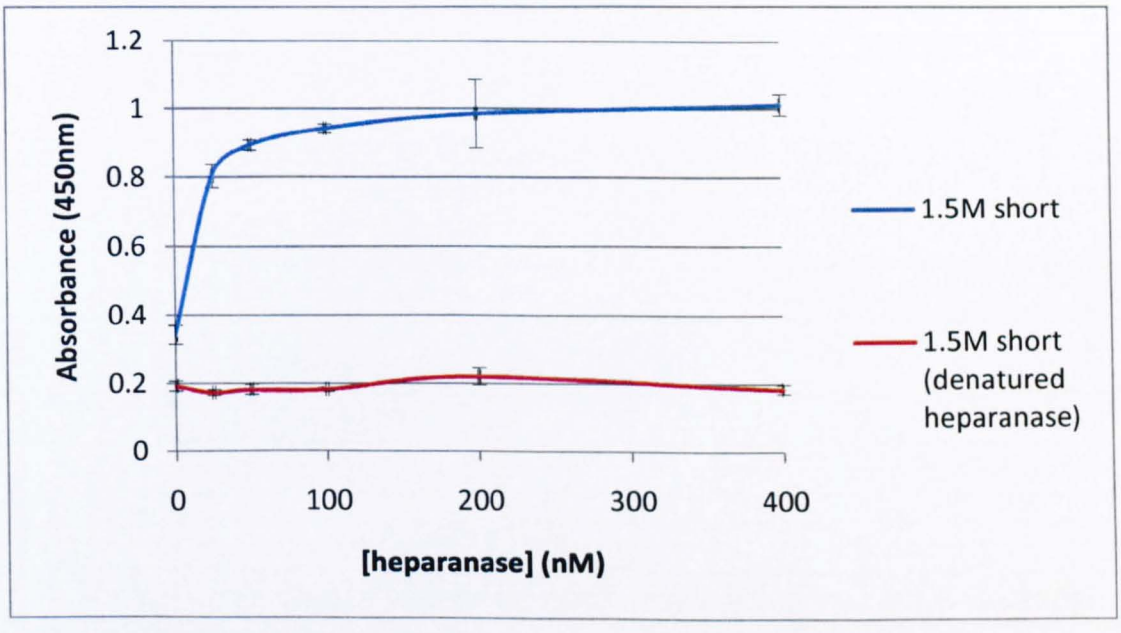

Figure 4.9 - A streptavidin ELISA carried out by immobilising 200nM 5' biotinylated 1.5M short aptamer to the wells of streptavidin-coated PCR tubes overnight at 4°C. After a wash step, denatured or active heparanase were added and the ELISA run to completion. Results showed that 1.5M short aptamer bound active heparanase similarly to the previous assays. However, the aptamer did not bind heat denatured heparanase as the absorbance did not increase upon increasing the concentration of heat denatured heparanase. Error bars represent standard deviation of the mean from triplicate experiments.

The results clearly indicate that all aptamers recognised and bound active heparanase as the absorbance showed a clear increase from that of the denatured heparanase, which did not increase at all upon adding increasing concentrations of the enzyme. Therefore, not only did the enzyme denature at 95°C but the selected aptamers did not recognise it,

suggesting that the aptamer recognises residues of the protein in its structured conformation.

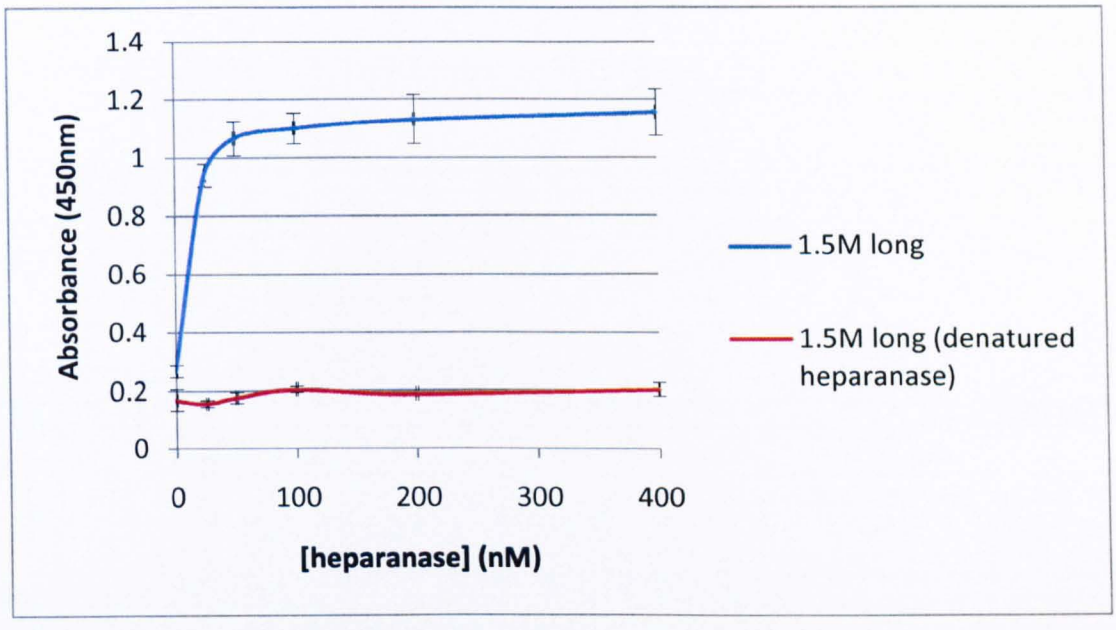

Figure 4.10 - A streptavidin ELISA carried out as above, using 200nM 5' biotinylated 1.5M long aptamer. Results showed that the aptamer bound active heparanase similarly to the previous assays. However, the aptamer did not bind heat denatured heparanase as the absorbance did not increase upon increasing the concentration of heat denatured heparanase.

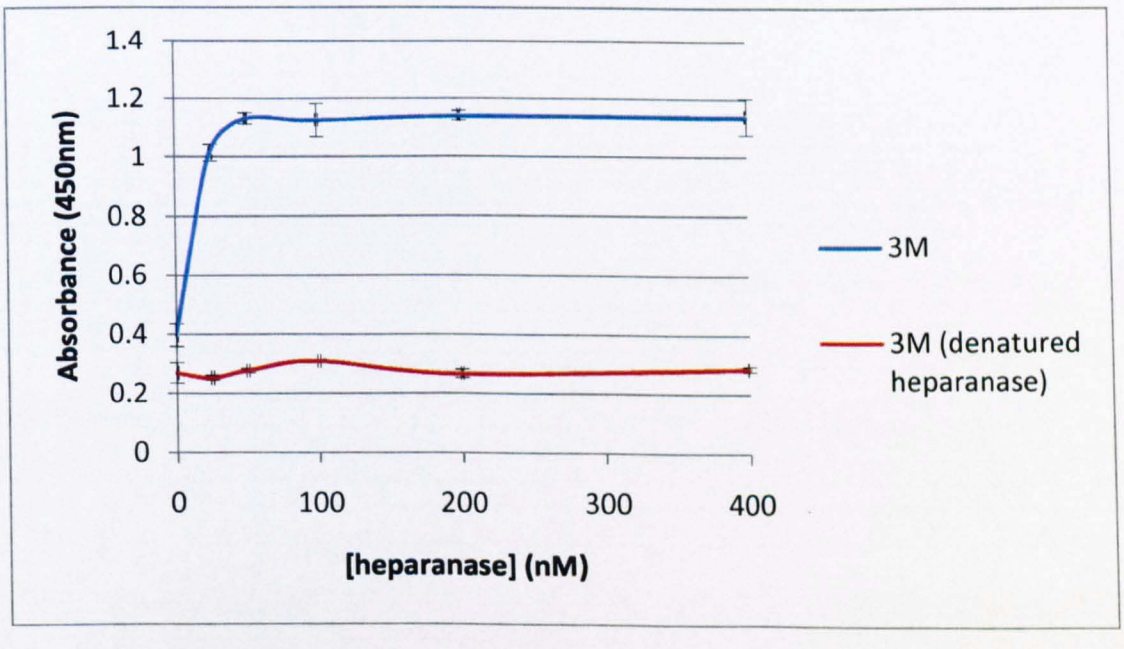

Figure 4.11 - A streptavidin ELISA carried out as above, using 200nM 5' biotinylated 3.0M aptamer. Results showed that the aptamer bound active heparanase similarly to the previous assays. However, the aptamer did not bind heat denatured heparanase as the absorbance did not increase upon increasing the concentration of heat denatured heparanase.

4.3 Fluorescence Quenching Titrations

To enable a fluorophore to fluoresce, it undergoes three main processes. Firstly, it must be excited by subjecting it to a photon of light at a particular wavelength, usually the same as that where it has its maximum absorbance. This causes it to maintain an excited state of high energy for a short amount of time when it is able to interact with other molecules and undergo structural changes. This causes some energy to dissipate and a consequent emission at a certain wavelength. Quenching, or decrease in fluorescence emission of a fluorophore in a peptide or protein may also occur with an excited fluorophore, and can be due to complex formation (static quenching) or collisional (dynamic quenching) between fluorophores and a quencher [3, 4]. Fluorophores then emit a photon of energy at a longer wavelength than the excitation wavelength, due to some of the energy already having been dissipated, returning them to their ground state. This process can be used to measure binding interactions, using an appropriate equation to plot the changes in fluorescence emission against concentration of the reactant added to the emitting molecule [3].

Both human polymorphic recombinant heparanase and GST fusion linker peptide contain tryptophan, tyrosine and phenylalanine residues, which have natural intrinsic fluorescence contained by dense populations of delocalised electrons in their aromatic rings [3]. Tryptophan is the major emitter of the three residues and if excited at 280nm forms an emission peak between 300 and 350nm depending on whether the tryptophan residues are exposed or 'hidden' within the folding of the protein [3]. Human recombinant mutant heparanase contains 6 tryptophan residues, all within the 50kDa subunit at sites 199, 220, 295, 340, 365 and 405. Linker peptide contains 2 tryptophan residues at sites 118 and 144.

In these experiments, aptamers generated for both the linker peptide and human recombinant heparanase were titrated with their respective targets based on [3]. Due to limited volumes of heparanase being available, it was decided to titrate volumes of aptamer to a heparanase solution, to continuously increase the concentration of aptamer until it was in excess over heparanase. This however, would add volume to the cuvette and dilute the total sample concentration. Thus, to assess the effects of this, salt solution was titrated in place of aptamer and the effect of the dilution was observed.

To analyse the data, fluorescence counts obtained from each addition were inserted into Microcal Origin, plotted and non-linear curve analyses drawn using equation 1.

$$\mathrm{Acalc(P0)} = \left[\left[\frac{(E1-E2)\left[(1+K\cdot D+K\cdot P0)-\sqrt{(1+K\cdot D+K\cdot P0)^2-4\cdot K\cdot K\cdot D\cdot P0}\right]}{2\cdot K}\right]+E2\cdot D\right]\cdot\frac{1}{D}$$

Equation 4.1 – Quadratic equation for fitting non-linear binding curves [3]. Acalc(P0) represents the maximum fluorescence of free heparanase divided by the fluorescent signals in presence of aptamer (F). P0 is the total aptamer concentration. K represents the equilibrium association constant. D is concentration of enzyme. E1 is the maximum value of Acalc(P0) and E2 is F when F is equal to F_0. To achieve 'best fit', figures for K and E1 can be modified to a degree.

Analysing the data in this way yields important information about the interactions of protein and aptamer, as it allows the calculation of association constants K_A for each aptamer to their cognate target.

Preliminary experiments were conducted using linker peptide, heparanase and aptamer alone to ensure that heparanase and its linker peptide showed a distinguishable peak if excited at 280nm (their absorption wavelengths) and that the aptamer did not show the same fluorescence emission profile (figures 4.12 and 4.13). Results showed evidence for the tryptophan peak at 335-340nm in both heparanase and the linker peptide, with no

peak from aptamer only, indicating this experiment's suitability for the study of aptamer-target protein interactions. Concentrations of 250nM heparanase and 500nM linker peptide were also derived from this experiment as they showed intense fluorescence signals, and 100mM salt solution was deemed as a suitable diluent, as no interference was observed. To minimise the dilution effect the aptamers would have on the concentration of heparanase, 20µM aptamer stock solution was used. This allowed two additions of 1.25µl to achieve the first two ratios of 10:1 (heparanase:aptamer) and 5:1, then the volume was doubled for each subsequent addition so that a total volume of 20µl was added to reach a final ratio of 0.625:1.

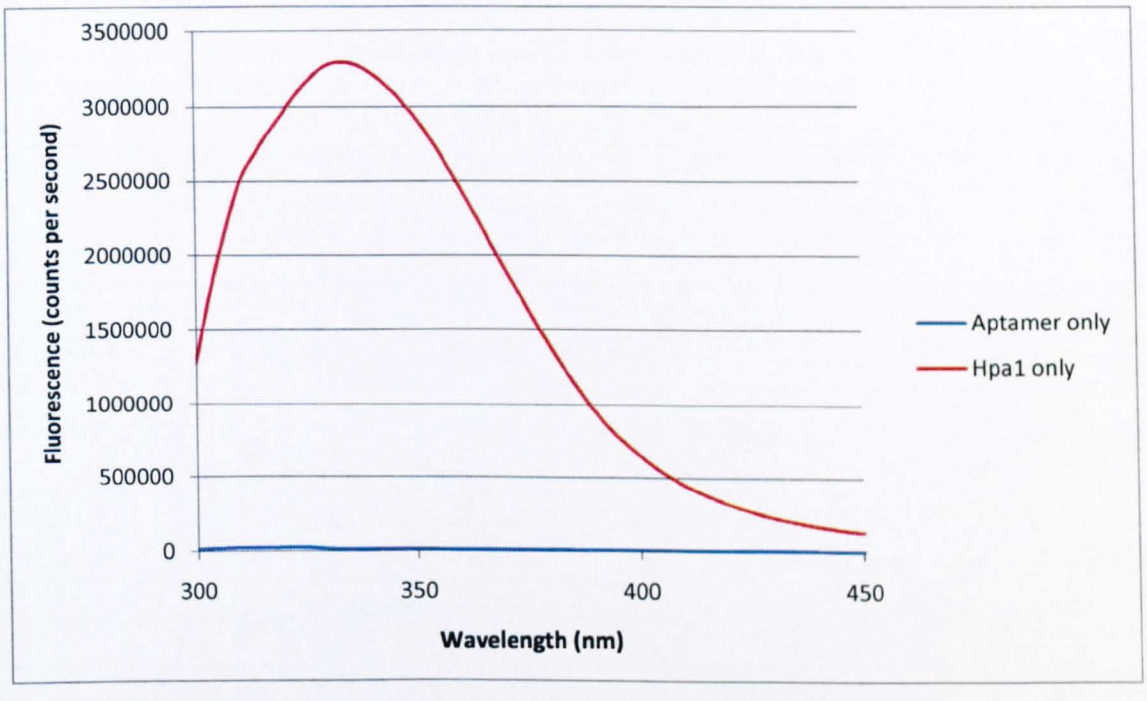

Figure 4.12 - Emission acquisition of 250nM heparanase only (red line) and 500nM 3.0M aptamer only (blue line), diluted in 100nM salt solution, to determine the presence of natural fluorescence in heparanase and that the spectrum of aptamer does not interfere.

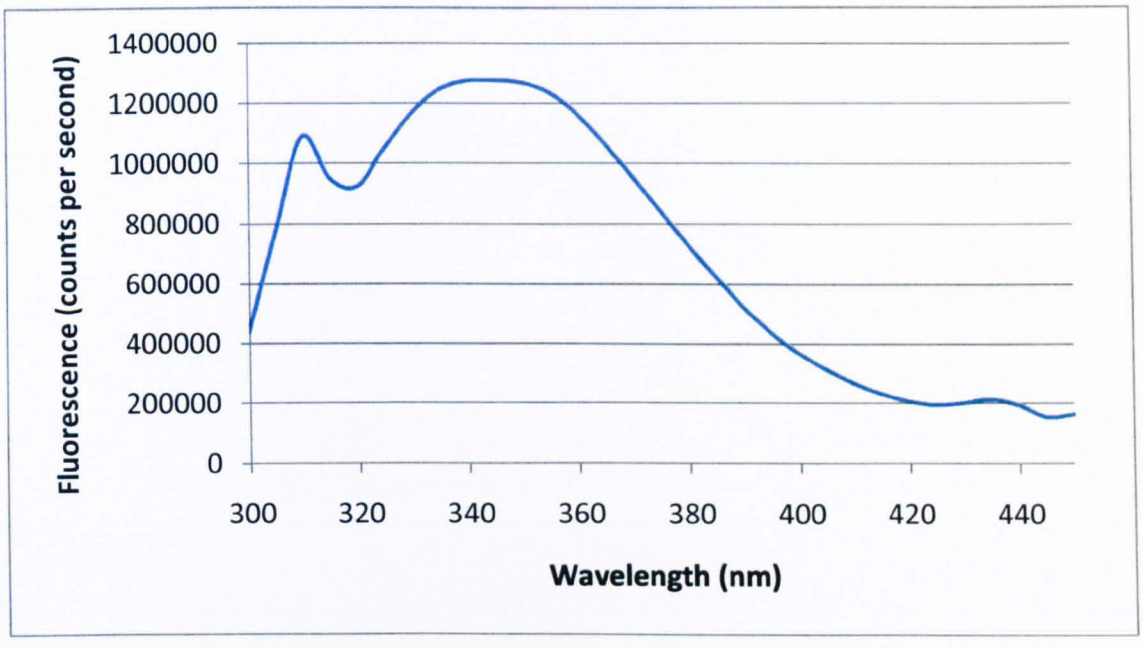

Figure 4.13 - Emission acquisition of 500nM linker peptide, diluted in salt solution, to determine its natural fluorescence spectrum.

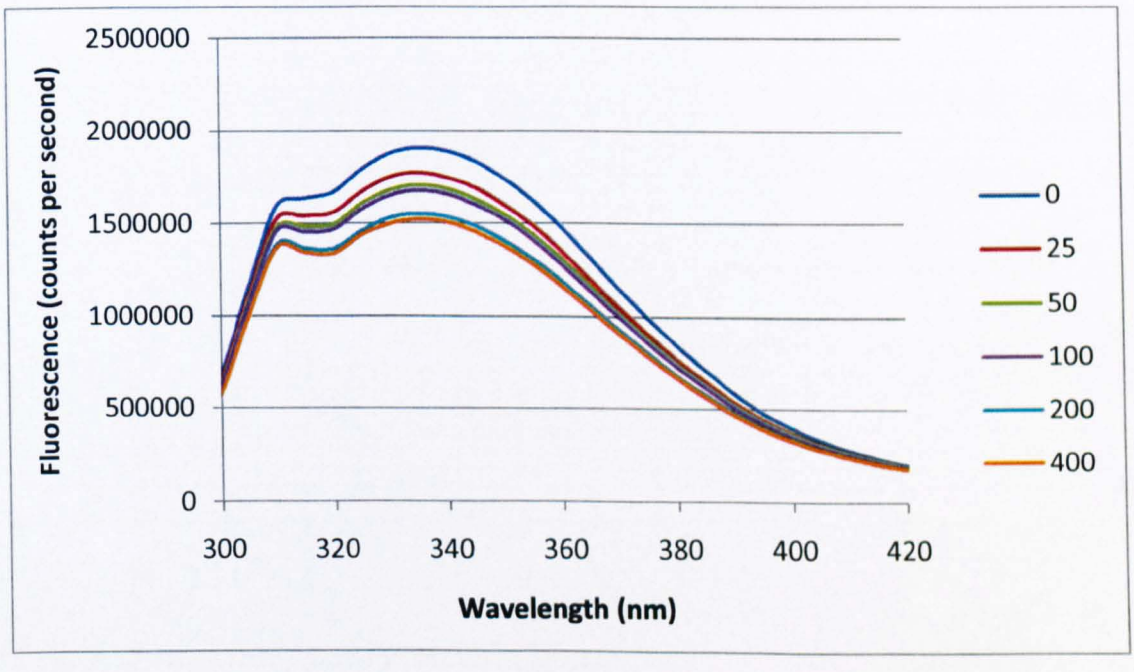

Figure 4.14 - Dilution effects upon 250nM heparanase. A total of 20µl 100mM salt solution was titrated in place of aptamer to observe any decrease in fluorescence. A total decrease of 20.2% was observed between the first and last titrations and maximum fluorescence signal was observed at 335nm.

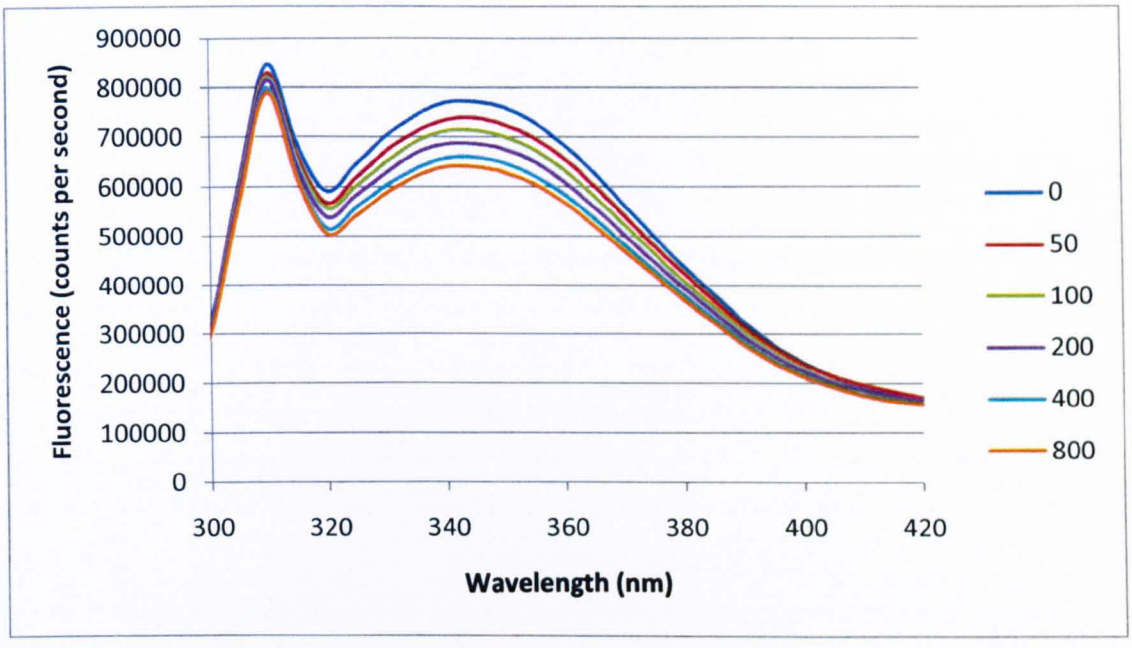

Figure 4.15 - Dilution effects upon 500nM linker peptide. A total of 20µl 100mM salt solution was titrated in place of aptamer to observe any decrease in fluorescence. A total decrease of 17.1% was observed between the first and last titrations and maximum fluorescence signal was observed at 345nm.

Figures 4.14 and 4.15 show experiments conducted when titrating 100mM salt solution in place of aptamer to observe the effect of time and dilution upon the change in fluorescence of heparanase and linker peptide. Unfortunately, even though the volumes added were the minimum the pipette could accurately dispense, it still decreased the fluorescence by 20.2% and 17.1% respectively.

Figure 4.16 shows the results of titrating 250nM heparanase with short aptamer. In the experiment, the fluorescence counts at 335nm decreased by 38% after addition of the last aliquot of aptamer, clearly indicating that the reduction in fluorescence was due to the interaction between the protein and the aptamer and not just a dilution effect.

Analysis of the decrease in fluorescence using the quadratic equation indicated above, suggested an association constant of $7.3 \times 10^{7} M^{-1}$ between the short aptamer and heparanase.

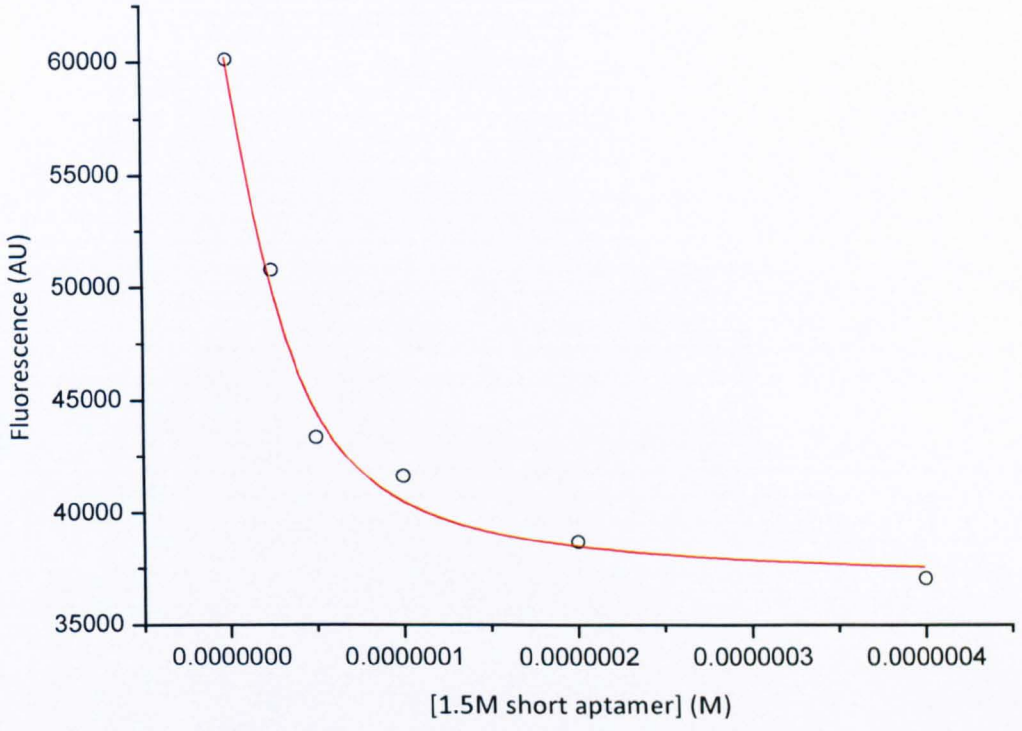

Figure 4.16 - Analysis of titration between 250nM heparanase and 1.5M short aptamer. After fitting the curve using the quadratic equation, a K_A of $7.3x10^7M^{-1}$ was determined.

Upon titrating 1.5M long aptamer with heparanase, a significant decrease in fluorescence was also observed, indicating the binding of this aptamer to heparanase. Figure 4.17 shows the analysis for the data, which determines an affinity constant of $8.3x10^7M^{-1}$ for the long aptamer and the heparanase enzyme, similar to that obtained with the short aptamer, which is the variable region of the long aptamer, without the primer sequences. It appears that the primer sequences have an effect on binding, which is not, however, significant.

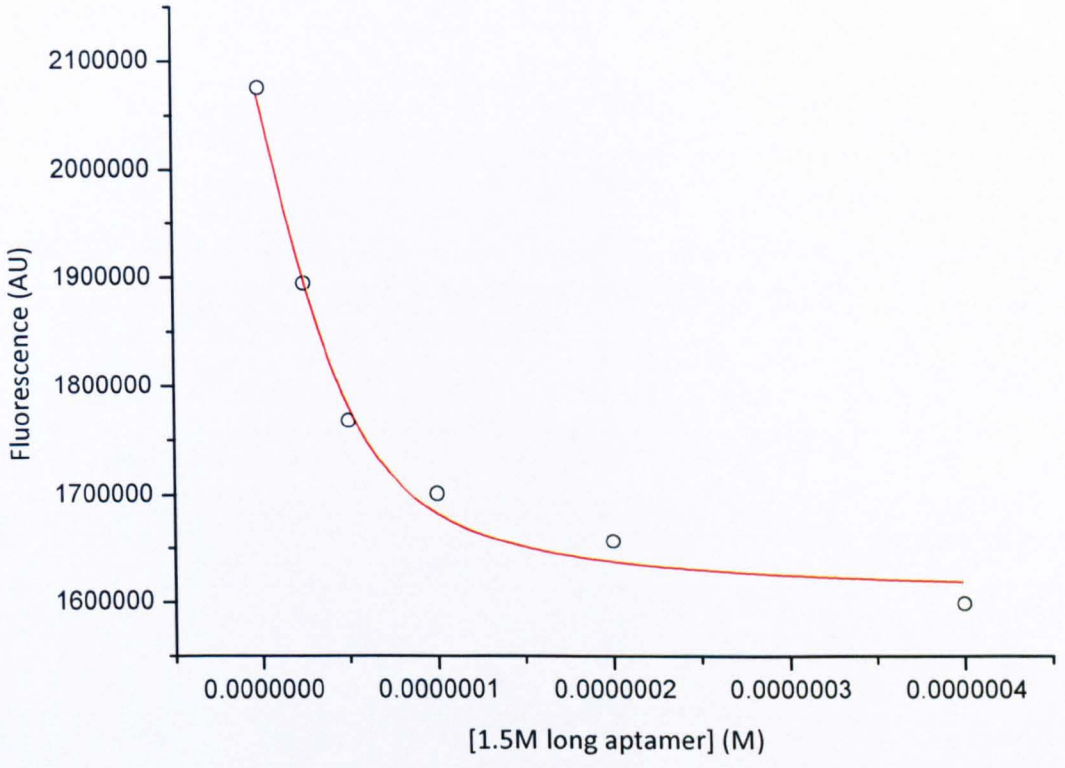

Figure 4.17 - Analysis of titration between 250nM heparanase and 1.5M long aptamer. After fitting the curve using the quadratic equation, the calculated K_A was $8.3x10^7M^{-1}$.

The 3.0M aptamer, when titrated into heparanase, also decreased the fluorescence counts, by 31%, showing a clear interaction of the aptamer with the enzyme. The calculated value for K_A after plotting the decrease in fluorescence versus aptamer concentration was found to be $7.7x10^7M^{-1}$, as seen in figure 4.18.

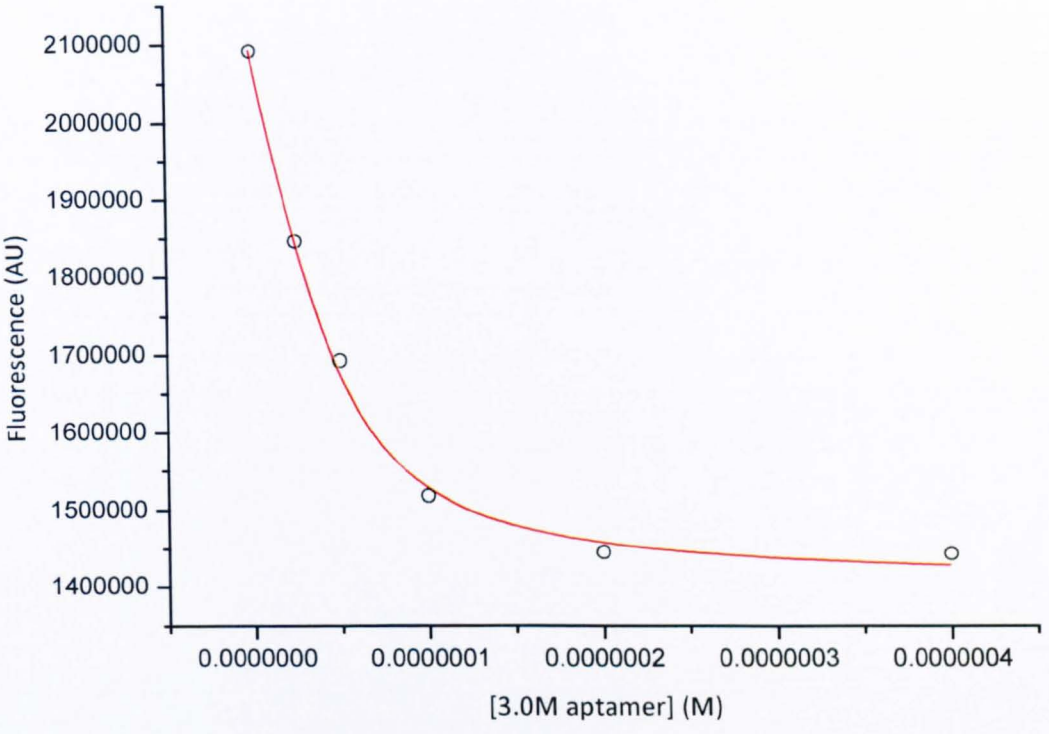

Figure 4.18 - Analysis of titration between 250nM heparanase and 3.0M aptamer. After fitting the curve using the quadratic equation, the calculated K_A was found to be $7.7x10^7M^{-1}$ for this aptamer against the heparanase enzyme.

When titrating the linker peptide with aptamers pink and yellow, both showed a 95% decrease in fluorescence between linker peptide alone and the last addition of aptamer, indicating an almost total loss of fluorescence emission upon aptamer binding. The two aptamers identified were also similar in their binding affinities for the peptide, as they displayed a K_A of 2.2 and $2.1x10^6M^{-1}$ respectively, shown in figures 4.19 and 4.20 respectively.

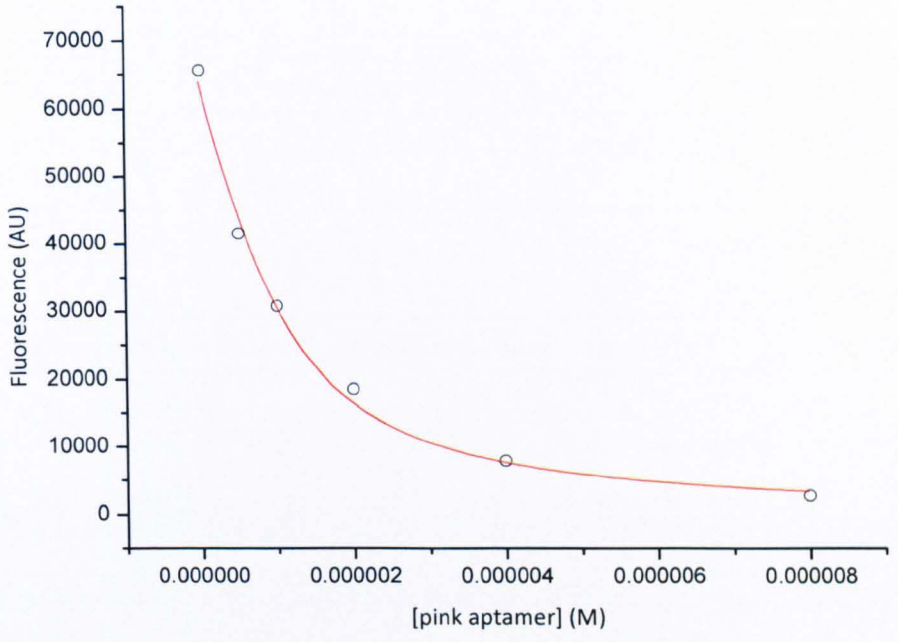

Figure 4.19 - Analysis of titration between 500nM linker peptide and pink aptamer. After plotting changes in fluorescence intensity versus aptamer concentration, the calculated K_A was found to be $2.2x10^6M^{-1}$.

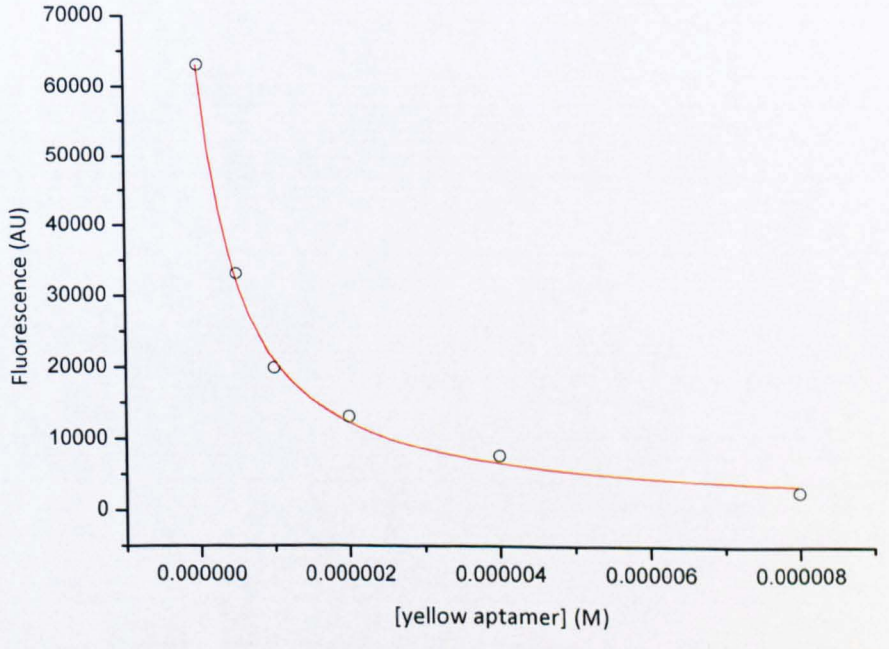

Figure 4.20 - Analysis of titration between 500nM linker peptide and yellow aptamer. After plotting changes in fluorescence intensity versus aptamer concentration, the calculated K_A was found to be $2.1x10^6M^{-1}$.

4.5 Discussion

These studies have shown that the aptamers selected against heparanase using the heat elution method did not bind heparanase, as indicated by ELISA and EMSA data. Therefore, it is possible that these aptamers were generated nonspecifically through binding to the wells of the 'Top Yield' tubes, which are designed specifically to bind to such biological molecules as proteins and nucleic acids. It was postulated that a reason why the ten round heat method did not generate aptamers was because the data in figure 4.3 suggested the aptamers may not have been released by the enzyme, which could have been stabilised by the binding of the aptamer. It has, however, been determined (see figures 4.9 to 4.11) that the aptamers generated by the salt round of selection did not recognise previously heat denatured heparanase, further supporting the evidence that the enzyme and aptamers form a stable complex that protects the enzyme from denaturation at these temperatures.

The streptavidin ELISAs all showed an increase of absorbance upon increasing heparanase concentration, suggesting binding between aptamer and heparanase (figures 4.8-4.11). Another piece of information obtained from the streptavidin ELISA in figure 4.8 was that the absorbance of the curves for 1.5M long and 3.0M aptamers reached a higher maximum than that of 1.5M short. This is likely due to more heparanase being retained in these two samples as 1.5M long and 3.0M aptamers are larger in size and less susceptible to steric hindrance than the smaller 1.5M short aptamer.

The fluorescence titrations tested all aptamers and yielded important information regarding the binding of the aptamers with the heparanase and heparanase linker peptide. The results of the fluorescence quenching titrations confirmed the results

obtained in the ELISA assays, demonstrating binding of the aptamers to the heparanase and heparanase linker peptide, and allowed the quantification of this interaction.

The decrease, or quenching, of the fluorescence counts (38% for 1.5M short, 23% for 1.5M long, 31% for 3.0M and 95% for both pink and yellow) indicate that both pink and yellow aptamers are binding in very close proximity to the two tryptophan residues at 118 and 144 and this is why the counts decreased so dramatically; nearly completely abolishing emission of fluorescence. As the linker peptide is only 6kDa compared to the aptamers' 22kDa, this could be expected if complexation between the two molecules were to occur, in agreement with the observations in our experiments. The lower quenching percentage from the heparanase-selected aptamers suggest they are binding further from a region containing one or more of the six tryptophan residues. As all tryptophans are spread within the 50kDa subunit at sites 199, 220, 295, 340, 365 and 405, it is likely that the binding of the aptamer would be closer to one or two tryptophans at a time, clearly accounting for the percentage of change observed in the fluorescence emission. It is even possible that the aptamer binds to the 8kDa subunit (which contains no tryptophan residues) or N-terminus, which carries a positive charge at physiological pH so would attract the negatively charged aptamer, but the aptamer binding to this part of the heterodimer causes such changes in the structure that they would affect the overall fluorescence emission of the tryptophans in the 50kDa subunit.

Binding of proteins and DNA occurs via intermolecular forces such as Van der Waals, electrostatic, and ionic and hydrogen bonding and is usually reversible; yielding a rate of association and dissociation. High affinity binding implies higher strength intermolecular forces, longer time of association between molecules and a low concentration of ligand needed to saturate the binding sites. Usually, the association constant (K_A) is used as a

measurement of binding affinity between aptamer and target, and is the inverse of the dissociation constant (K_D). This is shown by equation 4.2 below.

$$K_A = \frac{on-rate}{off-rate} = \frac{[aptamer.heparanase]}{[aptamer][heparanase]} = \frac{1}{K_D}$$

Equation 4.2 – Relationship between affinity constant (K_A) and dissociation constant (K_D) in binding studies [5].

Using this equation to obtain dissociation constants for the aptamers generated to heparanase yields 13.7nM, 12nM and 13nM for 1.5M short, long and 3.0M respectively, which compares with high affinity aptamers generated by other groups for their targets. For the linker peptide, 450 and 480nM for pink and yellow respectively unfortunately does not represent such a strong affinity, though this may be expected due to the fact that the target is a peptide and not a whole protein.

As these results were promising, the aptamers were subjected to further testing in *in vitro* studies using cell lines and invasion models to determine their selectivity among other proteins and enzymes, their functionality and their ability to inhibit the function of heparanase and linker peptide and also determine the presence of the heparanase and linker peptide in immunohistochemistry assays, which is the subject of the subsequent chapters of this.

References:

1. Ferreira, C.S., C.S. Matthews, and S. Missailidis, *DNA aptamers that bind to MUC1 tumour marker: design and characterization of MUC1-binding single-stranded DNA aptamers.* Tumour Biol, 2006. **27**(6): p. 289-301.
2. He, X., et al., *Hypoxia increases heparanase-dependent tumor cell invasion, which can be inhibited by antiheparanase antibodies.* Cancer Res, 2004. **64**(11): p. 3928-33.
3. Missailidis, S., *Targeting of antibodies using aptamers.* Methods Mol Biol, 2004. **248**: p. 547-55.
4. Silva, D., C.M. Cortez, and S.R. Louro, *Chlorpromazine interactions to sera albumins. A study by the quenching of fluorescence.* Spectrochim Acta A Mol Biomol Spectrosc, 2004. **60**(5): p. 1215-23.
5. Huading, Z., et al., *Binding affinities/avidities of antibody-antigen interactions: Quantification and scale-up implications.* Biotechnology and Bioengineering, 2006. **95**(5): p. 812-829.

CHAPTER FIVE

CELL AND TISSUE-BASED RECOGNITION BY APTAMERS

5.1 Background

Previous assays testing anti-heparanase aptamers' '1.5M short', '1.5M long' and '3.0M' recognition and binding of heparanase, showed promising results, with reasonable affinity constants, supported by results from streptavidin ELISAs. However, these were bench top assays containing a limited number of other proteins and enzymes, so it was unknown whether aptamers bound heparanase selectively under duress of an abundance of other different compounds *in vitro*.

It is well documented that the extracellular matrix (ECM) of the placenta and decidual tissue of the uterine wall are rich in heparan sulphate proteoglycans (HSPG), which are degraded by heparanase [1]. Heparanase is upregulated in the placenta [2, 3], and especially in cytotrophoblasts (as well as lymphocytes, monocytes, neutrophils and platelets) [4-10], making placenta an ideal tissue to use in experiments related to heparanase activity and/or inhibition.

The aim of these experiments was to stain cell lines and sections of different areas and time points of placenta with polyclonal heparanase antibody [11] to observe volume, patterns and distribution of staining. This was to provide a positive control with which to compare staining of the same tissue with three different aptamers: '1.5M short', '1.5M long' and '3.0M'; and give an indication of affinity and selectivity of the three aptamers for heparanase. Negative control antibodies, and aptamers raised against the 6kDa linker were also used, as well as an antibody that labels trophoblast cells. These experiments were carried out using immunohistochemical techniques; wax embedded sections and avidin peroxidase with 3,3'-Diaminobenzidine tetrahydrochloride (DAB) staining and

fixed, permeabilised endometrial cell lines labelled with streptavidin-fluorescein isothiocyanate (FITC) and propidium iodide (PI).

5.2 Immunohistochemistry (IHC) of paraffin-embedded placental tissue

The placenta is formed during the first stage of pregnancy when cells differentiate from the fertilised egg to form the blastocyst. This forms a barrier between the mother and foetus and allows exchange of oxygen, waste, hormones and antibodies, without which, the foetus would not survive.

The blastocyst contains an outer layer of cells called trophoblasts, which are invasive, eroding and metastasising cells; and the inner cell mass, which is located inside the trophoblast layer and later forms the foetus (figure 5.1). The blastocyst is formed in the first few days of pregnancy, when the trophoblasts immediately start secreting human chorionic gonadotropin (hCG, the hormone used in the pregnancy test), which make the endometrium receptive to implanting the embryo [12].

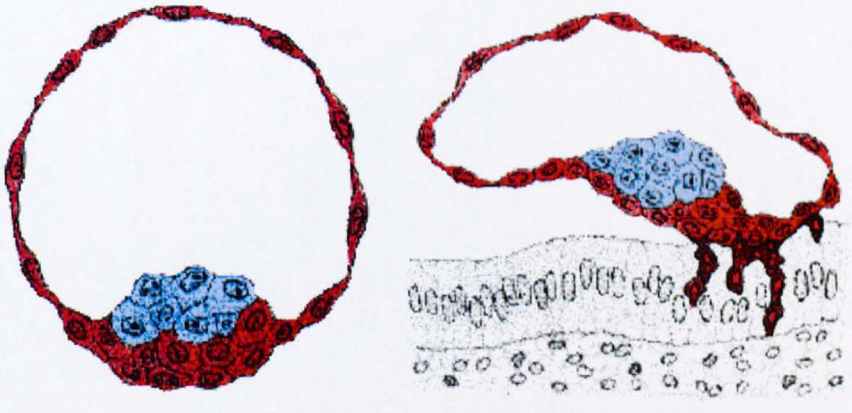

Figure 5.1 - Blastocyst at five days (left) formed by cytotrophoblasts (red) surrounding inner cell mass (blue), which later becomes the foetus. Placentation occurs (right) upon release of mucins and hormones from the cytotrophoblasts and endometrial wall, allowing the cytotrophoblasts to differentiate into invasive, anchoring and hormone-secreting trophoblasts (syncytiotrophoblasts), which all facilitate implantation. Modified from [13].

Mucins, which extend from the endometrium, slow the moving blastocyst and a complex release of hormones and protease inhibitors from both parties allow the trophoblasts to anchor to and invade the endometrium and myometrium (the inner and middle layers of the uterine wall) [12]. Cytotrophoblasts; the mononuclear precursor to all other trophoblasts, begin to differentiate upon the presence of these molecules, each type serving a different function, from secreting hormones (syncytiotrophoblasts), to anchoring the blastocyst, to becoming invasive and leading implantation at the front line [12]. Here, at two weeks of pregnancy, they begin remodelling the uterine spiral arteries – this is critical for a successful pregnancy [14]. The endometrium; now named decidua, forms the maternal part of the placenta [15].

At three weeks, the foetus has developed its blood system. Chorionic villi contain capillaries, which are the end-point of the foetal blood supply [12]. These are separated from the maternal blood by a layer of cyto- and syncytiotrophoblasts, which prevents immunological response and attack from the mother [12]. In between chorionic villi, inside the intervillous spaces, maternal blood is pooled, which forms the exchange site between the maternal and foetal blood supply.

First trimester and term chorionic villi show different morphology. First trimester chorionic villi show a mesenchymal core containing foetal capillaries, surrounded by a layer of cytotrophoblasts and syncytiotrophoblasts. Term chorionic villi show increased numbers of foetal capillaries, which lie close to the outer edge of the mesenchymal core to facilitate exchange of molecules between maternal and foetal blood. There are also fewer cytotrophoblasts, and increased syncytiotrophoblast clusters at the periphery of the villi [12].

5µm sections from different areas and time-points of the placenta were used to ascertain whether anti-heparanase aptamers '1.5M short', '1.5M long' and '3.0M' were competent at recognition and binding of heparanase in tissue previously shown to upregulate the enzyme. Characterisation of binding between the aptamers and target would clarify the most promising functional application for the aptamers; diagnostic or therapeutic. Experiments were repeated using tissue from different donors to ensure that all images displayed were representative and the results reproducible.

Sections were subjected to IHC by labelling with heparanase polyclonal antibody or anticytokeratin-7 antibody at 1:100 dilution in accordance with concentrations used in a previous study with these antibodies and tissue [1], biotinylated aptamers raised against the heparanase enzyme or linker peptide at a dilution of 1:200 to generate a similar molar concentration to that of the antibody, or a mouse negative control antibody added neat; followed by the respective secondary antibodies on the primary antibody treated samples only at a 1:200 dilution as used in a previous study [1]. Avidin peroxidase was used as the enzyme to develop the reaction of the DAB substrate, showing presence of heparanase as brown staining, whilst counterstaining with haematoxylin to show the nuclei in blue.

5.2.1 Term placenta

Term placenta experiments were repeated four times using tissue from different donors to ensure that all observations were accurate and representative. Overall, and as shown by figure 5.2, the sections stained with heparanase antibody have the highest level of staining, mainly around the periphery of the tissue and some within the foetal capillaries, showing the presence of heparanase. There is a high contrast between the levels of staining in this section with that seen in the negative control section. 1.5M long aptamer

showed the greatest result of all the aptamers; an identical staining pattern and intensity compared to the heparanase antibody. 1.5M short, pink and yellow aptamers only stained within the foetal capillaries and 3.0M showed a low level of stromal staining, which suggests that it is non-specific.

The morphology of the tissue and its staining by cytokeratin-7 antibody, suggests that this tissue is transverse section chorionic villi, and therefore, the cell types around the periphery that have shown presence of heparanase are cytotrophoblasts and syncytiotrophoblasts.

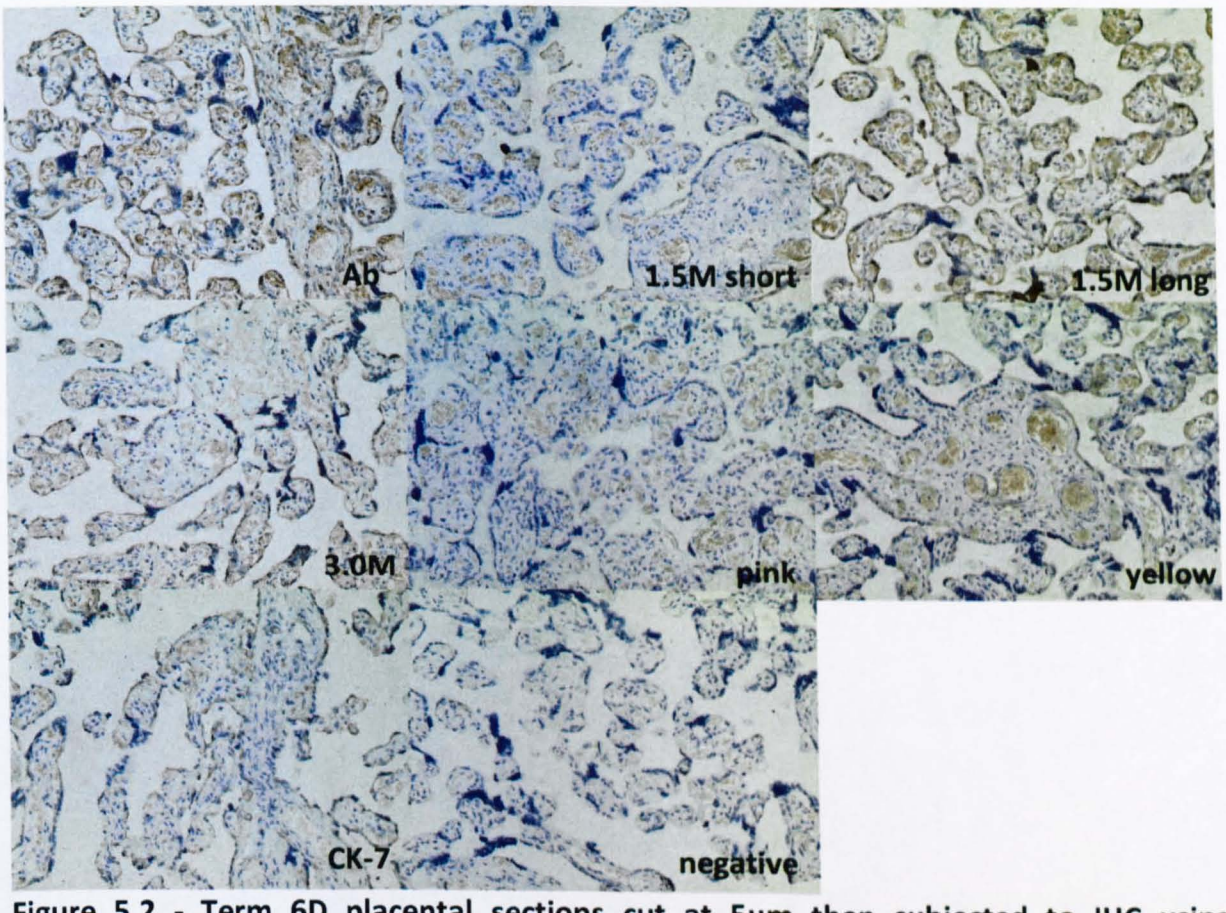

Figure 5.2 - Term 6D placental sections cut at 5µm then subjected to IHC using heparanase polyclonal antibody (Ab), biotinylated heparanase aptamers (1.5M short, 1.5M long, 3.0M), linker peptide aptamers (pink, yellow), positive control anti cytokeratin-7 antibody (CK-7) or a mouse monoclonal antibody as negative control (negative) and imaged at x20 magnification. Images are representative from four repetitions of reproducible results. Aptamer 1.5M long matched the staining pattern and intensity of the heparanase antibody, showing its specific recognition for heparanase, and the cytokeratin-7 antibody confirmed the heparanase-expressing cell types to be cyto- and syncytiotrophoblasts.

5.2.2 First trimester placenta

First trimester placenta experiments were conducted in triplicate. Figure 5.3 shows the different morphology this placental tissue has from that of term placenta. The immature chorionic villi are smaller in numbers and have larger diameters, together with a thicker trophoblast cell layer; shown by CK-7 antibody staining, compared to that of term placenta, correlating with the increased number of undifferentiated cytotrophoblasts. Heparanase-positive staining, shown by the heparanase antibody, was seen in the cytotrophoblasts lining the intervillous space of the chorionic villi, and in endothelial cells of the developing blood vessels. There was also some staining inside the villi in these sections in certain areas. No staining was observed when a mouse antibody was used as a negative control. Of the aptamers, 1.5M long and 1.5M short exhibited a staining pattern almost identical, although less intense than that of the antibody. 3.0M did show staining, although more uniformly throughout the stroma and not in the same pattern as the antibody, which suggests non-specific staining. Pink and yellow aptamers have exhibited little or no staining above the level of the negative control, suggesting there is no linker peptide in this sample.

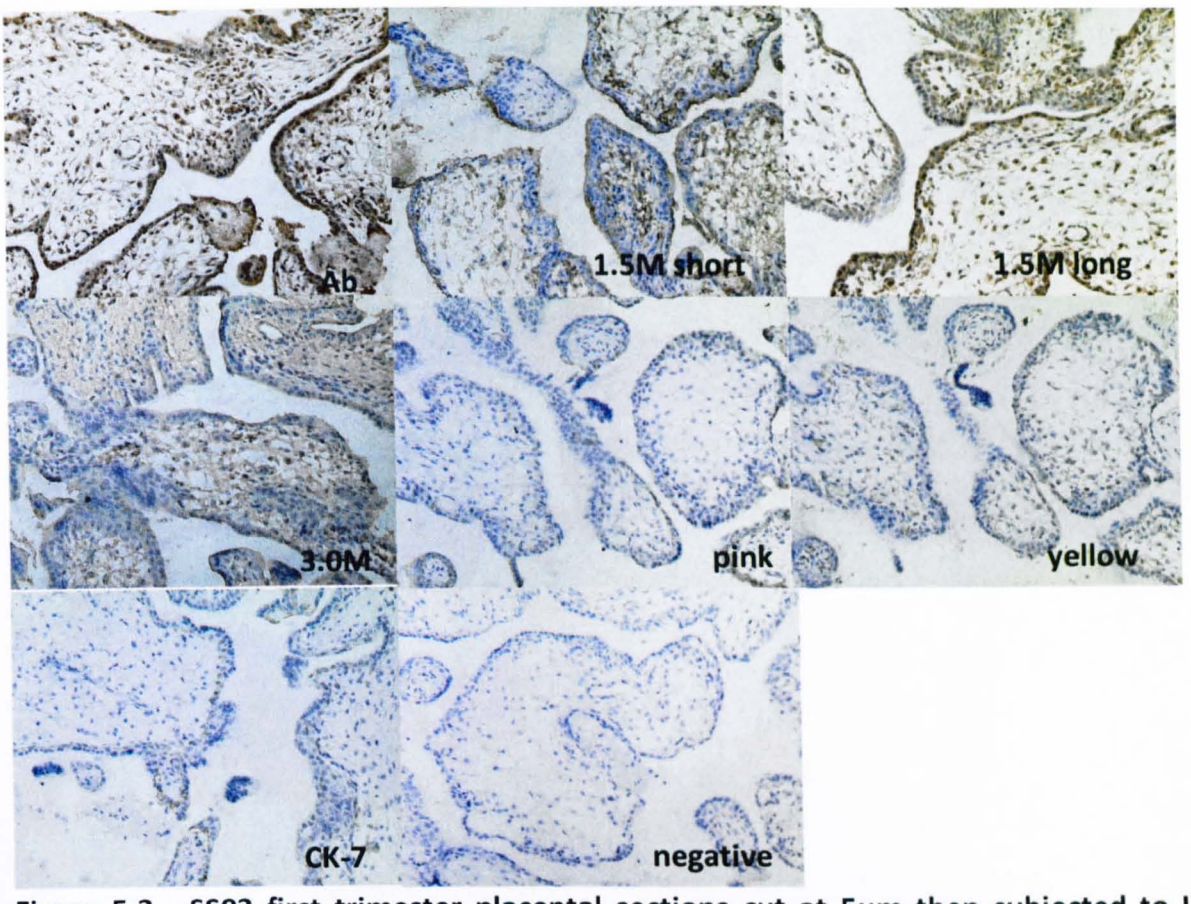

Figure 5.3 - SS03 first trimester placental sections cut at 5µm then subjected to IHC using heparanase polyclonal antibody (Ab), biotinylated heparanase aptamers (1.5M short, 1.5M long, 3.0M), linker peptide aptamers (pink, yellow), positive control anti cytokeratin-7 antibody (CK-7) or a mouse monoclonal antibody as negative control (negative) and imaged at x20 magnification. Images were representative of triplicate experiments, from which the results were reproducible. Of the aptamers, 1.5M long and short, respectively, showed a staining pattern and intensity close to that of the heparanase antibody.

5.2.3 Term decidua

In these sections there was only a very low level of staining so it is very difficult to form reliable conclusions. The cytokeratin-7 antibody has shown some trophoblasts around the periphery of the tissue in figure 5.4, but the aptamers and heparanase antibody have shown relatively low levels of heparanase compared with other tissue types in this study. This could be expected if heparanase is used for remodelling, as the tissue is term and therefore would be completely matured. The heparanase antibody has shown the highest level of staining, located within the tissue and around the periphery at the

location of trophoblasts shown by the cytokeratin-7 antibody. The negative control has shown staining inside the tissue; with its level higher than 1.5M short, 3.0M, pink and yellow aptamers, unfortunately reinforcing the observation that the conclusions from this tissue are not reliable. 1.5M long aptamer however, has once again shown a similar level of staining, although not so much at the location of the trophoblasts, as that by the heparanase antibody, continuing the pattern of the previous tissue samples.

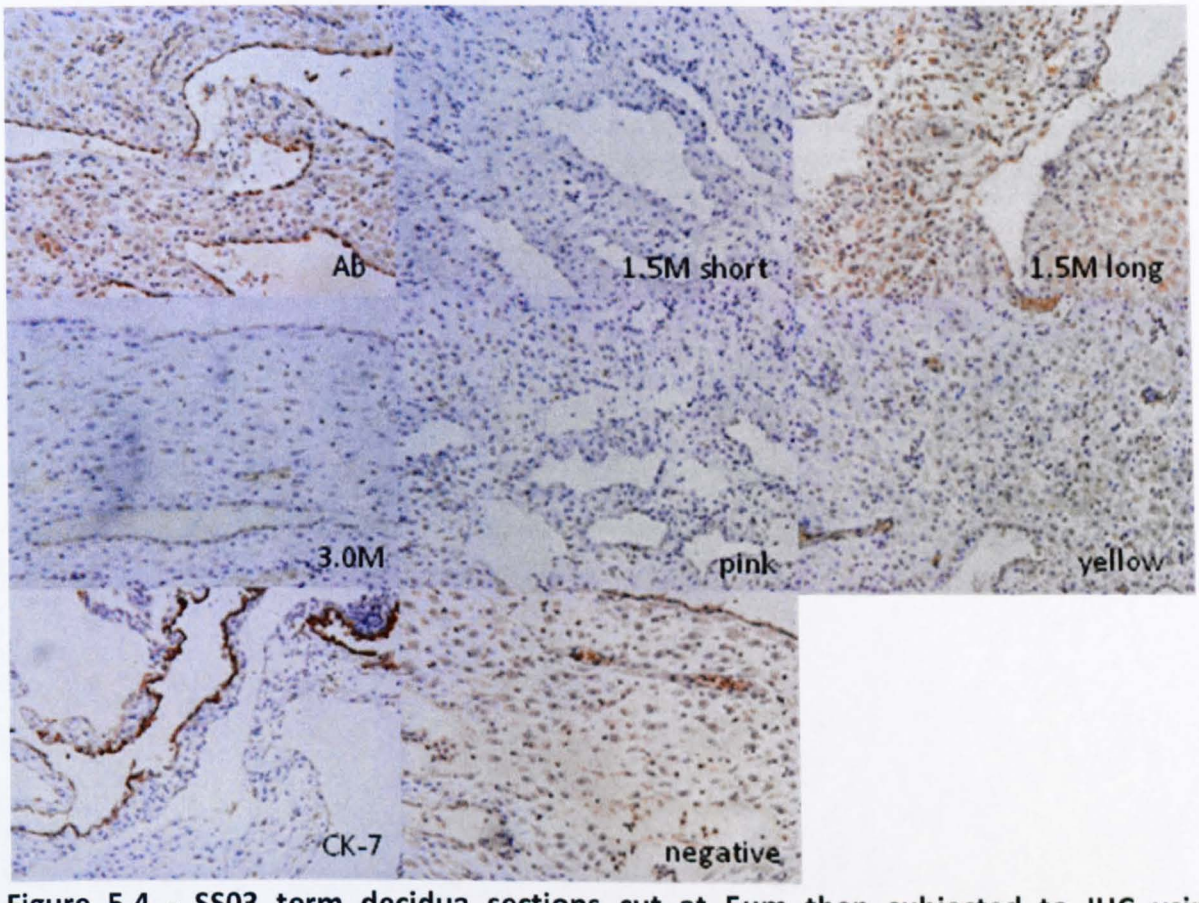

Figure 5.4 - SS03 term decidua sections cut at 5µm then subjected to IHC using heparanase polyclonal antibody (Ab), biotinylated heparanase aptamers (1.5M short, 1.5M long, 3.0M), linker peptide aptamers (pink, yellow), positive control anti cytokeratin-7 antibody (CK-7) or a mouse monoclonal antibody as negative control (negative) and imaged at x20 magnification. Images are representative from triplicate experiments. Aptamer 1.5M long showed a staining pattern most consistent with the heparanase antibody.

5.2.4 First trimester decidua

The overall results shown by experiments using first trimester decidual tissue are summarised by figure 5.5. Heparanase antibody has highlighted areas of heparanase in

the cyto- and syncytiotrophoblasts; confirmed by the presence of staining in the section labelled with CK-7 antibody, and in high volumes within the tissue itself. This high expression of heparanase is expected due to the rapid development of first trimester tissue. Of the heparanase aptamers, 1.5M short and 3.0M have shown a low level of staining throughout the tissue but not in the trophoblasts, and 1.5M long aptamer once again has shown the highest staining of heparanase, consistent with previous tissues, where it mirrored the staining patterns of the antibody. Pink and yellow aptamers have also shown high staining, suggesting presence of linker peptide within the tissue and trophoblasts, which would fit with the high levels of heparanase shown by the heparanase antibody, as one would expect to see linker within and around the trophoblasts due to their production and secretion of heparanase.

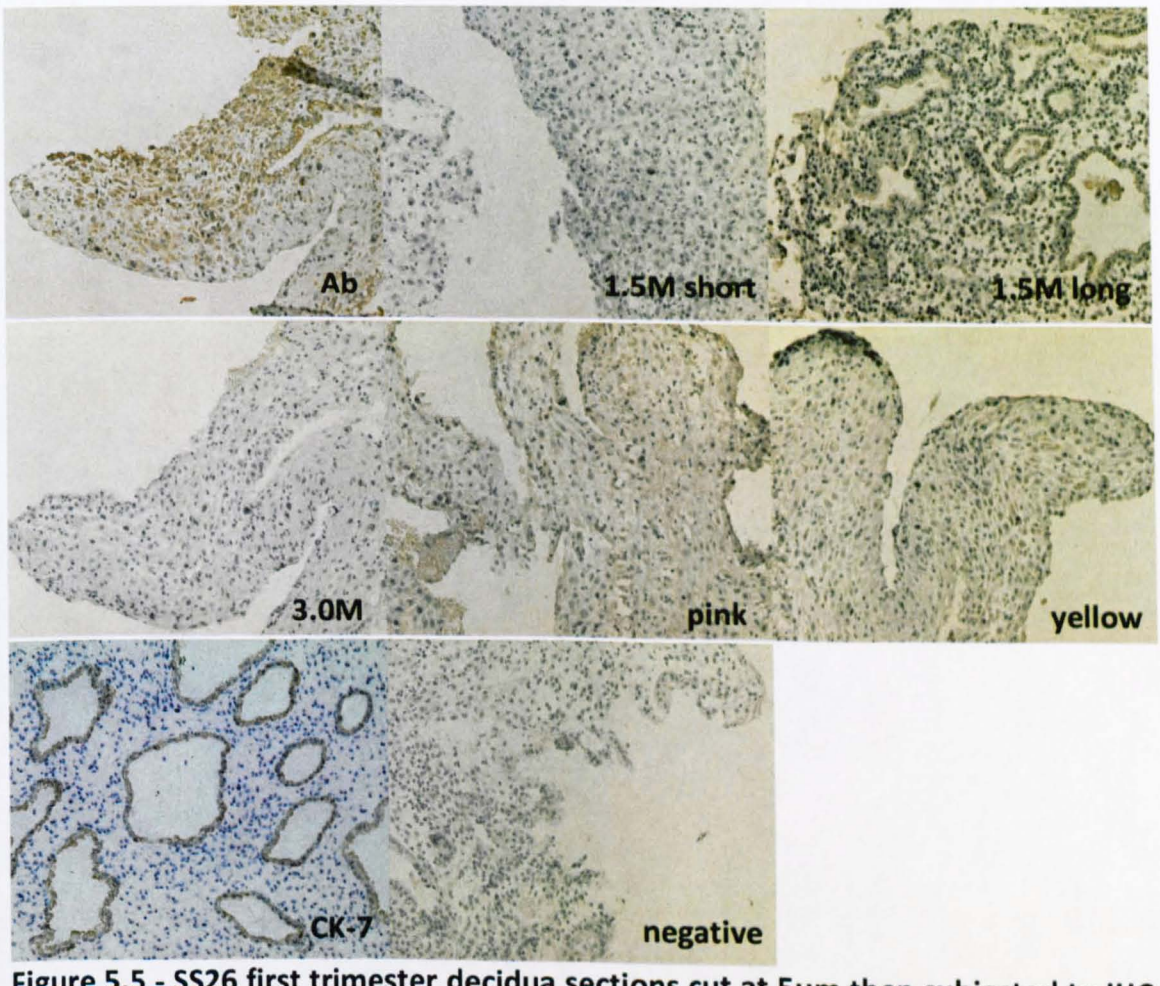

Figure 5.5 - SS26 first trimester decidua sections cut at 5µm then subjected to IHC using heparanase polyclonal antibody (Ab), biotinylated heparanase aptamers (1.5M short, 1.5M long, 3.0M), linker peptide aptamers (pink, yellow), positive control anti cytokeratin-7 antibody (CK-7) or a mouse monoclonal antibody as negative control (negative) and imaged at x20 magnification. Images are representative of triplicate

experiments. Heparanase aptamer 1.5M long and linker aptamers pink and yellow suggested presence of heparanase and linker peptide respectively, within the trophoblasts and tissue.

5.3 Immunofluorescence (IF) of placental-derived cell lines

Four different placental-derived cell lines were chosen for these experiments, BeWo; a trophoblast carcinoma cell line, Ishikawa; an endometrial carcinoma cell line, PL4; a first trimester immortalised trophoblast cell line, and first trimester placental stromal cells. Cells were grown on coverslips and were subsequently fixed and permeabilised in paraformaldehyde and triton-X 100, respectively, before being incubated with heparanase/cytokeratin-7/control mouse antibodies or heparanase/linker peptide biotinylated aptamers. Secondary antibodies were added to antibody-labelled coverslips, and then streptavidin-FITC conjugate was added to all coverslips, before being mounted with medium containing propidium iodide for labelling nuclei. Experiments were conducted in triplicate to gain consistency and ensure each cell line be treated with each label. The figures show the most representative images from each cell line and the overall conclusions are drawn from the reproducible results. In these fluorescent images, FITC molecules are responsible for the green staining showing heparanase presence, and propidium iodide for the red or blue staining, showing presence of the nuclei.

5.3.1 BeWo cells

From the results for heparanase antibody, it is clear that heparanase is present in the cytoplasm, plus inside the nucleus also in this cell line, as seen in figure 5.6. The appearance of heparanase is very granular. None of the aptamers have recognised

heparanase inside the nucleus in the same manner as the antibody; however, the aptamers selected for heparanase have all shown staining of granular appearance in the cytoplasm in accordance with that shown by the heparanase antibody, with 1.5M long aptamer looking the most promising. Pink aptamer showed a very low level of staining inside the cytoplasm and at the cell membrane and yellow aptamer showed staining at the cell membrane and exterior to the cells, not all in a granular form. Either could indicate presence of linker peptide, however, as they appeared no more pronounced than the negative control, it is likely to be background staining.

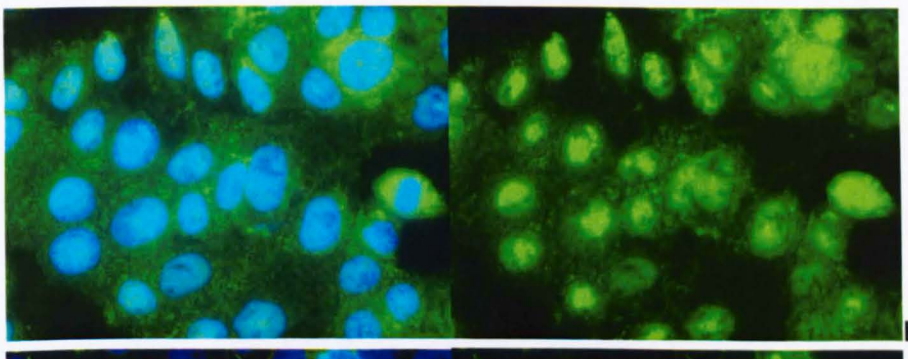

Heparanase antibody

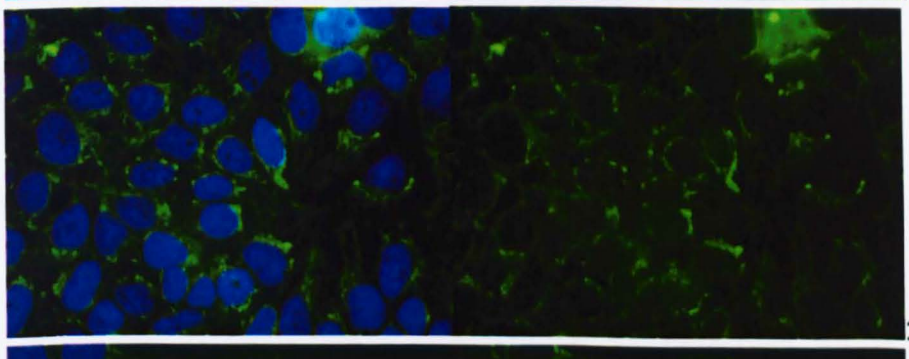

1.5M short aptamer

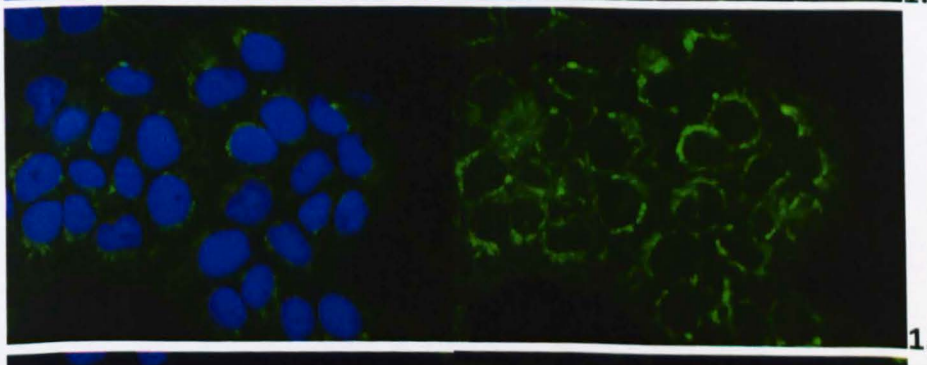

1.5M long aptamer

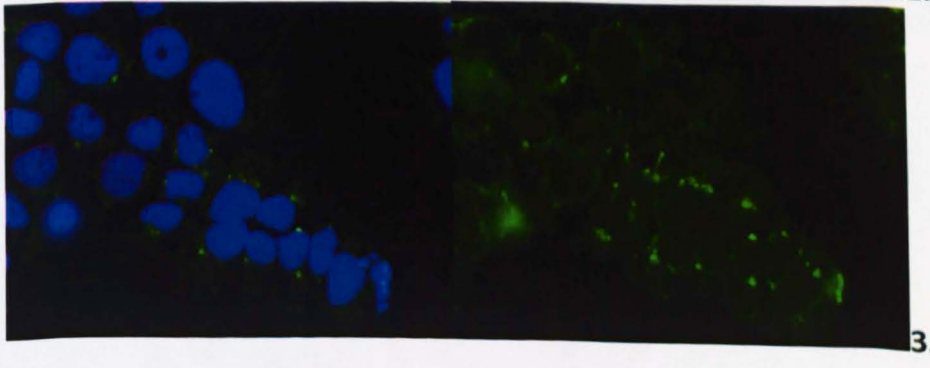

3.0M aptamer

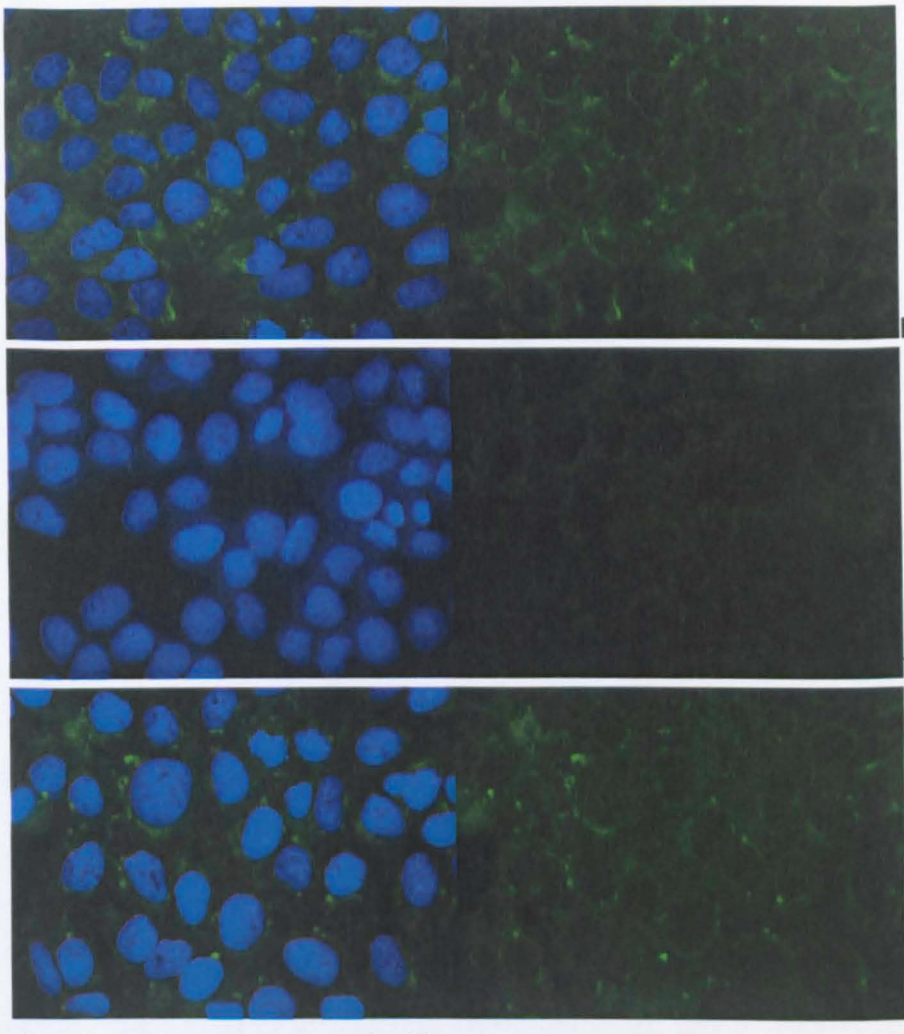

Figure 5.6 – BeWo trophoblast carcinoma cells subjected to IF using heparanase antibody, 1.5M short, long and 3.0M biotinylated heparanase-selected aptamers, pink and yellow biotinylated linker peptide-selected aptamers or a negative control mouse antibody, and imaged at x40 magnification showing heparanase expression (green) and nuclei (blue). Pink and yellow aptamers did not show increased volumes of staining from the negative control, whereas all of the heparanase-selected aptamers showed an increased level of staining, however, not as great as the heparanase antibody.

5.3.2 Ishikawa cells

In the Ishikawa cell line, the heparanase antibody has shown granular areas of staining in the cytoplasm and nucleus, as seen by figure 5.7. 1.5M short, 3.0M and pink aptamers show a low level of non-granular heparanase staining in the nucleus, which is different from the negative control as it has only showed staining in the cytoplasm. There are some small areas of granular staining with a more vibrant colour in the nucleus, but overall, these aptamers exhibit much less staining than exhibited by the antibody. 1.5M long aptamer shows the same granular vibrant staining patterns of the heparanase

antibody but not in as large a volume. Yellow aptamer has shown a very interesting result; it has completely stained the whole nucleus vibrant green, which does not appear to be background staining as the other samples do not show this. This could suggest a strong presence of linker peptide in the nucleus of these cells, which could be very exciting, as currently, little is known about the fate of the linker peptide after processing of the proenzyme.

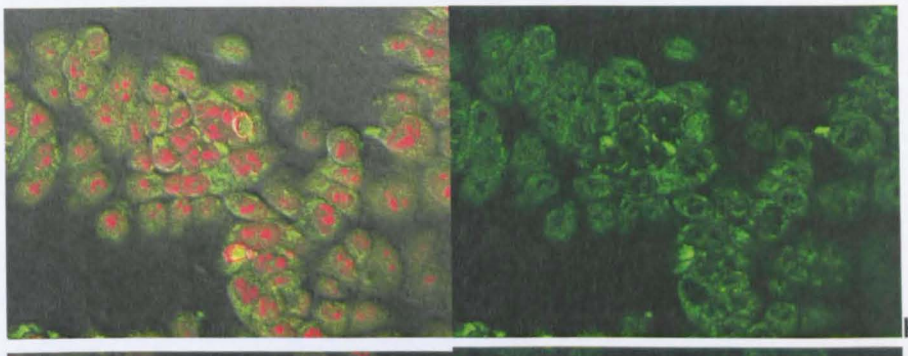

Heparanase antibody

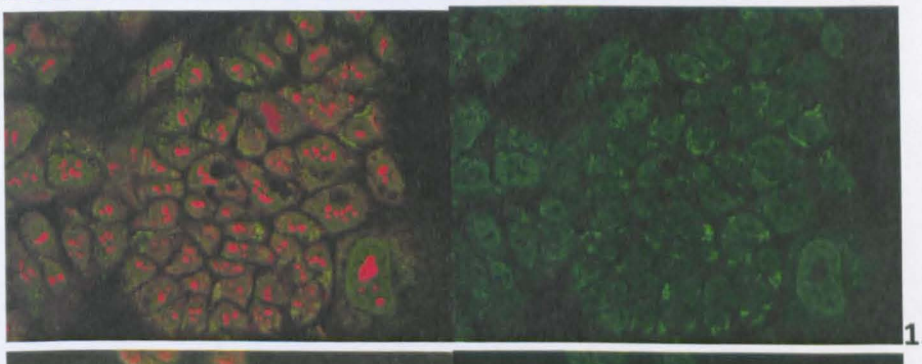

1.5M short aptamer

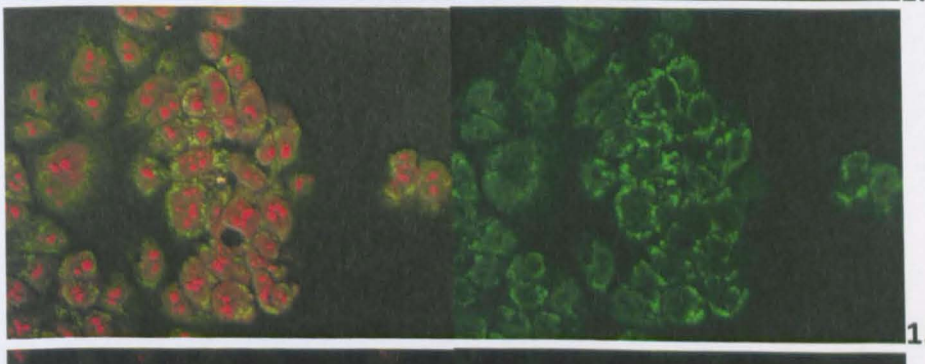

1.5M long aptamer

3.0M aptamer

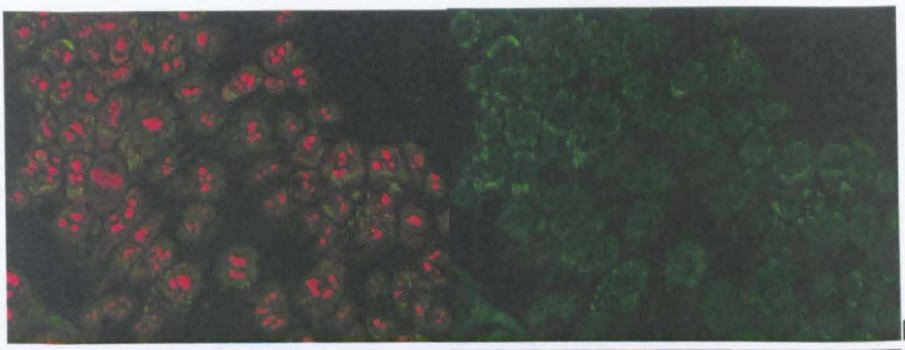

Pink aptamer

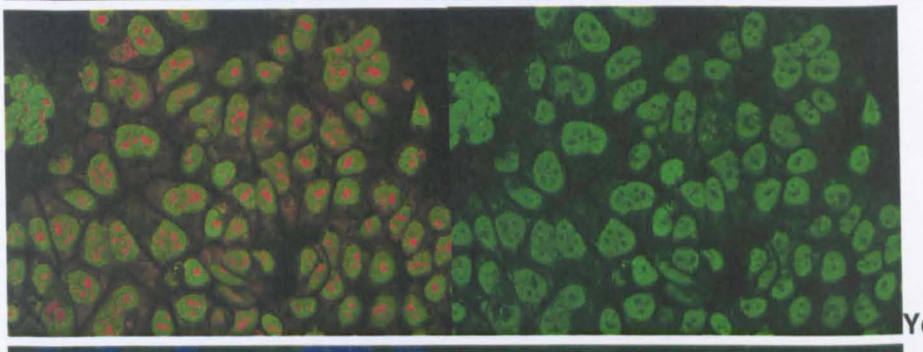

Yellow aptamer

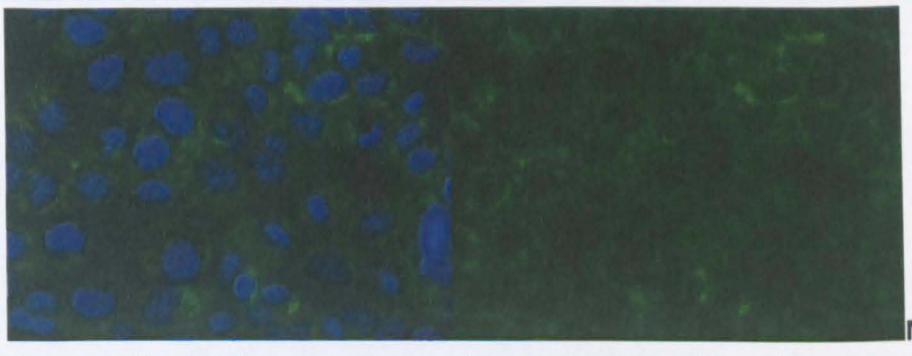

Negative control

Figure 5.7 - Ishikawa endometrial carcinoma cells subjected to IF using heparanase antibody, 1.5M short, long and 3.0M biotinylated heparanase-selected aptamers, pink and yellow biotinylated linker peptide-selected aptamers or a negative control mouse antibody, and imaged at x40 magnification showing heparanase expression (green) and nuclei (red or blue). Heparanase antibody and 1.5M long aptamer showed recognition of heparanase in the cytoplasm and nucleus and yellow aptamer stained the nucleus in large amounts, suggesting presence of linker peptide.

5.3.3 PL4 cells

The pattern of staining in the PL4 cell line shows high and granular heparanase levels mainly in the cytoplasm as shown by the heparanase antibody in figure 5.8, which was expected as the PL4 cell line is trophoblast. The signal was very strong using the antibody; however, it was just as strong with the aptamers selected for heparanase; 1.5M long aptamer even more so. Yellow aptamer showed a level of staining above the level of the negative control, which could indicate binding of the aptamer to linker peptide and its

presence in the cytoplasm. Pink aptamer did not show an elevated level of staining from the negative control, suggesting it did not recognise the presence of linker in this cell line.

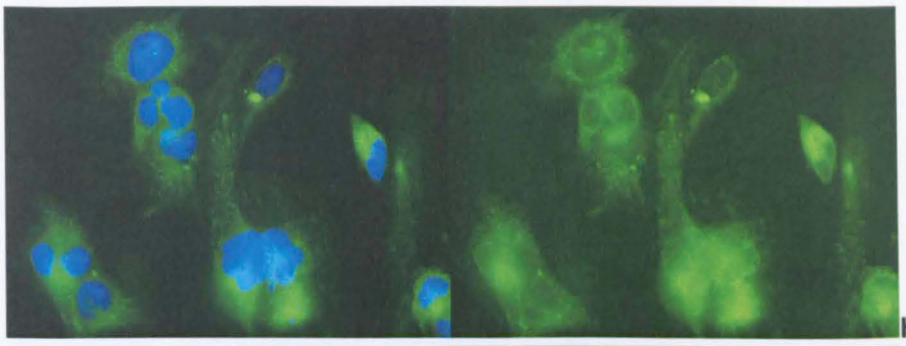

Heparanase antibody

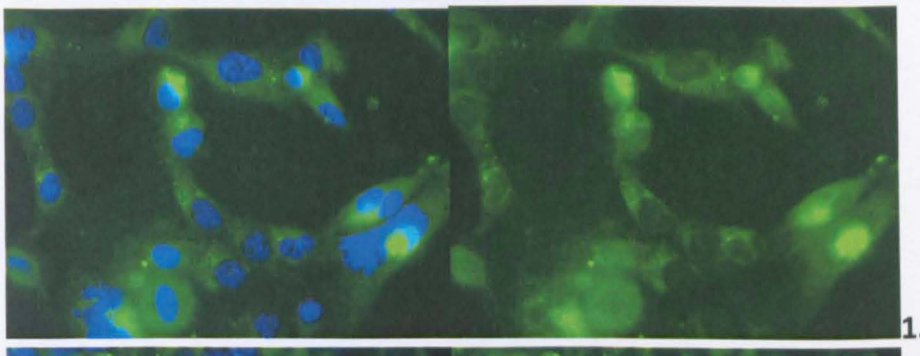

1.5M short aptamer

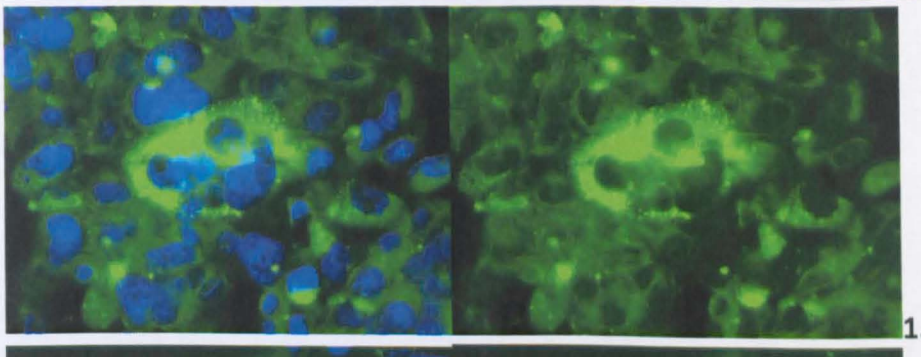

1.5M long aptamer

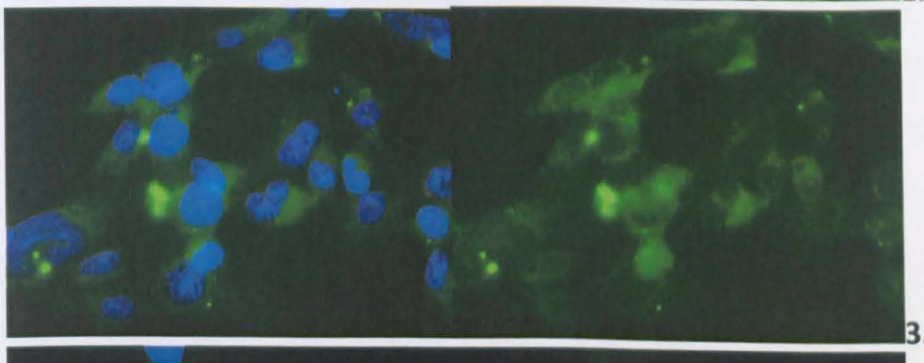

3.0M aptamer

Pink aptamer

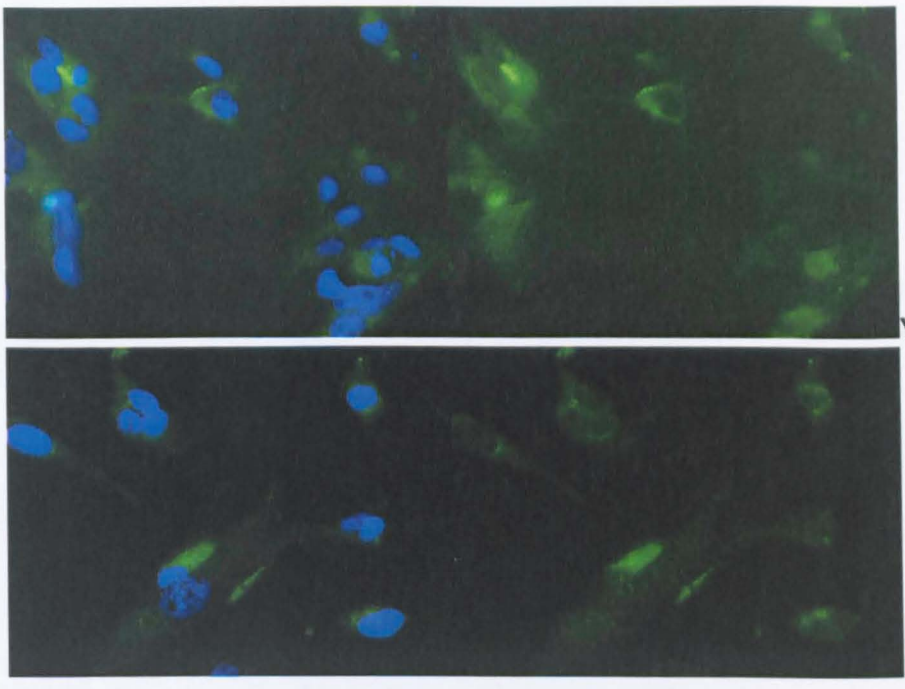

Figure 5.8 - PL4 immortalised trophoblast cells subjected to IF using heparanase antibody, 1.5M short, long and 3.0M biotinylated heparanase-selected aptamers, pink and yellow biotinylated linker peptide-selected aptamers or a negative control mouse antibody, and imaged at x40 magnification showing heparanase expression (green) and nuclei (blue). Heparanase antibody, aptamers 1.5M short, long and 3.0M all showed recognition of heparanase; mostly so by 1.5M long. Yellow aptamer also suggested presence of linker peptide in the cytoplasm.

5.3.4 Stromal cells

There was a very low level of heparanase staining in this cell type in general as seen in figure 5.9. As stromal cells are packing cells found inside the placenta, they may contain a low level of heparanase as they would undergo remodelling in pregnancy (as seen in the placental sections). However, they are not invasive cells by nature and so may not show the level of heparanase upregulation as trophoblast or carcinoma cell lines do. The heparanase antibody showed a low level of staining of a granular appearance in the cytoplasm and nucleus of the cells. All aptamers except for 1.5M short did not show a level of staining elevated from the negative control and 1.5M short was able to recognise heparanase to a higher extent in this tissue than the heparanase antibody.

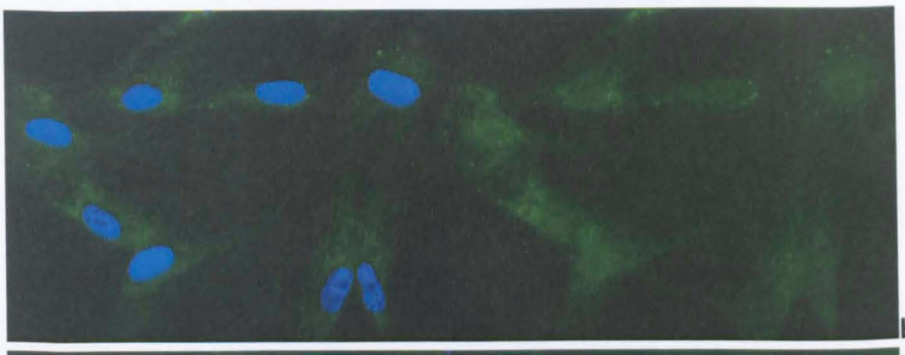

Heparanase antibody

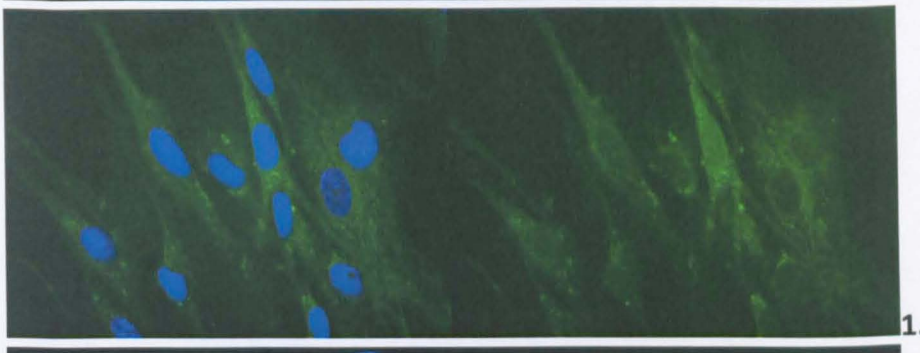

1.5M short aptamer

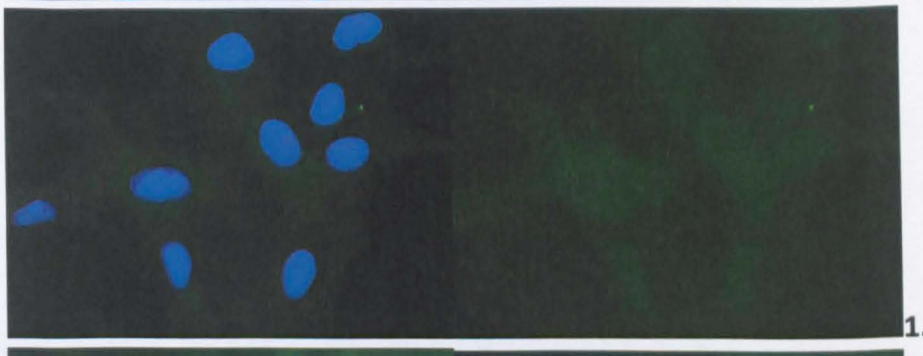

1.5M long aptamer

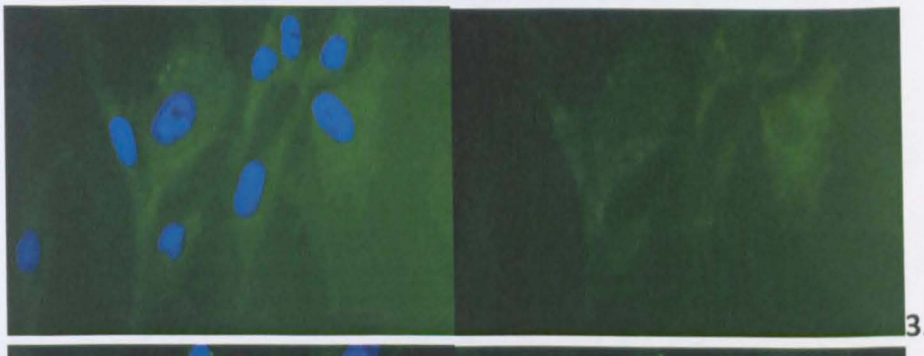

3.0M aptamer

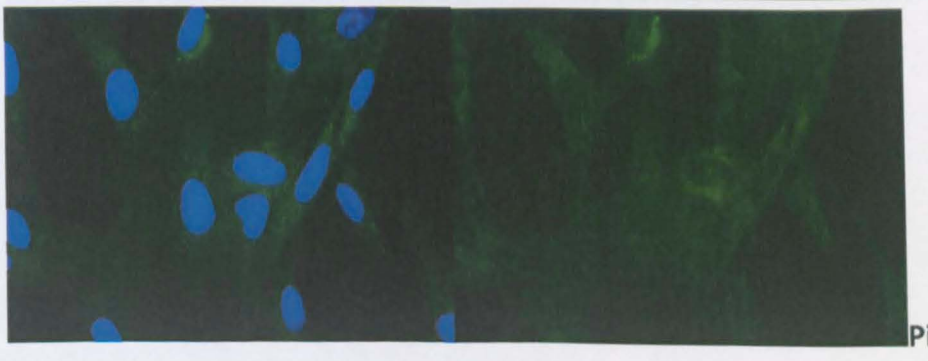

Pink aptamer

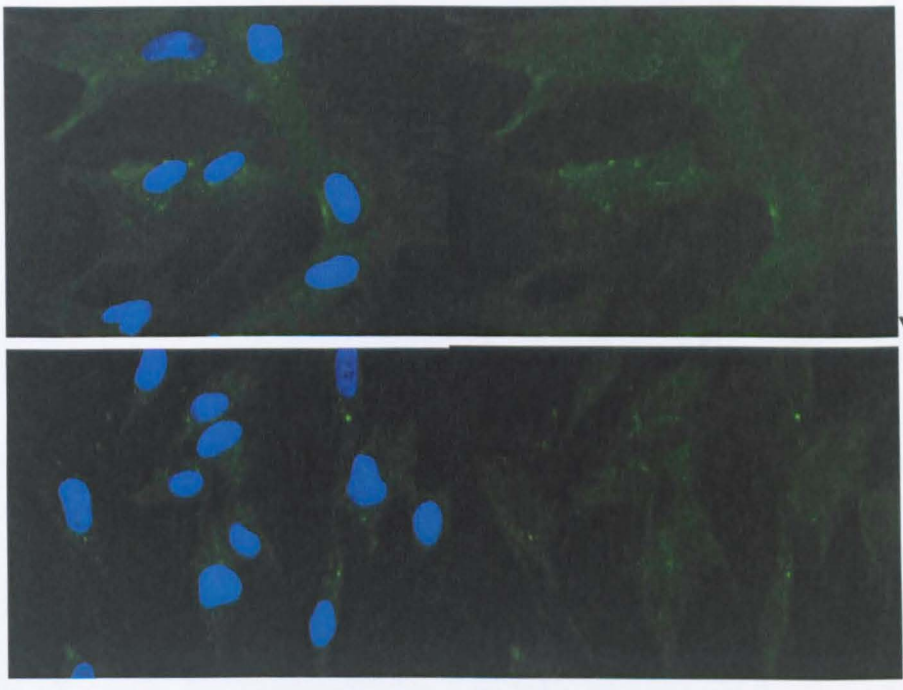

Figure 5.9 – Placental stromal cells subjected to IF using heparanase antibody, 1.5M short, long and 3.0M biotinylated heparanase-selected aptamers, pink and yellow biotinylated linker peptide-selected aptamers or a negative control mouse antibody, and imaged at x40 magnification showing heparanase expression (green) and nuclei (blue). 1.5M short aptamer, and to a lesser extent, heparanase antibody bound and recognised heparanase above the level of the negative control.

5.4 Discussion

Overall, these results compared the aptamers selected for heparanase favourably with the polyclonal antibody in terms of recognition and specificity for heparanase in cell and tissue sections.

The morphology and cytokeratin-7 staining in the placenta and decidual tissues suggests that the staining confined to the periphery displayed by the heparanase antibody and 1.5M long aptamer is from trophoblasts; confirming its identity as heparanase, as trophoblasts are heparanase-secreting invasive cells [2, 4].

1.5M long aptamer showed the most consistent staining in comparison with the heparanase antibody, with 1.5M short aptamer the next most promising. This may have been due to these both originating from the same aptamer and therefore they are

expected to share some structural features and/or binding nucleotides. In some sections 3.0M aptamer exhibited higher areas of staining than the negative control, however, as it was not in the same areas of the tissue that the heparanase antibody stained in, this suggests that it may have been non-specific.

Table 5.1 – A summary of representative data from immunofluorescence studies showing staining patterns of heparanase antibody, heparanase aptamers 1.5M short, 1.5M long and 3.0M; linker peptide aptamers pink and yellow, plus a negative control mouse antibody upon the cell lines tested. Location of staining is nuclear (N) and/or cytoplasmic (C) for each of the four cell lines.

Treatment	BeWo		Ishikawa		PL4		Stromal	
	N	C	N	C	N	C	N	C
Antibody	+	+	+	+	+	+	+	+
1.5M short	-	+	+	+	-	+	+	+
1.5M long	-	+	+	+	-	+	-	-
3.0M	-	+	+	+	-	+	-	-
Pink	-	-	+	+	-	-	-	-
Yellow	-	-	+	+	-	+	-	-
Negative	-	-	-	+	-	-	-	-

Table 5.1 summarises the data presented in the immunofluorescence studies. These showed volumes of heparanase located in the cytoplasm and nucleus of all cell lines, with bias toward nucleus or cytoplasm different in each cell line. Stromal cells did not show a large volume of heparanase and this was expected due to these cells not being invasive in nature, whereas Ishikawa, PL4 and BeWo cells were carcinoma, trophoblast and trophoblast carcinoma-derived cells respectively and are all invasive and would therefore be expected to express and secrete heparanase. In these studies the aptamers 1.5M long and short were shown to recognise heparanase to different extents in the different cell

lines; sometimes with better recognition than shown by the antibody. This further reinforces my previous results.

The aptamers selected for the linker peptide unfortunately cannot be confirmed as selective binders in the cell and tissue studies, as there is no antibody to compare them to, despite the high affinity shown for the linker peptide in previous studies (see chapter 4). However, the result for immunofluorescence using yellow aptamer definitely deserves further study as this suggested the presence of linker in the cytoplasm of trophoblast PL4 cells and its strong presence in the nucleus of carcinomal Ishikawa cells. Finding a way of proving that linker aptamers bind to the linker peptide, either by making an antibody or finding another inhibitor to compare them to in these assays, may provide useful information about the fate of the linker region after excision. Equally, the difference between the yellow and the pink aptamer, both of which were selected against the linker peptide, may be due to the ability of one to recognise the peptide both excised and as part of the proenzyme (yellow) whereas the other not (pink), explaining the reduced staining with the pink aptamer. Studying the potential inhibition of formation of active enzyme from the proenzyme by cathepsin L in the presence of yellow, but possibly not pink, aptamer could further confirm this hypothesis.

Investigations thus far had shown binding of the aptamers with reasonable affinity and recognition with specificity for the enzyme, especially exhibited by 1.5M long, shown by ELISA data and fluorescence quenching studies in which this aptamer also exhibited the highest K_A. Aptamer 1.5M short may not have shown the most promise in the previous studies with respect to binding affinity or retention of heparanase, but due to its smaller size than both antibody and the other aptamers, it may have been favoured in cell and

tissue-based studies, due to its increased tissue penetration in such assays. In addition to the binding and ability to label heparanase in cell and tissue studies, it was important to investigate the inhibitory effect, if any, of the aptamers on the enzymes function *in vitro*, as it is possible that the aptamers were able to bind to the enzyme without, however, inhibiting its function. This has been the subject of study in the following chapter, chapter 6, of this thesis.

References:

1. Harris, L.K., P.N. Baker, P.E. Brenchley, and J.D. Aplin, *Trophoblast-derived Heparanase is Not Required for Invasion.* Placenta, 2008. **29**(4): p. 332-7.
2. Goshen, R., A.A. Hochberg, G. Korner, E. Levy, R. Ishai-Michaeli, M. Elkin, N. de Groot, and I. Vlodavsky, *Purification and characterization of placental heparanase and its expression by cultured cytotrophoblasts.* Mol Hum Reprod, 1996. **2**(9): p. 679-84.
3. Haimov-Kochman, R., Y. Friedmann, D. Prus, D.S. Goldman-Wohl, C. Greenfield, E.Y. Anteby, A. Aviv, I. Vlodavsky, and S. Yagel, *Localization of heparanase in normal and pathological human placenta.* Mol Hum Reprod, 2002. **8**(6): p. 566-73.
4. Dempsey, L.A., T.B. Plummer, S.L. Coombes, and J.L. Platt, *Heparanase expression in invasive trophoblasts and acute vascular damage.* Glycobiology, 2000. **10**(5): p. 467-75.
5. Kizaki, K., H. Nakano, H. Nakano, T. Takahashi, K. Imai, and K. Hashizume, *Expression of heparanase mRNA in bovine placenta during gestation.* Reproduction, 2001. **121**(4): p. 573-80.
6. Vlodavsky, I., Y. Friedmann, M. Elkin, H. Aingorn, R. Atzmon, R. Ishai-Michaeli, M. Bitan, O. Pappo, T. Peretz, I. Michal, L. Spector, and I. Pecker, *Mammalian heparanase: gene cloning, expression and function in tumor progression and metastasis.* Nat Med, 1999. **5**(7): p. 793-802.
7. Freeman, C., A.M. Browne, and C.R. Parish, *Evidence that platelet and tumour heparanases are similar enzymes.* Biochem J, 1999. **342 (Pt 2)**: p. 361-8.

8. Laskov, R., R.I. Michaeli, H. Sharir, E. Yefenof, and I. Vlodavsky, *Production of heparanase by normal and neoplastic murine B-lymphocytes.* Int J Cancer, 1991. **47**(1): p. 92-8.

9. Mollinedo, F., M. Nakajima, A. Llorens, E. Barbosa, S. Callejo, C. Gajate, and A. Fabra, *Major co-localization of the extracellular-matrix degradative enzymes heparanase and gelatinase in tertiary granules of human neutrophils.* Biochem J, 1997. **327 (Pt 3)**: p. 917-23.

10. Sewell, R.F., P.E. Brenchley, and N.P. Mallick, *Human mononuclear cells contain an endoglycosidase specific for heparan sulphate glycosaminoglycan demonstrable with the use of a specific solid-phase metabolically radiolabelled substrate.* Biochem J, 1989. **264**(3): p. 777-83.

11. He, X., P.E. Brenchley, G.C. Jayson, L. Hampson, J. Davies, and I.N. Hampson, *Hypoxia increases heparanase-dependent tumor cell invasion, which can be inhibited by antiheparanase antibodies.* Cancer Res, 2004. **64**(11): p. 3928-33.

12. Kliman, H., *Trophoblast of the Human Placenta*, in *Encyclopedia of Reproduction*, E. Knobil and J. Neill, Editors. 1998, Academic Press.

13. Kliman, H. *From Trophoblast to Human Placenta*. [webpage] 1998 [cited; Available from: http://www.med.yale.edu/obgyn/kliman/placenta/articles/EOR_Placenta/Trophtoplacenta.html.

14. Cross, J.C., Z. Werb, and S.J. Fisher, *Implantation and the placenta: key pieces of the development puzzle.* Science, 1994. **266**(5190): p. 1508-18.

15. contributors, W. *Trophoblast*. Wikipedia, The Free Encyclopedia [Online Encyclopedia] 2008 25th April 2008 [cited 2008; Available from: http://en.wikipedia.org/w/index.php?title=Trophoblast&oldid=208056446

CHAPTER SIX

INHIBITION OF INVASIVE CELLS BY APTAMERS

6.1 Background

It has been demonstrated that aptamers 1.5M short, 1.5M long and 3.0M bind with high affinity and selectively recognise heparanase in ELISAs, fluorescence titrations and cell and tissue labelling at a different binding site than the polyclonal antibody. However, it was unknown what effect, if any, this binding had on the enzyme's function of hydrolysing heparan sulphate proteoglycans and invading the ECM. To investigate this further, two types of invasion assay were conducted; one using an artificial representation of ECM, and the other, a recently developed myoma model using human uterine leiomyoma tissue.

6.2 Matrigel Invasion Assay

Matrigel, a representation of ECM, is an extract of Engelbreth-Holm-Swarm (EHS) mouse sarcoma. It is a liquid that is rich in ECM proteins such as collagen IV, laminin and heparan sulphate proteoglycans and contains growth factors such as TGF-β, epidermal growth factor, insulin-like growth factor, fibroblast growth factor and tissue plasminogen activator and has been developed in response to the first documented invasion assays, which contained only type IV collagen and laminin on a base of type I collagen [1, 2]. Matrigel is now used widely in invasion assays (figure 6.1) in combination with an insert assembly; a small plastic transwell insert 'cup' with a filter or membrane as its underside, that usually fit into the wells of a 12 or 24-well plate.

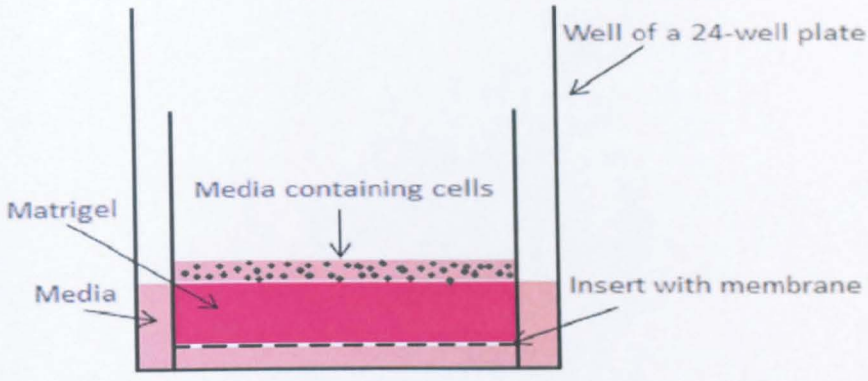

Figure 6.1 - Diagram of Matrigel assay setup.

Typically, the matrigel is left to polymerise before cells in their respective media (with or without inhibitors) are added on the upper surface. This is then left for a period of 24-48 hours in an incubator to allow the cells to permeate and invade the matrigel, before the experiment is completed by removing the contents of the upper surface of membrane, then fixing and staining the cells on its underside. The results are determined by the number of cells on the underside of the membrane, as those cells are the ones which have completely traversed the 'ECM'. This experiment has been widely used to assess the invasiveness of different cell lines and also to test different inhibitors of invasive cells.

The matrigel invasion assay is simple to perform and analyse, not time-consuming or particularly labour-intensive; however as the matrigel itself is an extract of mouse sarcoma, there are thoughts that it may not show an accurate representation of the nature of invading cells in human tissue, as tumour invasion is not just dependent on the tumour cell, but on the numbers and types of cells in the tissue which it is invading.

This experiment was conducted using 2 different cell lines; first trimester immortalised trophoblast cell line; PL4, and ovarian carcinoma cell line; OC MZ-6. Both cell lines had been previously tested in this experiment [3] and a high level of heparanase had also

been observed by immunofluorescence. A polyclonal anti-heparanase antibody that had also previously been used in this assay [4] was used as a positive control. This antibody was shown to inhibit the invasion of OC MZ-6 cells, although it was determined that it did not significantly inhibit the invasion of PL4 cells, whose activity was attributed to different mechanisms than the sole function of heparanase [3].

Anti-heparanase aptamers 1.5M short, 1.5M long and 3M were used as potential inhibitors, together with linker peptide aptamers pink and yellow (all at 1μM) and the aforementioned polyclonal anti-heparanase antibody (0.7μM). The concentration of antibodies was based on their previous optimisation in this assay [3], whilst the aptamers' concentration was chosen to fall within the range of IC_{50} of another small molecule heparanase inhibitor [5]. The controls used were cells only, with no inhibitor, showing the maximum invasion from both cell types, and a negative control mouse antibody to show that any inhibitory effect of the anti-heparanase antibody is due to its heparanase specificity. Cells were also grown on a coverslip with no matrigel or inhibitor, purely to demonstrate that they were at a suitable confluency for the experiment. After ending the experiment, cells on the top of the membrane were removed and those on the underside were haematoxylin-stained. Each membrane was removed and mounted, 8-10 images from representative areas on each membrane were taken and the cells were manually counted. Data were analysed using Microsoft Office Excel and, to assess the statistical significance, an unpaired two-tailed t-test was conducted.

Experiments using PL4 cells (figure 6.2) were conducted in duplicate. The coverslips showed adequate cell confluency for each experiment. The treatments of no inhibitor and control mouse antibody show similar values, as expected due to no relevant inhibitor

added to either. There is a significant decrease in number of cells traversing the ECM and membrane between no inhibitor at 42.13 ± 5.25 and the heparanase antibody 21.86 ± 7.43 (p=0.00009), thus showing significant inhibition of invasion. Between no inhibitor and 1.5M long aptamer 32.75 ± 7.09 there was a weak significance of inhibition (p=0.01), as was with the pink aptamer 32.6 ± 10.3 (p=0.04). None of the other aptamers exhibited significant inhibitory effects in these experiments as all were similar to no inhibitor and control mouse antibody.

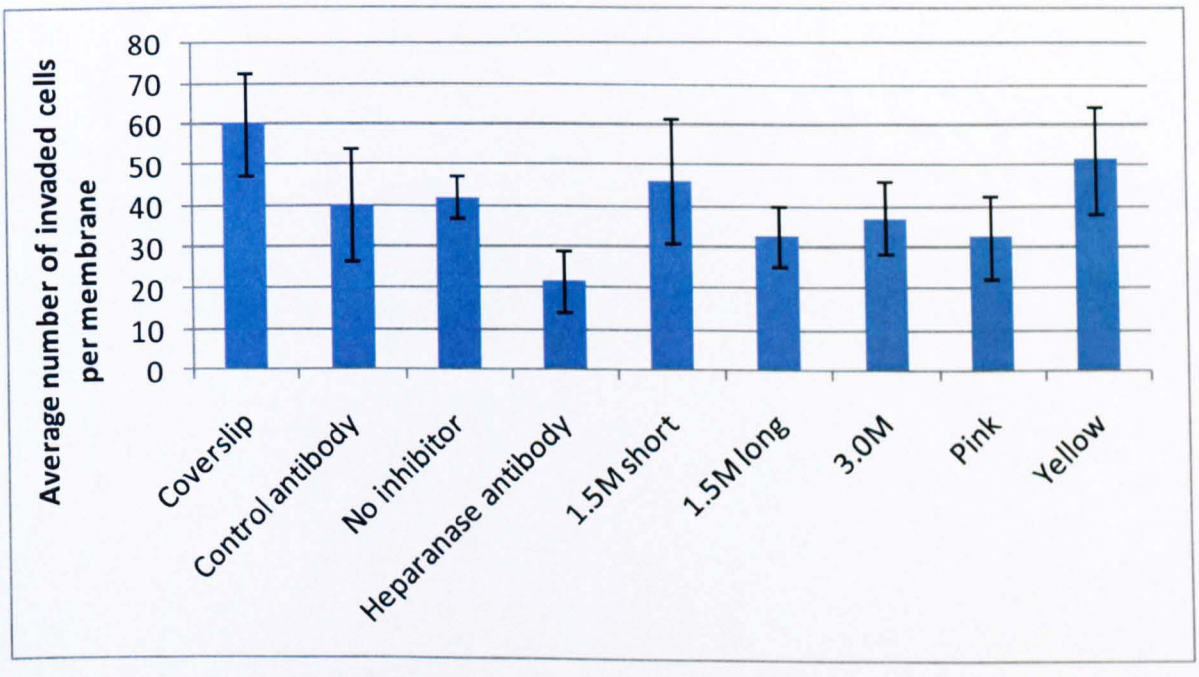

Figure 6.2 - PL4 cells cultured in medium supplemented with heparanase antibody, 1.5M short, 1.5M long, 3.0M, pink and yellow aptamers. The negative controls were represented as no inhibitor and a control mouse antibody. Figures represent the average of triplicate experiments and error bars show standard deviation of the mean. There was a significant inhibition of invasion between no inhibitor and heparanase antibody treatments (p=00009), and a weak significance between no inhibitor and the 1.5M long and pink aptamers (p=0.01, p=0.04).

Experiments with OC MZ-6 cells (figure 6.3) were conducted in triplicate. Once again, the cells were cultured to suitable confluency for the experiment and no inhibitor and control mouse antibody showed similar values. Heparanase antibody showed significantly decreased numbers of cells through the matrigel, with 40.6 ± 7.13 cells compared to no inhibitor at 74.4 ± 34.28 (p=0.0164) and compared with a negative control antibody at

66.6 ± 15.77 (p=0.0008). This corresponds to previous experiments with heparanase in this model [3, 4]. 1.5M long aptamer, however, inhibited the migration of cells with 26.9 ± 5.49 cells compared with no inhibitor (p= 0.0032) and with the negative control antibody (p< 0.0001). Aptamers 1.5M short showed little inhibition, whereas 3.0M did not significantly inhibit migration of cells in these studies, and neither did pink and yellow aptamers. These results suggest that 1.5M long is a significant inhibitor of cell invasion in this model.

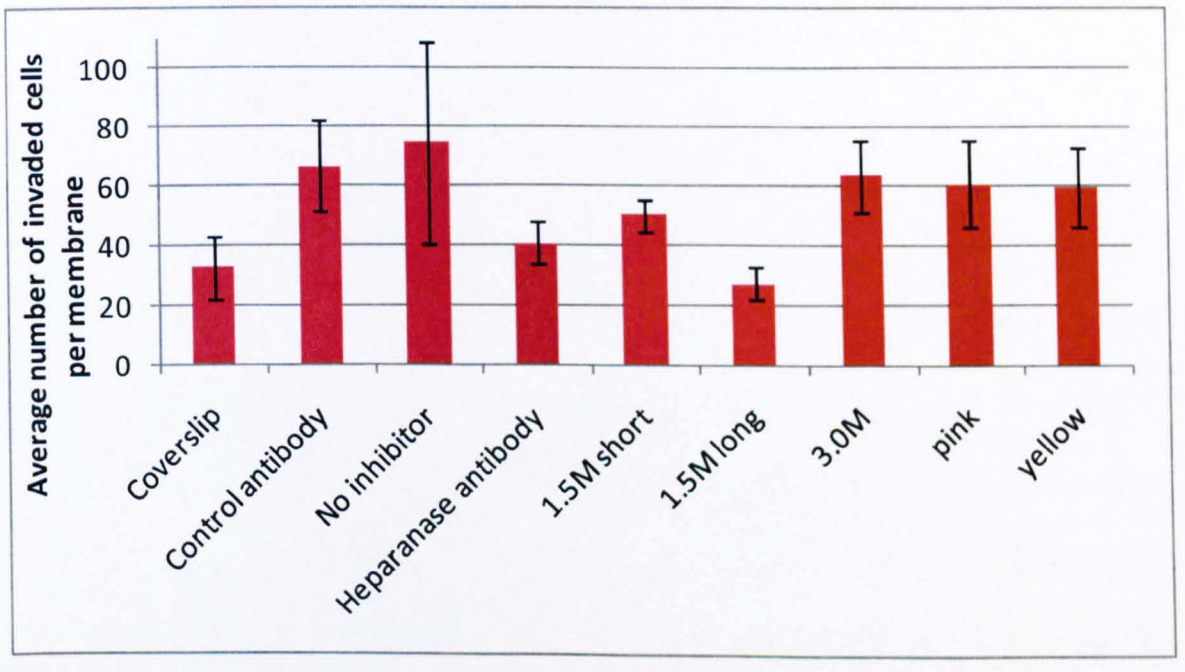

Figure 6.3 - OC MZ-6 cells cultured in medium supplemented with heparanase antibody, 1.5M short, 1.5M long, 3.0M, pink and yellow aptamers. The negative controls were represented as no inhibitor and a control mouse antibody. Figures are representative of the average of triplicate experiments and error bars show standard deviation of the mean.

6.3 Myoma Organotypic Model of Invasion

The organotypic myoma model of invasion overcomes the problem of using mouse or artificial tissue in these assay types [6]. It is a developing technique which uses human uterine leiomyoma tissue (commonly known as fibroid tissue) in place of matrigel. It is more laborious and time-consuming, as the cells are cultured for two-weeks of invasion.

However, more analytical techniques can be employed upon termination of the experiment and a better understanding of invasion gained.

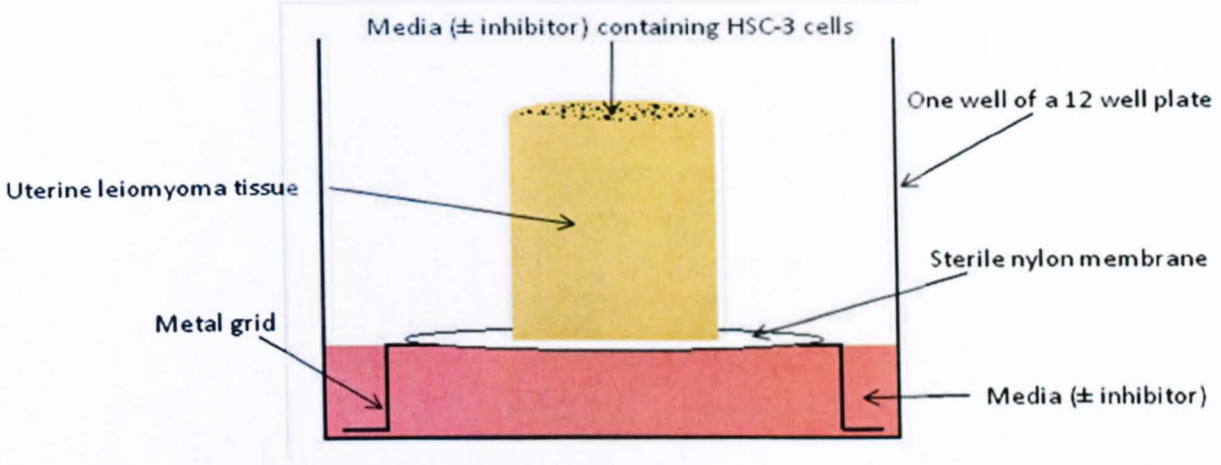

Figure 6.4 – Diagram of Myoma organotypic model setup.

After excision from the donor, myomas were cut into 8mm discs and transferred to 6.5mm transwell inserts inside 24 well plates. $7x10^5$ human tongue squamous carcinoma cells (HSC-3), shown to express and secrete heparanase [7], in 50µl medium with or without inhibitor (at identical concentrations as used in the Matrigel invasion assay) were added to the upper surface of the tissue and the cells were allowed to adhere (figure 6.4). After incubation for 24 hours, the myomas were placed atop a disc of nylon membrane upon a steel grid, where the cells were cultured for 14 days.

Termination of the experiment yielded four changes of media (which were retained at -20°C) and the myoma tissue itself, which were bisected longitudinally, dehydrated and embedded in paraffin for immunohistochemical analysis. ELISA and RIA were carried out on the collected media to check for collagen degradation products using antibodies raised in rabbits by immunisation with synthetic peptide sequences from type III collagen, since in previous studies HSC-3 cells were shown to degrade type III collagen [8]. ELISA detected the N-terminal telopeptide from type III collagen, whilst RIA detected the C-terminal telopeptide.

The experiment was conducted in triplicate, to make the results more reliable, with no cells in two of the samples. This showed the natural 'background' of the tissue without influence of cells or inhibitors. As another control, cells were added to the myoma tissue but no inhibitor added. This showed the maximum invasion potential of the cells through the tissue, assuming that none of the inhibitors acted as agonists! An unrelated aptamer (selected against a target involved in Alzheimer's disease) was also used in one sample, to show that any inhibitory effect of heparanase aptamers were not due to aptamers in general. Also used were 1.5M short, 1.5M long and 3M anti-heparanase aptamers, pink and yellow linker peptide aptamers and (2-{4-[(E)-3-(4-bromophenyl) acryloylamino]-3-fluorophenyl} benzooxazol-5-yl) acetic acid, abbreviated to BAFB, which was shown to have inhibitory effects upon heparanase in previous studies [5]. After day 14, when the experiment was terminated by dehydrating, fixing, wax-embedding then subjecting the sections to IHC, nine representative images (at x100 magnification) were taken from each repeat of every treatment. Each image was analysed using ImageJ software to determine the maximum invasion depth (distance from the surface of the tissue to the deepest invaded cell), maximum invaded area and invasion index [1- (noninvading area/total area)]. Figures were analysed using Microsoft Office Excel and unpaired, two-tailed t-tests to assess the statistical significance.

6.3.1 Invasion Data

Figure 6.5 shows two images gained from this study. One shows the migration of cells through myoma tissue when exposed to fresh medium only with no inhibitor added. This section clearly shows that a dense population of HSC-3 cells have invaded the upper layer of tissue, and interspersed through the rest of the tissue there are a number of large cell populations. The opposite is shown from the second image, which is derived from cells

exposed to 1.5M short aptamer. This section shows no cells at all have invaded the middle and lower areas of the tissue, and much less have invaded the upper surface. These findings suggest that the cells exposed to 1.5M short aptamer were not able to invade the tissue.

Between the two sections there is a clear difference in total HSC-3 cell numbers, with many more cells present in the section not exposed to inhibitor over that exposed to 1.5M short aptamer. However, care was taken to administer the same numbers of cells to all samples at the beginning of each experiment by aliquoting them from a universal mixture. This suggests that cells exposed to no inhibitor were able to proliferate over the 14 day period, whereas those exposed to 1.5M short aptamer did not proliferate at such a high rate. An explanation for this would be that because the non-inhibited cells were able to invade, they could gain confluency due to the increased surface area available to them, whilst because the inhibited cells did not invade, they had less available surface area in which to proliferate. It is also possible that 1.5M short aptamer has cytotoxic properties and for this reason the cells have not shown proliferation. However, in this particular image, a small number of cells have invaded a short distance into the tissue, and figures 6.6 to 6.8 show that invasion was not completely halted; rather reduced, suggesting the cells were still viable.

Figure 6.5 – Representative images derived from immunohistochemistry of myoma sections after termination of the experiment at day 14. Magnification is x100. The image on the left shows dense invasion from HSC-3 cells and has not been exposed to inhibitor, whereas the image on the right was exposed to 1.5M short aptamer and shows little invasion localised to the upper surface of the tissue.

Figure 6.6 shows the maximal invasion depths from all treatments represented as upper and lower quartiles, median, maximum and minimum values. The tissues exposed to heparanase antibody were the only treatments that showed a significant decrease in maximal invasion depth 228.9µm ± 241.2 from those without inhibitor added 1712.3µm ± 145.5 ($p<0.0001$). Treatments of unrelated aptamer, BAFB and those where no inhibitor were added show a much lower dispersal of the data than those from the heparanase and linker-generated aptamers, which, as shown by the boxes, have a larger spread of data towards the lower invasion depths. This suggests that although the result of the means for heparanase and linker-selected aptamers are not statistically lower than that for no inhibitor added, the datasets showed a proportion of images showing lower invasion depths.

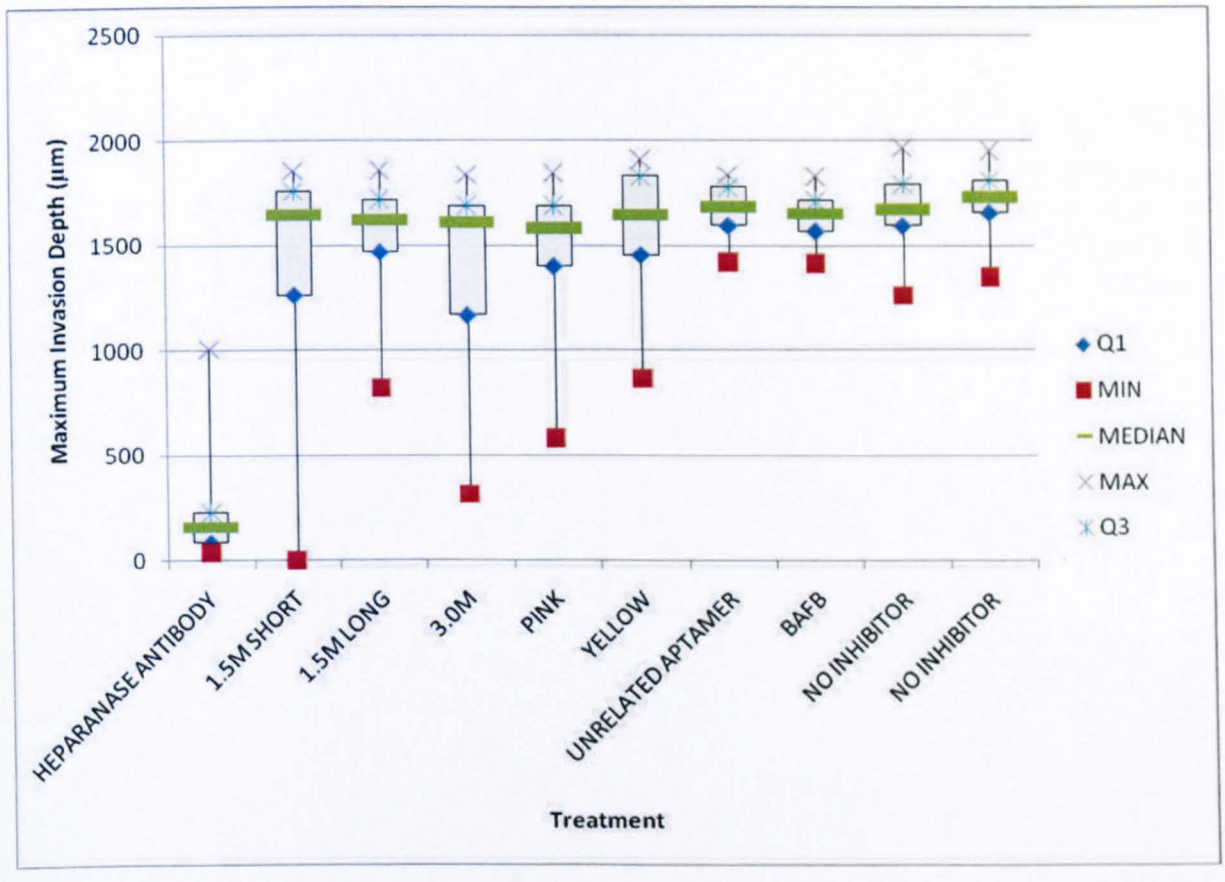

Figure 6.6 – A box and whisker diagram showing maximum invasion depth (n=27 samples) represented as upper (Q3) and lower (Q1) quartiles, median, minimum (min) and maximum (max) values. Heparanase antibody-treated tissue was the only treatment showing a significantly lower maximum invasion depth from tissues not exposed to inhibitor ($p<0.0001$).

Figures 6.7 and 6.8 show the total invasion area and invasion index from each treatment. Heparanase antibody (13809.9 ± 13608µm^2) and 1.5M short aptamer (67492.8 ± 74483.8 µm^2), both showed significantly less invasion ($p<0.0001$) compared to no inhibitor added (354354.6 ± 173621.9 µm^2). No significant differences were observed by the other treatments, which were all similar to the negative control (no inhibitor). These results suggest that both heparanase antibody and 1.5M short aptamers are effective inhibitors of invasion of HSC-3 cells, but that 1.5M long, 3.0M, pink and yellow aptamers together with BAFB do not function as inhibitors in this study. In studies using BAFB [5], solubility in aqueous solutions were an issue, and addition of small amounts of solvent such as DMSO were necessary before the compounds would dissolve. However, for this assay,

the tissues were stored frozen in a low percentage DMSO solution in medium and upon defrosting, were washed numerous times to remove the DMSO for the experiment. Therefore, it was not possible for the introduction of DMSO into the experiment via this inhibitor so a decision was made to attempt to dissolve the inhibitor in PBS only and mix well. Unfortunately this may not have been successful, and could explain why this compound did not show any inhibitory effects in this study.

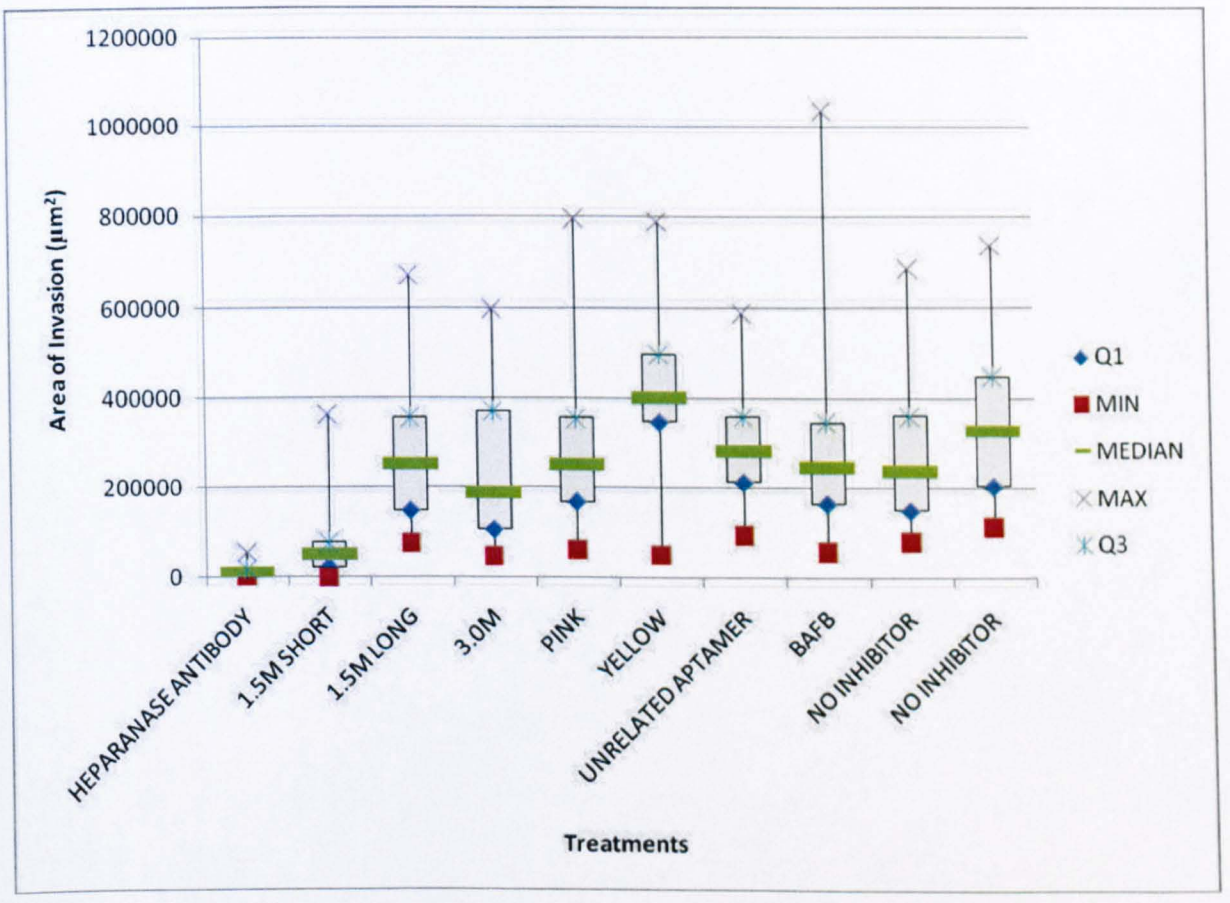

Figure 6.7 – A box and whisker diagram showing area of invasion (n=27 samples) from myoma tissues subjected to different treatments represented as upper (Q3) and lower (Q1) quartiles, median, minimum (min) and maximum (max) values. Heparanase antibody and 1.5M short both showed sigificantly less inavsion than the other treatments ($p<0.0001$).

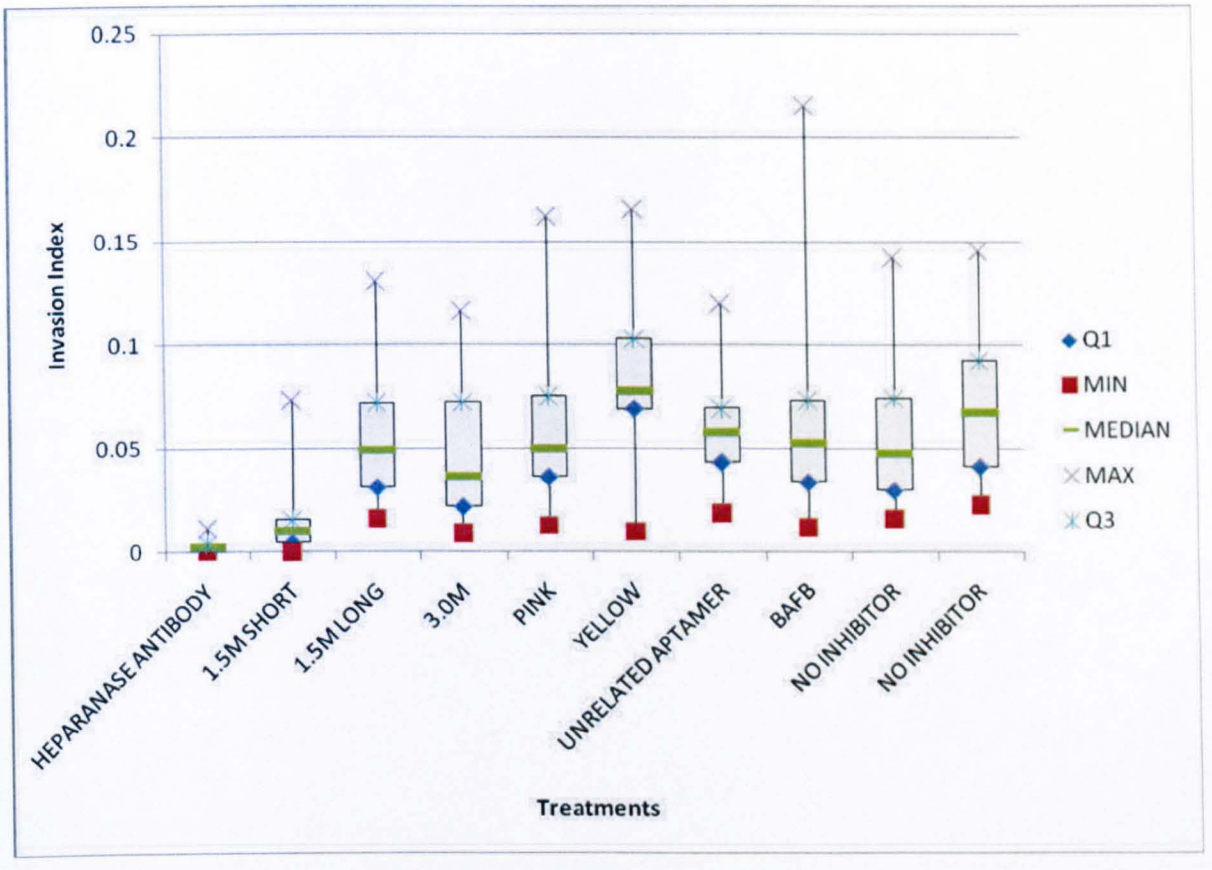

Figure 6.8 - A box and whisker diagram showing invasion index [1- (noninvading area/total area)] (n=27 samples) from myoma tissues subjected to different treatments represented as upper (Q3) and lower (Q1) quartiles, median, minimum (min) and maximum (max) values. Heparanase antibody and 1.5M short both showed sigificantly less inavsion than the other treatments (p<0.0001).

6.3.2 RIA

Radioimmunoassays were conducted to detect the C-terminal telopeptide from type III collagen by incubating the media samples in a reaction with a tracer (iodine-conjugated synthetic C-terminal telopeptide) and primary antibody (raised against synthetic C-terminal telopeptide) for two hours at 37°C. The primary antibody favourably binds collagen degradation product from the media sample in competition with tracer, hence the existence of large concentrations of collagen degradation product will create loss of the unbound tracer in a subsequent wash step and lower the counts in that sample. Figures 6.9 to 6.12 show radioimmunoassay data obtained for days 4, 7, 10 and 14. The media change from day 4 showed no significant differences from the control, to which no inhibitor was added. This was expected as the cells would not have had enough time at

four days to equilibrate, divide and invade the tissue. The media change upon termination of the experiment at day 14 only showed statistical significance from the treatment with no cells added (p=0.001). At day 14, it is possible that the cells had ceased invasion and were subject to senescence due to the volume of waste products that had accumulated on the tissues' surface.

Days 7 and 10 showed the most promising results. From day 7, the treatments of heparanase antibody (p=0.001), no cells (p=0.0002), and aptamers 1.5M short (p=0.0006), long (p=0.0004), 3.0M (p=0.001) and pink (p=0.003) all showed significantly lower collagen degradation products than that for the tissue with no inhibitor added. Treatments with yellow and unrelated aptamers and BAFB had no significant effect on collagen degradation product.

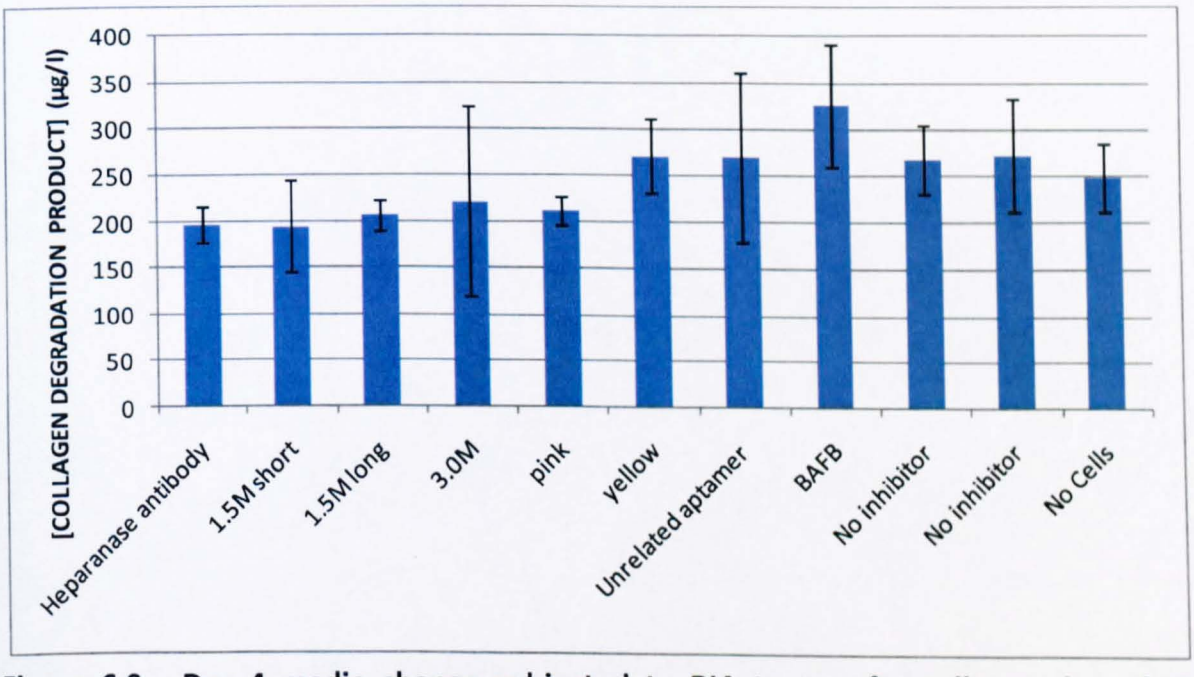

Figure 6.9 - Day 4 media change subjected to RIA to test for collagen degradation products. There were no significant differences between any of the treatments. Data shown are the means from triplicates of each of three samples of media and error bars represent standard deviation of the mean.

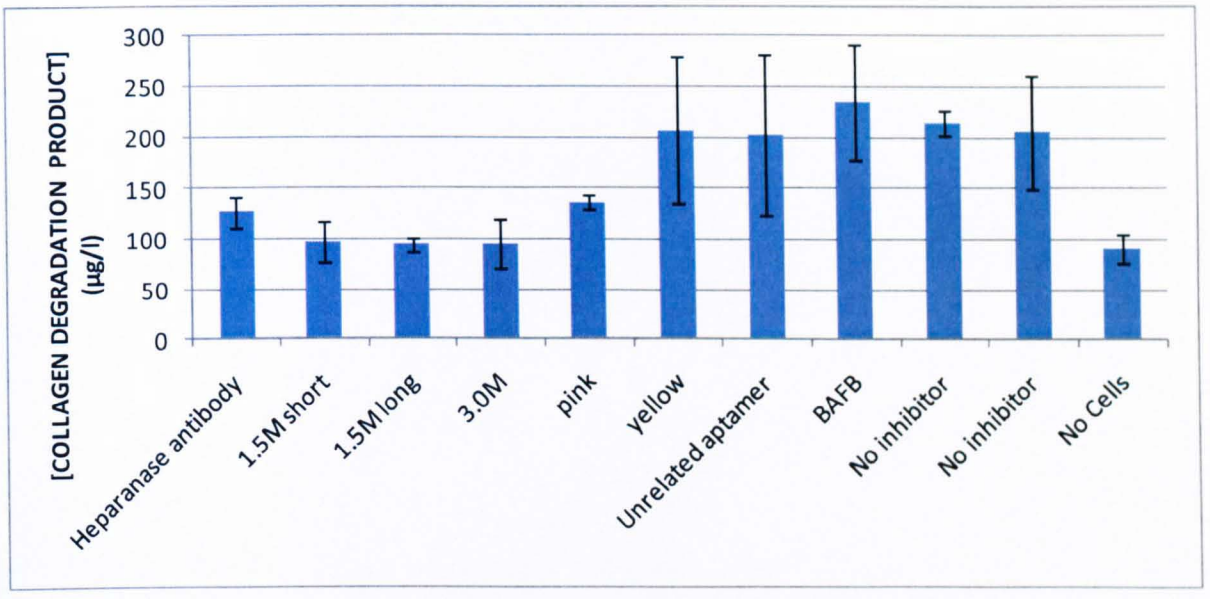

Figure 6.10 - Day 7 media change subjected to RIA for collagen degradation products. Treatments with heparanase antibody (p=0.001), 1.5M short (p=0.0006), long (p=0.0004), 3.0M (p=0.001), Pink (p=0.003) aptamers and no cells (p=0.0002) were all significantly lower than the control with no inhibitor added. Data shown are the means from triplicates of each of three samples of media and error bars represent standard deviation of the mean.

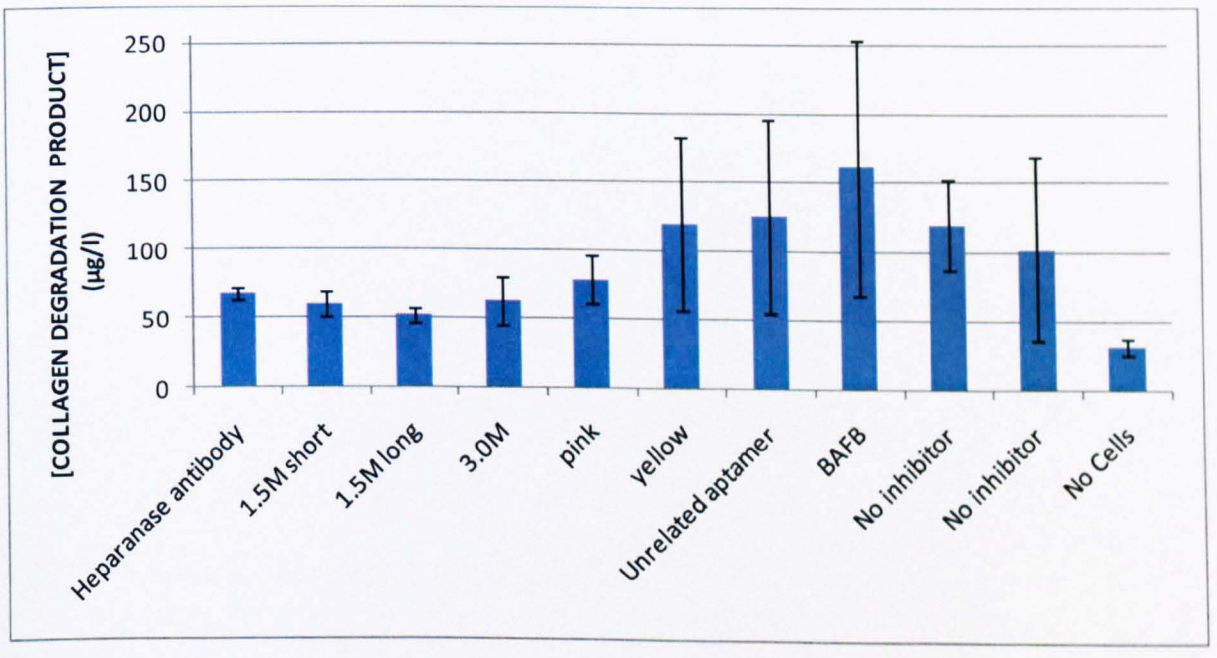

Figure 6.11 - Day 10 media change subjected to RIA for collagen degradation products. Treatments with no cells (p=0.009) were significantly lower, and heparanase antibody (p=0.07), 1.5M short (p=0.04), long (p=0.02) and 3M aptamers (p=0.06) were lower with slight significance than the control with no inhibitor added. Data shown are the means from triplicates of each of three samples of media and error bars represent standard deviation of the mean.

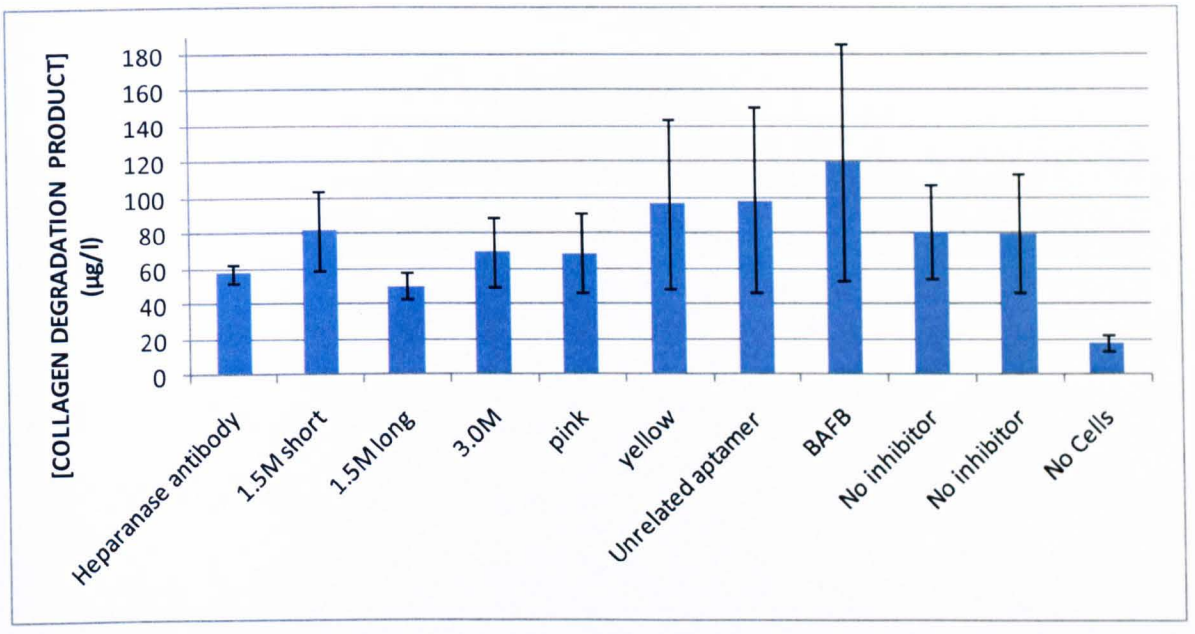

Figure 6.12 - Day 14 media change subjected to RIA for collagen degradation products. Treatments with no cells (p=0.001) were significantly lower and heparanase antibody (p=0.09) and 1.5M long aptamer (p=0.04) were lower with weak significance than the control with no inhibitor added. Data shown are the means from triplicates of each of three samples of media and error bars represent standard deviation of the mean.

Day 10 results show that the values for collagen degradation product in experiments to which no HSC-3 cells were added still remained significantly lower than the control with no inhibitor (p=0.009), which was expected as invasion should not occur in the absence of invasive cells. Heparanase antibody (p=0.07) and 1.5M short (p=0.04), long (p=0.02) and 3.0M aptamers (p=0.06) showed less collagen degradation product by a weak significance. However, aptamers pink, yellow and unrelated, with BAFB once again showed no significant decrease in collagen degradation product than the negative control, indicating that they were not acting as succesful inhibitors of invasion.

6.3.3 ELISA

This assay shows a negative correlation between collagen degradation product and absorbance as the primary antibody was firstly incubated with the medium sample before being exposed to the synthetic peptide coating the wells of the ELISA plate. This meant

that if there were collagen degradation products in the medium the antibody would bind them and not the synthetic peptide, giving less colour.

Figures 6.13 to 6.16 show ELISA data obtained from media changes on days 4, 7, 10 and 14 respectively. The pattern of data was similar throughout all media changes and the only significant increase in absorbance was seen from the heparanase antibody (p=0.01 on day 4, 0.03 on day 7, 0.03 on day 10 and 0.02 on day 14), 1.5M short aptamer (p=0.01, 0.02, 0.007 and 0.02 respectively) and 1.5M long aptamer (no significance on day 4, p=0.07 on day 7, and 0.03 on both days 10 and 14). Unfortunately the data for aptamer 3.0M was very variable, shown by the error bars, so a statistical significance in relation to the treatments with no inhibitor could not be obtained in any of the media changes. This is likely due to the condition of the cells or tissue in the experiment as all of the media changes show the same variability. None of the other treatments, including the treatment without cells, showed any significant difference in absorbance and therefore collagen degradation product from samples without inhibitor, suggesting that only heparanase antibody and 1.5M short and long aptamers, and possibly the 3M, were able to successfully inhibit the invasion of HSC-3 cells.

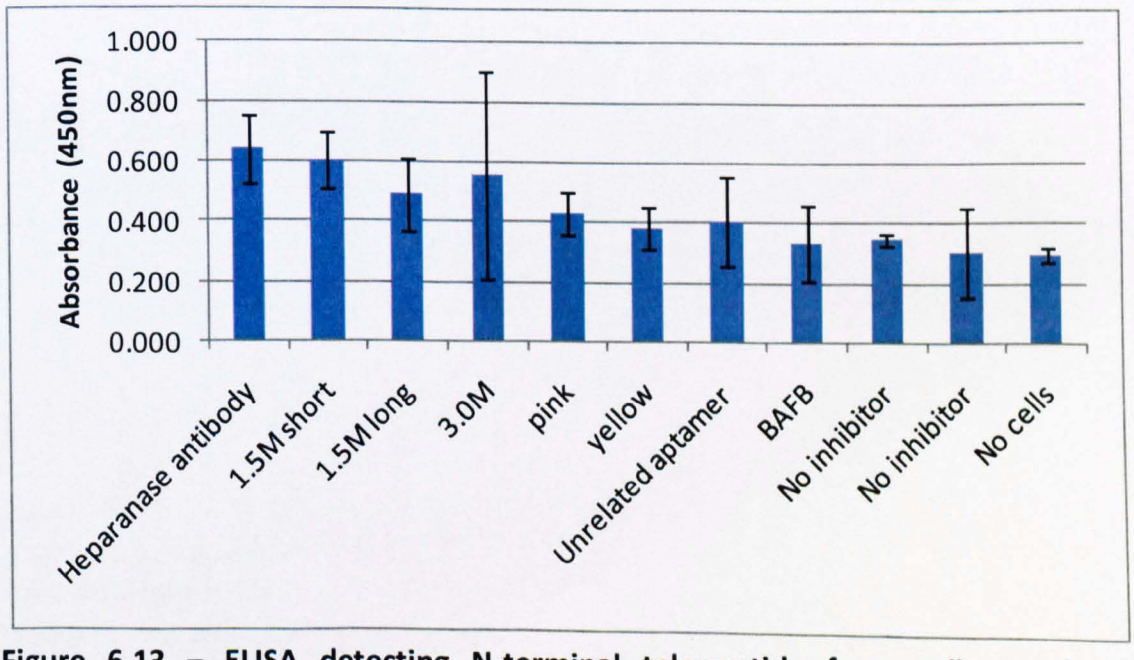

Figure 6.13 – ELISA detecting N-terminal telopeptide from collagen degradation products at day 4 media change. Heparanase antibody (p=0.01) and 1.5M short

aptamer (p=0.01) showed increased absorbance (therefore less collagen degradation product present). Data shown are the means from triplicates of each of three samples of media and error bars represent standard deviation of the mean.

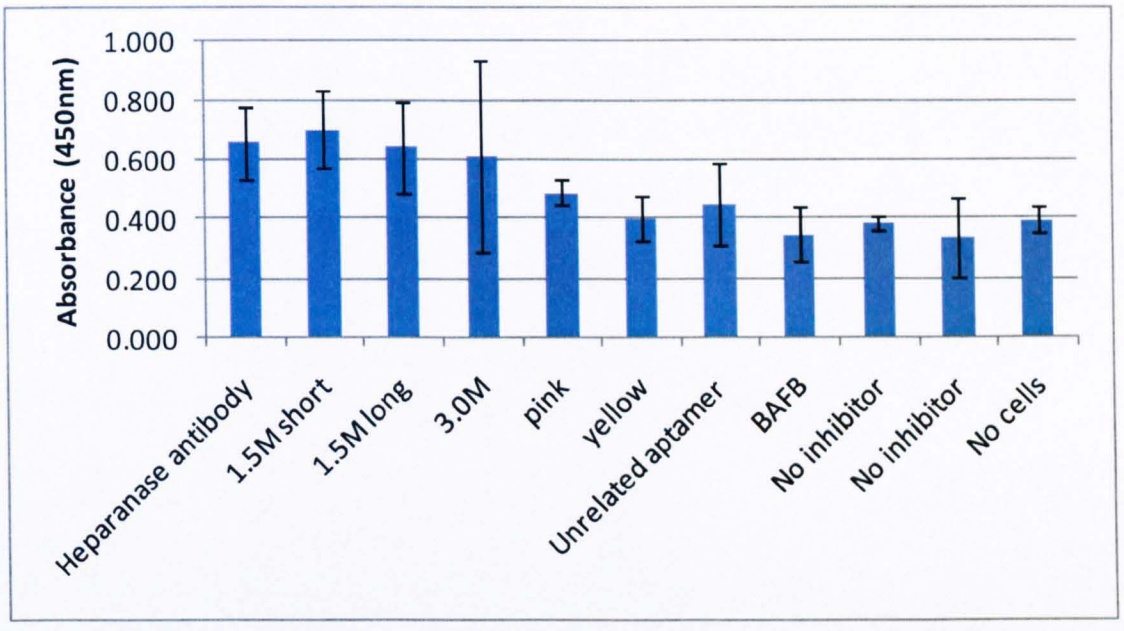

Figure 6.14 - ELISA detecting N-terminal telopeptide from collagen degradation products at day 7 media change. Heparanase antibody (p=0.03), 1.5M short aptamer (p=0.02) and 1.5M long aptamer (p=0.07) showed increased absorbance (therefore less collagen degradation product present). Data shown are the means from triplicates of each of three samples of media and error bars represent standard deviation of the mean.

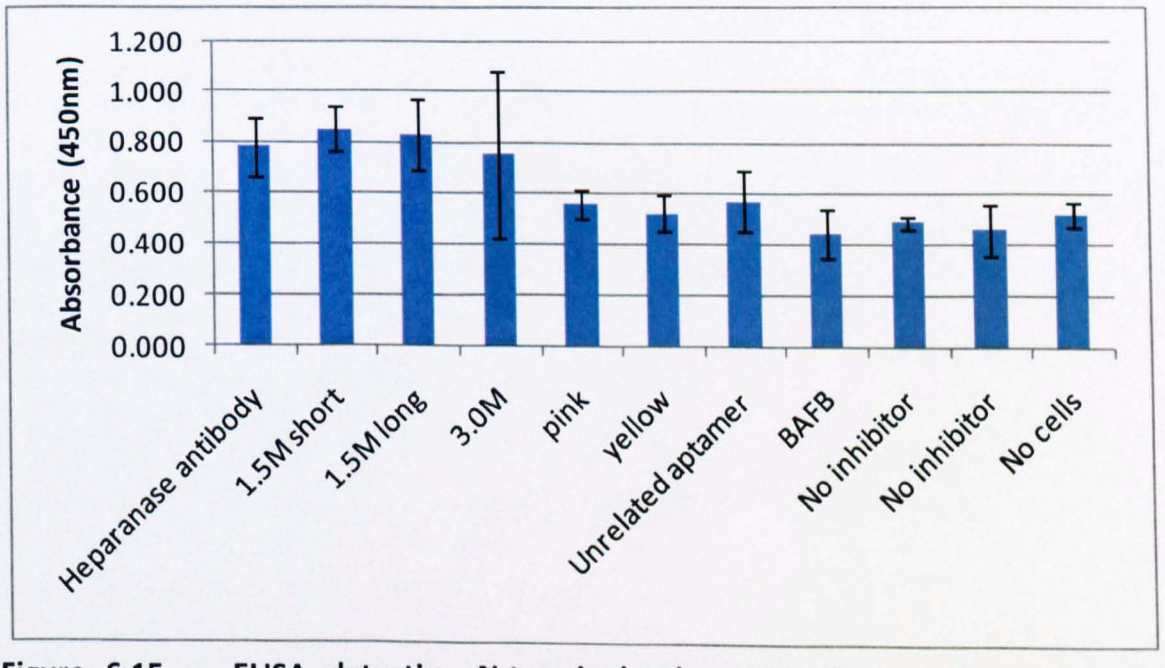

Figure 6.15 - ELISA detecting N-terminal telopeptide from collagen degradation products at day 10 media change. Heparanase antibody (p=0.03), 1.5M short aptamer (p=0.007) and 1.5M long aptamer (p=0.03) showed increased absorbance (therefore less collagen degradation product present). Data shown are the means from triplicates of each of three samples of media and error bars represent standard deviation of the mean.

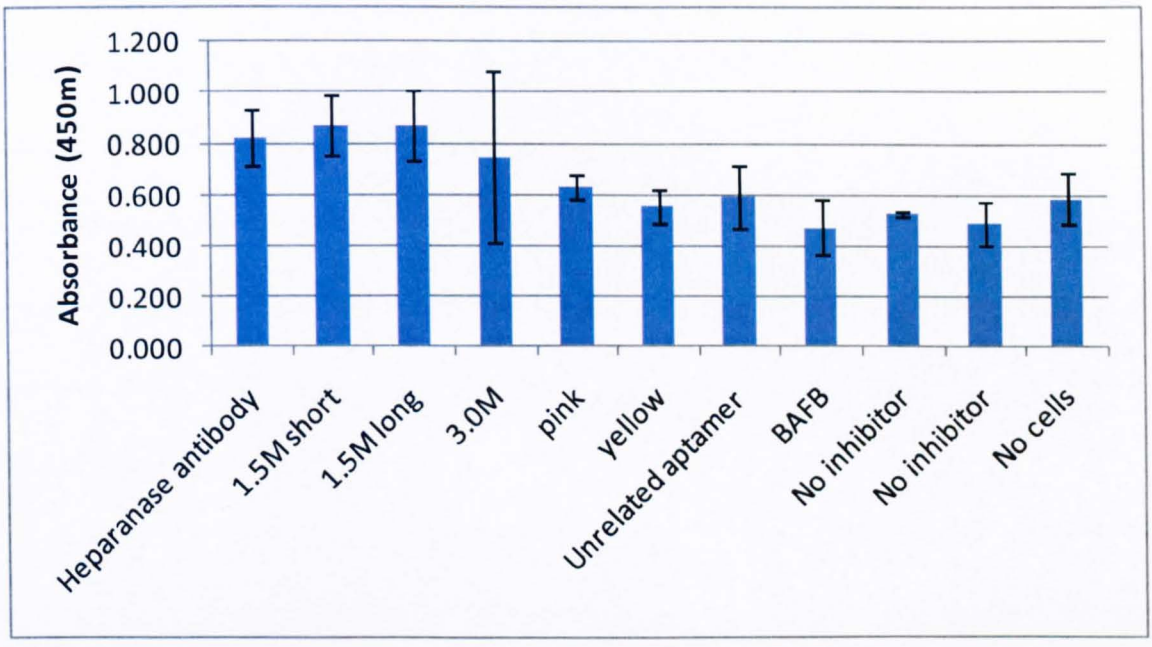

Figure 6.16 - ELISA detecting N-terminal telopeptide from collagen degradation products at day 14 media change. Heparanase antibody (p=0.02), 1.5M short aptamer (p=0.02) and 1.5M long aptamer (p=0.03) showed increased absorbance (therefore less collagen degradation product present). Data shown are the means from triplicates of each of three samples of media and error bars represent standard deviation of the mean.

6.4 Discussion

These studies were conducted in order to examine the effect that heparanase and linker peptide-selected aptamers have on the formation, secretion and function of active heparanase in invasion assays, using cells that had been previously shown to express heparanase [3, 4, 7].

The results of the matrigel invasion assay showed that both the PL4 and OC MZ-6 cell lines were successfully inhibited by the polyclonal heparanase antibody, which for the OC MZ-6 line, correlates with previous results using this antibody [3, 4]. Similarly, in this assay, the 1.5M long aptamer showed significant inhibition of OC MZ-6 cells at a concentration of 1µM, to a greater degree than the heparanase antibody, although to a

lesser extent for the PL4 cells. Both the 1.5M long and pink aptamers only showed a weak statistical decrease in number of PL4 cells traversing the membrane. This would correlate with the results of the previous study by Harris *et al.* [3] that the primary function of heparanase in these cells is one of either a transcriptional regulator of COX-2 expression (and subsequent migration as seen in a different trophoblast cell line) and/or as the inactive proenzyme stimulating migration via PI3K or p38, rather than strictly direct invasion and remodelling.

In the organotypic model of invasion, measurements taken from the images show significantly lower invasion depth, area of invasion and invasion index for the tissues treated with heparanase antibody and significantly lower invasion area and invasion index from tissues treated with 1.5M short aptamer. The former was expected, as in previous studies and chapters of this thesis the polyclonal heparanase antibody has been shown to be a functional inhibitor and superior for labelling and staining of heparanase [3, 4]. 1.5M short aptamer, however, has not shown the greater promise in other experiments detailed in this thesis, although it has similar affinity for heparanase as indicated by binding assays. Furthermore, this is the first experiment in which human tissue has been used and perhaps the truncated nature of this aptamer has favoured it with this cell line. In experiments conducted to ascertain the localisation of heparanase within oral cancer cell cultures [7], heparanase activity was found in cell extracts and intact cells, but not in the conditioned medium, suggesting that heparanase acts at the plasma membrane or within the cytoplasm of the cell itself, which would correlate with the processing of proheparanase to its active form inside the late endosomes/lysosomes before secretion to the cell surface. As the full-length version of this aptamer (i.e. 1.5M long) was not shown to significantly inhibit invasion in this assay, and other than the antibody, the only

aptamer that had any significant inhibitory effect was 1.5M short (the only severely truncated aptamer), this suggests a possible perfusion of 1.5M short aptamer across the plasma membrane to inhibit heparanase before its secretion to the cell surface or at the cell surface itself, where it would be subject to less steric hindrance by other molecules, due to its small size.

It is possible that inhibition of invasion of cells in both assays by aptamers 1.5M long and short aptamers respectively, could be due to a direct cytotoxic effect they exhibit on the cells. However, as the cells treated with these aptamers have shown reduced and not complete invasion, it would suggest that the cells were still viable. An assay to determine the aptamers' natural cytotoxicity over these cells would further complement the results shown in this chapter.

The RIA, and to some extent, ELISA data reinforce these results as both the heparanase antibody and 1.5M short aptamer are suggested to inhibit invasion. However, 1.5M long, 3.0M and even pink aptamer (in RIA) are also suggested to exhibit inhibitory activity. This would correlate with previous results in this thesis, where these aptamers have shown to bind heparanase or linker peptide. Binding to the linker peptide may cause inhibition of heparanase due to the prevention of the formation of the active enzyme, through blocking the digestion of the linker peptide in the proenzyme. Failure of the yellow aptamer to have the same effect may be due to the fact that, although this aptamer also binds the linker peptide, may bind in such a way as not to prevent proteolytic cleavage. The invasion depths for these aptamers, although statistically non significant, showed lower minimum values, and lower median values in invasion area and index than yellow and unrelated aptamers, BAFB and no inhibitor, suggesting that a proportion of them may have been subject to inhibition. The RIA and ELISA data may not have been replicated on

the same scale in the image data because the RIA and ELISA are more sensitive to small changes in collagen degradation.

Overall, aptamers in these studies were found to have the ability to inhibit heparanase activity and tissue penetration, often at a level similar or superior to the polyclonal antibody. The most promising aptamer sequence was shown to be the one identified after elution from the 1.5M salt, although, depending on the assay, and perhaps the accessibility of the protein, it was either the 'long' or the 'short' form of this aptamer that exhibited the highest activity. Lack of significant activity by the 3.0M aptamer may be due to the position of the binding of this aptamer to the enzyme. All aptamers were originally selected for affinity for the enzyme, but not for inhibitory action. Thus, it is possible that a higher binding species may bind to such site as to not have any or little functional effect, whereas another species of lower affinity may be a better functional inhibitor. Similarly, although the aptamer species against the linker peptide have contributed significant information as to the fate of the peptide, or presence of proenzyme in the cell (see chapter 5), it appears that one of the peptide-derived aptamers has an inhibitory affinity, whereas the other does not. Again, this may be that the one of the aptamers prevents proteolytic cleavage of the linker peptide, whereas the other aptamer does not. It may also be due to the fact that both aptamers were selected against the synthetic peptide, and thus, one may be able to bind to the peptide in the holoenzyme (proenzyme), whereas the other does not and binds only to the already cleaved peptide (as shown by the fluorescence quenching experiments, see chapter 4).

References:

1. Albini, A., Y. Iwamoto, H.K. Kleinman, G.R. Martin, S.A. Aaronson, J.M. Kozlowski, and R.N. McEwan, *A rapid in vitro assay for quantitating the invasive potential of tumor cells.* Cancer Res, 1987. **47**(12): p. 3239-45.
2. Terranova, V.P., E.S. Hujanen, D.M. Loeb, G.R. Martin, L. Thornburg, and V. Glushko, *Use of a reconstituted basement membrane to measure cell invasiveness and select for highly invasive tumor cells.* Proc Natl Acad Sci U S A, 1986. **83**(2): p. 465-9.
3. Harris, L.K., P.N. Baker, P.E. Brenchley, and J.D. Aplin, *Trophoblast-derived Heparanase is Not Required for Invasion.* Placenta, 2008. **29**(4): p. 332-7.
4. He, X., P.E. Brenchley, G.C. Jayson, L. Hampson, J. Davies, and I.N. Hampson, *Hypoxia increases heparanase-dependent tumor cell invasion, which can be inhibited by antiheparanase antibodies.* Cancer Res, 2004. **64**(11): p. 3928-33.
5. Courtney, S.M., P.A. Hay, R.T. Buck, C.S. Colville, D.J. Phillips, D.I. Scopes, F.C. Pollard, M.J. Page, J.M. Bennett, M.L. Hircock, E.A. McKenzie, M. Bhaman, R. Felix, C.R. Stubberfield, and P.R. Turner, *Furanyl-1,3-thiazol-2-yl and benzoxazol-5-yl acetic acid derivatives: novel classes of heparanase inhibitor.* Bioorg Med Chem Lett, 2005. **15**(9): p. 2295-9.
6. Nurmenniemi, S., T. Sinikumpu, I. Alahuhta, S. Salo, M. Sutinen, M. Santala, J. Risteli, P. Nyberg, and T. Salo, *A novel organotypic model mimics the tumor microenvironment.* Am J Pathol, 2009. **175**(3): p. 1281-91.
7. Ikuta, M., K.A. Podyma, K. Maruyama, S. Enomoto, and M. Yanagishita, *Expression of heparanase in oral cancer cell lines and oral cancer tissues.* Oral Oncol, 2001. **37**(2): p. 177-84.

8. Ziober, B.L., M.A. Turner, J.M. Palefsky, M.J. Banda, and R.H. Kramer, *Type I collagen degradation by invasive oral squamous cell carcinoma.* Oral Oncol, 2000. **36**(4): p. 365-72.

CHAPTER SEVEN

DEVELOPING APTAMERS AS USEFUL DIAGNOSTIC OR THERAPEUTIC TOOLS

7.1 Background

Previously, aptamers were selected against human polymorphic recombinant heparanase and the 6kDa linker peptide using a salt selection method. Three aptamers selected for heparanase and two for the linker peptide were suggested to bind with high affinity, shown by ELISA and fluorescence quenching studies. These aptamers were also tested for specificity and inhibition of formation or activity of active heparanase in *in vitro* cell and invasion assays. 1.5M short and long aptamers were the most promising in these studies; showing K_Ds of 13.7 and 12nM respectively, were seen to label heparanase in cell lines and tissue sections and suggested significant inhibition of tumour cell lines through tissue in cell invasion assays; 1.5M long aptamer significantly inhibiting ovarian carcinoma cell line OC MZ-6 in a Matrigel invasion assay and 1.5M short aptamer significantly inhibiting human tongue squamous carcinoma cells (HSC-3) in a myoma organotypic model. As these aptamers showed the greatest promise, assessing their functionality as therapeutics or in a diagnostic assay was essential.

7.2 Serum Stability Assays

To assess the aptamers' suitability as therapeutic agents, it was necessary to have an understanding of how stable the unmodified aptamers would be in the body, as, in the bloodstream alone, there are many nucleases capable of degrading the aptamers, rendering them inactive [1]. A simple experiment to achieve this was conducted by incubating 5μM of each aptamer in 17μl human or mouse serum for different time periods, then stopping the reaction using 1M EDTA and running the product on a 12%

native polyacrylamide gel, stained with ethidium bromide. Figures 7.1 to 7.5 show the results for each aptamer with human and mouse serum.

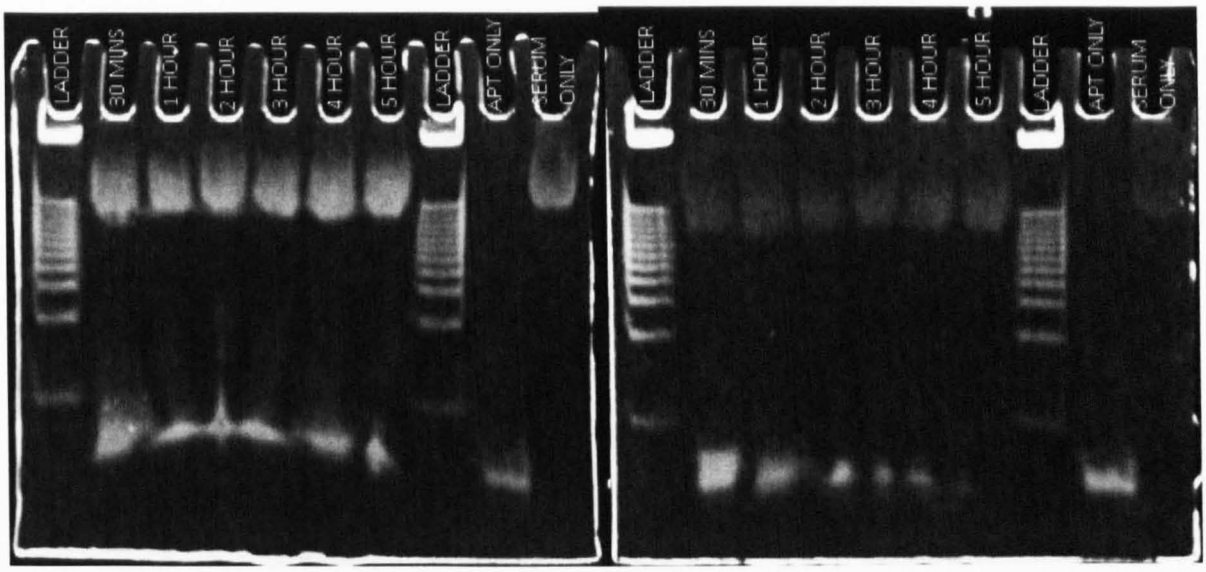

Figure 7.1 - Products of '1.5M short' aptamer incubated with human (left) or mouse (right) serum for different lengths of time, then the reactions stopped and products run on a 12% native PAGE, stained with ethidium bromide. Lanes are marked with duration of incubation time. Each band of the DNA ladder represents 25bp, beginning with 25bp.

Comparison of bands on the gels for 1.5M short aptamer (figure 7.1) incubated for different time points with human and mouse serum, with that of aptamer only showed that 1.5M short aptamer was not subject to nuclease degradation from human serum as the bands did not show any smearing or decrease in size or intensity from aptamer only, and hence, no breakdown of the aptamer into smaller fragments was observed. With mouse serum, there was a decrease in primary band intensity at five hours' incubation time, suggesting that nucleases may have degraded the aptamer into smaller fragments not visible on the gel.

Figure 7.2 shows the results obtained from incubation of 1.5M long aptamer with human and mouse serum for different time periods. Upon increasing the time of exposure to both human and mouse serum, an increase of smearing below the aptamer's main band

is observed. However, with human serum, the samples have not run in a straight line and therefore the increase in smearing may be due to the lack of lane width for the sample incubated for four hours. The band nevertheless disappeared altogether at 5 hours for human serum and 3 hours in mouse serum. This suggests that at these times, the aptamers have been completely digested by nucleases present in the serum and are present in such small fragments that ethidium bromide either cannot intercalate with them at all or they have run off the bottom of the gel.

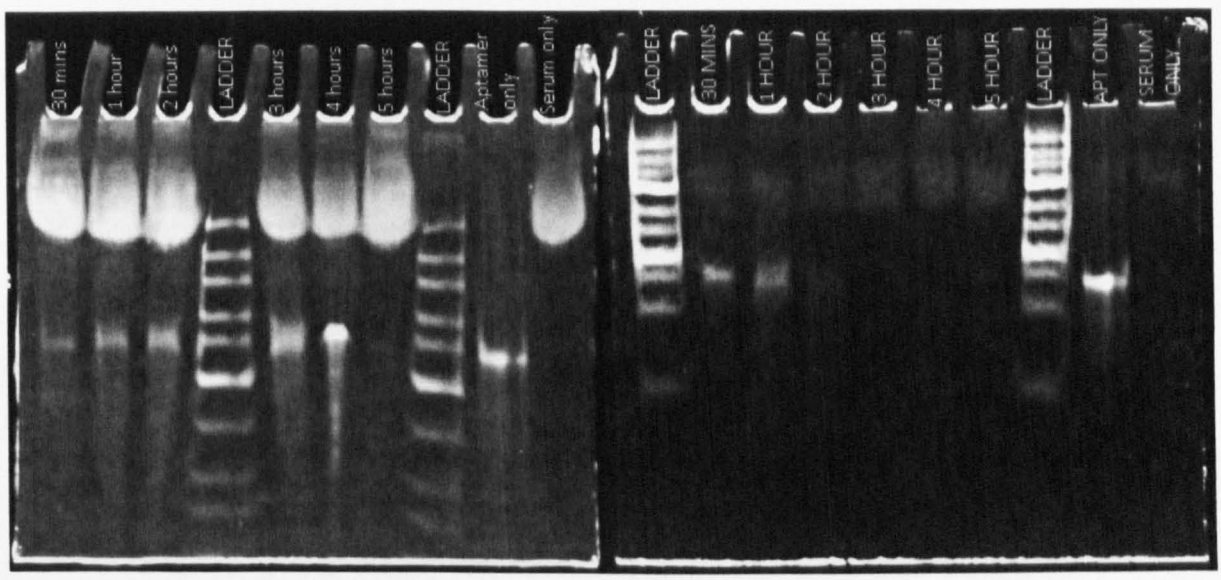

Figure 7.2 – Products of '1.5M long' aptamer incubated with human (left) or mouse (right) serum for different lengths of time, then the reactions stopped and products run on a 12% native PAGE, stained with ethidium bromide. Lanes are marked with duration of incubation time. Each band of the DNA ladder represents 25bp, beginning with 25bp.

Figure 7.3 shows the results obtained for 3.0M aptamer when exposed to human and mouse serum. There is an increase in smearing from three hours onwards in human serum; however, as the aptamer has not run in a straight line, the smear may appear more intense due to the aptamer having less gel width. With mouse serum, there is a decrease in band intensity and an increase of smearing from only 30 minutes, suggesting that 3.0M aptamer is very susceptible to degradation by mouse serum.

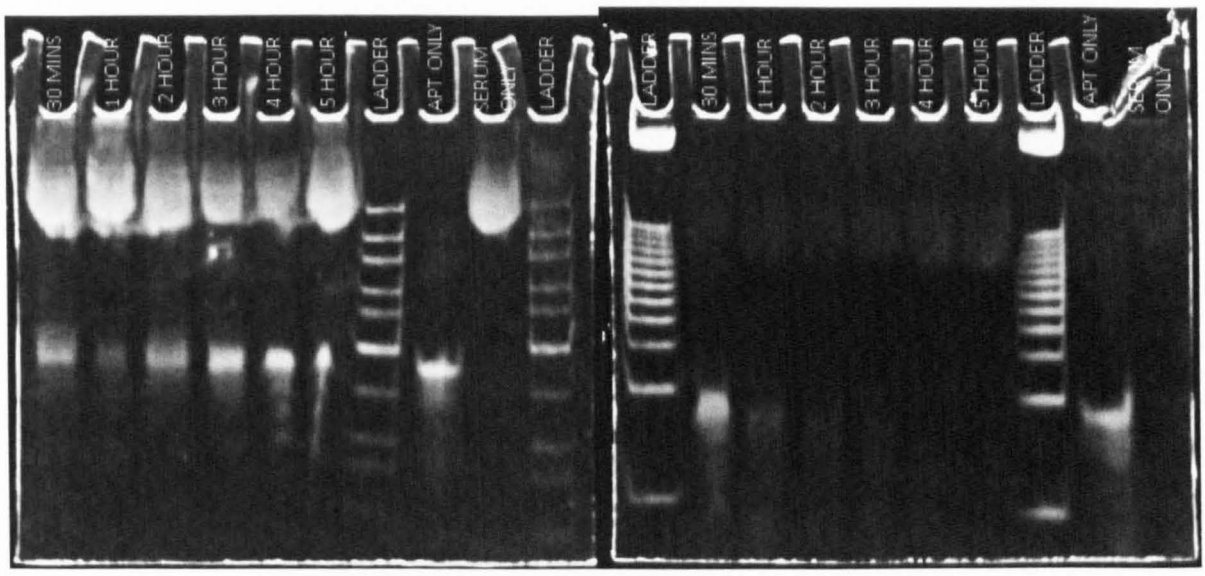

Figure 7.3 - Products of '3.0M' aptamer incubated with human (left) or mouse (right) serum for different lengths of time, then the reactions stopped and products run on a 12% native PAGE, stained with ethidium bromide. Lanes are marked with duration of incubation time. Each band of the DNA ladder represents 25bp, beginning with 25bp.

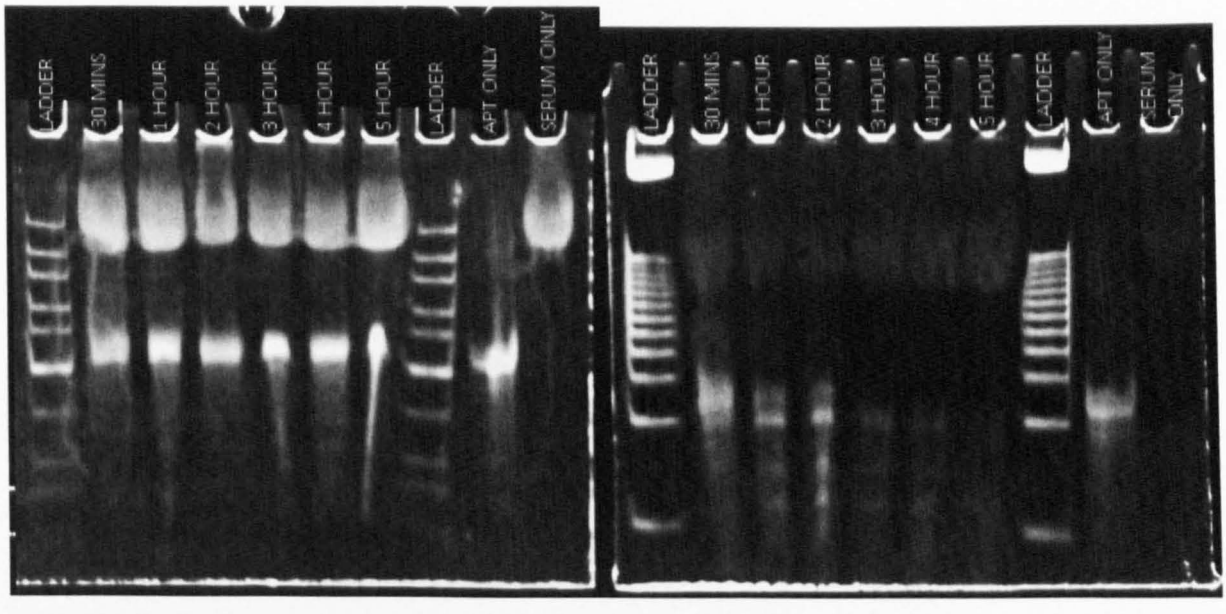

Figure 7.4 - Products of 'pink' aptamer incubated with human (left) and mouse (right) serum for different lengths of time, then the reactions stopped and products run on a 12% native PAGE, stained with ethidium bromide. Lanes are marked with duration of incubation time. Each band of the DNA ladder represents 25bp, beginning with 25bp.

Upon incubating pink aptamer (figure 7.4) with human serum, there is no reduction of band intensity or increase in smearing in comparison to the band shown by the aptamer alone. This suggests that pink aptamer is not susceptible to degradation by human serum. Mouse serum however, has caused a decrease in band intensity and increase in

smearing from three hours in comparison to the band of aptamer alone, suggesting that it has been degraded by nucleases present in the serum in this time frame.

Yellow aptamer (figure 7.5) has shown an unexpected result in the case of human serum. There is a very weak band for human and yellow aptamer incubated for 30 minutes, which does not correspond with the rest of the results for this serum which are all intense bands. If nuclease degradation had happened with this aptamer, one would expect to see a decrease in intensity of bands and increase in intensity of smearing with increase of incubation time. Therefore, this suggests that this result is an error perhaps caused by an incorrect concentration of aptamer being added to the serum in the first place. Upon incubating yellow aptamer with mouse serum, all of the bands show decreased intensity and increased smearing, with the primary aptamer band disappearing from three hours onwards. This suggests that yellow aptamer is subject to nuclease degradation from nucleases present in mouse serum.

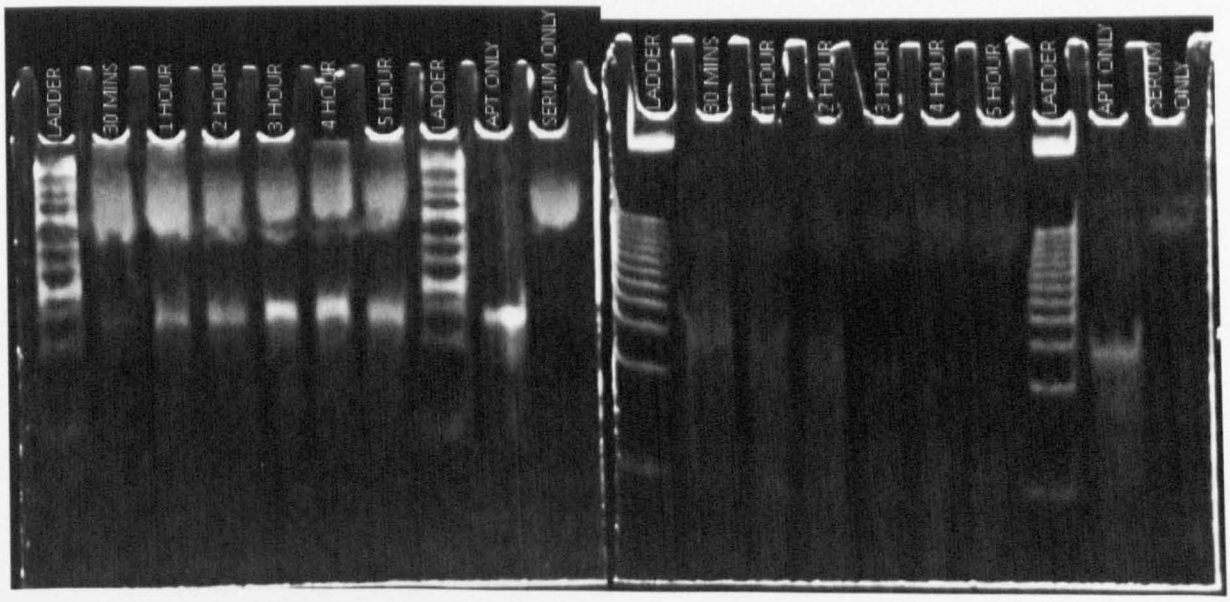

Figure 7.5 - Products of 'yellow' aptamer incubated with human (left) or mouse (right) serum for different lengths of time, then the reactions stopped and products run on a 12% native PAGE, stained with ethidium bromide. Lanes are marked with duration of incubation time. Each band of the DNA ladder represents 25bp, beginning with 25bp.

7.3 Interactions with Serum Albumins

Serum albumin is a 67kDa protein found in the blood or serum of vertebrates, where it constitutes approximately 60% of the total plasma proteins. At pH 7.4 it is negatively charged and acts as a transporter as many ligands are able to reversibly bind it non-covalently via its many binding sites [2, 3]. The binding of drugs to serum albumin in the bloodstream has important consequences on the bioavailability of those drugs, as their free and active concentrations in the bloodstream affects the intensity of their effects as well as the time spent in the body [2], although it has been found in the interactions of albumin with pesticides, that their affinity for albumin is lower than that for their primary targets [4].

To investigate the possible interactions between 1.5M short and long aptamers to human serum albumin (HSA), fluorescence quenching techniques were used, similar to chapter four, where aptamers were titrated into heparanase or its linker peptide. Experiments were performed at 37°C in a 3ml cuvette containing 1ml HSA diluted to concentration using PBS, pH 7.4. Excitation was performed at 290nm and emission was displayed from 300-400nm, with the slits narrowed to ± 3nm and a time interval of 90 seconds between each addition.

Aptamers 1.5M short and long were firstly titrated stepwise into water and PBS, pH 7.4 at 37°C, generating concentrations between 0-8μM to investigate their intrinsic fluorescence, as the presence of any aromatic ring in the molecular chain can invoke natural fluorescence [5]. It is seen from figure 7.6 and 7.7 that both aptamers have intrinsic fluorescence as there are peaks at 380nm, which increases in fluorescence

intensity upon increasing the aptamer concentration; 1.5M short showing less fluorescence than 1.5M long. Water was used as a diluent to show that the aptamer and not PBS was the cause of the fluorescence, although the fluorescence for 1.5M short increased upon using PBS as the diluent, however this was likely due to a difference in pH as in fluorescence spectroscopy, pH changes have a significant influence on results. Fluorescence of the aptamers caused a problem since the aptamers at these concentrations would obscure any quenching of HSA; therefore the concentration of HSA had to be high enough and the aptamer concentrations low enough to eliminate the interference. The optimum concentrations were therefore found to be 60μM HSA; which is 1/10th of the maximum level in plasma, and additions of aptamer from 0-7.4μM, corresponding to a maximum of 200μg/L; within the same range found in patients' plasma in clinical trials of aptamer ARC1779 to vWF [6].

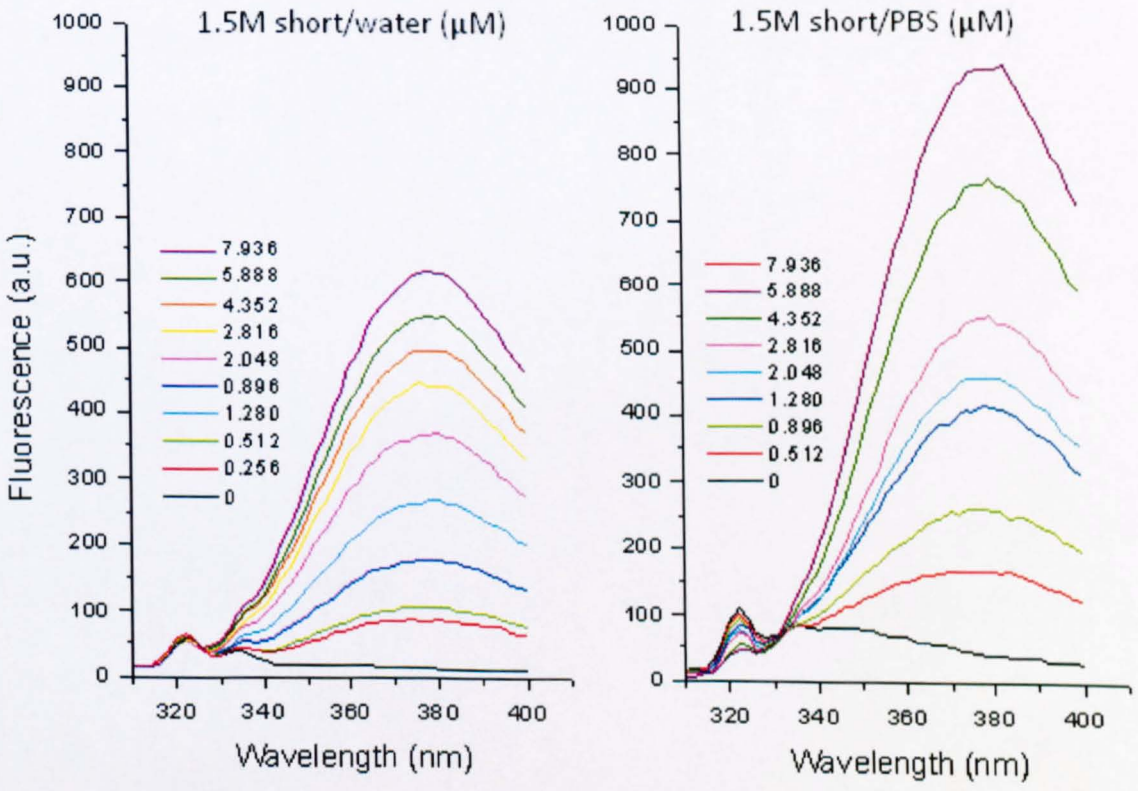

Figure 7.6 – Fluorescence spectra of 1.5M short aptamer in water (left) and PBS buffer (right) at 37°C. Fluorescence increases upon increasing the concentration of aptamer in both PBS and water, showing that although the fluorescence is higher in PBS, the aptamer is in fact the cause and the pH difference in water and PBS is the most likely reason for the increase of fluorescence of the aptamer in PBS.

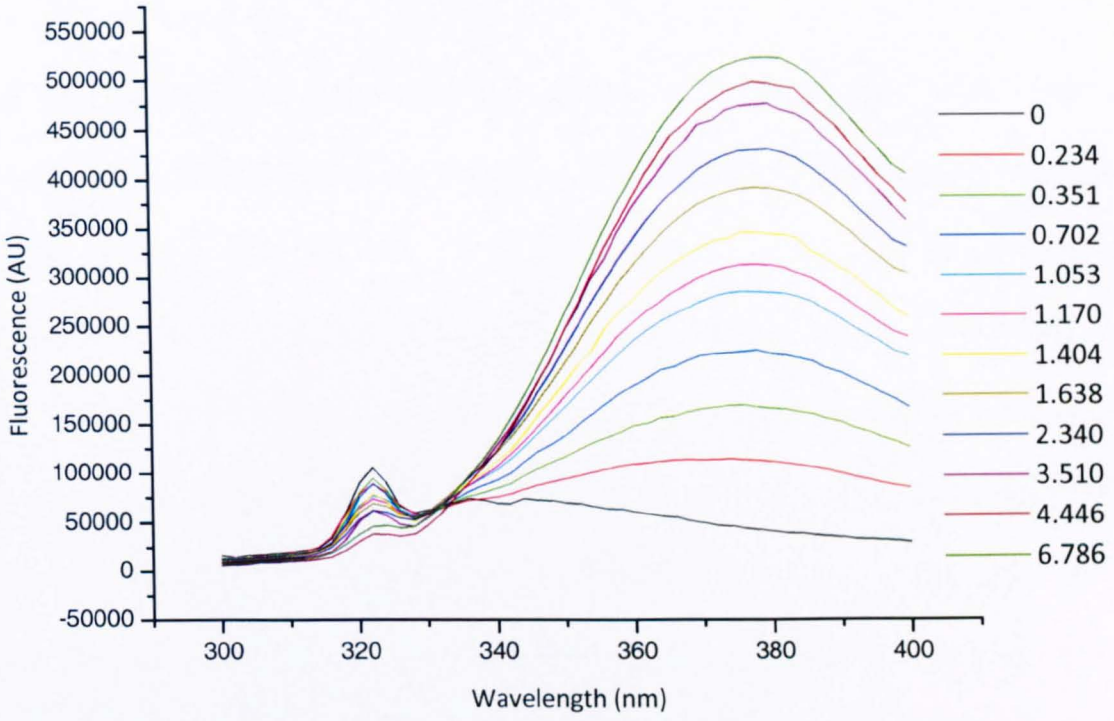

Figure 7.7 – Fluorescence spectrum of increasing concentrations of 1.5M long aptamer in water showing the intrinsic fluorescence of this aptamer.

When carrying out fluorescence studies, a decrease in fluorescence intensity not due to the quenching i.e. interaction between species can occur, and is termed the inner filter effect (IFE) [7]. The cause of this effect is the absorption of (in this case) the aptamer at the excitation or emission wavelength of the fluorophore, known as primary and secondary IFE respectively [7]. The IFE can masquerade as true quenching from the interactions of aptamer and HSA and therefore must be corrected using the appropriate equation. Therefore, the titrations were carried out in parallel using a spectrophotometer to determine the absorption at excitation and emission wavelengths. The sIFE was found to be negligible as neither aptamer was found to absorb at 380nm (data not shown), whereas the pIFE i.e. absorption of the aptamer at the excitation wavelength of 290nm was a contributing factor. Therefore, Parker's equation was used to correct this effect [7].

Figure 7.8 and 7.9 show the means of three fluorescence spectra obtained from stepwise titrations of 1.5M short and long aptamers with HSA at 37°C. Figure 7.10 is a normalised plot of the fluorescence quenching for both aptamers, plotted as HSA F/F_0 ratio against aptamer concentration, using an average of six values with standard deviations not higher than 11%, measured at the maximum emission of 345nm. As shown in the graph, 1.5M short aptamer is able to quench the fluorescence of HSA at 37°C by 1.5% (± 0.03%) and 9% (± 1.2%) at 1:100 and 1:10 molar ratios respectively, with quenching of 10% achieved by a molar concentration 9.1 times lower than HSA. 1.5M long aptamer is able to quench the fluorescence of HSA by 10% at a concentration 18.2 times lower than HSA, and by 2.4% (± 0.1%) and 16% (± 0.6%) at 1:100 and 1:10 molar ratios. The results show that both aptamers are able to quench the fluorescence of HSA, although 1.5M long is more effective.

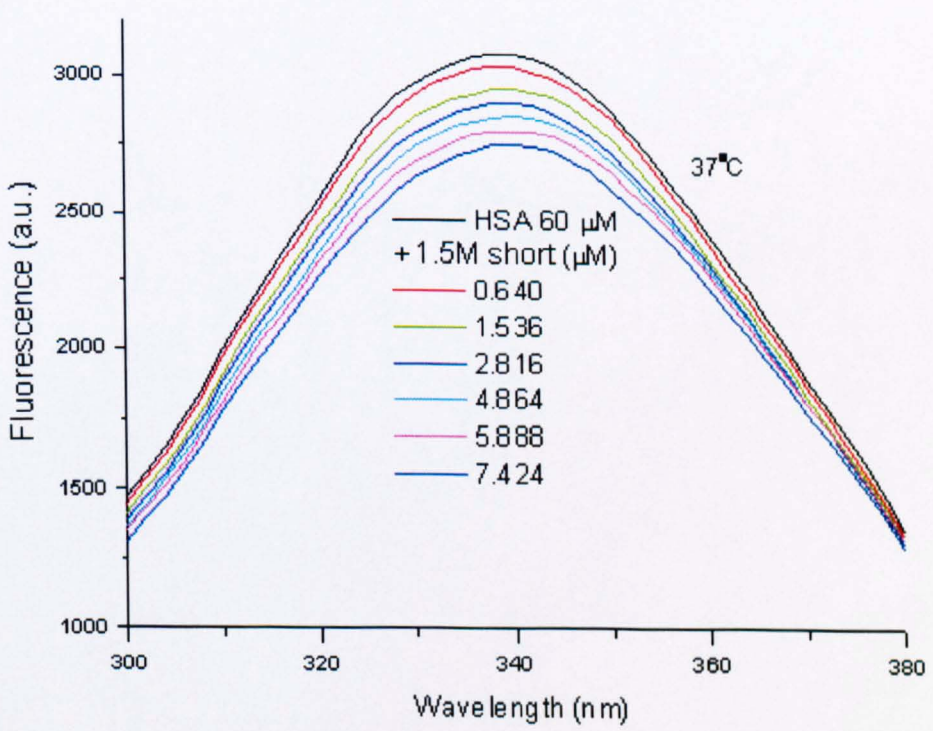

Figure 7.8 – Means of three experiments showing gradual HSA fluorescence quenching by increasing concentrations of 1.5M short aptamer at 37°C in PBS.

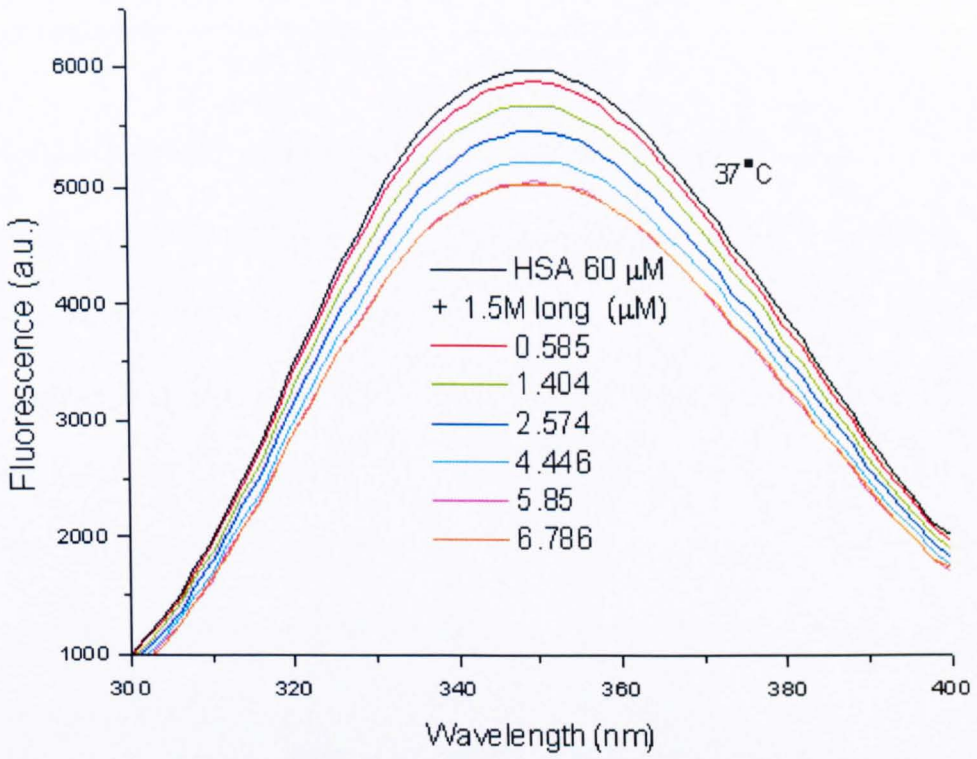

Figure 7.9 - Means of three experiments showing gradual HSA fluorescence quenching by increasing concentrations of 1.5M long aptamer at 37°C in PBS. The decrease in fluorescence is more pronounced than by 1.5M short aptamer.

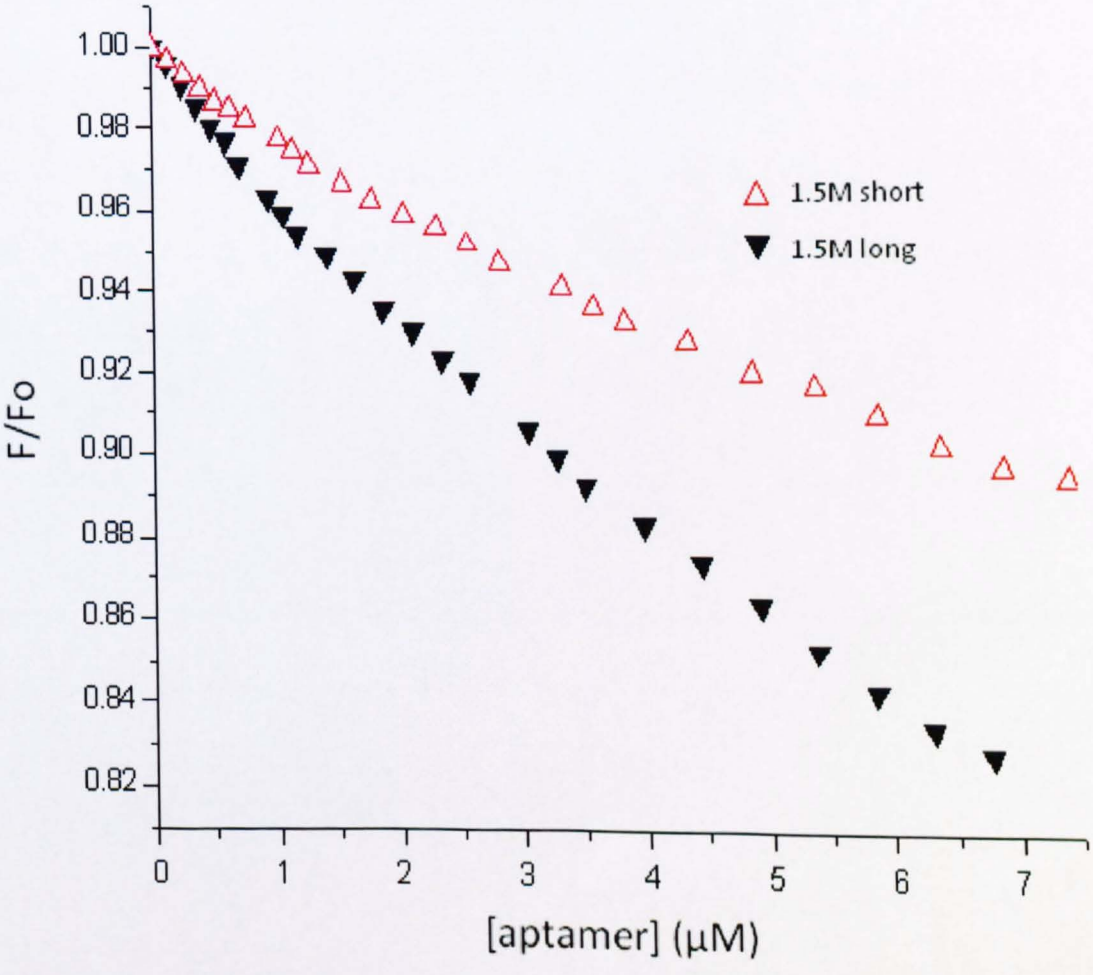

Figure 7.10 – Normalised plots of fluorescence quenching of HSA by 1.5M short and long aptamers in PBS at 37°C at the wavelength of maximum emission (345nm). Data is the

mean of six values showing no greater standard deviation than 11%. The quenching effect is more considerable for 1.5M long than short.

To gain more information about the type of interaction occurring between the aptamers and HSA, UV spectrometry titrations were carried out by titrating increasing concentrations of aptamers 1.5M short and long into PBS and 6μM HSA diluted in PBS (figures 7.11 and 7.12). The addition of both aptamers to PBS and HSA increased the overall absorbance, showing that the aptamer was responsible for this increase and not HSA. The increase was more pronounced for 1.5M long than short, and both produced a shift of the maximum absorbance to the left upon addition of increasing concentrations of aptamer The shift seen from 1.5M short aptamer moved 6nm to the left, suggesting that only a slight conformational change in the protein was occurring [5] and therefore, HSA quenching by this aptamer is most likely due to dynamic quenching. However, in the case of 1.5M long, not only was there a substantial shift in the maximal absorption by 20nm to the left, but a complete change in the shape of the peak was observed, incorporating the peak at 260nm of the aptamer, suggesting that one complex was formed and that the quenching was due to the static quenching phenomenon with 1.5M long aptamer [5].

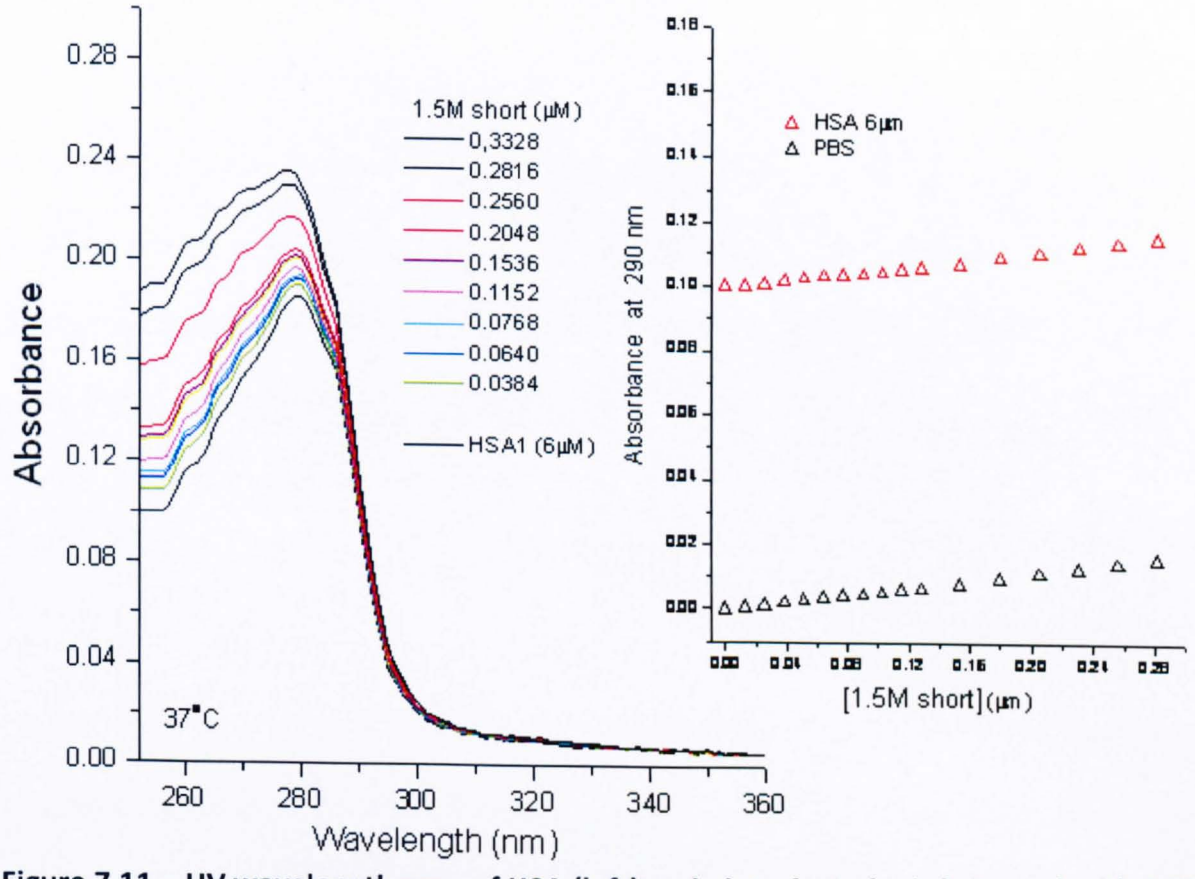

Figure 7.11 – UV wavelength scan of HSA (left) and plot of PBS (right) titrated with 1.5M short aptamer.

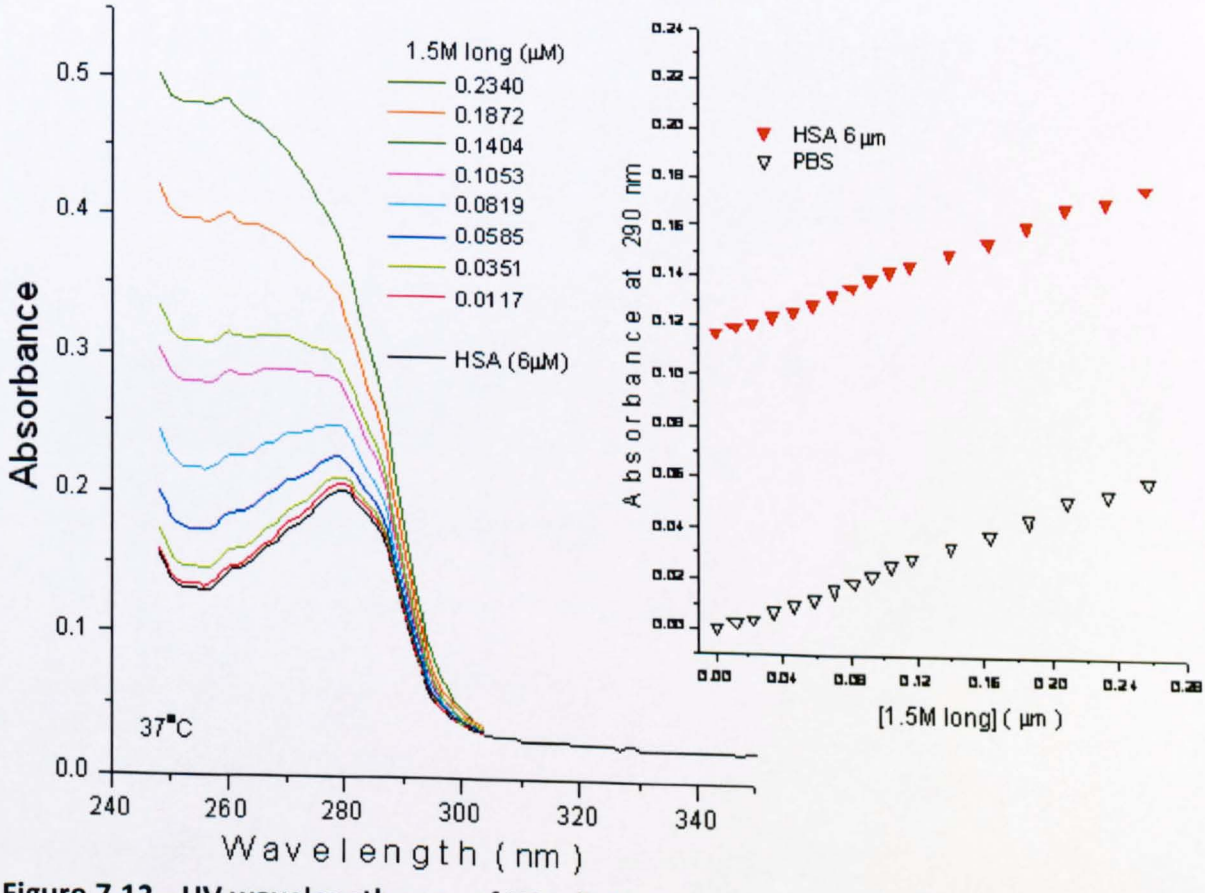

Figure 7.12 - UV wavelength scan of HSA (left) and plot of PBS (right) titrated with 1.5M long aptamer.

7.4 Development of a Piezoelectric Aptasensor

A biosensor is a device used for detection of a specific analyte and is composed of a sensitive biological agent (e.g. aptamer or antibody), which interacts selectively with the analyte of interest; a transducer, which transforms the signal generated from this interaction to the electronic equipment, which analyses and displays the signal in a user-friendly way.

The field of biosensors, and in particularly, electronic aptamer-based biosensors (aptasensors) has recently progressed due to the technique's many advantages [8]. These include being able to detect the presence of the compound of interest quickly when compared to techniques such as ELISA, which uses a chemical reaction after several incubations of successive detection labels. There are no radioactive compounds involved; making aptasensors a safer alternative to assays such as RIA. Also, real-time measurements are possible in many of the different detection systems, as is the opportunity of automation, which makes for high throughput assays [8].

Several approaches to development of analytical aptasensors have been used. Most of these use aptamers conjugated with functional groups or moieties at their 5' or 3' end so that they may be coupled to the solid support and used as a receptor. The disadvantages of using these types of assay then become apparent, i.e. the need to couple functional moieties to the aptamer can be time consuming and expensive, but also may change the binding properties the aptamer has for its target, leading to reduced sensitivity and/or selectivity, although research is ongoing to overcome this, and the multiple advantages of using aptasensors far outweigh these problems [8].

The quartz crystal microbalance (QCM) is a technique that has been employed by groups to study the interactions between immobilised aptamers and their respective target proteins [9-11]. A gold-coated quartz crystal forms the solid support, which when coupled with the microbalance equipment, oscillates at a certain frequency. Frequency of its oscillation is directly related to the thickness of deposit on the surface of the crystal, which when immobilised aptamers recognise and bind their protein target, the mass at the surface increases causing the frequency of oscillation to decrease. This is demonstrated by the Sauerbrey equation (equation 7.1), where Δf_r is the change of resonance frequency in Hertz, Δm is the change in nanogram mass on the quartz surface, A is the size of the aptamer-coated surface in square centimetres and c_f is the sensitivity constant. The sensitivity constant is calculated as shown in equation 7.1, by use of the original frequency (f_r) e.g. 5MHz, the density (ρ_q) and velocity of sound (v_q) of the quartz crystal [10].

$$\Delta f_r = -c_f \frac{\Delta m}{A} \quad \text{using} \quad c_f = \frac{2f_r^2}{\rho_q v_q}$$

Equation 7.1 – Sauerbrey equation [10] linking change in resonance frequency with a change in mass at the crystal surface.

In order to provide the basis of a useful diagnostic technique using QCM, heparanase-selected aptamers must:

1. immobilise to the crystal's surface
2. retain recognition specifically for heparanase
3. have the ability to be regenerated and reused
4. recognise heparanase at low concentrations and in the presence of other proteins
5. the results must be reproducible and accurate

Immobilisation of 5' biotinylated heparanase-selected aptamers to the surface of a 5MHz crystal was carried out using a solution of 4mg/ml 3,3'-dithiodipropionic acid-di(N-succinimidylester) (DSP), diluted in water-free N,N-dimethylacetamide (DMA), in accordance with other group's methods [10, 12] and immobilises free amino groups of lysine residues of streptavidin by peptide bonds. These act as a 'spacer' between the gold surface and the biotinylated aptamer, as it has been found that use of the spacer, rather than direct immobilisation of amino-modified aptamers to DSP on the surface, increases the sensitivity of the device [8, 10]. Experiments were conducted with use of a flow cell and stop-flow system to maintain the crystal's surface in solution at all times and PBS was used as the buffer and diluent.

Firstly, upon addition of the crystal to the flow cell, it was important to allow enough time for the crystal to equilibrate, so the frequency was monitored immediately after inserting the crystal and immersing it in PBS. It was determined necessary to allow between 100-140 minutes before beginning any experiments. Therefore, each experiment was allowed this time of incubation in PBS inside the flow cell before any readings were taken.

To investigate whether immobilising 1.5M short and long aptamers to the quartz crystal surface would retain their recognition for heparanase and if the crystals could be regenerated, experiments were conducted on newly immobilised crystals. Inside the flow cell, which was exposed to room temperature and humidity, the capacitance was adjusted so the microbalance equipment was 'locked on' to the frequency of the crystal, then the crystals were incubated in PBS for 140 minutes to equilibrate and a base reading taken for approximately ten minutes to ensure the crystal had equilibrated. After pausing the reading of measurements, 800nM heparanase in PBS was introduced to the flow cell

by use of the peristaltic pump. Immediately after stopping the pump, when the heparanase had been introduced to the flow cell, the readings were resumed. After the readings had stabilised, the program was paused, PBS was added to the flow cell via the pump and the readings resumed once again. This served as a 'wash step' by removing any heparanase which was unbound, and any plateau of frequency was used to determine the maximum decrease from addition of heparanase. The crystal was then regenerated by introducing 100mM EDTA and 3.0M NaSCN wash steps, followed by returning the crystal to PBS, pausing the readings and using the pump to make each addition. The experiments were also repeated using 800, 400, 200 and 100nM heparanase, corresponding to 50, 25, 12.5 and 6.25µg/ml respectively; 10^4 times over the upregulated heparanase levels in cancer patients [13]. These results are shown in figure 7.13 and show that higher heparanase concentrations decrease the frequency of the crystal by a bigger margin, due to more heparanase becoming bound by the aptamers.

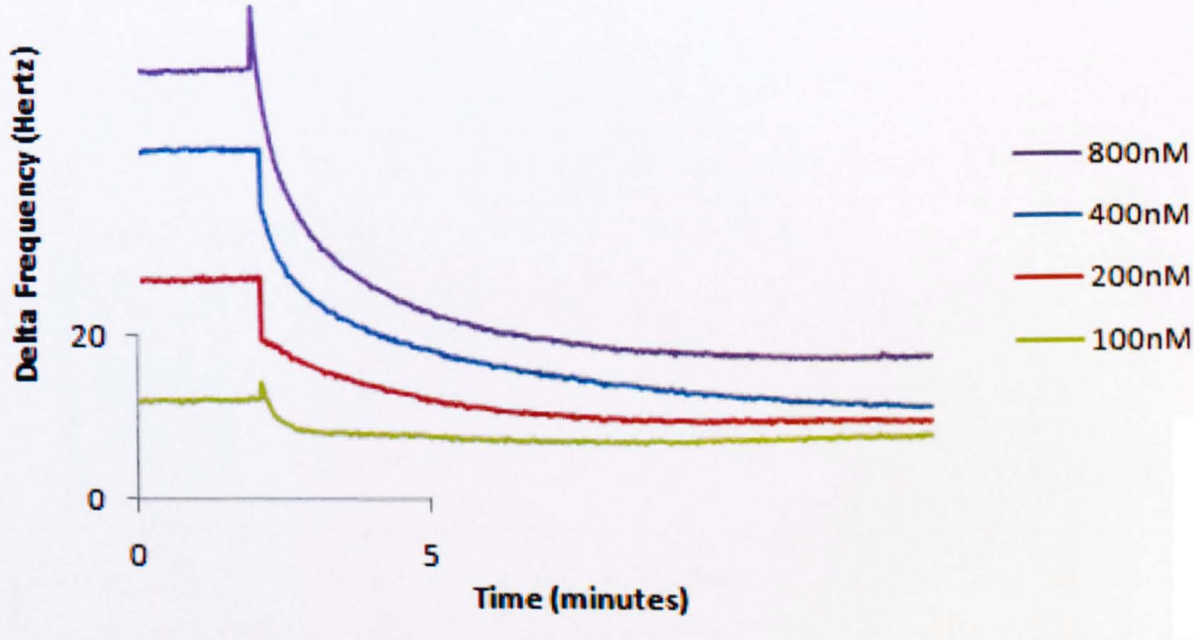

Figure 7.13 – Binding sensogram showing decrease in frequency of crystals immobilised with 1.5M short aptamer exposed to different concentrations of heparanase. Higher concentrations of heparanase exhibited a greater decrease in frequency.

Figures 7.14 and 7.15 show the results when 800nM heparanase diluted in PBS were added to crystals immobilised with 1.5M short and long aptamers. The results both show a considerable decrease upon exposure to heparanase, by 42.97Hz and 50.35Hz respectively. Washing with PBS liberated only 5.51Hz and 4.39Hz, giving total Δf_r of 37.46Hz and 45.96Hz for 1.5M short and long aptamers respectively. This suggests that heparanase was recognised and bound by both aptamers.

Returning the crystals to PBS after performing regeneration washes using 100mM EDTA and 3.0M NaSCN increased the frequencies to 0.61Hz below the level of original equilibration for the crystal immobilised with 1.5M short aptamer and 3.09Hz lower than that of 1.5M long aptamer. This suggests that the crystals were almost totally regenerated, liberating almost all of the bound heparanase and leaving behind the immobilised aptamers.

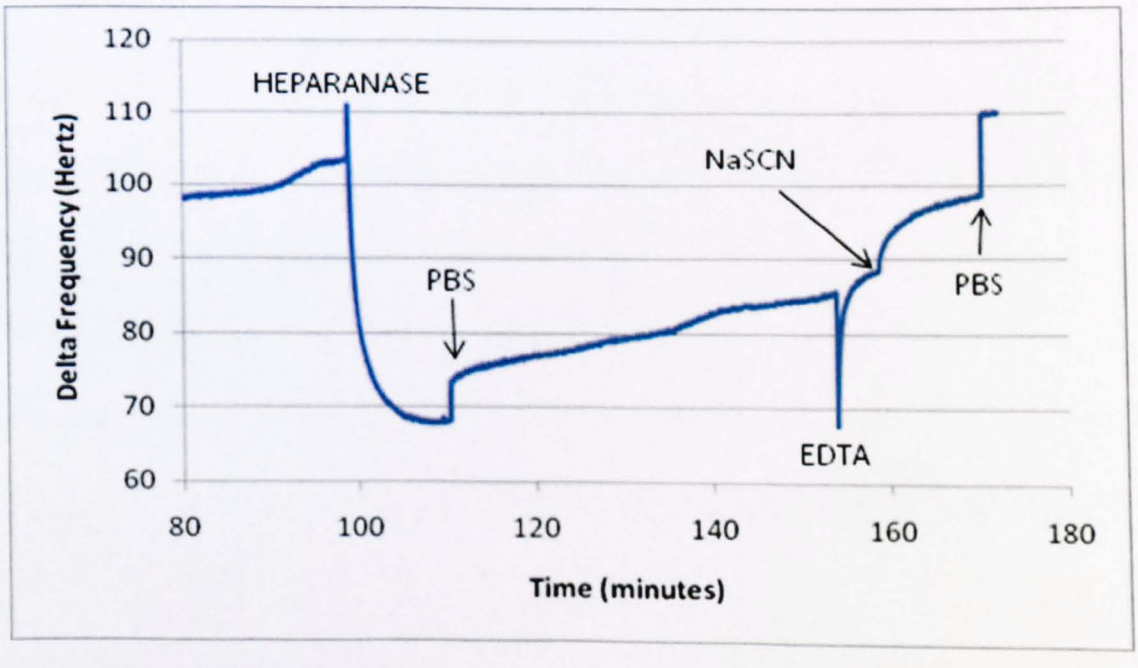

Figure 7.14 – Binding and regeneration sensograms for addition of 800nM heparanase to quartz crystal immobilised with 1.5M short aptamer. After a wash with PBS, an Δf_r of 37.46Hz was observed. Washing with 100mM EDTA then with 3.0M NaSCN allows total regeneration of the crystal.

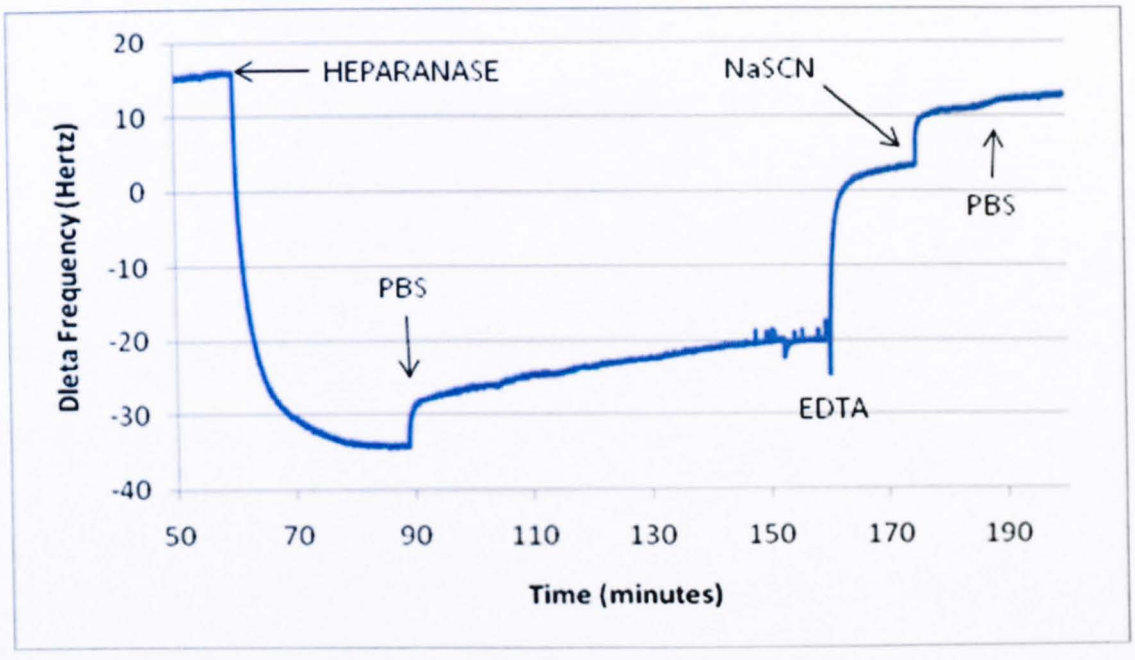

Figure 7.15 – Binding and regeneration sensograms for addition of 800nM heparanase to quartz crystal immobilised with 1.5M long aptamer. Washing with PBS determined an Δf_r of 45.96Hz, then with 100mM EDTA and 3.0M NaSCN allowed almost total regeneration of the crystal.

7.5 Discussion

The results from these experiments suggest that heparanase and linker peptide-selected aptamers are stable in human serum for up to five hours, with the exception of 1.5M long aptamer, which succumbed to nuclease degradation upon incubation with serum in between four and five hours. Mouse serum, on the contrary, caused complete nuclease degradation of all of the aptamers within five hours; 3.0M and yellow aptamers exhibited degradation from 30 minutes, whilst pink and 1.5M long aptamers both showed nuclease degradation between two and three hours and 1.5M short aptamer between four and five hours. These results suggest that without modification, aptamers may be stable in the blood of humans for up to five hours, which correlates with the results shown by Bates [14] and Xu [15], with the nucleolin aptamer AS-1411, which is an unmodified 26 nucleotide DNA aptamer also not subject to nuclease degradation through its formation

of a G-quadruplex structure alone. Therefore, these aptamers may form promising therapeutics, which may be a consequence of their secondary structures as also reported by Di Giusto [16] with circularised aptamers. Conversely, the data also suggests that without modification, aptamers would not be stable in the blood of a mouse for longer than 30 minutes, so either the aptamers would require modification, or the mouse may not form a suitable model for animal testing.

Fluorescence quenching experiments with human serum albumin showed that 1.5M short aptamer was able to quench the fluorescence by 10% at a concentration 9.1 times lower than HSA, and 1.5M long aptamer at 18.2 times lower. In a similar study by Silva *et al.* [17] a pesticide, Methyl Parathion, was required in excess of HSA to generate a quenching of 10%, suggesting that these aptamers may bind in closer proximity to the one tryptophan residue found in HSA than this pesticide [2]. This tryptophan residue is located at site 214 in subdomain IIA, within which there is a large hydrophobic cavity with many arginine residues near the surface [2, 4], which have been shown in different studies to serve as anchor points for aptamers [18]. The UV titrations suggested that 1.5M short aptamer did not form a complex with HSA and that the interactions were due to dynamic quenching, whereas 1.5M long was suggested to form a ground state complex with HSA. These results could be further reinforced by carrying out further titrations at a different temperature and applying the Stern-Volmer theory used in previous studies of drugs and serum albumins [3, 17, 19].

Preliminary results from the QCM experiments with 1.5M short and long aptamers suggested that the aptamers had bound successfully to the quartz crystals and that they retained the capacity to recognise and bind heparanase; shown when heparanase was

introduced to the flow cell and the frequency decreased and remained 37.46 and 45.96Hz lower respectively after a wash with PBS, confirming binding. Different concentrations of heparanase were also distinguished from 800 to 100nM, in which an increase in concentration correlated with a greater decrease in frequency.

The regeneration steps were successful as the crystals returned to within 4Hz of their original frequency before the addition of heparanase. This was in accordance with other groups [10] and was expected due to the absence of mono or bivalent metal ions in EDTA, which are required for the formation of the aptamers' complex structures. Removal of these ions causes unfolding of the aptamers and release of the bound heparanase. As a precaution, 3.0M NaSCN, the final elution of the selection process, was also used due to its ability to remove the remainder of bound aptamers from heparanase in selection. It was expected that addition of PBS would renew the crystal by causing the refolding of the immobilised aptamers due to PBS containing Magnesium ions [10]. These preliminary results were very promising for the future use of these aptamers in a diagnostic assay; however, further experiments need to be conducted. To provide information regarding the longevity of immobilised crystals, their limits of detecting heparanase and binding data between aptamers and heparanase, it is necessary to conduct experiments consecutively and immediately after immobilisation of 1.5M short, long and an unrelated (negative control) aptamer to each crystal. Firstly, experiments repeated using 800nM heparanase, followed by regeneration would determine reproducibility at that concentration, and could be used to determine binding data such as K_A and K_D for each aptamer using this methodology. Repeats of each experiment using a series of different concentrations down to 10pM would determine if the lowest concentrations of heparanase detected by the system would correspond to heparanase levels in the sera of cancer patients [13]. The first experiments of addition of 800nM heparanase would then

be repeated and compared to the original results. This would show whether the crystal's capacity to recognise heparanase was diminished after so many regeneration steps and the whole set of experiments would give a clear indication as to how many times the crystal could be regenerated and reused, and if it were a reliable and accurate way of detecting concentrations of heparanase in solution and therefore be used as a diagnostic tool. Many assays have been generated to reliably test the activity of heparanase and its inhibitors that could be transferred into a diagnostic setting. However, their disadvantages; the use of radiation [10, 11], cost [20, 21], or the time consuming element [22-24] could mean that a reliable QCM-based assay with the ability for regeneration of crystals as well as specific detection of heparanase at low concentrations in real time upon addition of sample, would be highly desirable.

References:

1. Shaw, J.P., et al., *Modified deoxyoligonucleotides stable to exonuclease degradation in serum.* Nucleic Acids Res, 1991. **19**(4): p. 747-50.
2. Kragh-Hansen, U., *Molecular aspects of ligand binding to serum albumin.* Pharmacol Rev, 1981. **33**(1): p. 17-53.
3. Silva, D., C.M. Cortez, and S.R. Louro, *Chlorpromazine interactions to sera albumins. A study by the quenching of fluorescence.* Spectrochim Acta A Mol Biomol Spectrosc, 2004. **60**(5): p. 1215-23.
4. Kratochwil, N.A., et al., *Predicting plasma protein binding of drugs: a new approach.* Biochem Pharmacol, 2002. **64**(9): p. 1355-74.
5. Lakowicz, J.R., ed. *Principles of Fluorescence Spectroscopy*. Second ed. 1999, Kluwer Academic Publishers/Plenum Press: New York. 237-259.
6. Gilbert, J.C., et al., *First-in-Human Evaluation of Anti von Willebrand Factor Therapeutic Aptamer ARC1779 in Healthy Volunteers.* Circulation, 2007. **116**(23): p. 2678-2686.
7. Puchalski, M.M., M.J. Morra, and R. Vonwandruszka, *Assessment of Inner Filter Effect Corrections in Fluorometry.* Fresenius Journal of Analytical Chemistry, 1991. **340**(6): p. 341-344.
8. de-los-Santos-Álvarez, N., et al., *Aptamers as recognition elements for label-free analytical devices.* TrAC Trends in Analytical Chemistry, 2008. **27**(5): p. 437-446.
9. Furtado, L.M., et al., *Interactions of HIV-1 TAR RNA with Tat-derived peptides discriminated by on-line acoustic wave detector.* Anal Chem, 1999. **71**(6): p. 1167-75.

10. Liss, M., et al., *An aptamer-based quartz crystal protein biosensor.* Anal Chem, 2002. **74**(17): p. 4488-95.

11. Tombelli, S., et al., *Aptamer-based biosensors for the detection of HIV-1 Tat protein.* Bioelectrochemistry, 2005. **67**(2): p. 135-41.

12. Hianik, T., et al., *Influence of ionic strength, pH and aptamer configuration for binding affinity to thrombin.* Bioelectrochemistry, 2007. **70**(1): p. 127-33.

13. Shafat, I., et al., *Heparanase levels are elevated in the plasma of pediatric cancer patients and correlate with response to anticancer treatment.* Neoplasia, 2007. **9**(11): p. 909-16.

14. Bates, P.J., et al., *Antiproliferative activity of G-rich oligonucleotides correlates with protein binding.* The Journal of biological chemistry, 1999. **274**(37): p. 26369-26377.

15. Xu, X., et al., *Inhibition of DNA replication and induction of S phase cell cycle arrest by G-rich oligonucleotides.* The Journal of biological chemistry, 2001. **276**(46): p. 43221-43230.

16. Di Giusto, D.A. and G.C. King, *Construction, stability, and activity of multivalent circular anticoagulant aptamers.* J Biol Chem, 2004. **279**(45): p. 46483-9.

17. Silva, D., et al., *Methyl parathion interaction with human and bovine serum albumin.* Toxicol Lett, 2004. **147**(1): p. 53-61.

18. Hermann, T. and D.J. Patel, *Adaptive recognition by nucleic acid aptamers.* Science, 2000. **287**(5454): p. 820-5.

19. Silva, D., et al., *The interaction of methyl-parathion with serum and albumin of the neo-tropical fish Piaractus mesopotamicus.* Ecotoxicology and Environmental Safety. **73**(1): p. 32-37.

20. Enomoto, K., et al., *A simple and rapid assay for heparanase activity using homogeneous time-resolved fluorescence.* J Pharm Biomed Anal, 2006. **41**(3): p. 912-7.

21. Tokuda, C., L. Jacquemart, and M. Preaudat. *Development of a Homogenous Heparanase Assay using HTRF Technology.* [cited; Cisbio international technical document]. Available from: http://www.htrf-assays.com.

22. Behzad, F. and P.E. Brenchley, *A multiwell format assay for heparanase.* Anal Biochem, 2003. **320**(2): p. 207-13.

23. Hammond, E., C.P. Li, and V. Ferro, *Development of a colorimetric assay for heparanase activity suitable for kinetic analysis and inhibitor screening.* Anal Biochem, 2009. **396**(1): p. 112-6.

24. Inc., T.B. *Heparan Degrading Enzyme Assay Kit.* [cited; Available from: http://takaramirusbio.com/.

CHAPTER EIGHT

CONCLUSION AND FURTHER WORK

The aim of this project was to select for aptamers against human recombinant polymorphic heparanase and its excised linker peptide with the aim of inhibition of the active enzyme or its cleavage of the linker peptide from the proenzyme to form the active enzyme, or its identification in biological samples to provide the basis for a future therapeutic or diagnostic reagent in the field of cancer medicine.

Using an amplified library with each species containing a 25 nucleotide variable sequence; hence allowing complex structures to be formed, a modified SELEX protocol was optimised for the targets. Target proteins were incubated with the aptamer library and bound aptamers were eluted using a salt elution series. The higher salt elutions containing aptamers were chosen for testing based on them containing species with higher affinity as those with low affinity would have eluted at lower salt concentrations. These were 1.5M NaCl and 3.0M NaSCN for heparanase and 3.0M NaSCN for the linker peptide. After cloning and sequencing aptamers from these fractions, it was determined that the 1.5M NaCl elution had produced one species with consensus and the 3.0M NaSCN showed aptamers that shared consensus in all sequenced samples with one exception. In the case of the linker peptide, two sequences were repeated with the highest frequency amongst those generated. Based on their predicted structures using Mfold, the aptamers were truncated as much as possible to remove any nucleotides not implicated in structure formation; generating a 30 and 72 nucleotide sequence from the 1.5M NaCl elution of heparanase, named '1.5M short' and '1.5M long' respectively and a 55 nucleotide sequence from the 3.0M elution; named '3.0M'. In terms of the linker, both sequences were retained as 72 nucleotides based on their predicted structures, and were named 'pink' and 'yellow'.

Preliminary assays were carried out to determine that the aptamers did indeed bind their respective target before carrying out *in vitro* testing. A sandwich-based ELISA utilising the biotin-streptavidin interaction to immobilise biotinylated 1.5M short, 1.5M long and 3.0M aptamers to the solid support of the well was manipulated, and adding increasing concentrations of heparanase determined that the aptamers did indeed bind heparanase. However, binding of the aptamers was not at the antibody binding site, as its interactions were not disrupted in a competition ELISA with increasing aptamer concentrations. It was also determined that the aptamers selected for heparanase did not recognise the heat-denatured enzyme, suggesting that they recognise a sequence of residues in a structured conformation. This could be further investigated by subjecting the aptamer to circular dichroism analysis or structural NMR spectroscopy.

The almost complete quenching of the intrinsic fluorescence generated by tryptophan residues of the linker peptide by aptamers pink and yellow suggested that their binding obscured the signal by both tryptophan residues, supported by the fact that the aptamers are larger, at 22kDa, compared to the linker peptide at 6kDa. Quenching of one third of the intrinsic fluorescence of heparanase by aptamers 1.5M short, long and 3.0M suggested that the aptamers either bound and obscured the signal of two out of the six tryptophans within the 50kDa subunit, or within a different area, possibly the 8kDa subunit, therefore altering the enzyme's structure enough to show this level of quenching. Fluorescence titrations also demonstrated the association constants between heparanase and its aptamers were in the range of high affinity of $10^7 M^{-1}$, with the most promising aptamer shown to be the 1.5M long. Affinity constants for linker peptide with aptamers pink and yellow were in the range $10^6 M^{-1}$, perhaps due to the lower conformational structure of a peptide in comparison to a full-length protein.

In vitro assays using the selected aptamers to label heparanase and linker peptide in immunohistochemistry and immunofluorescence studies showed that overall the favoured aptamers for detection of heparanase in tissue and cell samples were the 1.5M long and short respectively. They both showed similar staining, both in terms of pattern and intensity, as the heparanase antibody, which is expected as they originated from the same sequence and therefore may share some structural features or binding nucleotides. Of the aptamers selected for the linker peptide, yellow was favoured in these studies as it most frequently showed a level of staining over the negative control and suggested it may be able to recognise linker peptide either cleaved or uncleaved from the proenzyme, and pink may not. This could be further confirmed by conducting an assay into the processing of proheparanase using cathepsin L in the presence of both aptamers separately, plus the relevant controls. Further fluorescence assays using the biotinylated aptamers used for IHC and IF labelling could also be conducted to determine the effect of biotin on the aptamer affinity for heparanase as compared with the unmodified aptamers.

Invasion assays using all aptamers selected, plus the heparanase polyclonal antibody and a small-molecule inhibitor of heparanase, BAFB [1] as inhibitors, determined that the polyclonal antibody was the most successful inhibitor of invasion of tumour-derived cells in both assays, which corresponds to previous experiments [2, 3]. 1.5M short aptamer showed a decrease in invasion area and index in human uterine leiomyoma tissue, suggesting it was favoured because of its size and may have been able to travel through the plasma membrane or act at the plasma membrane itself to inhibit heparanase, where the longer aptamers may not, due to the steric hindrance or non-specific interaction with other molecules. Aptamers 1.5M long, 3.0M and pink were all suggested to show a degree of inhibition, which was anticipated due to their performance in the previous

binding and labelling studies. Unfortunately, small molecule inhibitor, BAFB, was not able to show any inhibition in these assays due to its low solubility in the appropriate buffer for the assay. Thus, attempting to dissolve the BAFB in a more suitable solvent and repeating the assay would show a suitable comparison of inhibition by a small molecule of a different variety to an aptamer. Due to time and financial constraints, it was not possible to test different concentrations and/or cell lines in these experiments; however, this would be an interesting further line of study, as it would allow us to elucidate the effect of increasing concentrations of 1.5M long, 3.0M and pink aptamers would have on heparanase inhibition. Furthermore, the extent of inhibition in hypoxic conditions could also be determined, as culturing the cells using 1% rather than 20% O_2 was previously shown to enhance invasion in the ovarian carcinoma cell line [3]. To further demonstrate that the aptamers in this study did indeed reduce invasion due to their inhibitory effect on heparanase and not a cytotoxic effect upon the cells directly, a cytotoxicity assay could be conducted to complement these results.

Aptamers have been shown to be stable in human serum, suggesting their potential for therapeutic applications, although their lack of resistance in mouse serum would have an adverse effect in their study in this model, requiring them to be appropriately modified to increase stability. Previous in vivo testing of small molecule inhibitors for heparanase have been carried out using Fischer 344 rats immunised with mammary adenocarcinoma 13762 MAT cells [4]. Therefore, testing the stability of these aptamers in rat serum would be appropriate, and if the aptamers showed stability, would allow a comparison experiment to be conducted with the other relevant small molecule inhibitors. Longer time incubations with aptamers and human serum would also give an indication of the maximum amount of time the aptamers would be stable for, as in the assays conducted in this study, some aptamers still remained stable at the maximum time point of five

hours. Aptamers' stability is likely to be linked to increased structural conformations, as this has been previously shown to be a crucial factor in nuclease degradation experiments. Additionally, aptamers have been studied for their interaction with serum proteins to evaluate the effect these may have in the pharmacokinetic properties of the aptamers. Both aptamers studied have shown an interaction with HSA, which, however, has been significantly lower than their interaction with heparanase although the longer aptamer has shown a higher affinity for HSA than the short one.

Selected aptamers have also been shown to have a diagnostic potential, both from the results obtained in the early ELISA studies and in subsequent studies using quartz crystal microbalance, which offers a number of advantages for point of care delivery of diagnosis. Aptamers were shown to perform well in the QCM system, and were able to be immobilised on the crystal and used in a variety of concentration and sufficiently regenerated for further measurements. However, additional experiments would be necessary to establish limits of upper and lower detection of heparanase, reproducibility, regeneration and lifespan of crystal. Further work using spiked human serum would demonstrate the limits of detection of heparanase in biological samples using this technique.

This project has achieved its objectives of generating high affinity and specificity aptamers for recombinant polymorphic heparanase and its linker peptide. These aptamers have shown the ability to recognise their cognate targets both in spectroscopic and biochemical assays as well as in tissue and cell culture analysis. Furthermore, they have shown the potential to inhibit heparanase activity and recognise heparanase in diagnostic platforms. Thus, this research has opened the possibility for developing and optimising these molecules into future therapeutic and diagnostic modalities.

References:

1. Courtney, S.M., P.A. Hay, R.T. Buck, C.S. Colville, D.J. Phillips, D.I. Scopes, F.C. Pollard, M.J. Page, J.M. Bennett, M.L. Hircock, E.A. McKenzie, M. Bhaman, R. Felix, C.R. Stubberfield, and P.R. Turner, *Furanyl-1,3-thiazol-2-yl and benzoxazol-5-yl acetic acid derivatives: novel classes of heparanase inhibitor.* Bioorg Med Chem Lett, 2005. **15**(9): p. 2295-9.
2. Harris, L.K., P.N. Baker, P.E. Brenchley, and J.D. Aplin, *Trophoblast-derived Heparanase is Not Required for Invasion.* Placenta, 2008. **29**(4): p. 332-7.
3. He, X., P.E. Brenchley, G.C. Jayson, L. Hampson, J. Davies, and I.N. Hampson, *Hypoxia increases heparanase-dependent tumor cell invasion, which can be inhibited by antiheparanase antibodies.* Cancer Res, 2004. **64**(11): p. 3928-33.
4. Parish, C.R., C. Freeman, K.J. Brown, D.J. Francis, and W.B. Cowden, *Identification of sulfated oligosaccharide-based inhibitors of tumor growth and metastasis using novel in vitro assays for angiogenesis and heparanase activity.* Cancer Res, 1999. **59**(14): p. 3433-41.